

**A TRANSMEMBRANE MUTATION IN Fc γ RIIB REVEALS THE
ROLE OF CERAMIDE IN PHAGOCYTOSIS AND AUTOIMMUNITY**

NURHUDA ABDUL AZIZ

NATIONAL UNIVERSITY OF SINGAPORE

2013

**A TRANSMEMBRANE MUTATION IN F_{cγ}RIIB REVEALS THE ROLE OF
CERAMIDE IN PHAGOCYTOSIS AND AUTOIMMUNITY**

NURHUDA ABDUL AZIZ

B.Sc (Forensic Science)(Hons), Curtin University of Technology, Australia

A THESIS SUBMITTED

FOR THE DEGREE OF DOCTOR OF PHILOSOPHY

**NUS GRADUATE SCHOOL FOR INTEGRATIVE
SCIENCES AND ENGINEERING**

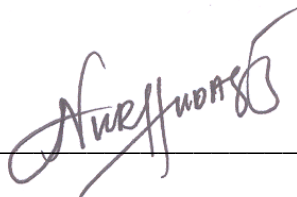
NATIONAL UNIVERSITY OF SINGAPORE

2013

Declaration

I hereby declare that this thesis is my original work and it has been written by me in its entirety. I have duly acknowledged all the sources of information which have been used in the thesis.

This thesis has also not been submitted for any degree in any university previously.

A handwritten signature in black ink, appearing to read 'Nurhuda Abdul Aziz', is written over a horizontal line.

Nurhuda Abdul Aziz

Acknowledgements

There are many people who were involved in the successful completion of this project and production of this thesis:

I would like to thank Assoc. Prof Markus R. Wenk for supervising me. I am grateful for the time and advice that he has so generously provided.

My gratitude also goes to Assoc. Prof Paul A. MacAry for being a great supervisor. I have benefited tremendously from his expertise and experience in cell biology. I could not have done this thesis work without the supervision and encouragement from such a patient and understanding supervisor.

My great appreciation goes to Asst. Prof Gijsbert Grotenbreg and Asst. Prof Brandon J. Hanson for their insightful comments and valuable suggestions. Special thanks to Dr Olivia Oh for working closely with me to see through this project well as to Dr Gan Shu Uin and Dr Paul Hutchinson helping me with various technical issues related to this project. I would also like to extend my appreciation to Dr Shui Guanghou for his help with the mass spectrometry, and Ms Duan Xinrui for her assistance with statistical analysis.

Lastly, I would like to thank all my lab colleagues, past and present for your friendship and for being a part of my research experience.

Table of Contents

CHAPTER 1	1
INTRODUCTION	1
1.1 Phagocytosis	2
1.1.1 The immune system and phagocytosis.....	2
1.1.2 Receptors involved in phagocytosis	4
1.1.3 Fc γ receptor mediated phagocytosis	5
1.1.3.1 Particle internalization and formation of phagocytic cup.....	5
1.1.3.2 Formation of Early Phagosomes	7
1.1.3.3 Formation of Late Phagosomes	8
1.1.3.4 Phagosome – lysosome fusion.....	9
1.2 Fragment Crystallizable γ Receptors (FcγRs)	11
1.2.1 Regulation of phagocytosis signaling by Fc γ receptors	15
1.2.2 The role of Fc γ RIIb in host defense and human autoimmunity.....	18
1.2.3 Mechanism for loss of Fc γ RIIb inhibitory function by Ile232Thr polymorphism.....	20
1.3 The molecular biology of lipids	21
1.3.1 Lipid diversity, role and importance	21
1.3.2 Classification of the repertoire of lipids	24
1.3.3 The influence of lipids on membrane curvature.....	28
1.3.4 Lipid distribution and contribution in phagocytosis	32
1.3.5 Lipid rafts: Overview	45
1.3.5.1 Rafts in signal transduction	47
1.3.5.2 A role for ceramide in lipid rafts	48
1.3.6 Lipidomics: emerging lipid analytics.....	50
1.4 Objectives and thesis outline	53
CHAPTER 2	55
MATERIALS AND METHODS	55
2.1 Solutions and Buffers	56
2.1.1 Buffers for phagosome preparation.....	56
2.1.2 Buffers for plasma membrane isolation.....	57
2.1.3 Buffers for SDS – PAGE and western blotting	57
2.1.4 Buffers for flow cytometry.....	59
2.1.5 Buffers for confocal microscopy	59
2.1.6 Buffers for mycobacterial infection	59
2.2 Reagents	60

2.2.1	Latex beads.....	60
2.2.2	Antibodies.....	60
2.2.3	Plasmids and Cell lines	61
2.3	Cell culture	66
2.3.1	Cell culture and maintenance.....	66
2.3.2	Differentiation of U937 monocytes into macrophages.....	66
2.4	Detection of Protein kinase C activity assay	67
2.5	Preparation of plasma membrane isolates	67
2.6	Assessment of phagocytosis and phagosome maturation.....	68
2.6.1	Generation of IgG opsonized latex beads	68
2.6.2	Phagosome Formation and Isolation.....	69
2.6.3	Phagosome quantitation.....	70
2.6.4	Western blot analysis	70
2.6.5	Flow cytometry analysis	72
2.7	Confocal Microscopy.....	74
2.8	Mycobacteria infection assays.....	76
2.8.1	Culture of Mycobacteria.....	76
2.8.2	BCG infection and survival assays by U937 macrophages.....	76
2.8.3	Bioplex Cytokine Array	77
2.9	Lipid Analysis.....	78
2.9.1	Extraction of lipids from samples.....	78
2.9.2	Lipid fingerprinting by mass spectrometry.....	79
2.10	Statistical Analysis	80
CHAPTER 3.....		81
RESULTS I: GENERATION OF CELL LINES, REAGENTS AND MODEL SYSTEMS FOR STUDYING Fcγ RECEPTOR MEDIATED PHAGOCYTOSIS .		81
3.1	Introduction	82
3.2	Characterization of Fcγ receptors on U937 cells.....	83
3.3	Establishment of conditions for phagocytosis in U937 cells.....	88
3.3	Use of latex beads for an <i>in vitro</i> phagosome model	92
3.4	Isolation of maturing phagosomes with step sucrose gradients	96
3.5	Extraction of plasma membrane	104
3.6	Discussion.....	108
CHAPTER 4.....		112
RESULTS II: ANALYSING THE EFFECTS OF FcγRIIB^{232I} AND FcγRIIB^{232T} ON LATEX BEAD PHAGOCYTOSIS		112
4.1	Introduction	113

4.2 Evaluation of phagocytic indexes of Fc γ RIIb ^{232I} and Fc γ RIIb ^{232T} macrophages	114
4.3 Assessment of phagosomal maturation	116
4.3 Assessment of phagosome acidification	119
4.4 Quantification of ROS produced in maturing phagosomes	122
4.5 Impact of Fc γ RIIb on calcium responses during phagocytosis.....	126
4.6 Discussion	129
CHAPTER 5.....	133
RESULTS III: INVESTIVGATING THE PHAGOCYTIC BACTERICIDAL ACTION OF FcγRIIB^{232I} AND FcγRIIB^{232T} ON A PATHOGEN MODEL.....	133
5.1 Introduction	134
5.2 Ensuring Fc receptor mediated phagocytic uptake	135
5.3 Measurement of bacterial ingestion and killing	138
5.4 Assessment of inflammatory cytokines following phagocytosis.....	144
CHAPTER 6.....	153
RESULTS IV: Lipidomic Fingerprinting and Analysis.....	153
6.1 Introduction	154
6.2 Lipid composition of plasma membrane	154
6.3 Lipid composition in maturing phagosomes	162
6.4 Comparison of lipid profiles between plasma membrane and phagosomes 166	
6.4 Discussion.....	172
CHAPTER 7	174
RESULTS V: INVESTIVGATING THE ROLE OF CERAMIDE IN PHAGOCYTOSIS	174
7.1 Introduction	177
7.2 Generation and characterization of cell lines	179
7.3 Effect of ceramide on BCG killing and cytokine secretion.....	185
7.4 Discussion.....	195
CHAPTER 8.....	198
DISCUSSION.....	198
Discussion	199

APPENDICES.....	208
Appendices	209
Appendix 1: Optimized MRM parameters for lipid species detected by LC-MS/MS.....	209
Appendix 2: Trends of individual lipid species in maturing phagosomes.....	215
REFERENCE	225
References	226

Summary

Receptor-mediated phagocytosis is a phylogenetically ancient biological process employed for the protection of organisms from microbial infection and in the maintenance of tissue homeostasis through clearance of cellular debris. The best characterized cellular receptors that underlie this process are the receptors for immunoglobulins-particularly IgG termed Fc γ Rs and this form of phagocytosis is termed opsonization. Fc γ Rs can be broadly classified into activatory or inhibitory receptors based on the presence of Immuno-Tyrosine Activatory Motifs (ITAM) or Immuno-Tyrosine Inhibitory Motifs (ITIM) in their cytoplasmic domains. The inhibitory receptor is proposed to regulate and dampen pro-inflammatory signaling and hyper-aggressive phagocytic activity mediated by the activatory receptors. The principle inhibitory receptor Fc γ RIIb also plays a role in controlling autoimmunity for a single Isoleucine to Threonine substitution in its transmembrane domain termed Fc γ RIIb^{232T} renders the receptor non-functional and confers susceptibility to systemic lupus erythematosus (SLE). The Fc γ RIIb^{232T} receptor is excluded from membrane microdomains where the WT receptor regulates activatory Fc γ Rs. In this study, we conduct a comprehensive analysis of the lipid composition of phagosomes as these organelles invaginate, internalize and mature through the endocytic pathway from the macrophage plasma membrane. We demonstrate that maturing phagosomes captured at different time points post phagocytosis, exhibit a distinct lipid composition from the plasma membrane. Using cell lines stably transfected with either Fc γ RIIb^{232I}

or Fc γ RIIb^{232T}, we also demonstrate that Fc γ RIIb^{232T} impacts upon cellular ceramide expression/metabolism and this is linked to the observed hyperaggressive phagocytic activity of these macrophages. These findings represent the first comprehensive map of lipid composition and functionality in FcR-mediated phagocytosis and highlight a novel role for ceramide in this vital biological process.

List of Figures

Introduction

Fig 1.1: IgG opsonized particles stimulates Fc γ receptor clustering in mediating recognition of target particles for phagocytosis.	5
Fig 1.2: Schematic representation of phagosome maturation highlighting the molecules involved in relation to events along the endocytic pathway. ...	7
Fig 1.3: Stages of phagosome formation and maturation.	10
Fig 1.4: Schematic representation of human Fc γ Rs.	14
Fig 1.5: Diagrammatic representation of general Fc γ R signaling.....	17
Fig 1.6: The basic structure of cell membrane is the lipid bilayer.	22
Fig 1.7: Structure of phospholipid (specifically, phosphatidylcholine).	24
Fig 1.8: Basic structure of sphingolipid backbone and its various head groups.	26
Fig 1.9: Sterols such as cholesterol are defined by their planar and rigid tetracyclic ring	27
Fig 1.10: Spontaneous curvature mediated by lipids depends on their molecular geometry.	31
Fig 1.11: Lipids are heterogeneously distributed between membranes and across the membrane bilayer.	32
Fig 1.12: PI serves as the basic building block for the synthesis of PIPS.....	37
Fig 1.13: Schematic illustration of PIP composition at different stages of a forming phagosome.	39

Fig 1.14: PIP species detected in maturing phagosomes.....	40
Fig 1.15: Cholesterol preferentially partitions into areas with sphingolipids.	43
Fig 1.16: Lipid rafts are microdomains described as floating islands in a sea of phospholipids.	46
 <u>Results I</u>	
Figure 3.1: U937 cells and the Fc γ RIIb knock –ins express Fc γ RI and Fc γ RII but not Fc γ RIII.	85
Figure 3.2: U937 knock – in cells express similar levels of Fc γ RII.....	86
Figure 3.3: Fc γ RIIb, the inhibitory receptor, is not expressed in U937.....	87
Fig 3.4: Effects of PMA stimulation on PKC activation.	90
Fig 3.5: Cells differentiated with GM-CSF and PMA have increased phagocytic capacity.	91
Fig 3.6: Rabbit IgG coated latex beads are most efficiently taken up via Fc receptors.	94
Fig 3.7: IgG particles interact with Fc γ receptors and is internalized into the phagolysosomal pathway.	95
Figure 3.7: Latex bead phagosomes were isolated by flotation on step sucrose gradients.	99
Fig 3.8: Latex bead phagosomes were isolated at different stages of maturation.	100
Fig 3.9: Phagosome isolates were devoid of major contamination from other intracellular organelles.	101

Fig 3.10: Phagosome concentration is normalized according to absorbance at 600nm.	102
Fig 3.11: Equal loading of phagosomes was verified by silver stain.....	103
Fig 3.12: Coating of cells with cationic silica beads enables isolation of the plasma membrane from internal membranes.	106
Fig 3.13: Silver staining of proteins in plasma membrane extracts.....	107

Results II

Fig 4.1: Fc γ RIIb ^{232T} macrophages exhibit enhanced phagocytosis.	115
Fig 4.2: Fc γ RIIb ^{232T} polymorphism on the cell surface is sufficient to enhance the rate of maturation of IgG opsonized beads.	118
Fig 4.3: Phagosomes expressing Fc γ RIIb ^{232T} displayed a more rapid acidification kinetic compared to Fc γ RIIb ^{232I} phagosomes.	121
Fig 4.4: Fc γ RIIb ^{232T} phagosomes produced more ROS over time compared to wild type Fc γ RIIb ^{232I} phagosomes.	125
Fig 4.5: A more notable calcium response was observed during phagocytosis by Fc γ RIIb ^{232T} macrophages.	128

Results III

Fig 5.1: Anti – 2F12 opsonized BCG activates Fc γ receptor mediated phagocytosis.	137
Fig 5.2: Fc γ RIIb ^{232T} expressing macrophages internalize more mycobacteria.	140
Fig 5.3: Macrophages expressing Fc γ RIIb ^{232T} have a much higher capacity to kill ingested bacteria as compared to Fc γ RIIb ^{232I} expressing macrophages.	142

Fig 5.4: Killing capacities of macrophages were not affected by the increased bacterial burden.	143
Fig 5.5: Macrophages expressing Fc γ RIIb ^{232T} secrete higher levels of IL-1 β and TNF α 48h following BCG infection.....	147
Fig 5.6: Pro – inflammatory cytokine secretion was enhanced by macrophages expressing Fc γ RIIb ^{232T} following 24 h incubation with BCG.....	148
Fig 5.7: Increased production of pro – inflammatory cytokines 48 h after Fc γ receptor phagocytosis of BCG by Fc γ RIIb ^{232T} macrophages.....	149

Results IV

Fig 6.1: Major lipid species in the plasma membrane.....	156
Fig 6.2: Individual lipid species in the plasma membrane revealed significant differences between Fc γ RIIb ^{232I} and Fc γ RIIb ^{232T} macrophages.....	157
Fig 6.3: Fc γ RIIb232T resulted in increased levels of phospholipid species with long acyl chains.....	159
Fig 6.4: Impact of Fc γ RIIb ^{232I} or Fc γ RIIb ^{232T} on saturation of plasma membrane phospholipids.	161
Fig 6.5: Comparison of phagosome lipids from Fc γ RIIb ^{232I} and Fc γ RIIb ^{232T} macrophages.	164
Fig 6.6: Heatmap representation of changes in individual lipid species of phagosome lipids.	165
Fig 6.7: The lipid composition of the plasma membrane differed significantly from that of phagosome membranes.	167
Fig 6.8: Comparison of ceramide species in both the Fc γ RIIb232I and Fc γ RIIb232T phagosomes.	170

Fig 6.9: Raft lipids were enriched in cells expressing Fc γ RIIb²³²¹ 171

Results V

Figure 7.1: Establishing the expression of SMPD1 gene in transduced U937 cell lines..... 181

Figure 7.2: SMPD1 expression levels were confirmed by western blotting. 182

Figure 7.3: Surface expression of ceramide was altered after over-expression or silencing of SMPD1 gene..... 183

Figure 7.4: SMPD1 can modify the levels of ceramide on the plasma membrane. 184

Fig 7.5: High level of ceramide retards the uptake of BCG into macrophages. 188

Fig 7.6: Ceramide mediated raft modification is critical for pathogen survival. . 189

Fig 7.7: Ceramide influences the secretion of pro-inflammatory cytokines..... 192

Fig 7.8: A low level of ceramide enhances excessive cytokine production after 48h Fc γ R phagocytosis. 193

Fig 7.9: Production of IL-10 in culture supernatant after Fc γ R phagocytosis.... 194

List of Tables

Table 1: Molecular markers of endocytic organelles proposed to interact with phagosomes.....	10
Table 2: Fc- receptor polymorphisms in human autoimmune diseases.....	18
Table 3: Classification system for phospholipids.	25

Abbreviations

ASMase	Acid sphingomyelinase
BCG	Bacillus Calmette-Guérin
BSA	Albumin from bovine serum
Cer	Ceramide
CFU	Colony forming units
Cho	Cholesterol
EEA-1	Early endosome antigen 1
ESI-MS	Electrospray ionization mass spectrometry
ER	Endoplasmic reticulum
Fc γ R	Fc receptor for immunoglobulin G
G-CSF	Granulocyte colony stimulating factor
GFP	Green fluorescent protein
GM-CSF	Granulocyte-macrophage colony stimulating factor
IgG	Immunoglobulin G
IFN- γ	Inteferon gamma
IL	Interleukin

ITAM	Immunoreceptor tyrosine activatory motif
ITIM	Immunoreceptor tyrosine inhibitory motif
LAM	Lipoarabinomannan
LAMP-1	Lysosome-associated membrane protein 1
LBPA	lysobisphosphatidic acid
MHC	Major histocompatibility complex
MIP-1 α	Macrophage inflammatory protein 1 alpha
MIP-1 β	Macrophage inflammatory protein 1 beta
MOI	Multiplicity of infection
PA	Phosphatidic acid
PAMP	Pathogen-associated molecular pattern
PBS	Phosphate buffered saline
PC	Phosphatidylcholine
PI	Phosphoinositol
PIPS	Phosphoinositides
PE	Phosphoethanolamine
PMA	Phorbol 12-myristate 13-acetate

PS	Phosphatidylserine
ROS	Reactive oxygen species
RT-PCR	Reverse transcriptase-polymerase chain reaction
shRNA	Short hairpin RNA
SLE	Systemic lupus erythmatosus
SM	Sphingomyelin
SMPD1	Sphingomyelin phosphodiesterase 1
SNARE	SNAP and NSF attachment receptor
TNF- α	Tumor necrosis factor alpha

CHAPTER 1

INTRODUCTION

1.1 Phagocytosis

1.1.1 The immune system and phagocytosis

Phagocytosis is an essential component of our innate immune system. It is the process by which foreign particles that are larger than 0.5 μm including microbial pathogens, apoptotic bodies and cellular debris are internalized by phagocytic cells and digested/eliminated. This process of recognition and engulfment of pathogens or tissue debris that accumulate during infection, inflammation or wound repair is essential for successful host defense. As such, phagocytosis serves two vital functions: – (i) The removal of apoptotic cells or cellular debris and (ii) the elimination of infectious agents [1-3].

Phagocytosis is an evolutionarily conserved process that was first observed by the Russian biologist Elie Metchnikoff in the late 1800s and has been extensively studied for over one hundred years [3-6]. Whilst the proteinaceous components of this process have been characterized there remains a significant gap in our knowledge about the role of lipids despite these being the major molecular constituents of the phagosome membrane.

All eukaryotic organisms, with the exception of yeast, possess the ability to phagocytose. In mammalian cells, phagocytosis is mediated primarily by a specialized subset of immune cells termed “professional phagocytes”. This includes monocytes, macrophages, neutrophils and dendritic cells. Professional phagocytes are equipped to rapidly and efficiently ingest invading

microorganisms in contrast to non-professional phagocytes, which are far less efficient and are unable to eliminate as large a variety of targets. Non-phagocytic cells include natural killer cells, basophils and eosinophils [7-10].

Phagocytosis is initiated by the interaction of specialized phagocytic receptors on the plasma membrane of the phagocyte with ligands on the surface of the foreign particle. The receptor-ligand interaction activates signal transduction pathways that result in the internalization of the target particle. The internalized particle is contained in a plasma membrane derived vacuole, termed a phagosome. The phagosome subsequently undergoes maturation by interactions with endocytic compartments, converting them into an effective microbicidal and degradative compartment for the elimination/digestion of the internalized particle [7, 11].

Phagocytosis constitutes a mechanism in the first line of host defense through the uptake and clearance of infectious targets and contributes to the maintenance of tissue homeostasis, control of immune responses and the resolution of inflammation. The understanding of the phagocytic process is important as inappropriate clearance of apoptotic bodies can give rise to autoimmune disorders, while a failure to engulf and kill pathogens can result in deadly infections. Ingested pathogens are not only killed but are digested to generate peptides that can be loaded onto class II major histocompatibility complexes (MHC-II) for antigen presentation to cells of the adaptive immune response. Hence, phagocytosis also serves to coordinate the link between the innate and adaptive immune response [3, 11-14].

1.1.2 Receptors involved in phagocytosis

The surface of the phagocyte is adorned with a variety of phagocytic receptors that are able to recognize and bind to invading microorganisms. The expression of an array of specialized phagocytic receptors attributes to the cell's unique ability to efficiently internalize a variety of targets while also allowing for the discrimination of pathogens from host self [15, 16].

Receptors involved in phagocytosis include pattern recognition receptors that directly recognize the target pathogen through pathogen-associated molecular patterns (PAMPs) such as surface carbohydrates, lipoproteins and lipopolysaccharides that are present on bacteria, viruses or fungi; and receptors that recognize targets coated in opsonic molecules [2, 10-13, 16].

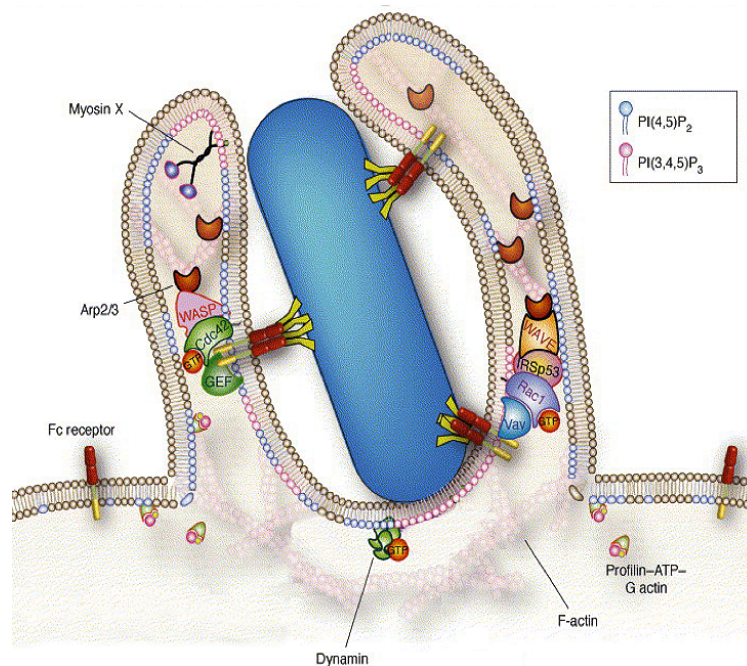
Major opsonins include circulating serum immunoglobulin G (IgG) and components of the complement cascade [2, 12]. Opsonization renders the target particle more susceptible to engulfment by phagocytic cells. Complement receptors (CR) recognize complement-opsonized pathogens, which get displaced inwardly, gently "sinking" into the phagocytic cell without pseudopod extension. In contrast, IgG opsonized particles are eliminated by Fc receptor (FcR) mediated phagocytosis. The conserved Fc domain of IgG distributed over the surface of an opsonized microbe is recognized by Fc γ Rs present on the phagocytes and is rapidly internalized by actin-dependent extension of the plasma membrane around the target particle. The extending pseudopods eventually surround and

internalize the target particle through a “zipper-like” process where the $Fc\gamma R$ s interact sequentially with IgG on the surface of the particle [3, 12, 13, 17].

1.1.3 $Fc\gamma$ receptor mediated phagocytosis

1.1.3.1 Particle internalization and formation of phagocytic cup

The engagement of $Fc\gamma$ receptors on the plasma membrane with IgG molecules on the surface of the foreign particles triggers the formation of an actin-rich phagocytic cup as shown in **Fig 1.1**.



(adapted from Yeung et al, 2006)

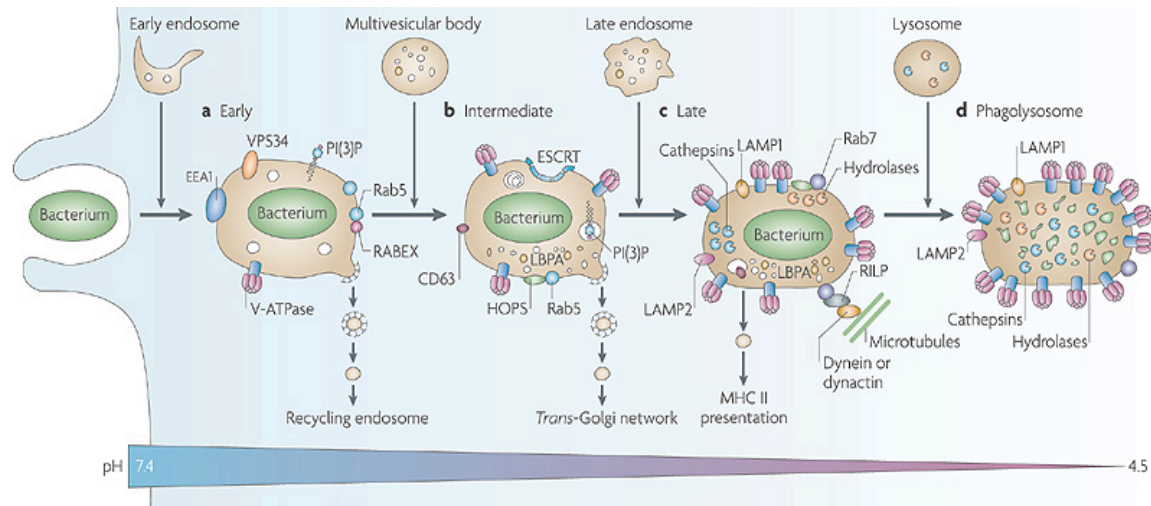
Fig 1.1: IgG opsonized particles stimulates $Fc\gamma$ receptor clustering in mediating recognition of target particles for phagocytosis.

This leads to membrane extension and actin polymerization resulting in the internalization of the target bound to the Fc receptor into the cell.

The target particle is surrounded by the extending of pseudopods of the plasma membrane that eventually engulfs the target particle. This ultimately results in the delivery of the internalized particle into the cell interior within a plasma membrane derived vacuole – the phagosome [17-19].

After internalization, actin is shed from the nascent phagosome. The phagosome, derived from the plasma membrane does not initially possess microbicidal ability and thus undergoes a coordinated maturation process similar to that observed for early to late endosomes within the the endocytic pathway. The endocytic pathway is organized as a continuum of organelles from early endosomes to lysosomes. Phagosome maturation modifies the composition of the phagosomal membrane and its luminal contents to endow the phagosome with an array of microbicidal and digestive molecules needed to degrade the internalized particle. Current phagosome maturation models imply the continuous removal and addition of material from the endocytic compartments to the early phagosome to convert it into a microbicidal phagolysosome (**Fig1.2**) [3, 10, 18]. The interplay between the phagosomal and endosomal pathways has been described as a “kiss and run” mechanism in which the partial and transient fusion of endosomes and phagosomes (kiss) allows for the transfer of membrane and luminal contents and is immediately followed by fission (run) which prevents complete mixing of the two compartments. Therefore, in addition to the receptors and ligands that participate in phagocytosis, other molecules provide unique characteristics to each stage of phagosome maturation. These include molecules that regulate the

internal pH and vesicle docking, fusion and budding [3]. The following sections dissect the discrete stages of phagosome maturation and the mechanisms known to regulate this process.



(adapted from Flannagan et al, 2009)

Fig 1.2: Schematic representation of phagosome maturation highlighting the molecules involved in relation to events along the endocytic pathway. Following scission from the plasma membrane, the internalized particle undergoes a maturation process sequentially interacting with endosomes and lysosomes ultimately becoming a phagolysosome.

1.1.3.2 Formation of Early Phagosomes

Once the phagosome has been sealed off from the cell membrane, the nascent phagosomes first fuse with early endosomes. Early endosomes have a mildly acidic pH and the endosome-phagosome fusion introduces early endosomal membranes and proteins such as Rab 5 and Early Endosome Antigen 1 (EEA1) to phagosomes. Rab 5 is primarily found on early endosomes and stimulates the

fusion of nascent phagosomes with early endosomes. The precise mechanism of the recruitment of Rab 5 to the phagosome has remained elusive but has been reported to be essential for the subsequent progression to the late phagosome stage of phagocytosis. The recruitment of EEA1 to early phagosome facilitates docking and fusion with early endosomes. EEA1 also interacts with soluble N-ethylmaleimide-sensitive factor attachment protein receptor (SNARE). SNARE proteins bind to target vesicles very tightly and promotes membrane fusion contributing further to phagosome maturation by mediating the fusion of early endosomes with the phagosome [3, 20].

1.1.3.3 Formation of Late Phagosomes

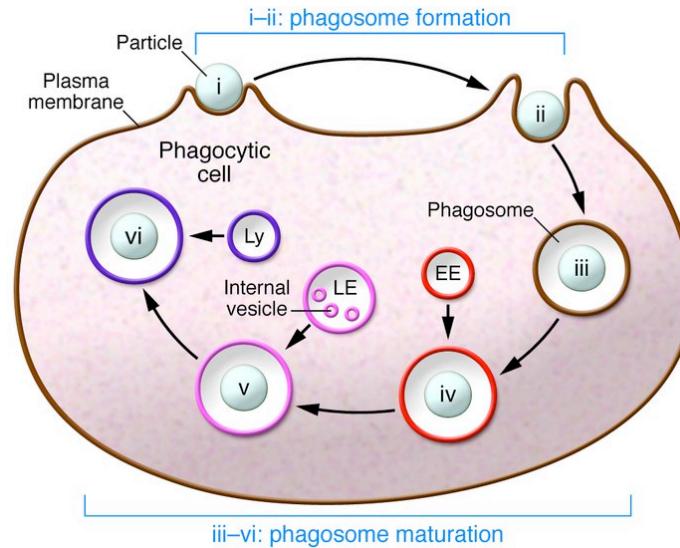
As phagosomes progress through the endocytic pathway they become enriched in late endosome components. Late phagosomes are more acidic (~pH 5.5) compared to early phagosomes due to the accumulation of additional proton pumps. Proton pumps are catalyzed by vacuolar ATPase (V-ATPase), a protein complex that translocates H⁺ across phagosomal membranes at the expense of ATP. The transition of early phagosome into a late phagosome is signaled by the loss of early endosomal markers and the acquisition of late endosomal components, best exemplified by Rab 7 and lysobisphosphatidic acid (LBPA). Rab 7, a small GTPase found predominantly on late endosomes is vital for the completion of phagosome maturation. The impairment of Rab 7 acquisition on phagosome have been shown to block phagosome-lysosome fusion and acidification [3].

1.1.3.4 Phagosome–lysosome fusion

Late endosomal markers such as LBPA are lost as phagosomes fuse with lysosomes, the last compartment of the endocytic pathway to generate a phagolysosome. Lysosomes are the main hydrolytic compartment and are enriched in acid hydrolases, hydrolytic proteases such as cathepsin D as well as other lysosome associated membrane proteins (LAMP). As such, phagolysosomes possess a number of complementary degradative properties, including very low pH ($\text{pH} < 5$) and are rich in hydrolytic enzymes and oxidative compounds. The phagosome lumen becomes highly acidic and oxidative creating an extremely hostile environment that results in the degradation of the encapsulated particle [1, 14].

As pathogens and apoptotic bodies are degraded, phagosomes decrease in size, undergo fragmentation and eventually disappear [14]. The steps leading to the formation of the phagolysosome, which is the terminal stage of the maturation sequence, are illustrated in **FIG 1.3**.

Table 1 shows a list of protein or lipid markers from compartments along the endocytic pathway that is commonly used to identify the stage of phagosome maturation.



(adapted from Steinberg and Grinstein, 2008)

Fig 1.3: Stages of phagosome formation and maturation.

Phagocytosis events are carefully orchestrated beginning with (i) receptor engagement, followed by (ii) membrane pseudopod extension, “zippering” of the membrane around the target, (iii) scission of the nascent vacuole from the plasma membrane and (iv-vi) finally maturation by sequential interactions with endosomes and lysosomes for the acquisition of microbicidal and degradative capabilities.

Organelle	pH	Markers
Early endosome	6.0	EEA1, Rab5, PI(3)P, syntaxin -13, transferrin receptor
Late endosome	5.0-6.0	Rab7, Rab9, Mannose -6- phosphate receptor, LAMP, LBPA
Lysosome	4.5 – 5.0	LAMP, mature cathepsin D

Table 1: Molecular markers of endocytic organelles proposed to interact with phagosomes.

The lumen of the phagosome undergoes gradual acidification from near – neutral pH to pH < 5 as it merges with components of the endocytic pathway.

1.2 Fragment Crystallizable γ Receptors (Fc γ Rs)

Structural properties and antibody binding interactions

Most cells of the immune system express FcRs on their surfaces. FcRs are transmembrane glycoproteins that bind to the constant fragment crystallizable (Fc) region of immunoglobulins. FcRs are classified according to the immunoglobulin subclass to which they bind. Five classes of FcRs exist for all classes of immunoglobulins; Fc α R binds IgA, Fc δ R binds IgD, Fc ϵ R binds IgE, Fc γ R binds IgG and Fc μ R binds IgM [21-24].

Of these, Fc γ Rs are the most extensively studied and well-characterized, and are expressed by most types of leukocytes including macrophages, monocytes, neutrophils, dendritic cells [25, 26].

In humans, Fc γ receptors fall into three structurally distinct classes: Fc γ RI (CD64), Fc γ RII (CD32) and Fc γ RIII (CD16). Several genes encode Fc γ Rs in each class. Three genes, known as A, B and C exist for both Fc γ RI and Fc γ RII. Two genes, A and B, code for Fc γ RIII. These genes are located on chromosome 1 at q21-23 [23, 27]. Fc γ receptors share similarity in their extracellular immunoglobulin-like domains, but they differ primarily in their transmembrane and intracellular domains [28].

Fc γ RI consists of three extracellular domains. This feature is thought to be responsible for its high IgG binding affinity. Fc γ RII and Fc γ RIII have only two

domains, which make them low affinity receptors for IgG. The first two domains are homologous in all three Fc γ Rs but the third domain, which is closest to the cell surface, is different and confers Fc γ RI its high affinity for the Fc region of IgG and restricted isotype specificity thus, Fc γ RI binds monomeric IgG. Fc γ RII and Fc γ RIII both have low affinity for the antibody constant region but a broader isotype binding specificity that binds to multimeric immune complexes [23, 29-32].

Functionally, Fc γ Rs can be distinguished by the signals in which they transmit. Activating receptors trigger a variety of biological cellular responses such as promoting phagocytosis, the release of various inflammatory cytokines and the production of reactive oxygen species. The inhibitory receptor on the other hand serves to regulate the threshold of the activation responses [15, 21, 29, 33].

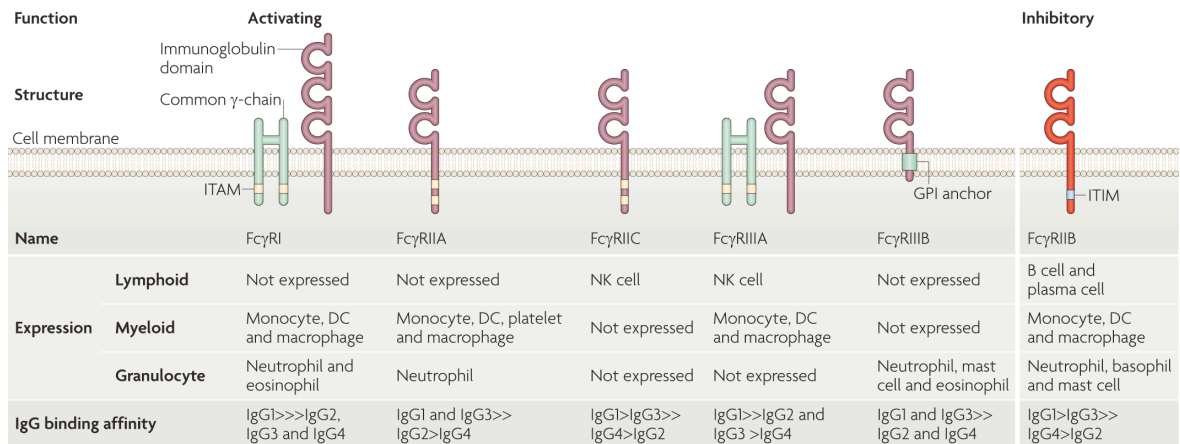
Most of the identified human Fc γ Rs fall within the activation class. Activatory receptors can be characterized by the presence of an immunoreceptor tyrosine based activatory motif (ITAM) in its cytoplasmic tail. ITAM comprises of 2 copies of the amino acid sequence YxxL. Fc γ RIIIa is the most abundantly expressed activatory receptor in humans. Among the three classes of Fc γ Rs, Fc γ RIII isoforms are unique in that their ITAM signaling domains are found within the cytoplasmic tail and as such do not require the presence of a separate signaling subunit. This allows Fc γ RIIIa to transmit its activation signals in the absence of the common γ chain. Fc γ RI and Fc γ RIII in contrast do not contain signaling

domains by themselves but associate with γ subunits that contain the signaling ITAM domains. The activating receptors are switched on when the Fc portion of IgG binds to Fc γ Rs resulting in receptor cross-linking and subsequent phosphorylation of the ITAM. This initiates a signaling cascade that results in the activation of the immune cell function leading to phagocytosis, calcium mobilization, oxidative burst and cytokine release [21, 23, 29-31, 34-36].

As opposed to the activating Fc receptors, Fc γ RIIb, is a single chain inhibitory receptor that encodes immunoreceptor tyrosine-based inhibitory motif (ITIM) containing inhibitory residues in its cytoplasmic tail. Fc γ RIIb is the only Fc γ R that expresses an ITIM motif. ITIM consists of the 13 amino acid residues AENTITYSLLKHP. Once phosphorylated during FcR engagement, the ITIM recruits protein and lipid phosphatases that downregulate the phosphorylation signaling of the activating receptors and dampens the activatory signals thus limiting the phagocytic response [22, 29, 33, 36, 37].

The activating and inhibitory receptors function in concert and this paired expression on a given cell allows for a balanced immune response [29, 33, 36, 38]. The differences and expression of the Fc γ Rs are summarized in **Fig 1.4**.

Fc γ RIIb is present exclusively on neutrophils and is a glycosylphosphatidylinositol (GPI)-linked receptor lacking transmembrane and cytoplasmic domains. No subunits are known to associate with it but Fc γ RIIb is thought to signal with the cooperation of other receptors [23, 36].



(adapted from Smith and Clatworthy, 2010)

Fig 1.4: Schematic representation of human FcγRs.

Humans express three structurally different FcγRs: FcγRI, FcγRII and FcγRIII. The various FcγRs bind the distinct IgG subclasses with different affinity. Based on their function; FcγR can mediate activating signals via ITAM. FcγRIIb, the inhibitory receptor bears an ITIM on its intracellular tail negatively regulating the response of the activating receptors. This establishes a threshold for the response to phagocytosis is sufficient to clear the pathogen but limited so that the excessive response is not damaging thus protecting the host.

1.2.1 Regulation of phagocytosis signaling by Fc γ receptors

Activating signaling by ITAM-containing Fc γ Rs

Phagocytosis of IgG immune complexes is initiated by the ligation of IgG with the Fc γ Rs on the cell surface. This induces the clustering of activating Fc γ Rs on the cell as multiple IgG molecules on the immune complex are engaged securely capturing the immune complex. Receptor aggregation results in downstream signaling via the ITAM motifs on the activatory receptors or the ITIM motifs on the inhibitory receptors [37].

Cross-linking of activatory receptors results in phosphorylation of the ITAM located in either the cytoplasmic tail of Fc γ RIIA or in the associated γ subunit by tyrosine kinases of the Src family. Src, Hck, Lyn and Fgr are examples of predominant family members of the Src family that have been identified in phagocytic cells. However, it remains to be seen as to which family member phosphorylates ITAM as this may depend on the cell type involved and the Fc γ Rs engaged [23, 33, 39].

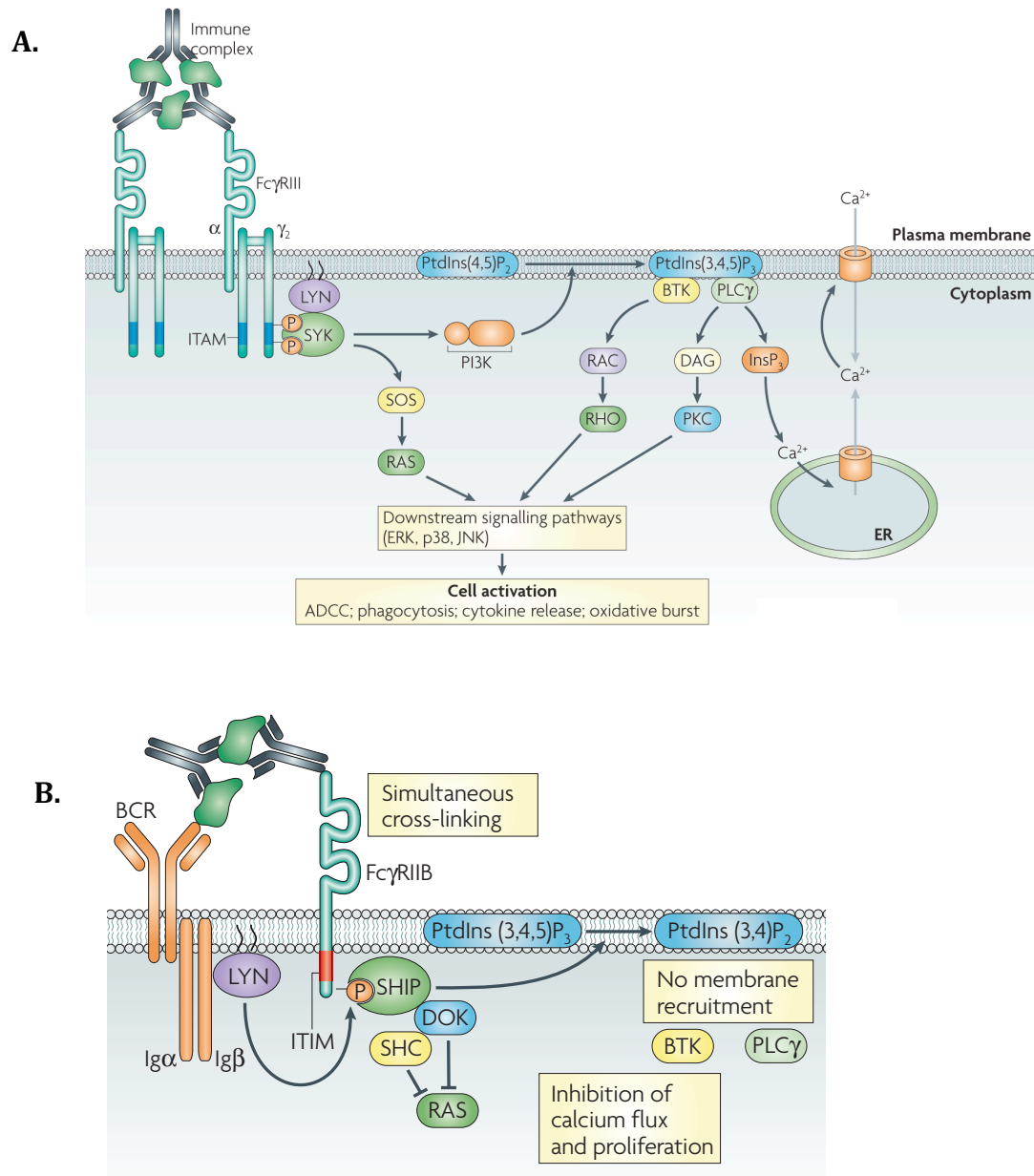
The phosphorylated ITAMs serve as docking sites for the recruitment of Src homology (SH2) domain containing Syk tyrosine kinase. Syk in turn promotes multiple downstream signaling pathways most notably the activation of phosphatidylinositol 3-kinase (PI3K) which leads to the production of phosphatidylinositol-3,4,5-triphosphate [PI(3,4,5)P₃]. [PI(3,4,5)P₃], recruits Bruton's tyrosine kinase (BTK) and phospholipase C γ (PLC γ). The activation of

PLC γ generates diacylglycerol (DAG) and inositol-1,4,5-P $_3$ (IP $_3$). The latter is responsible for the mobilization of intracellular calcium (Ca $^{2+}$) from internal reserves and triggering of further downstream signaling events. Besides calcium-dependent pathways, the MAPK (mitogen-activated protein kinase) pathway is also activated by ERK following Fc γ crosslinking and is of central importance for cell activation. These events have been identified to mediate particle internalization, production and release of proinflammatory cytokines and reactive oxygen species during phagocytosis.

Inhibitory signaling by ITIM-containing Fc γ RIIb

Co-engagement of the inhibitory receptor, Fc γ RIIb to an ITAM containing receptor leads to tyrosine phosphorylation of the ITIM by Lyn kinase. This results in the recruitment of the phosphatases Src homology 2 domain- containing inositol 5'-phosphatase (SHIP) to the ITIM motifs of Fc γ RIIb. The major function of SHIP is to dephosphorylate PI(3,4,5)P $_3$ into phosphatidylinositol-3,4-bisphosphate PI(3,4)P $_2$ inhibiting phagocytosis.

The interruption or inhibition of the activation signaling cascade through ITIM bearing receptors suppresses ITAM activation events and is crucial for maintaining homeostasis and controlling inappropriate activation signals that may be over-inflammatory and destructive [21, 30, 33, 38]. **Fig 1.5** illustrates the signaling mechanisms of ITAM and ITIM regulatory Fc γ R signaling.



(Falk Nimmerjahn & Jeffery V. Ravetch, 2008)

Fig 1.5: Diagrammatic representation of general Fc γ R signaling.

(A) The clustering of activatory Fc γ Rs such as Fc γ RIII activates Lyn kinases. Lyn phosphorylates the ITAM which in turn stimulates Syk and PI3K. This leads to the recruitment of BTK and PLC γ generating a calcium flux and triggering further downstream signaling events. **(B)** Simultaneous cross-linking of the activatory receptors with Fc γ IIb leads to the phosphorylation of the ITIM in the cytoplasmic tail of Fc γ RIIb by Lyn. This results in the recruitment of SHIP, which inhibits the recruitment of BTK and PLC γ leading to the block of Ca²⁺ influx and PKC activation.

1.2.2 The role of Fc γ R11b in host defense and human autoimmunity

Fc γ 11b contains ITIM motifs that can recruit phosphatases that inhibit phagocytosis. Over-expression of Fc γ R11b can inhibit phagocytosis. The tight regulation of the activatory and inhibitory Fc γ Rs play a key role in a balanced immune response. Genetic polymorphisms that modify the expression or function of Fc γ Rs have been implicated with susceptibility to a wide range of inflammatory and autoimmune diseases. This has resulted in significant global interest in the field of Fc γ R biology. The major polymorphisms of human Fc γ Rs are shown in

Table 2.

Autoimmune Disease	Polymorphism in Fc γ Rs			Reference
	Fc γ R11a	Fc γ R11b	Fc γ R11a	
Systemic Lupus Erythematosus (SLE)	Arg131His	Ile232Thr	Val158Phe	Duits et al., 1995; Manger et al., 1998 Wilcocks et al, 2010 Koene et al., 1998; Wu et al., 1997
Rheumatoid Arthritis			Val158Phe	Kastbom et al., 2005; Morgan et al., 2000; Nieto et al., 2000
Multiple Sclerosis	Arg131His			Myhr et al., 1999
Guillain – Barré syndrome	Arg131His			van der Pol et al., 2000; Vedeler et al., 2001
Myasthenia gravis (MG)	Arg131His			Raknes G et al., 1998
Idiopathic thrombocytopenic purpura (ITP)	Arg131His Arg131Arg		Val158Phe Phe158Phe	Foster et al., 2001; Williams Y., 1998; Fujimoto TT., 2001

Table 2: Fc- receptor polymorphisms in human autoimmune diseases.

Polymorphisms in human Fc γ Rs and their possible relations between have been described in patients with various autoimmune diseases.

Of particular interest is the single nucleotide polymorphism in Fc γ RIIb, in which a single T to C nucleotide change results in the substitution of isoleucine (I) to threonine (T) at position 232 within the transmembrane region of the receptor [40, 41].

There is evidence that indicates that the polymorphism in Fc γ RIIb influences susceptibility to systemic lupus erythematosus (SLE)[42-45]. SLE is a systemic autoimmune diseases characterized by autoantibody production. Patients with SLE have defective clearance of apoptotic cells and immune complexes. SLE affects a variety of organs and the build up of immune deposits result in inflammatory lesions [46, 47]. Several studies also suggest a role for Fc γ RIIb in modulating tolerance in mouse models for autoimmunity. The Fc γ RIIb deficient mouse has been shown to develop SLE-like manifestations. Macrophages from these mice also exhibited increased intracellular calcium flux, superoxide production and pro-inflammatory cytokine release following activatory Fc γ R cross-linking. This supports the notion that Fc γ RIIb could prevent the initiation of autoimmunity by mediating a negative feedback cascade that limits the activity of the activatory receptors [33, 37, 48].

Associations of the Fc γ RIIb^{232T} have been suggested to contribute to an increased susceptibility to SLE in several racial groups. Studies have shown that the Fc γ RIIb^{232T} genotype was found to be significantly over-represented in Japanese [49], Chinese [50], Thais [51], Indians [52], and Caucasian [53] SLE

patients. This polymorphism has also been known to be higher in population areas where malaria is endemic such as Southeast Asia and Africa. This suggests that the non-inhibitory Fc γ RIIb^{232T} is selected as a result of a protective effect in malaria infection, which carries a high risk of mortality, especially in infancy and children. Studies using Fc γ RIIb deficient mice have observed increased clearance of malarial parasites. Hence an impaired Fc γ RIIb function may be beneficial in the context of parasitic infections because defective Fc γ RIIb^{232T} leads to increased pathogen clearance [37, 53, 54].

1.2.3 Mechanism for loss of Fc γ RIIb inhibitory function by Ile232Thr polymorphism

Previous studies have shown that Fc γ RIIb^{232T} variant receptors that underwent substitution of isoleucine to threonine at position 232 within the transmembrane domain were excluded from specialized membrane domains known as “lipid rafts”. As a consequence, it is unable to interact with activatory receptors and exert its inhibitory effect on cellular function. Cells bearing this receptor variant have been reported to exhibit enhanced phagocytic capacity. This suggests that the failure to associate with lipid rafts disrupts normal Fc γ RIIb function resulting in exaggerated activatory receptor activity thought to promote SLE [42, 55].

1.3 The molecular biology of lipids

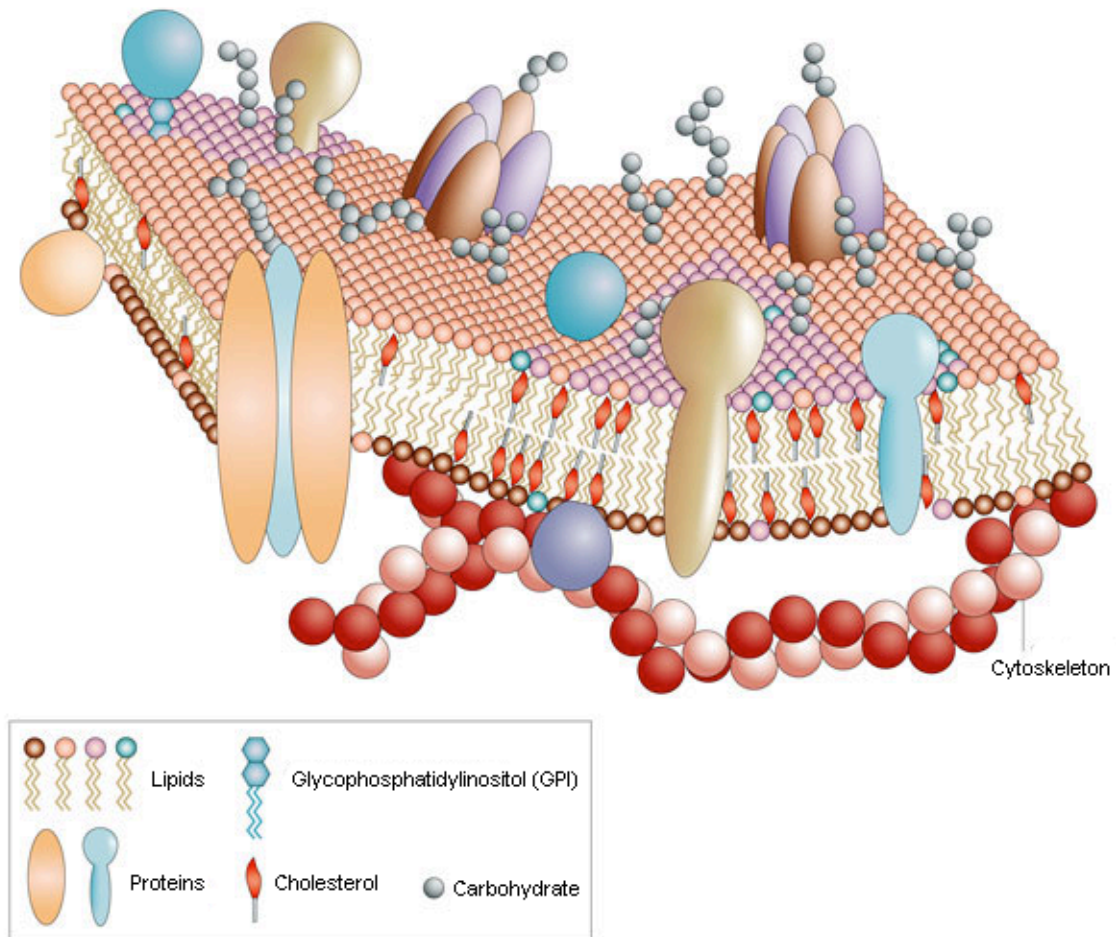
1.3.1 Lipid diversity, role and importance

Lipids are loosely defined as biological molecules which are soluble in organic solvents such as chloroform, ether or toluene. Lipids are amphipathic in nature consisting of polar hydrophilic head groups that face the cytoplasmic and extracellular spaces and non-polar hydrophobic tails that face each other. Lipids exhibit immense structural diversity and biological function due to the various combinations of polar headgroups, fatty acyl chains and aliphatic hydrocarbon chains structures. The headgroup of the lipids can vary, as can the fatty acids, which differ in length and degree of saturation, as can the bonds linking hydrocarbon chains. This extensive range of unique chemical structures encode for distinct functions within biological systems [56-58].

Lipids fulfill a multitude of different and essential functions in the cell. A primary role of lipids in cellular function is the formation of a membrane that separates the inside of a cell from the outside of a cell. In 1972, Singer and Nicholson introduced the fluid mosaic model (**Fig 1.6**). This model describes cell membranes as composed of a lipid bilayer which are intercalated with transmembrane proteins. Now, forty years later, this model is still a widely accepted model of the cell membrane [59].

Lipid bilayers form the core structure of membranes that define each cell and also subdivide the intracellular compartments of a cell as membranes envelop

each cellular organelle. The membranes surrounding each organelle have specific lipid composition and the distribution of lipid composition between various organelle membranes are unique [58, 60, 61].



(adapted from Pietzsch, J., 2004).

Fig 1.6: The basic structure of cell membrane is the lipid bilayer.

The schematic depicts membrane lipid asymmetry and also shows the association of membrane proteins viewed as icebergs embedded in a sea of lipids. Singer and Nicolson proposed this fluid mosaic model of the membrane structure in 1972. The Singer-Nicolson fluid mosaic concept is still the textbook model of how the cell membrane is organized.

In addition to being a cell membrane barrier, lipids play essential roles in cell structure and organization, signaling events and intracellular membrane trafficking. For example, lipids provide membranes for budding, fission and fusion; characteristics that are essential for cell division, biological reproduction and intracellular membrane trafficking [62].

Lipids form microdomains within the plasma membrane where signaling platforms assemble. Lipid species participate in signaling by acting as both substrates for and as activators of enzymes responsible for the generation of secondary messengers. The role of lipids in signal transduction is important for cellular communication and regulation of cellular responses. Aberrant communication among cells or dysregulation in signaling transduction pathways contribute to many diseases and pathological conditions such as chronic inflammation, autoimmunity and cancer [58, 62-64].

Finally, lipids have an additional role in membrane microdomain organization and are important determinants for the distribution of membrane proteins. Lipids can induce the organization of membrane lipids into microdomains that control the interaction of signaling proteins. Transmembrane proteins contain one or more hydrophobic regions that can transverse the membrane bilayer allowing these proteins to become closely exposed to membrane lipids. These transmembrane proteins also segregate into microdomains according to the nature of surrounding lipids. As such, lipids provide the matrix and so facilitate membrane bound proteins to aggregate and interact and/or allow others to disperse [58, 63-65].

In summary, lipids not only form the matrix of the cell membrane but they also determine the nature of all communication within the cell.

1.3.2 Classification of the repertoire of lipids

The basic structure of biological membranes is the lipid bilayer, which is mainly formed from three different lipid classes: phospholipids, sphingolipids and sterols. Phospholipids are the most abundant class of membrane lipids. Phospholipids are composed of two fatty acid tails, glycerol, a phosphate group and a polar headgroup as shown in **Fig 1.7**. The fatty acids can vary in length and can be saturated (no double bonds) or unsaturated (one or more double bonds). Based on the differences in chemical groups that are linked to the phosphate group, phospholipids can be classified into multiple different classes (**Table 3**). The major classes of phospholipids include phosphatidylcholine (PC), phosphatidylethanolamine (PE), phosphatidylserine (PS), phosphatidylinositol (PI) and phosphatidic acid (PA) [58, 60, 66].

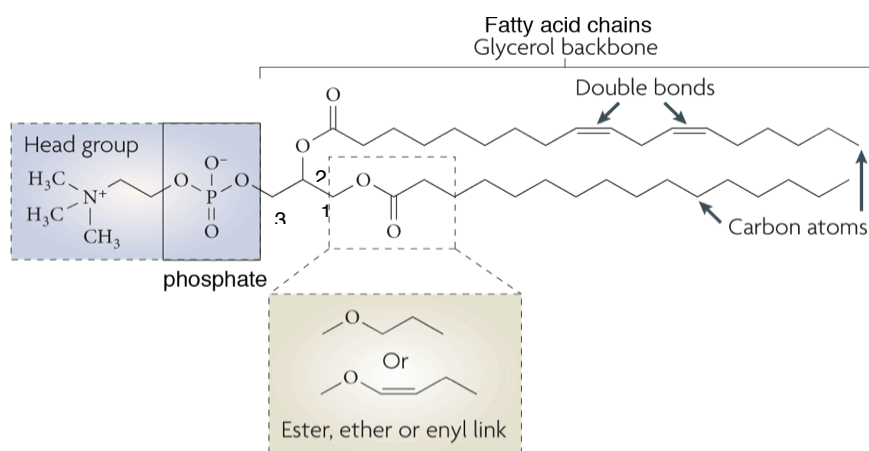


Fig 1.7: Structure of phospholipid (specifically, phosphatidylcholine).

A phospholipid is composed of two fatty acids, a glycerol unit, a phosphate group and a polar molecule at sn-3. Each phospholipid class in turn consists of numerous molecular species, i.e. lipids that have the same structural head group but differ in respect of the acyl chains. The length of the alkyl chain typically varies from 14 to 24 carbons and the number of double bonds from 0 to 6 [67].

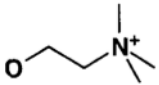

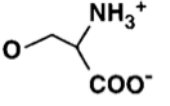
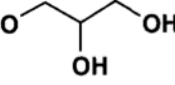
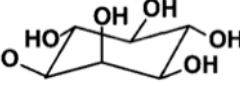
Class	Nomenclature	Headgroup	Structure of headgroup
Phosphatidylcholine	PC	Choline	
Phosphatidylethanolamine	PE	Ethanolamine	
Phosphatidylserine	PS	Serine	
Phosphatidylglycerol	PG	Glycerol	
Phosphatidylinositol	PI	Inositol	
Phosphatidic acid	PA	Phosphate	H

Table 3: Classification system for phospholipids.

Phospholipids can have many different head groups as a substituent attached to the phosphate group (which forms PA). Examples of these head groups include serine (PS), ethanolamine (PE), choline (PC), glycerol (PG) and inositol (PI).

Sphingolipids consist of a sphingoid base backbone (typically 18-20 carbon) instead of a glycerol molecule backbone, which is linked through an amide bond to a fatty acid to which may be attached to a head group. Sphingolipids are defined by the structure of the head group. The simplest of sphingolipids is ceramide, which consists of just hydroxyl groups whereas more complex

sphingolipids have phosphates and sugar residues attached (**FIG 1.8**). The lipid moiety can vary in terms of chain length of the fatty acids and in the degree of saturation and hydroxylation of the sphingoid base. Also, variations in the type, number and linkage of sugar residues give rise to a wide range of sphingolipids. The most abundant mammalian sphingolipid is sphingomyelin (SM) which is the addition of a phosphocholine headgroup on its ceramide backbone [68].

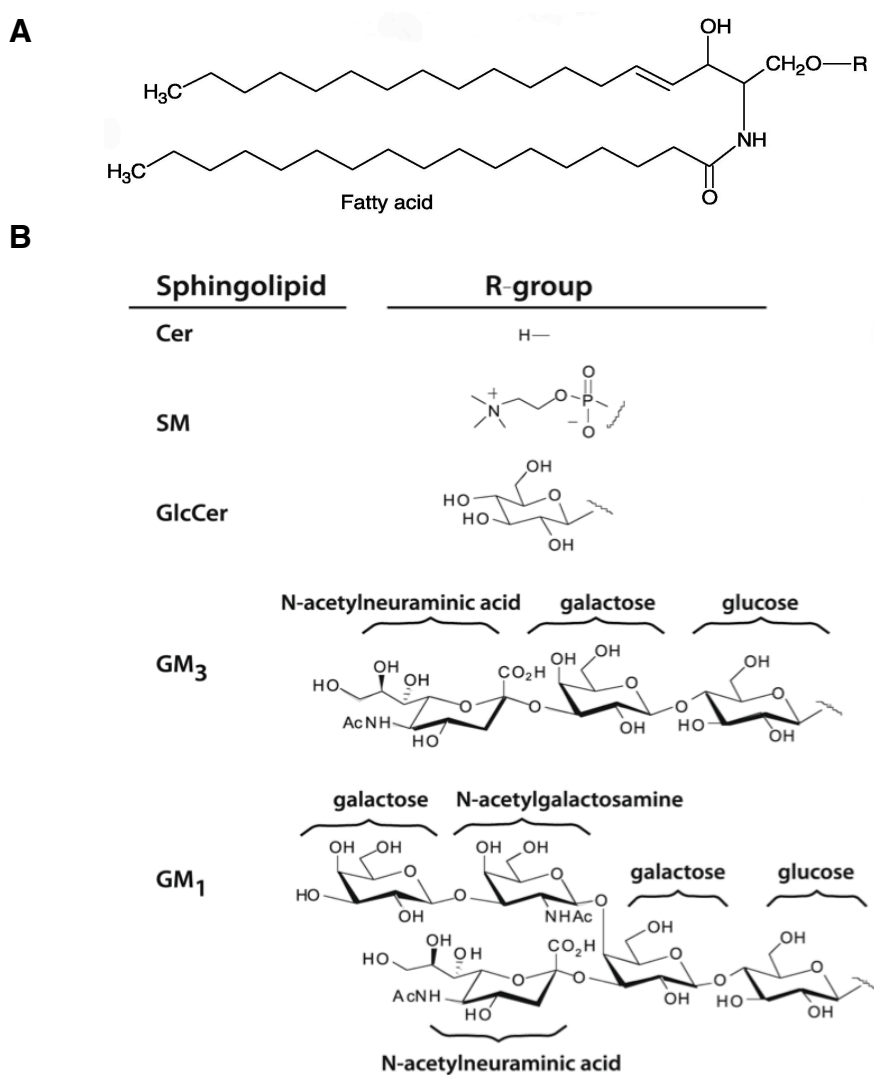


Fig 1.8: Basic structure of sphingolipid backbone and its various head groups.

Ceramide constitutes the backbone of all complex sphingolipids. The sphingolipid headgroup can be phosphocholine (which produces SM), glucose (to produce GlcCer) or can be further decorated with monosaccharides to create a wide range of glycosphingolipids, for example GM3.

Sterols represent the major non-polar lipids of cell membranes with cholesterol being the most predominant sterol lipid. Cholesterol is based on a four-ring structure that consists of three six-carbon rings and one five-carbon ring. One of the six-carbon rings has a double bond and all the rings are joined together to form the rigid and planar structure of the molecule (**Fig 1.9**) [60].

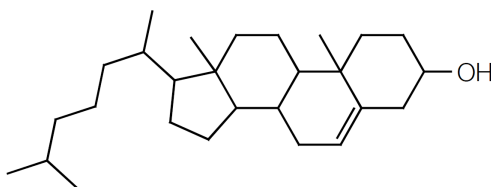


Fig 1.9: Sterols such as cholesterol are defined by their planar and rigid tetracyclic ring

In most biological membranes, phospholipids co-exist and function together with sphingolipids and cholesterol [57].

1.3.3 The influence of lipids on membrane curvature

Lipid membranes must be flexible enough to bud or invaginate for example when budding to form vesicles or fusing with other membranes during membrane trafficking. Phagocytosis involves extensive remodeling of the plasma membrane to shape the phagocytic cup around the target, followed by membrane closure then fusion and fission events with intracellular membranes such as endosomes and lysosomes during maturation. The unique chemical structure of each lipid group can favour different membrane curvatures. This is determined largely by the size of the individual lipid molecules polar head group and its hydrophobic tail. Curvature inducing lipids may foster membrane fusion and fission [57, 64, 69].

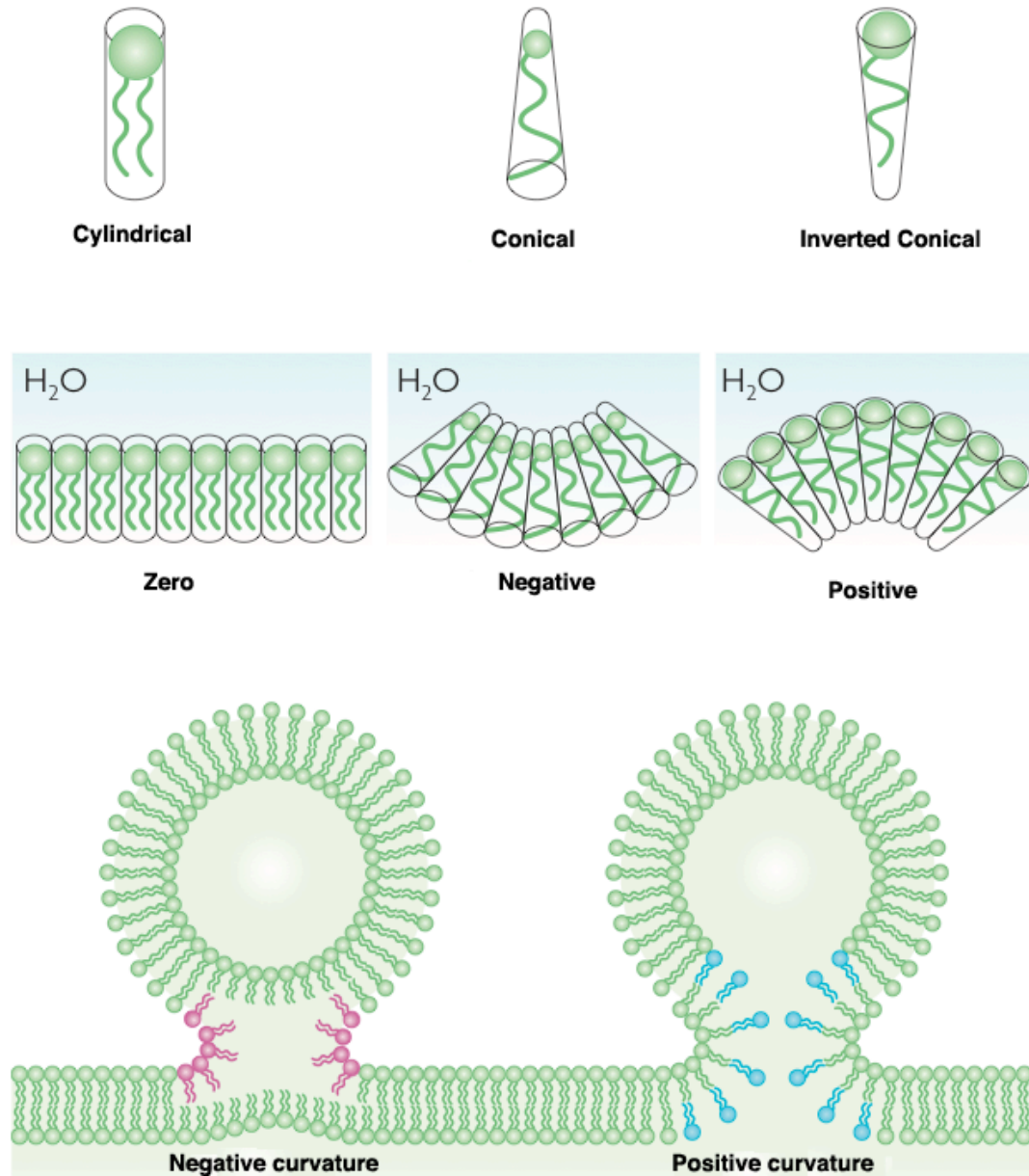
Lipids that have head groups with cross-sectional areas relatively equal to the area occupied by the fatty acyl tails have a cylindrical molecular geometry, for instance, PC with its hydrophobic tails facing each other and the polar head groups facing the aqueous phase. Lipid species with large head groups compared to the hydrophobic tail such as lysophospholipids will assume an inverted conical form. This will give rise to a positive curvature monolayer whereas lipids such as PA and PE have a relatively small head group compared to its fatty acid chain. These lipids will assume a conical molecular geometry bringing about negative curvature as the head groups will pack more tightly than the tail end. Curvature is induced when the two membrane leaflets in the bilayer do not contain the same lipids. A lipid quantity imbalance between the two

leaflets can also contribute to membrane bending. Any bend within a bilayer will create a positive curvature in one monolayer and a negative curvature in the other monolayer (**Fig 1.10**) [60, 70].

Lipid geometry also depends on the acyl chains. A double bond in the hydrophobic tail induces a “kink” in the chain and so occupies a larger area. Fatty acid chains that have more double bonds have more kinks in their structure and take up more space. Thus, as the number of double bond increases, the membrane becomes more fluid because the fatty acid tails fit less closely. Conversely, the fewer the number of double bonds, the more tightly the fatty acid tails fit together and the membrane becomes less fluid. Sphingolipids have saturated tails and as such are able to form taller and narrower cylinders than PC lipids of the same chain length. This allows them to pack more tightly, adopting a solid “gel” phase and separate from the surrounding phospholipids which are more loosely packed due to their kinked unsaturated chains. In contrast, phospholipids tend to exist in a liquid crystalline state as they contain saturated and unsaturated acyl chains of variable length in which the acyl chains are fluid and disordered. In the absence of other lipids, membranes containing only phospholipids and sphingolipids phase separate into a highly ordered gel phase made of sphingolipids and a disordered phase that contains phospholipids. Addition of sterols to such membranes allows for the formation of liquid – ordered phase in which the saturated acyl chains are highly organized as in the gel phase but exhibit mobility similar to that of the liquid crystalline state. As sterols

preferentially associate with sphingolipids, the cylindrical combination of SM plus cholesterol resists membrane bending that is required for fission and fusion [58, 60, 71, 72].

Lipid composition is an important determinant that can influence membrane curvature in fission and fusion events that define phagosome formation and maturation as they generate membrane areas with positive or negative curvature around the forming or maturing phagosome [64, 73].



(adapted Piomelli et al., 2007)

Fig 1.10: Spontaneous curvature mediated by lipids depends on their molecular geometry.

The physical structure of the lipids, whether cylindrical, conical (when the tail is larger) or inverted conical (when the head group is larger) can affect the intrinsic curvature of membranes altering their geometry. Cylindrical shaped lipids produce zero curvature while lipids with head groups that point away from the centre of the arc is said to exhibit a positive curvature. Conversely head groups that point towards the centre of the arc is said to exhibit negative curvature as the bilayer bends around the lipid head group.

1.3.4 Lipid distribution and contribution in phagocytosis

Lipids are not randomly distributed over the membrane. Instead, lipid levels are tightly regulated spatially and temporally within cellular membranes [74]. Different lipid species are also non-randomly distributed in cellular membranes as well as between subcellular organelles and the distribution of lipids in each membrane is unique and specific as shown in **Fig 1.11** [75]. The plasma membrane contains high amounts of sphingolipids, sterols and saturated phospholipids all of which pack at high densities to promote bilayer rigidity and impermeability. On the other hand, the endoplasmic reticulum membrane primarily contains unsaturated phospholipids that make the membrane more fluid to facilitate the incorporation of newly synthesized proteins [76].

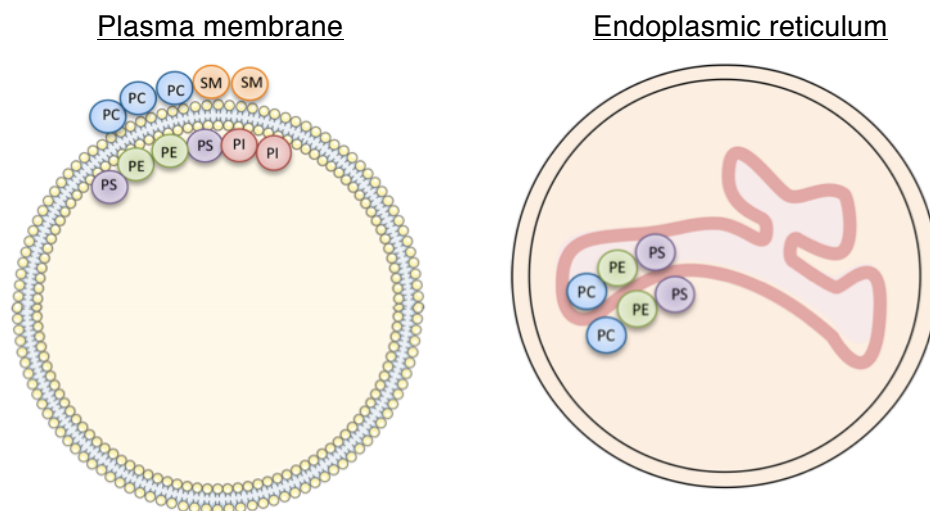


Fig 1.11: Lipids are heterogeneously distributed between membranes and across the membrane bilayer.

The plasma membrane has an asymmetric lipid arrangement while the ER on the other hand is assumed to have a symmetric lipid distribution.

In addition to the heterogeneous distribution of lipids among various organelle membrane compartments, there are also striking differences in the distribution of lipids across the membrane bilayer. For instance, an essential feature of the plasma membrane is the asymmetric distribution of lipids with its outer leaflet (luminal) concentrated in choline-containing lipids such as PC and SM whereas its inner (cytosolic) leaflet is enriched in PE, PS and PI. Cholesterol however, is distributed on both leaflets [60, 67, 77]. The asymmetric distribution of lipids has important functional consequences. For example, PS is exclusively enriched in the inner leaflet of the plasma membrane in healthy cells while in apoptotic cells, PS is externalized to the outer leaflet of the plasma membrane. PS externalization is a result of a calcium induced scramblase (enzymes that promote the translocation of PS to the outer leaflet of the PM) mechanism. The externalized PS serves as a recognition signal for clearance by phagocytic cells [19, 64].

Phosphatidylserine (PS)

PS which makes up 2-10% of the total phospholipid pool, is particularly enriched in the cytoplasmic leaflet of the plasma membrane and in organelles of the endocytic pathway. PS is proposed to confer a negative charge to the inner leaflet and promote the recruitment of positively charged proteins with C2 domains such as PKC isoforms and PI3K to the plasma membrane. Both

enzymes play a role in phagocytosis, which hints at the importance of PS at the phagocytic cup and on phagosomal membranes. In addition Yeung et al., 2009 have shown that the level of PS remains relatively unchanged in maturing phagosomes and its concentration is maintained through ongoing fusion with endosomes and lysosomes. Nevertheless, the function of PS in cellular membranes remains poorly defined [57, 61, 64, 73, 78, 79].

Whereas all lipids are asymmetrically distributed between the two leaflets of the plasma membrane, the ER membrane bilayer displays a symmetric distribution of lipids and primarily contains unsaturated lipids that make the membrane flexible [80].

Phosphatidylcholine (PC)

PC is the most abundant lipid in cells accounting for 45-55% of total lipids. It is the key building block of membrane bilayers as it spontaneously forms a bilayer structure in an aqueous environment. PC is enriched slightly in the outer leaflet of the plasma membrane and has a cylindrical shape. PC is often regarded as a structural component of cell membranes [57]. PC is a precursor for various signaling molecules. For example, PC can be hydrolysed by phospholipase D1 and 2 (PLD) to generate PA. [19]. Iyer *et al.* (2004) generated inactive mutants of PLD1 and PLD2, which individually exhibited partial inhibition (55-65%) on phagosome formation. The combination of these mutants led to almost total abolishment of phagocytosis (91%) suggesting that PLD and by extension PA,

play an important role in the early stages of phagocytosis, namely in particle engulfment [81]. Beyond the role of PC as a structural component of cellular membranes and its role as a substrate for the production of signaling lipids such as PA, very little is known about the function of PC itself [57]

Phosphatidic acid (PA)

In resting cells, PA accounts for 1-2% of cellular lipids. PA has a small head group compared to its fatty acid portion. The accumulation of this cone shape lipid induces negative curvature and has been suggested to facilitate in phagosome sealing and membrane fission. As such, the conversion of PC, which is a cylindrical lipid into PA, would dynamically change the conformation of the membrane. PA may therefore assist in phagosome sealing and fission by accumulating at the tips of extending pseudopods [19, 57]. The production of PA has been observed both at the phagocytic cup and on the extending pseudopods using PA-specific fluorescent probes [82]. However, to date there are no definitive measurements of the PA content of phagosomes and no quantitative attribution of its source [64].

Phosphatidylethanolamine (PE)

PE is the second most abundant lipid and accounts for almost 20% of the total cellular lipids. PE comprises 15-25% of mammalian phospholipids and similar to PC, functions mainly as a structural component of membranes. PE is enriched in

the inner leaflet of the plasma membrane. PE is also found in most subcellular compartments but is enriched in the mitochondria. PE has a relatively small headgroup and so adopts a conical shape inducing negative curvature [57]. PE does not form bilayers by themselves and this property is essential for the functional embedding of membrane proteins and for processes such as membrane fission and fusion [83].

Phosphoinositol (PI)

PI comprises of 10-15% of the cellular lipids. PI is present in various organelles in varying concentration and is more abundant in the inner leaflet of the plasma membrane. PI is unique among all phospholipids because its inositol ring can undergo transient and reversible reactions through kinases and phosphatases at any one of three positions (D3, D4, D5) to yield monophosphoinositides that can be further phosphorylated to yield the bis- and tris-phosphorylated species as shown in **Fig 1.12** [14, 64].

All phosphoinositides (PIP) are localized on the cytosolic leaflet of the plasma membrane and of intracellular organelles. Despite being minor constituents, PIP are key regulators of membrane traffic and most of the known PIP have been identified on forming and/or maturing phagosomes. Using fluorescent probes, the distribution and fate of PIP have been studied in most detail to monitor the dynamics of these lipids during phagocytosis [57, 64, 84].

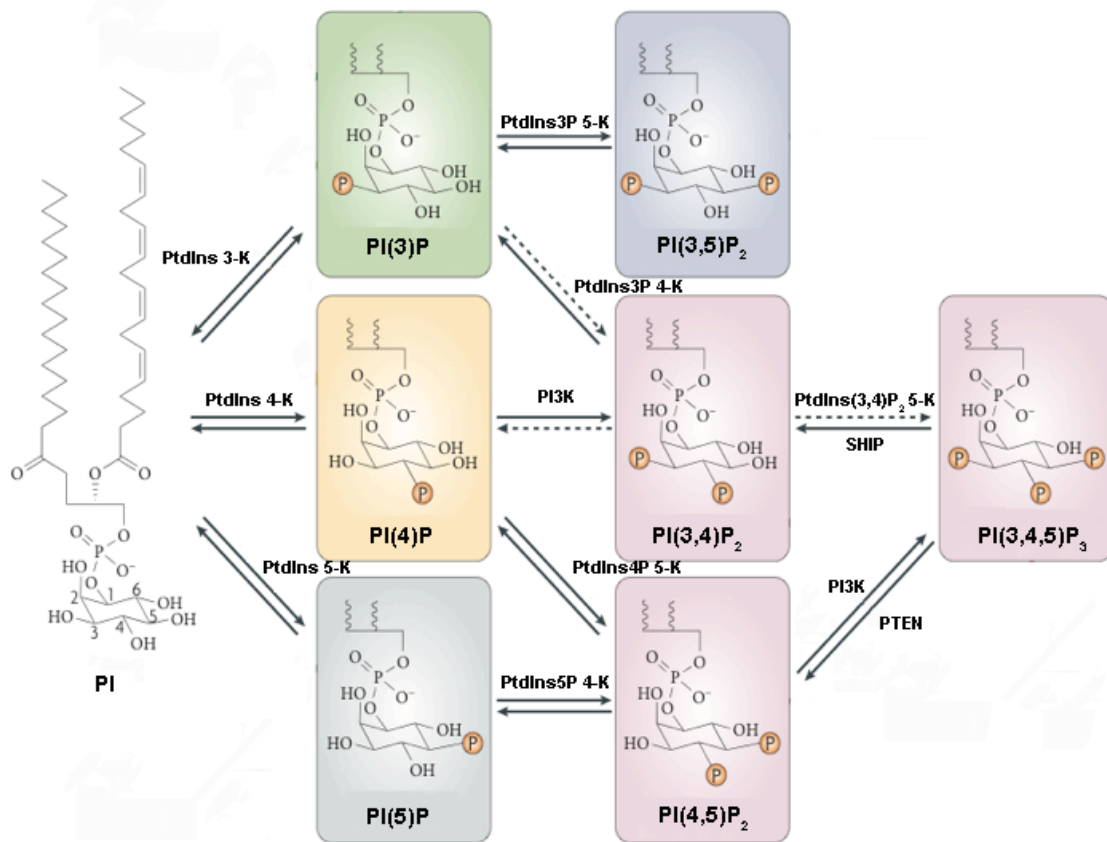
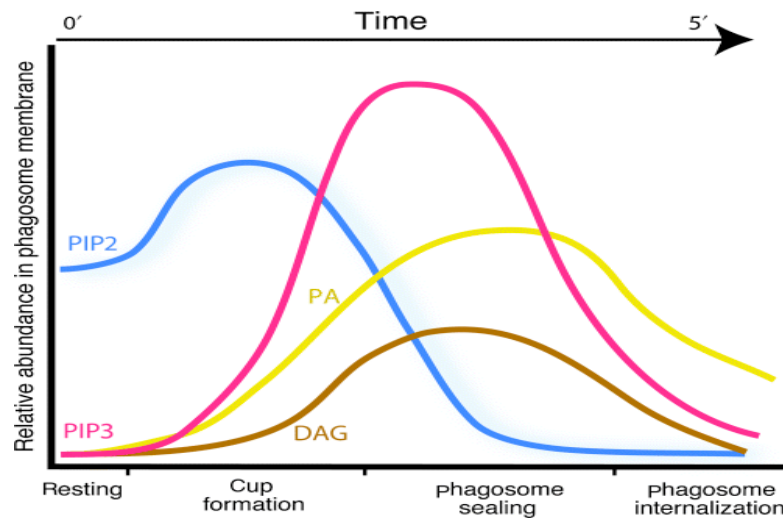


Fig 1.12: PI serves as the basic building block for the synthesis of PIPs.

There are seven phosphoinositides (PIP) species that can be interconverted through the action of kinases or phosphatases. The inositol ring can be phosphorylated at position 3, 4, or 5 to generate seven PIP species. The resulting monophosphoinositides: phosphatidylinositol 3 – phosphate [PI(3)P], phosphatidylinositol 4 – phosphate [PI(4)P], and phosphatidylinositol 5 – phosphate [PI(5)P] can be further phosphorylated to form phosphatidylinositol-4,5-*bis*phosphate [PI(4,5)P₂], phosphatidylinositol-3,5-*bis*phosphate [PI(3,5)P₂] and phosphatidylinositol-4,5-*tris*phosphate [PI(3,4,5)P₃].

PI(4,5)P₂ is constitutively present in the plasma membrane. It transiently accumulates at the phagocytic cup and propagates with pseudopods as they extend to surround the target particle. As pseudopods advance, PI(4,5)P₂ disappears abruptly from the base of the forming phagosome and is completely

undetectable in the sealed phagosome. The disappearance of PI(4,5)P₂ closely parallels the course of actin disassembly to complete particle engulfment [19, 84-86]. The inhibition of PI(4,5)P₂ has been shown to impair phagocytic efficiency [87]. Interestingly, the retention of PI(4,5)P₂ on the plasma membrane has also been observed to abort phagosome formation thereby reducing phagocytosis as its retention prevents actin disassembly which is necessary for the completion of phagosome engulfment [88]. The disappearance of PI(4,5)P₂ is largely due to hydrolysis by phosphoinositide-specific phospholipase C_γ (PLC_γ) to produce diacylglycerol (DAG) and inositol-3,4,5-trisphosphate (IP₃). The inhibition of PLC_γ has been documented to suppress the production of DAG which in turn abolishes phagocytosis [89]. PI(4,5)P₂ is also eliminated by the action of class I phosphatidylinositol 3-kinase (PI3K) which phosphorylates PI(4,5)P₂ to produce PI(3,4,5)P₃. PI(3,4,5)P₃ accumulates selectively in nascent phagosome and its accumulation is confined to the phagocytic cup with little enrichment in other regions of the plasma membrane (**Fig 1.13**). Hence, not only does the lipid composition vary between the two leaflets, but within a given membrane, lipids can be transiently enriched in areas [19, 57].



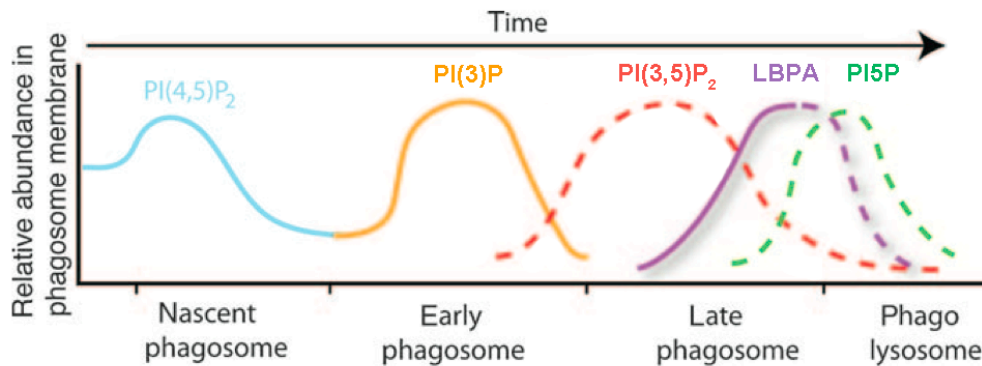
(adapted from Yeung and Grinstein, 2007)

Fig 1.13: Schematic illustration of PIP composition at different stages of a forming phagosome.

The intracellular distribution of PIP can be conveniently studied by transfecting cells with green fluorescent protein tagged PH, PX and FYVE domains that bind to these PIP species. PI(4,5)P₂ accumulates during the phagocytic cup formation. PI(4,5)P₂ disappears from the base of the forming phagosome and is undetectable in the sealed phagosome. PI(4,5)P₂ can be eliminated by either degradation by PLC γ into DAG or IP₃ or phosphorylation to PI(3,4,5)P₃ by PI3K. PI(3,4,5)P₃ is formed at the phagocytic cup and rapidly disappears after the phagosome has been sealed off from the plasma membrane.

PI-3-Phosphate [PI(3)P] which is normally found on early endosomes is also detectable on early phagosomes. PI(3)P is generated by the phosphorylation of PI at the 3 position of the inositol headgroup by class III PI3K, hVps34. It is still unclear how PI(3)P is removed from maturing phagosomes but it has been hypothesized to undergo hydrolysis by the recruitment of SHIP phosphatases or phosphorylation by kinases to PI(3,5)P₂ (**Fig 1.14**) [64]. PI(3)P has been highlighted to be important in phagocytosis as PI3K inhibitors such as

wortmannin and LY294002 have been shown to inhibit the phagocytosis of large particles ($>3 \mu\text{m}$). While phagocytosis of smaller particles ($< 3 \mu\text{m}$) can still proceed in the presence of these inhibitors, phagosome maturation is blocked [19, 57, 84, 90].



(adapted from Yeung et al., 2006)

Fig 1.14: PIP species detected in maturing phagosomes.

A high level of PI(3)P is synthesized at the phagosome membrane immediately after sealing from the plasma membrane and is not present in the late phagosome compartments.

Although, it is clear that PIP play a crucial role in orchestrating phagocytosis in signaling its initiation and contributing to the cytoskeletal and membrane remodeling that underlie engulfment and maturation, the fate of other lipids during phagocytosis remains to be defined [84].

Lysobisphosphatidic acid (LBPA)

Lysobisphosphatidic acid (LBPA) is exclusively found in late endosomes and lysosomes. LBPA seems to be synthesized at the location where it is found. In this respect it differs from other conventional phospholipids which are mostly synthesized in the ER or to a lesser extent in the Golgi, with the exception of PE which is synthesized in the mitochondria [57]. Studies have shown that LBPA controls the expression of cholesterol in late endosomes and that the accumulation of cholesterol decreases the LBPA level [91]. LBPA is an example of an inverted cone-shaped lipid that promotes positive membrane curvature facilitating the formation of invaginations characteristic of the late endosomes. Experiments with pure lipid liposomes have suggested that LBPA is instrumental in the formation of multivesicular structures, which are typical of late endosomes but only if the pH is acidic, as in the case in the phagosomal lumen. LBPA has been detected in maturing phagosomes. However, the contribution of LBPA to phagosome maturation is poorly defined. [57, 64, 92].

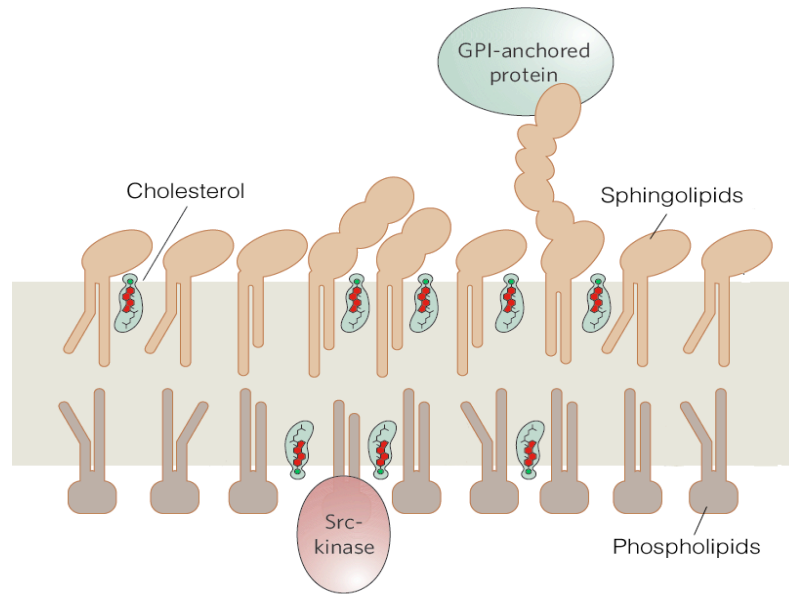
Cholesterol

Cholesterol is enriched in the plasma membrane where it typically accounts for 20-25% of cellular lipids. It is distributed differentially among the different endocytic compartments. Most of the cholesterol content in the endocytic pathway is confined to the early and late endosomes whereas lysosomes are

nearly devoid of cholesterol. Cholesterol has a planar and rigid structure, which provides rigidity to the fluid membrane so as to reduce passive permeability and to increase the mechanical durability of the lipid bilayer [19, 64]. It does so by occupying the spaces between the saturated hydrocarbon chains of the sphingolipids (**Fig 1.15**). However, too much ordering (cohesion and packing) can be detrimental because it slows down the diffusion of membrane proteins [93, 94].

Cholesterol is also believed to be essential for the formation and maintenance of lipid rafts as the disruption of lipid rafts using cholesterol depleting statins or methyl- β -cyclodextrin (M β CD) impairs Fc receptor mediated signaling and phagocytosis [95, 96]. Interestingly, studies have also shown that cholesterol depletion have no effect on the ability of cells to ingest opsonized particles [97]. In addition, Hyunh et al., 2008 reported that excessive cholesterol accumulation impaired phagosome maturation by interfering with fusion with lysosomes, however the early stages of phagosome maturation was unaffected [98].

Cholesterol is a highly mobile lipid that can translocate between membranes very quickly. It preferentially associates with sphingolipids, especially sphingomyelin (SM) to form microdomains known as “lipid rafts” towards which specific proteins have affinity. This conceivably helps to cluster proteins in functional assemblies for diverse processes such as signal transduction and membrane trafficking [93, 94]. These specialized microdomains and their possible role in phagosome formation are discussed in detail below.



(adapted from Maxfield and Tabas, 2005)

Fig 1.15: Cholesterol preferentially partitions into areas with sphingolipids.

The headgroup of sphingolipids and the hydroxyl group of cholesterol stabilize these lipid domains via hydrophilic interactions, whereas the acyl chains of sphingolipids and the sterol ring form hydrophobic interactions. Cholesterol is also much smaller than other lipids so flip – flops between the leaflets of the membrane bilayer can readily occur. Cholesterol can increase the order in membranes through its rigid structure and is able to fill interstitial spaces.

Sphingomyelin (SM)

SM differs from glycerol-containing phospholipids in that it is composed of long and mostly saturated fatty acid tails. These straight, hydrophobic tails allow sphingomyelin to adopt a taller cylindrical shape than PC of the same length and thus pack more tightly, adopting a solid gel phase that can be fluidized by sterols [83].

SM is the most abundant sphingolipid in cellular membranes with 80-90% of SM localized on the outer leaflet of plasma membrane. SM can be hydrolysed by acid sphingomyelinases (ASMase) to generate ceramide. As SM is a major constituent in the outer leaflet of the cell membrane, its capacity as a source for ceramide is enormous. ASMase is an enzyme which is expressed by all cell types and is located principally in secretory vesicles on the outer leaflet of the plasma membrane and in late endosomes and lysosomes. It is activated upon receptor clustering and is translocated from the intracellular stores onto the extracellular leaflet of the cell membrane [19, 99-103].

Ceramide

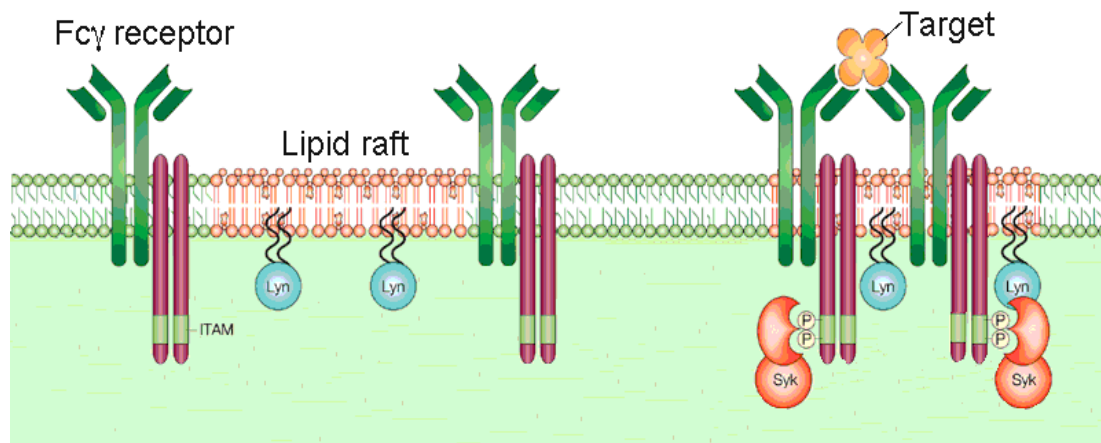
Ceramides have been implicated in a variety of cellular processes, such as infection and apoptosis. Ceramide is highly hydrophobic and as such is confined to the membranes of phagosomes or lysosomes or the extracellular leaflet of the plasma membrane [102]. Ceramide is capable of stabilizing lipid microdomains and may function in a manner analogous to cholesterol [84]. Ceramide molecules have a unique property of fusing membranes thus triggering spontaneous fusion of raft microdomains to form large, ceramide enriched membrane platforms [104]. Ceramide being a cone-shaped lipid will spontaneously form negative curvatures that will lead to membrane invagination and budding [102].

Studies have shown that ceramide is involved in the kinetics of phagosome maturation and its subsequent fusion with endocytic compartments during phagosome maturation. Schramm et al., 2008 reported that ceramide derived from ASMase is crucial for proper phagosome maturation and acquisition of bactericidal properties. Utermohlen et al., 2008 showed that ceramide is required for phago-lysosomal fusion in infected macrophages. In addition, ceramide has also been identified to be an important requirement for the assembly of actin filaments on phagosomes [100, 105].

1.3.5 Lipid rafts: Overview

While the fluid mosaic model proposes that the cell membrane is a homogeneous solution of phospholipids, the membrane raft theory proposes the existence of microdomains randomly distributed on the membrane surface. These are known as “lipid rafts”. Lipid rafts are cholesterol and sphingolipid rich, and compartmentalize the plasma membrane into distinct regions that serves as signaling platforms that can preferentially recruit signaling proteins during receptor stimulation (**Fig 1.16**). The membrane surrounding the rafts is more fluid, as it consists of mostly unsaturated phospholipids and cholesterol while the phospholipids in the lipid rafts tend to be more highly saturated allowing for close packing with sphingolipids. This tight packing of lipids leads to phase separation

responsible for the signature property of lipid rafts to form distinct liquid-ordered phases in the lipid bilayer, dispersed in a liquid-disordered matrix of phospholipids [72, 106]. Lipid rafts harbour glycosylphosphatidylinositol (GPI)-anchored proteins and transmembrane proteins whose activity is controlled by their localization to these rafts. This has led to the consensus that these lipid domains play an important role in the process of signal transduction [76, 107].



(Susan K. Pierce, (2002), *Nature Reviews Immunology*, 96-105)

Fig 1.16: Lipid rafts are microdomains described as floating islands in a sea of phospholipids.

The plasma membrane has also been suggested to be patchy, with segregated portions that are distinct in structure and function that can vary in thickness and composition [108].

1.3.5.1 Rafts in signal transduction

Cells use lipid rafts as signaling platforms that couple events on the outside of the cell with signaling pathways inside the cell. Lipid rafts can modulate signaling events in a variety of ways. A cell surface receptor might reside outside of the raft but can be translocated there upon ligand binding. Translocation of signaling molecules in and out of lipid rafts could then control the ability of cells to respond to various stimuli [109]. Rafts may also contain incomplete signaling pathways that are activated when a receptor or a required molecule is recruited [107].

Within the immune system, it has been shown that many immunoreceptors including Fc γ receptors associate with lipid rafts in response to ligand-induced cross-linking. Binding of a ligand to a receptor located within lipid rafts may initiate compartmentalized signaling within rafts. The segregation of receptors into microdomains would select and concentrate these receptors in a microenvironment that would initiate and allow for enhanced access to particular downstream signaling proteins. Receptor activation within a lipid raft protects the signaling complex from non-raft enzymes such as membrane phosphatases that could otherwise affect the signaling process. Lipid rafts might also be involved in negatively regulating signals by sequestering molecules in an inactive state or may be translocated out of lipid rafts. This allows for efficient and specific signaling in response to stimuli [106, 109-112].

During $Fc\gamma$ receptor phagocytosis, cross-linked receptors are recruited to lipid rafts as Src family kinases e.g. Lyn reside in lipid rafts. These kinases are responsible for the phosphorylation of the ITAM, which is the key initiating event in the signal transduction cascade that leads to phagocytosis [19]. Accordingly, Flotillin-1, a lipid raft protein have also been reported by Garin et al., 2001 to be present on phagosome membranes. This suggests a potential involvement of lipid rafts in the regulation of phagocytosis and/or phagosome maturation.

1.3.5.2 A role for ceramide in lipid rafts

Like the cholesterol-containing rafts, ceramide-rich rafts remain in a highly ordered state. However, cholesterol and ceramides both have small polar headgroups and thus compete for association with rafts because of a limited capacity of raft lipids with large headgroups to accommodate these smaller lipids [113]. Ceramide-enriched membrane domains are not part of a specific signaling pathway but serve as a general mechanism for cellular signaling. Hence, a variety of receptors and stimuli, including $Fc\gamma RII$ trigger the release of ceramide and/or the formation of ceramide rich membrane domains [100, 114, 115].

Numerous studies have demonstrated lipid rafts may not be pre-existing domains but are dynamic membrane regions that can fuse together to form larger rafts or signaling platforms enriched in ceramide [108]. This fusion of small rafts may be

induced in different cell types upon stimulation via many receptors or infection by different pathogens [108, 114].

One of the most important properties of lipid rafts is that they can control numerous protein-protein and lipid-protein interactions at the cell surface. This function is possible because of the capacity of lipid rafts to include or exclude signaling proteins selectively and its ability to coalesce into larger domains. Small rafts in “resting” cells might be important to maintain signaling proteins in the “off” state and stimulation would induce raft clustering, forming specialized domains in which signaling partners could meet and be activated. Since ceramide molecules have the tendency to spontaneously associate with other ceramide-enriched membrane domains, the fusion of ceramide rafts to form larger platforms could simply cluster receptor molecules present in the rafts. However, as many receptors are also outside of these rafts, ceramide could also function to trap these receptor molecules upon activation. Thus, ceramide rich platforms may function primarily to re-organize receptors and signaling molecules in and at the cell membrane to facilitate and amplify signaling processes via a specific receptor [100, 114, 116].

The molecular mechanisms of receptor clustering in general remain to be defined. However, it has been shown that ceramide is essential for clustering of Fc γ RII in lipid rafts and as such, for signal transduction. Studies by Abdel Shakor et al., 2004 showed that ceramide production at the cell surface facilitates Fc γ RIIIa recruitment to lipid rafts.

In addition to the trapping of an activated receptor in rafts, ceramide may also function to stabilize the interaction with the receptor ligand. The clustering of a receptor in a ceramide lipid raft could lead to a change in receptor conformation. This could result in the preferential interaction of the receptor with ceramide or ceramide lipid rafts and might also stabilize the interaction of a receptor with its ligand [100].

1.3.6 Lipidomics: emerging lipid analytics

Lipidomics entails the detailed analysis and global characterization both spatial and temporal, of the structure and function of lipids in cells [117]. As a field, lipidomics has lagged in comparison to the development of genomics and proteomics and our knowledge of the lipidome of most cells remains rudimentary. One of the reasons for the delay in understanding of lipidomics is due to the analytical challenge arising from the high complexity of the large chemically diverse molecular species. Nevertheless, several developments in analytical instrumentation and molecular tools are emerging and have pushed the lipidomic field forward [74, 118].

Optical methods such as the use of fluorescent lipid probes that can be genetically encoded and delivered into cells for live cell imaging has allowed for spatial and temporal imaging in intact cells. This approach is based on the generation of chimeric constructs consisting of a fluorescent protein bound to the

headgroup of the lipid of choice. However, the selection of probes are limited and may not be specific resulting in binding to more than one lipid species. Another limitation of fluorescent probes is that they often do not allow for reliable quantification [74, 85].

Specific antibodies to lipids are rare and such antibodies would be useful tools for research in membrane trafficking. However, the method for the generation of antibodies against lipids is difficult because lipids often display little specific binding due to their hydrophobicity but if successful and proven highly specific, the antibody could be used for clinical applications such as diagnostic or therapeutic purposes [118].

Thin-layer chromatography (TLC) and gas chromatography (GC) have been extensively used for studying most lipid classes with relatively non-specific detection techniques such as the visualization of phosphorus by spray reagents but this technique requires large amounts of lipids to be extracted. This requirement limits the analysis of low abundant lipids. The analyses of fatty acid substituents by GC typically involve the scraping of TLC spots followed by the extraction and derivatization to make the analyte more volatile. This approach destroys the phospholipid structure, compromising the ability to study chemical details of the phospholipids present in the TLC spot [74, 119].

Liquid Chromatography Electrospray Ionisation Mass Spectrometry (LC-ESI-MS) is rapidly becoming a method of choice for profiling complex lipid mixtures. It

provides for high sensitivity, resolution and throughput of a variety of lipid species in different biological matrices. The high resolution aids in the identification of previously uncharacterized lipids and allows for discrimination between lipids with similar mass and chemical structures [118]. The availability of synthetic and pure lipids as internal standards and the scope of lipids that they represent have also improved. This allows for the absolute quantification of the lipid species in moles as opposed to relative fold changes from minute amounts of samples. The precise identification and quantification of the lipid constituents present in a biological sample has established mass spectrometry as the preferred instrumental analytical platform for comprehensive analysis of the lipidome [74].

Overall, developments in technology have revolutionized the lipidomics research offering insights into the astounding range of their biological activities and extend our understanding in lipid-related diseases such as obesity, atherosclerosis and Alzheimer's disease. This knowledge holds great promise for addressing the specific roles of lipid molecular species in cellular function and dysfunction as well as identifying potential biomarkers for establishing preventive or therapeutic treatment [118, 120, 121].

1.4 Objectives and thesis outline

This study aims to address three major questions namely:

1. *The lipid composition of maturing phagosomes*

The roles of lipids in phagosome formation and maturation have not been thoroughly researched. Related research by Grinstein *et al.* utilizes microscopy techniques to study lipid dynamics during phagocytosis. While investigations have elucidated roles for certain classes of lipids in various parts of Fc γ mediated phagocytosis, to date no investigations have yet followed the roles of these lipids through the entire process of phagocytosis. In this project, phagosomes will be isolated by flotation on step sucrose gradients. This yields highly purified phagosomes. The lipidome of phagosomal membranes will be determined using mass spectrometry. Phagosome lipids will be compared to that of the plasma membrane. This will allow us to monitor the relationship of these lipids and Fc receptors; from the plasma membrane to the engulfment and destruction of the opsonized target.

2. *The effect of the presence or absence of Fc γ RIIb^{232I} / Fc γ RIIb^{232T} on lipid composition and its link to autoimmunity?*

Evidence showing that Fc γ RIIb^{232T} loses its inhibitory function through exclusion from lipid rafts leads to hyperactive macrophages and is associated with the pathogenesis of systemic lupus erythematosus. While the relationship between lipid rafts and Fc receptors have been the focus of many projects,

very few studies have been done to look into the roles of lipid rafts in Fc γ receptor mediated phagocytosis. Here, focus is on lipid biology in Fc receptor signaling.

3. Determining the contribution of ceramide lipid rafts for signal transduction and phagosome function

IgG coated latex beads bind to Fc γ Rs on the plasma membrane of phagocytes, which leads to the crosslinking and clustering of numerous Fc γ Rs. After cross-linking, receptors translocate to areas with a specific lipid environment. It has been suggested that these regions on the plasma membrane are enriched in ceramide. Reports by Abdel Shakor et al., 2004 have postulated that cell surface ceramide controls Fc γ RII clustering and phosphorylation in lipid rafts which are important for inducing the phagocytosis of opsonized pathogens. Others have showed the importance of the transmembrane domain of Fc γ Rs for their association with lipid rafts. In line with this thinking, we explored if ceramides can regulate the function of both the activatory and the inhibitory responses by Fc γ RII receptors in the context of phagocytosis.

CHAPTER 2

MATERIALS AND METHODS

2.1 Solutions and Buffers

Deionized water was obtained from a Milli-Q water system (Millipore). The composition of solutions and buffers used are as follows:

2.1.1 Buffers for phagosome preparation

10 x Tris Buffered Saline (TBS): 121.1g of Tris base (Sigma-Aldrich) and 876.6g of sodium chloride (Sigma-Aldrich) were dissolved in 800ml of deionized water. pH was adjusted to 8.0 and the volume made up to 1L with deionized water.

2mM sodium orthovanadate (Na_3VO_4): 3.68mg of Na_3VO_4 (Sigma-Aldrich) was made up to 10ml with deionized water.

Homogenization buffer base: 42.79g of sucrose (Sigma-Aldrich) and 0.102g of imidazole (Sigma) were weighed out and made up to 500ml with 1 x TBS pH 7.4.

Homogenization buffer: 50 μl of 0.5M EDTA (1st Base) and 100 μl of 2mM Na_3VO_4 was made up to 10ml with homogenization buffer base. Protease inhibitors (Roche) were added prior to use.

3mM imidazole, pH 7.4: 2.04mg of imidazole was made up to 100ml with TBS.

Sucrose solutions (w/v): 10, 25, 35, 62g of sucrose were weighed out and made up in 100ml of 3mM imidazole, pH 7.4.

2.1.2 Buffers for plasma membrane isolation

Plasma membrane coating buffer (PMCB): 20ml of 1M MES (Sigma-Aldrich), 140ml of 2M sorbitol (Sigma-Aldrich) and 30ml of 5M NaCl were mixed together and pH adjusted to 5.5 – 6.0 with concentrated NaOH. The volume was made up to 1L with deionized water.

Lysis buffer: 8.51mg imidazole (Sigma-Aldrich) was dissolved in 500 ml of deionized water. Protease inhibitors were added prior to use.

70% (w/v) nycodenz: 100% (w/v) nycodenz (Sigma-Aldrich) was prepared by dissolving 10g nycodenz in lysis buffer to a final volume of 5.5ml. 7ml of 100% (w/v) stock solution was diluted to 10ml with lysis buffer to make 70% (w/v) nycodenz.

1 mg/ml PAA/PMCB: Polyacrylic acid (PAA)(Sigma-Aldrich) was dissolved in PMCB. The solution was pH adjusted with pH paper (Merck) to pH 6.0 – 6.5 with concentrated NaOH.

2.1.3 Buffers for SDS – PAGE and western blotting

1 x RIPA lysis buffer: 5ml of 1M Tris pH 7.4 (1st Base), 10ml of 10%(v/v) Nonidet-P40 (Sigma), 5ml of 5M NaCl, 1ml of 100mM EDTA (1st Base) were made up to 100ml with deionized water. This buffer was supplemented with protease inhibitor and 2mM Na₃VO₄ prior to use.

5 x SDS-PAGE sample loading dye: 2.5ml of 1M Tris HCl pH 6.8 (1st Base), 1g of sodium dodecylsulphate (SDS) (Sigma-Aldrich), 0.5ml of glycerol (Invitrogen),

0.5ml of 14.7M β -mercaptoethanol (Sigma-Aldrich), 1.25ml of 0.5M EDTA (1st Base) and 10mg of bromophenol blue (Sigma-Aldrich) were mixed and made up to a final volume of 50ml with deionized water.

Polyacrylamide resolving lower gel Tris buffer pH 8.8: 91g of Tris base (Sigma-Aldrich) was dissolved in 400ml of deionized water and adjusted to pH 8.8. 20ml of 10% SDS (1st Base) was added and the solution made up to a final volume of 500ml with deionized water.

Polyacrylamide stacking upper gel Tris buffer pH 6.8: 6.05g of Tris base was dissolved in 40ml of deionized water and adjusted to pH 6.8. 4ml of 10% SDS was added and the final volume of the solution was made up to 100ml of deionized water.

10% (w/v) ammonium persulfate (APS): 0.1g APS (Sigma-Aldrich) was dissolved in 1ml deionized water.

SDS/Glycine running buffer: 3.03g of Tris base, 14.04g of glycine (Fisher Scientific) and 1g of SDS were made up to 1L with deionized water.

Transfer buffer: 5.81g of Tris base, 2.93g of glycine and 0.375g of SDS were dissolved in 500ml of deionized water. 200ml of methanol (Merck) was added and the mixture was adjusted to a final volume of 1L with deionized water.

0.2% (v/v) TBS-Tween (TBST): 1 x of TBS was obtained by 1:10 dilution of 10 x TBS. 2ml of Tween 20 (Bio-Rad) was added to make up the final solution.

2.1.4 Buffers for flow cytometry

1% paraformaldehyde (PFA): 5g of PFA (Sigma-Aldrich) was dissolved in 450ml deionized water. The solution was heated to 50°C on a hotplate. When the solution was totally clear, 50ml of 10 x PBS was added. This solution was pH adjusted to 7.2 - 7.4 with concentrated NaOH.

2.1.5 Buffers for confocal microscopy

Methanol:Acetone fixative: 1 part volume of methanol (Merck) was added to 1 part volume of acetone (Merck). The mixture was subsequently stored at -20°C.

Phosphate saline buffer (PBS): 10 x PBS (1st Base) was diluted 1:10 with deionized water. The final solution was adjusted to pH 7.4.

10mM glycine in PBS: 0.751g glycine (Fisher Scientific) was made up in 1 x PBS pH 7.4 to a final volume of 1L.

Permeabilisation Buffer: 5ml of fetal bovine serum (FBS) (Gibco), 25mg of saponin (Sigma-Aldrich) and 0.5ml of 1M HEPES pH 7.4 (Invitrogen) were made up in a final volume with 50ml of 10mM glycine in PBS.

2.1.6 Buffers for mycobacterial infection

20% (v/v) Tween 80: Tween 80 (Applichem) was diluted 1:5 with deionized water.

0.1% (v/v) Triton-X: Triton-X (USB Corporation) was diluted 1:1000 with deionized water.

2.2 Reagents

All solvents used were of high performance liquid chromatography (HPLC) grade. All lipid standards were purchased from Avanti Polar Lipids.

2.2.1 Latex beads

1 μ m Fluoresbrite® Yellow Orange (YO) Carboxylate Microspheres and Polybead® Carboxylate Blue Dyed Microspheres were obtained from Polysciences.

2.2.2 Antibodies

The following antibodies were used: Anti-Rab5 antibody (Cell Signaling Technology), anti-Rab7 antibody (Cell Signaling Technology), anti-lysosomal associated membrane protein (LAMP-1) antibody (Abcam), anti-calnexin antibody (Abcam), anti-58k Golgi antibody (Abcam), anti-flotillin1 antibody (Cell Signaling Technology), anti-actin antibody (Abcam), anti-Na⁺K⁺-ATPase (Cell Signaling Technology), anti-human CD32 (BD Pharmingen) were used at 1:1000 for western blotting and 1:100 for immunofluorescent staining. For western blots, horseradish peroxidase (HRP)-coupled goat anti-mouse or anti-rabbit IgGs (Thermo Scientific) were used at 1:5000 dilution. Anti-human CD64, CD32 and CD16 preconjugated with fluorescent dye Alexa Fluor 488 (BD Pharmingen) were used for flow cytometry.

2.2.3 Plasmids and Cell lines

2.2.3.1 Generation of plasmids

Wild type human Fc γ R11b cDNA was cloned by RT-PCR from primary monocytes and introduced into pLenti6/V5 with the directional TOPO[®] cloning kit (Invitrogen) according to manufacturer's instructions. The primer pair used to clone for Fc γ R11b was:

5' –CACCATGGGAATCCTGTCATTCTTACC – 3' (forward) and

5' – CTAAATACGGTTCTGGTCATCAGGC – 3' (reverse)

The Fc γ R11b^{232T} was generated from wild type via QuickChange II XL site-directed mutagenesis kit (Stratagene) following manufacturer's instructions. The mutagenic primer pair used was:

5' – GTGGCTGTGGTCACTGGGACTGCTGTAGCGGCCATTGTTG – 3'
(forward) and

5' – CAACAATGGCCGCTACAGCAGTCCCAGTGACCACAGCCA – 3' (reverse)

SMPD1-EGFP in a pLenti6/V5 vector was purchased from Genescript. Stbl3 E.coli strains were used for the amplification of all pLenti6/V5 lentiviral plasmids.

Plasmids were purified using the EndoFree Plasmid Maxiprep kit (Qiagen) following manufacturer's instructions. Plasmid concentrations were quantified using the Nanodrop ND-1000 spectrophotometer (Biofrontier).

2.2.3.2 Generation of stable knock-in cell lines

Fc γ RIIb^{232I} and Fc γ RIIb^{232T} were stably transfected into U937 cells using Superfect (Qiagen) according to manufacturer's instructions. The cells were subjected to blasticidin (Invitrogen) selection.

SMPD-1 was transfected into Fc γ RIIb stable cells by Superfect (Qiagen) according to manufacturer's instructions. Cells were selected for GFP expression using MoFlow (Beckman Coulter).

Lentiviral shRNA particles for SMPD1 were purchased from Sigma-Aldrich and transfected into Fc γ RIIb U937 cells. The cells were selected with puromycin (Sigma-Aldrich).

2.2.3.3 RT-PCR for expression levels Fc γ RIIb

Isolation of RNA from cells

Approximately 10×10^6 cells were used for each cell type. RNA was isolated from the cells using the High Pure RNA Isolation kit (Roche) following manufacturer's instructions. Briefly, the cells were resuspended in 200 μ l PBS and 400 μ l of the supplied lysis buffer. The cells were vortexed and the mixture was loaded onto the supplied High Pure filter tube. These tubes were centrifuged and its flow

through discarded. 10 μ l of DNase I diluted in 90 μ l DNase incubation buffer was added to the column. The column was washed with 500 μ l of wash buffer I followed by 500 μ l of wash buffer II. This was followed by the addition of another 200 μ l wash buffer II and the extracted RNA was eluted out from the column in 50 μ l elution buffer.

cDNA synthesis from total RNA

Total RNA was converted into first strand cDNA by using SuperScript III First-Strand Synthesis System for RT-PCR (Invitrogen) according to manufacturer's instructions. Briefly, 5-10 μ g of total RNA was mixed with oligo dT₂₀ (1 μ l, 50 μ M) and dNTP (1 μ l, 10mM). DEPC treated water was added to make up to a final volume of 10 μ l. The samples were incubated for 10 min at 70°C to allow for primer hybridization and chilled on ice for 1 min. 10 μ l of reaction mixture containing 10 x reaction buffer (2 μ l), 25 mM MgCl₂ (4 μ l), 0.1 M DTT (2 μ l), 40 U/ μ l RNase out (1 μ l) and SuperScript III reverse transcriptase (1 μ l) were added to each sample tube. The contents of the tubes were mixed and incubated for 2 min at 42°C then for 50 min at 50°C. The samples were then incubated for 5 min at 85°C to terminate cDNA synthesis. RNase H (1 μ l) was added to remove RNA followed by incubation of the tubes for 20 min at 37°C. The cDNA was stored at -20°C.

PCR amplification of cDNA

2 μ l of reverse transcribed cDNA was used for amplification with specific primer pairs for Fc γ R1Ib, our transcript of interest and β -actin was used as an internal control to ensure equivalent amounts of RNA from the different cell lines.

The primer pair used for Fc γ R1Ib was:

5' –CACCATGGGAATCCTGTCATTCTTACC – 3' (forward) and

5' – CTAAATACGGTTCTGGTCATCAGGC – 3' (reverse)

The primer pair used for actin loading control was:

5' – GCTCCGGCATGTGCAA – 3' (forward) and

5' – AGGATCTTCATGAGGTAGT – 3' (reverse)

Cycling conditions were:

Initial denaturation	95°C	10 s	
Denaturation	95°C	30 s	} 34 cycles
Annealing	60°C	30 s	
Extension	72°C	60 s	
Final extension	72°C	7 min	

Storage 4°C hold

The PCR products were loaded onto a 1% agarose gel and ran at 100 V. The gel was stained with ethidium bromide. PCR fragments were visualized using the ChemiDoc imaging system (Bio-Rad)

2.2.3.4 Analysis of surface Fc γ Receptors on U937 cells

1 X 10⁶ cells were resuspended in 50 μ l of PBS. 1 μ l of monoclonal antibody directed against Fc γ RI, Fc γ RII or Fc γ RIII (BD Pharmingen) or the appropriate isotype control was added to the cells and incubated in the dark for 1 h at 4°C. The cells were washed with PBS to wash off the excess antibodies and resuspended in 50 μ l of PBS. 1 μ l of goat anti-mouse (F'ab)₂ secondary antibody pre-conjugated with Alexa Fluor 488 was then added to the tubes. The tubes were further incubated for 30 min at 4°C in the dark. Excess secondary antibodies were washed off and the cells were resuspended and fixed with 500 μ l of 1% PFA before being acquired by the Dako Cyan flow cytometer with Summit software (Beckman Coulter).

2.2.3.5 Intracellular Fc γ RIIb quantification

Cells were permeabilized and fixed with BD Cytotfix/Cytoperm solution (BD Biosciences) according to the manufacturer's instructions. Cells were resuspended in 50 μ l of BD Perm/Wash solution (BD Biosciences) and labeled for 30 min at 4°C with 1 μ l of primary monoclonal antibody directed against Fc γ RIIb (Abcam). Excess antibody was washed off and 1 μ l of goat anti-mouse (F'ab)₂

secondary antibody preconjugated with Alexa Fluor 488 was added. Cells were incubated for 15 min at 4°C. Cells were washed and resuspended in 1 % PFA followed by flow cytometry acquisition by Dako Cyan.

2.3 Cell culture

2.3.1 Cell culture and maintenance

Wild type U937 cells were obtained from the American Type Culture Collection (ATCC). All cell lines were cultured in suspension in RPMI 1640 media with L-glutamine (HyClone) supplemented with 10% fetal bovine serum (FBS) (Gibco) and 1% penicillin-streptomycin (Gibco). The cells were grown at 37°C under a humidified 5% CO₂ atmosphere.

2.3.2 Differentiation of U937 monocytes into macrophages

50 x 10⁶ cells were plated in 500 cm² tissue culture plates and stimulated with 50ng/ml granulocyte macrophage colony stimulating factor (GM-CSF) (PeproTech Inc.) and 5ng/ml phorbol 12-myristate 13-acetate (PMA) (Sigma-Aldrich) in IMDM with L-glutamine and 25mM HEPES (PAA Laboratories) media supplemented with 10% FBS and 1% penicillin-streptomycin. Cells were allowed to adhere for 48 h at 37°C. The media was removed and fresh complete RPMI media was added. The cells were further incubated for 24 h at 37°C in a 5% CO₂ atmosphere. For all experiments, cells were differentiated as described prior to analyses even if not explicitly stated.

2.4 Detection of Protein kinase C activity assay

The assay of PepTag® non-radioactive detection of protein kinase C (PKC) (Promega) was performed accordingly to manufacturer's instructions. Briefly, 1×10^7 U937 differentiated macrophages were washed with cold 1 x PBS and resuspended in 0.5 ml of cold PKC extraction buffer and homogenized. After centrifugation for 5 min at 14,000g, the supernatants were purified on 1 ml column of DEAE cellulose pre-equilibrated in PKC extraction buffer and the PKC-containing fractions were eluted using 5 ml of PKC extraction buffer containing 200 mM NaCl. Samples were incubated at 30°C for 30 min with the fluorescent peptide substrate that is highly specific for PKC. The reactions were stopped at 95 °C for 10 min. The phosphorylated and non-phosphorylated forms of the PepTag® peptide were separated in a 0.8% agarose gel and photographed on a transilluminator. The positive control reaction contained 10 ng of PKC.

2.5 Preparation of plasma membrane isolates

Plasma membrane fractions were purified using cationic colloidal silica beads which was kindly supplied by Donna Beer Stolz from University of Pittsburgh School of Medicine. At least 50×10^6 cells were typically used for each experiment. Briefly, all buffers were pre-chilled and the experiment was performed at 4°C. Adherent U937 differentiated cells were detached from culture plates using a cell scraper. The cells were washed with 1 x PBS and resuspended in 10ml PMCB. The cell suspension was added dropwise to 5ml of

1% colloidal silica in PMCB. Excess unbound cationic silica beads were removed by washing the cells three times with 30ml of PMCB and centrifugation was carried out at 300 x g for 3 min at 4°C. After the third wash, the cells now bounded with the cationic silica beads were resuspended in 3 ml of PMCB. The cells were added dropwise into 5ml of 1mg/ml polyacrylic acid. The cells were washed twice with 20ml PMCB to remove the excess polyacrylic acid. The cells were then incubated in a lysis buffer supplemented with protease inhibitors for 30 min at 4°C. The cell suspension was then lysed using 20-30 strokes of a Dounce homogenizer. The cell lysate was centrifuged at 900 x g for 10 min at 4°C to remove internal membranes that were released. The pellet containing the nuclei and the silica bound plasma membrane fragments was resuspended in lysis buffer and diluted with an equal volume of 100% Nycodenz before being layered on top of a 10ml 70% Nycodenz solution. The gradient was centrifuged at 20,000 x g for 30 min using a swinging bucket rotor P40ST (Hitachi-Koki). The purified plasma membrane pellet which appeared glassy was washed three times with lysis buffer at 20,000 x g and subjected to mass spectrometry analysis and western blotting. Protein concentrations were determined using Bradford Protein Assay (Bio-Rad).

2.6 Assessment of phagocytosis and phagosome maturation

2.6.1 Generation of IgG opsonized latex beads

IgG coated latex beads were prepared by using 1 μ m carboxylate microspheres. Beads were covalently bound to BSA (Sigma) by using the PolyLink protein

coupling kit (Polysciences) according to manufacturer's instructions. Briefly, microparticles were washed and resuspended with coupling buffer. EDAC solution was added to the bead suspension. BSA was then added and the mixture incubated with end-to-end mixing at room temperature for 1 h. The tubes were centrifuged at 1000 x g for 10 min. The BSA coated latex beads were then opsonized with rabbit anti-BSA (Sigma-Aldrich) for 15 min at 37°C.

2.6.2 Phagosome Formation and Isolation

Phagosomes were formed by the internalization of IgG opsonized latex beads. Opsonized beads were diluted in cell culture media. Opsonized beads were added to the differentiated U937 cells and uptake was synchronized by incubation of beads with the cells for 2 h at 4°C. Unbound beads were washed off with 1% BSA in PBS. Pre-warmed media was immediately added. Cells with the surface bound beads were incubated for 5min, 45min or 105min at 37°C in a CO₂ incubator to induce phagocytosis. Phagocytosis was stopped by the addition of ice cold PBS and the cells were washed extensively to remove any non-internalized beads. Isolation of phagosomes was performed using a method described by Desjardins et al. 1994. Briefly, cells were gently scraped and spun down at 200 x g for 5 min at 4°C. The cell pellet was washed in 1ml of homogenization buffer containing protease inhibitors. Cells were cracked open by 20 strokes of a tight fitting Dounce homogenizer. The homogenate was centrifuged in a 15ml Falcon tube at 350 x g for 5 min to remove unbroken cells and nucleus. The supernatant was collected and mixed with a 62% (w/v) sucrose

solution to bring it to a final concentration of 42% sucrose. Phagosomes were then isolated on step sucrose gradients in a 14 ml polyallomer gradient tube (Beckman) in the following order (from bottom): a cushion of 1 ml 62% sucrose, the phagosome sample at 42% sucrose (2ml), 2ml of 35% sucrose, 2ml of 25% sucrose and 2ml of 10 % sucrose. The samples were centrifuged at 100 000 x g for 60 min at 4°C. After centrifugation, phagosomes were recovered from a single band at the 10%-25% sucrose interface. Phagosomes were then resuspended in 10ml cold PBS and centrifuged at 15 000 x g for 15 min at 4°C. The phagosome pellet was resuspended in an appropriate buffer for further analyses.

2.6.3 Phagosome quantitation

Phagosome samples from different preparations and time points were quantified by measuring absorbance at 600_{OD} nm. The measure of turbidity of the various phagosome samples allows for the normalization of equivalent amounts of phagosomes.

2.6.4 Western blot analysis

SDS polyacrylamide gel electrophoresis and protein transfer

Proteins from phagosome or plasma membrane samples were resolved with SDS-PAGE using the Biorad Mini-PROTEAN gel electrophoresis system. Phagosome samples were quantified by measuring light scattering at 600 nm as described to ensure equal loading of protein while plasma membrane samples were quantified by Bradford assay. Samples were solubilized in RIPA buffer

supplemented with protease inhibitors. Samples were denatured by the addition of 1 x sample buffer and heated at 95°C for 5 min. Samples were loaded onto a 10 % SDS polyacrylamide resolving gel with a 4% polyacrylamide stacking gel. Electrophoresis was carried out at a constant current of 15 mA in 1 x running buffer. A protein standard ladder (Invitrogen) was loaded to indicate band size. Following electrophoresis, the gels were either stained using a silver stain kit (Bio-Rad) or proteins were transferred onto methanol activated polyvinylidene fluoride (PVDF) membranes (Millipore) using a semi – dry transfer system (Bio-Rad) with 1 x transfer buffer at a constant current of 40 mA for 2 hr.

Immunoblotting

Following protein transfer, PVDF membranes were blocked by drying. Membranes were incubated with primary antibodies prepared in 5% (w/v) BSA in 0.2% (v/v) TBST solution overnight at 4°C with gentle shaking. Membranes were washed 3 x with 0.2 % (v/v) TBST solution for 5 min each time. Secondary HRP conjugated antibodies (Thermo Scientific) were prepared in TBST with 5% BSA. Incubations with secondary antibodies were carried out for 1 h at room temperature with gentle shaking. Membranes then washed three times with 0.2% TBST solution for 15 min each. Membranes were developed with the Western lightning enhanced chemiluminescence substrate reagent (PerkinElmer) and exposed to X-ray films (Thermo Scientific) before being imaged in an automated developer.

2.6.5 Flow cytometry analysis

For all flow cytometry analysis, data was acquired with the Dako Cyan flow cytometer and subsequently analyzed using the FlowJo software (Treestar).

2.6.5.1 Dynamics of uptake of various IgG immune complexes

Uptake of latex beads by Fc receptors was performed by seeding cells onto a 6 well plate. BSA coated latex beads were conjugated to anti-mouse (Sigma) or rabbit (Sigma) BSA as described. Phagocytosis experiments performed as described, and followed for 45 min at 37°C. Cells were scraped, collected and fixed with 1% PFA for flow cytometry analysis.

2.6.5.2 Assessment of phagocytic index

Phagocytic index was evaluated by the incubation of U937 differentiated cells with IgG-opsonized fluorescent latex beads. Phagocytosis was performed as described. After the desired time point, cells were scraped, collected and washed with PBS. The resulting cell pellet containing the latex bead phagosomes was resuspended in 500µl 1% PFA for flow cytometry analysis.

2.6.5.3 Measurement of ROS generated by maturing phagosomes

1×10^6 cells were differentiated into macrophages in a 6 well plate and phagocytosis was performed as described. After the uptake of IgG coated latex beads into the cells, the cells were scraped and washed with PBS. Intracellular ROS generation was evaluated by the addition and 30 min incubation of 100µM dihydrorhodamine 123 (Invitrogen), a fluorogenic substrate. This probe is non-

fluorescent but exhibits a green fluorescence when oxidized in the presence of reactive oxygen intermediates or species. After incubation, cells were washed and fixed with 1 % PFA. The amount of fluorescence was quantified via flow cytometry.

2.6.5.4 Determination of phagosomal pH

IgG latex beads were labeled with pHrodo™, succinimidyl ester (Invitrogen) according to manufacturer's instructions. pHrodo™ is a dye that is non-fluorescent at neutral pH and fluoresces red in acidic environments (e.g., phagolysosomes). Briefly, 500µl of latex bead suspension was resuspended in 100mM sodium bicarbonate buffer and labeled with a final concentration of 1mM pHrodo™ dye in 1ml reaction volume. Labelling was carried out at room temperature for 45min in the dark. Latex beads were washed with the provided wash buffer to remove any unincorporated dye. The beads were then washed with 100% methanol and finally resuspended in prewarmed RPMI media and vortexed for 30s. 1×10^6 U937 macrophages were incubated with the pHrodo™ labelled beads for 1h at 4°C to synchronise latex beads uptake and phagosome maturation. Unbound latex beads were discarded and the cells were flooded with prewarmed RPMI media and incubated at 37°C for 5 min, 45 min or 105 min. Thereafter, cells were scraped and pHrodo™ fluorescence of the macrophages was assessed by flow cytometry.

2.6.5.5 Intracellular calcium measurements

Cells were resuspended in 1ml of RPMI supplemented with 2% fetal calf serum and 25mM HEPES. Cells were incubated with 1.5 μ M Indo-1 AM (Invitrogen), a calcium sensitive dye for 45 min at 37°C. The cells were washed and resuspended before acquisition by flow cytometry by Aria II. Live-gated cells were acquired for 15 sec for baseline fluorescence, followed by a 3 min acquisition after IgG coated beads were added. An addition of final concentration of 1 μ g/ml calcimycin (Invitrogen) was used as a positive control.

2.7 Confocal Microscopy

Preparation of glass coverslips

Glass coverslips were handled using a watchmaker forceps. Coverslips were cleaned by dipping in deionized water followed by 100% ethanol and sterilized by flaming off residual ethanol.

Preparation of samples

Cells were stimulated and differentiated into macrophages directly on glass coverslips in 24 well flat-bottom plates. IgG fluorescent latex beads were added to the cells and phagocytosis was synchronized by centrifugation of the 24 well plate at 350 x g for 5 min at 4°C. Plates were incubated at 37° with various time points to stimulate phagosome maturation. Subsequently, coverslips were transferred to a new 24 well plate and fixed overnight in 1 ml methanol:acetone

(1:1) mix at -20°C.

Immunofluorescence staining

Fixed coverslips were washed four times with 2ml of 10mM Glycine PBS solution to remove all traces of the fixative. The coverslips were then incubated in a humidified chamber with 50µl permeabilization solution containing primary antibodies at the manufacturer's recommended dilutions for 2 h at room temperature. After primary incubation, the coverslips were washed four times as above. Secondary F(ab')₂ antibodies pre-conjugated with Alexa Fluor dyes (Molecular Probes) were prepared in 50µl permeabilization solution and incubated with the coverslips in the dark for 1h at room temperature in a humidified chamber. When required, 0.5µl DAPI (Invitrogen) was added during secondary staining procedure. The coverslips were washed four times with 10mM Glycine PBS solution. Each coverslip was briefly dipped into a beaker of deionized water before being mounted onto microscope slides using ProLong® Gold Antifade (Invitrogen) mounting solution. The microscope slides were then stored horizontally at 4°C. Colourless nail varnish was used to adhere the coverslips onto the microscope slides to prevent the coverslips from moving in the course of image acquisition.

Image acquisition using confocal microscope

All confocal images were acquired using a Leica SP5 confocal microscope with

the accompanying LAS AF software.

2.8 Mycobacteria infection assays

2.8.1 Culture of Mycobacteria

M. Bovis BCG and *M. Bovis BCG* with green fluorescent protein (GFP) (a generous gift from Sylvie Alonso, National University of Singapore) and were cultured to mid log phase in Middlebrook 7H9 (Difco) supplemented with 10% OADC enrichment (Becton Dickinson and Co.), 0.2% Tween 80 (Applichem) and 0.1% glycerol (Invitrogen).

Mycobacterial cultures were adjusted to density of 1.0 at OD 600nm and aliquots were stored at -80°C for future use. Representative vials were thawed and plated on Middlebrook 7H11 agar (Difco) supplemented with 10% OADC to determine the number of colony forming units (CFU). Prior to use, mycobacterial aliquots were thawed and diluted in cell culture medium and briefly sonicated to ensure single cell suspension of mycobacteria.

2.8.2 BCG infection and survival assays by U937 macrophages

Cells were differentiated into macrophages in a 24-well format at a density of 5×10^4 cells per well. The assay was performed in quadruplicate for each data time-point. Prior to infection, the BCG innocuum was mildly sonicated. The BCG was opsonized with 15µg of 2F12 antibody (a gift from Brandon Hanson, DSO laboratories) for 15 min at 37°C. Media was removed from all wells and 500µl serum-free RPMI were added. Cells were infected with BCG at multiplicity of

infection (MOI) of 2 bacteria per cell. After 1 h of infection at 37°C, extracellular mycobacteria were removed by washing with 1 x PBS, and 1ml of RPMI media supplemented with 10% FCS was added to each well not due for lysis.

The number of viable intracellular bacteria was determined by lysing the macrophages with 500µl of H₂O containing 0.1% Triton X-100 at 0,1,3,4,7 days postinfection. The lysate was serial diluted in PBS and plated on 7H11 (Becton Dickinson and Co.) quadrant plates. Colony forming units were enumerated after 18 days of incubation at 37°C.

2.8.3 Bioplex Cytokine Array

Macrophage differentiated cells were infected with BCG at a MOI of 10 bacteria per cell in IMDM supplemented with 10% FBS. Prior to infection, BCG were mildly sonicated for 30 sec to disrupt aggregates. The infected cells were incubated at 37°C with 5% CO₂ for 24 h and 48 h. At the end of the incubation time point, culture supernatant was harvested and filtered through a 0.22µm filter. The supernatant was kept at -20°C until use for cytokine array analysis.

Analysis of the cytokines secreted by the cells in the next 24 h and 48h following the BCG infection was measured with either a 10-plex or 17-plex Human cytokine array (Bio-Rad) following instructions supplied with the kit. Cytokines measured for the 10-plex assay were: IL-1β, IL-2, IL-6, IL-8, IL-10, G-CSF, INF-γ, MIP-1α, MIP-1β, TNF-α. The cytokines measured were for the 17-plex assay were: IL-1β, IL-2, IL-4, IL-5, IL-6, IL-7, IL-8, IL-10, IL-12, IL-13, IL-17, G-CSF, GM-CSF, INF-γ,

MCP-1, MIP-1 β , TNF- α . Each sample was performed in duplicate. Cytokine levels were determined using a Bio-Plex array reader using the BioPlex Manager 5.0 platform (BioRad). Cytokine levels for infected samples were normalized against the corresponding basal levels in uninfected controls.

2.9 Lipid Analysis

2.9.1 Extraction of lipids from samples

Lipids were extracted from 40 OD_{600 nm} equivalents of phagosomes or from plasma membrane isolated from 50 x 10⁶ cells. Lipid extractions were performed according to the method of Bligh and Dyer. All buffers and reagents were pre-chilled in an ice-bath. Samples were washed and re-suspended in 50 μ l PBS. 600 μ l of chloroform:methanol (1:2) mixture were added to the samples and the mixture was vortexed vigorously three times for 1 min with a 5 min interval in between. Next, 300 μ l chloroform and 200 μ l 1M KCl was added to the tube and the mixture was again vortexed, three times for 30 s with intervals of 1 min in between. The mixture was then centrifuged for 2 min at 9,000 rpm to separate the phases. The lower organic layer was transferred to a clean microcentrifuge tube and the top aqueous phase re extracted with 300 μ l chloroform. The second organic phase extraction was combined with the first extraction and samples were dried under a gentle stream of N₂ gas.

2.9.2 Lipid fingerprinting by mass spectrometry

1,2-dimyristoyl-glycero-3-phosphocholine, 1,2-dimyristoyl-glycero-3-phosphoethanolamine, 1,2-dimyristoyl-glycero-3-phosphoserine, PA-17:0/17:0, PG-4:0/14:0, d31-PI-18:1/16:0, N-heptadecanoyl-Derythrosphingosine (C17 Cer), C12-SM and d6-cholesterol were spiked into samples as internal standards. The total lipid extracts were dissolved in a chloroform:methanol (1:1, vol/vol) mix. 10 μ l of sample was injected for analysis via an autosampler. Samples were analyzed using an Agilent 1200 HPLC system coupled with a 3200 QTrap (Applied Biosystems). Phospholipids were analyzed using electrospray ionization. Separation of individual lipid classes of phospholipids by normal phase HPLC was carried out using a Phenomenex Luna 3 μ silica column (inner diameter 150 \times 2.0 mm) with the following conditions: mobile phase A (chloroform: methanol: ammonium hydroxide, 89.5: 10: 0.5 [vol/vol/vol]), B (chloroform: methanol: ammonium hydroxide: water, 55: 39: 0.5: 5.5 [vol/vol/vol/vol]); flow rate of 300 μ l/min; 5% B for 3 min, then linearly changed to 30% B over 24 min and maintained for 5 min, and then linearly changed to 70% B over 5 min and maintained for 7 min. Then, the gradient was changed back to the original ratio over 5 min and maintained for 6 min for column re-equilibration.

Cholesterol was analyzed by reverse phase HPLC-atmospheric spray chemical ionization-MS. Separation was carried out on an Agilent Zorbax Eclipse XDB-C18 column (inner diameter 4.6 \times 150 mm) using an isocratic mobile phase chloroform, methanol, 0.1 M ammonium acetate (100: 100: 4 [vol/vol/vol]) at a

flow rate of 250 $\mu\text{l}/\text{min}$.

Quantification of individual molecular species was carried out using multiple reaction monitoring (MRM). The m/z transitions, declustering potential and collision energy used were optimized using the Quantitative Optimization function available for the Analyst 1.4.1 software (**Appendix 1**). The instrument was calibrated using polypropyleneglycol standards provided by the manufacturer. Lipid levels for each sample were calculated by summing up the signal intensities obtained for each individual lipid species measured by both the LC-MS methodologies, and then normalized to the appropriate internal standard.

2.10 Statistical Analysis

All the statistical analyses were performed with the GraphPad Prism software version 5 (GraphPad Software Inc.) Unless indicated, data are expressed as mean \pm SEM, from at least three independent experiments (n). The statistical significance of the mean difference was determined by students t test or one-way ANOVA. The asterisks indicate statistical significance: * $p < 0.05$; ** $p < 0.01$; *** $p < 0.001$.

CHAPTER 3

RESULTS I: GENERATION OF CELL LINES, REAGENTS AND MODEL SYSTEMS FOR STUDYING Fc γ RECEPTOR MEDIATED PHAGOCYTOSIS

3.1 Introduction

Fc γ RIIb is important for negatively regulating the activatory Fc receptors as a feedback mechanism to control phagocytosis allowing for optimal clearance and destruction of opsonized pathogens. Failure to regulate the activatory signals can result in hyperactive phagocytosis that will lead to autoimmunity and excessive inflammation [122].

As mentioned in the Introduction 1.2.2, research on Fc receptor polymorphisms identified a role for Fc receptors and autoimmunity [21, 22, 32]. The single amino acid polymorphism from isoleucine (I) to threonine (T) in the Fc γ RIIb region at position 232 of the transmembrane domain results in the loss of function of the inhibitory receptor and has been linked to autoimmune diseases such as systemic lupus erythematosus (SLE) [34, 40, 49-51].

To investigate the effect of Fc γ RIIb^{232I} (wild-type Fc γ RIIb) and Fc γ RIIb^{232T} (polymorphic form of Fc γ RIIb) on phagocytosis, we used a human monocytic cell line U937 that does not naturally express Fc γ RIIb [123] to generate stable lentiviral-based transfectants that expressed either the wild-type or the polymorphic variant. The isoleucine to threonine substitution was achieved by performing site directed mutagenesis as described in materials and methods.

Latex beads have been widely used for the study of phagocytosis [124-126]. For our experiments, we coated latex beads with IgG, thereby driving internalization via Fc γ receptors. With this system, we allowed U937 cells to take up these IgG

latex beads and isolated the latex bead phagosomes over time on step sucrose gradients. The isolation of phagosomes that is free from other host cell organelles is of utmost importance to allow for further fine biochemical analyses.

3.2 Characterization of Fc γ receptors on U937 cells

The U937 human monocytic cell line was used to dissect the impact of Fc γ RIIb and its non-functional counterpart Fc γ RII^{232T} on phagocytosis. The absence of Fc γ RIIb on U937 cells allowed for manipulation and expression of these inhibitory receptors. U937 were stably transduced with wild-type, Fc γ RII^{232I} or the polymorphic Fc γ RII^{232T}. These cell lines will permit the analysis of the contribution of these inhibitory Fc γ receptors on studies impacting phagocytosis.

The first thing we set out to do was to analyse surface Fc receptors present on U937 cells. Surface staining was performed as described and cells were analyzed by flow cytometry. The flow cytometric analysis of wild-type U937 cells indicated the presence of Fc γ RI and Fc γ RII but not Fc γ RIII on the cell surface. While Fc γ RI expression remained similar across all three cell types, there were marked increases in Fc γ RII expression in the transduced U937 cell lines compared to wild-type (**Fig 3.1**). As Fc γ RII is present as two isoforms, the activatory Fc γ RIIIa and the inhibitory Fc γ RIIIb [29], this suggests that the commercially available antibody against Fc γ RIIIb is not able to differentiate between Fc γ RIIIa and Fc γ RIIIb due to the similarities in the extracellular domains of these receptors.

Intracellular flow cytometry was performed to test for the total expression levels of Fc γ RII (Fc γ RIIa and Fc γ RIIb) in the transduced U937 cells. Our results indicate that the total level of Fc γ RII is similar in both transduced cell lines (**Fig 3.2**).

As commercially available antibodies do not distinguish between the wild type and the polymorphic form of Fc γ RIIb, RT-PCR was performed to specifically confirm the expression of Fc γ RIIb receptors in the transduced cell lines. The results showed that Fc γ RIIb was not expressed on wild type U937 cells but is expressed on both the U937 Fc γ RIIb transfectants with equivalent levels (**Fig 3.3**). We have confirmed equivalent expression of Fc γ RIIb mRNA and protein transcripts in both Fc γ RIIb^{232I} and Fc γ RIIb^{232T} transduced cell lines. More importantly, surface expressions of these two variants were also equivalent. This will allow direct scrutinization of the impact of Fc γ RIIb^{232T} on phagocytosis as compared to Fc γ RIIb^{232I}.

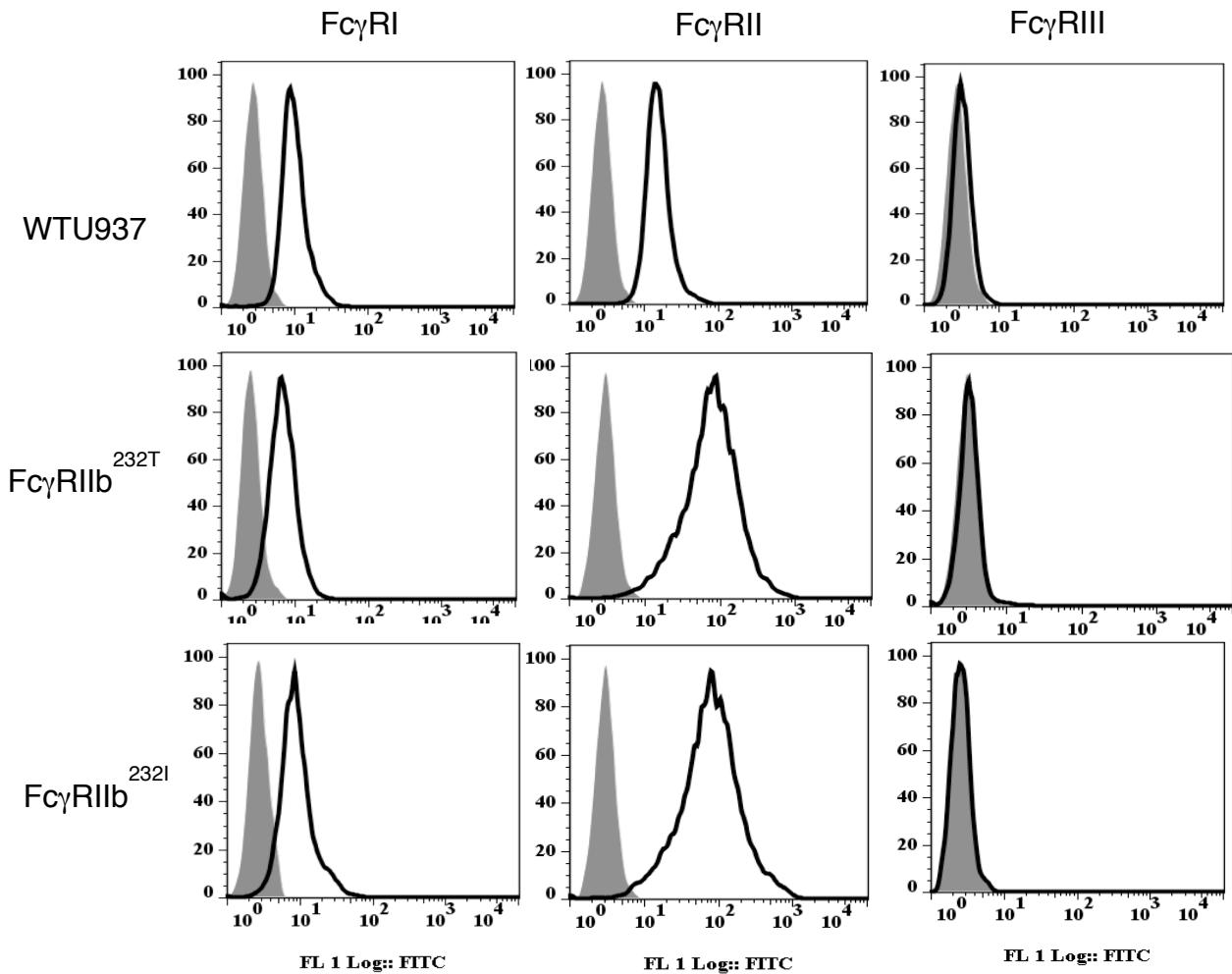


Figure 3.1: U937 cells and the Fc γ RIIb knock-ins express Fc γ RI and Fc γ RII but not Fc γ RIII.

Analysis of surface Fc γ R distribution by flow cytometry revealed that U937s express Fc γ RI, and Fc γ RII but not Fc γ RIII. The commercial antibody for Fc γ RII was not specific for Fc γ RIIIa or Fc γ RIIb leading to higher detection levels of total Fc γ RII in U937 cells that were transduced with either Fc γ RIIb^{232I} or Fc γ RIIb^{232T} than compared to the wild type U937 (WTU937). Grey shaded peak: isotype control. Open peak: Fc γ receptor staining.

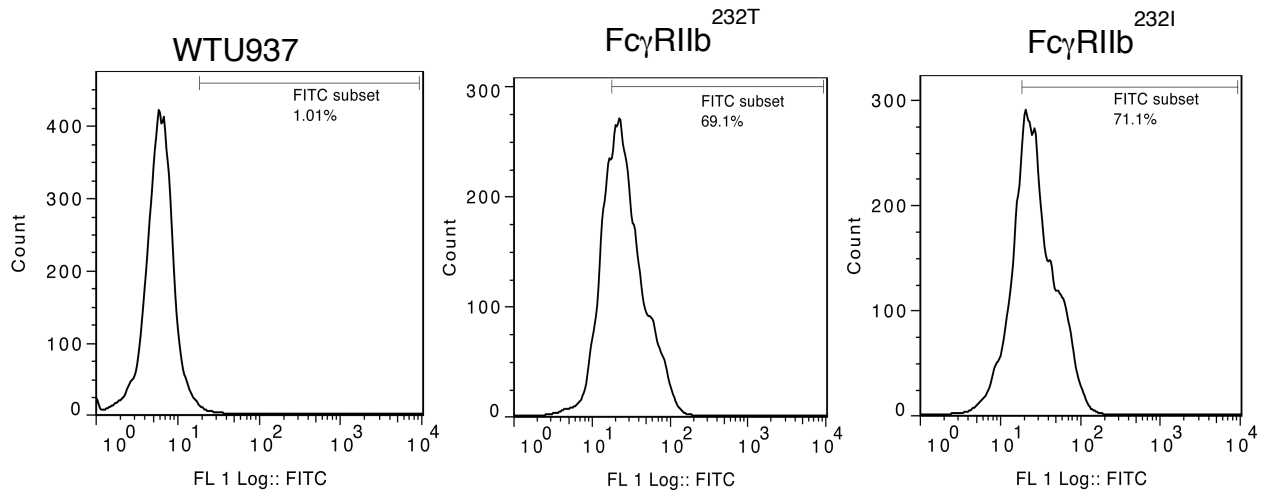


Figure 3.2: U937 knock-in cells express similar levels of Fc γ RII.

U937 cells were subjected to lentiviral stable transduction encoding for Fc γ RIIb and selected with blasticidin. Intracellular flow cytometry of the stable cell lines showed equivalent levels of total Fc γ RII expression.

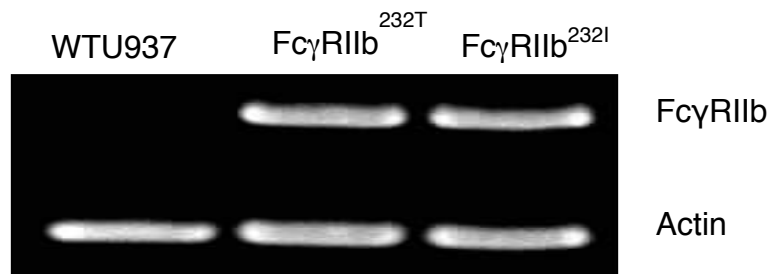


Figure 3.3: Fc γ RIIb, the inhibitory receptor, is not expressed in U937.

RT-PCR was performed on RNA extracted from these cells to confirm for the expression of Fc γ RIIb. Primers used were specific for Fc γ RIIb. The RT-PCR data shows that wild type U937 do not express Fc γ RIIb and that the stable knock in cells express similar levels of Fc γ RIIb. RT-PCR was also carried out on actin as an internal control, in order to ensure that equivalent amounts of RNA were used.

3.3 Establishment of conditions for phagocytosis in U937 cells

The use of a model cell line that mimics the behavior of differentiated tissue macrophages circumvents problems of limited primary cell numbers. Monocytic cell lines are widely used as they can be readily expanded for protocols requiring very large cell numbers.

U937 is a pro-monocytic cell line that can be differentiated towards a macrophage-like phenotype after treatment with GM-CSF and/or phorbol esters such as PMA [127-131]. U937 cells were stimulated with GM-CSF or the combination of both GM-CSF and PMA. Cells differentiated in the presence of GM-CSF and PMA changed from suspension to adherent growth. The adherent cells displayed cytoplasmic extension and membrane ruffling. PMA transiently induces activation of protein kinase C (PKC). As such, PMA was washed out and replaced with fresh media supplemented with 10% FBS after initial differentiation [132, 133]. The PMA-activated cells were cultured for a further 24 h to allow the cells to rest before phagocytosis (**Fig 3.4**).

These differentiated macrophages were then allowed to ingest latex beads as phagocytic targets. Flow cytometry was used to measure the phagocytic capacity of these cells 45 min after IgG fluorescent latex beads uptake. Fluorescent beads were used to readily allow for detection by flow cytometry and the quantification of a phagocytic index that is in proportion to the number of ingested particles. Treatment of U937 cells with 50ng/ml GM-CSF and 5ng/ml PMA for 48 h enabled

the cells to readily phagocytose a suspension of IgG latex beads whereas the phagocytic capacities of unstimulated cells or cells stimulated with GM-CSF only were weak and limited (**Fig 3.5**).

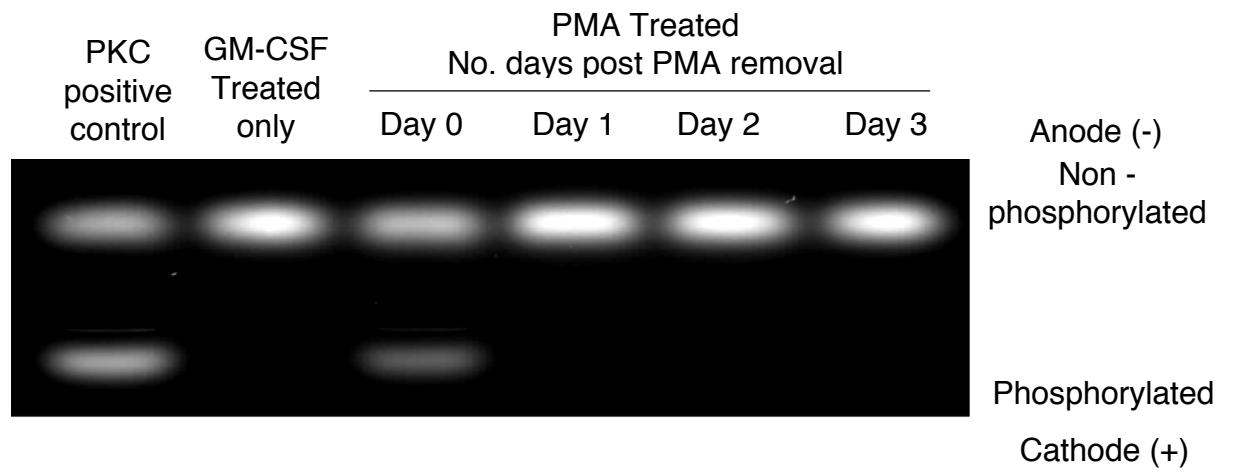


Fig 3.4: Effects of PMA stimulation on PKC activation.

Pretreatment of cells with PMA, a well-established activator of the signal transduction enzyme protein kinase C (PKC), transiently induces its activation. After washing out PMA, PKC activity levels were not detectable. The peptide substrate, phosphorylated by PKC if present in samples migrate to the cathode while the non – phosphorylated peptide migrate to the anode.

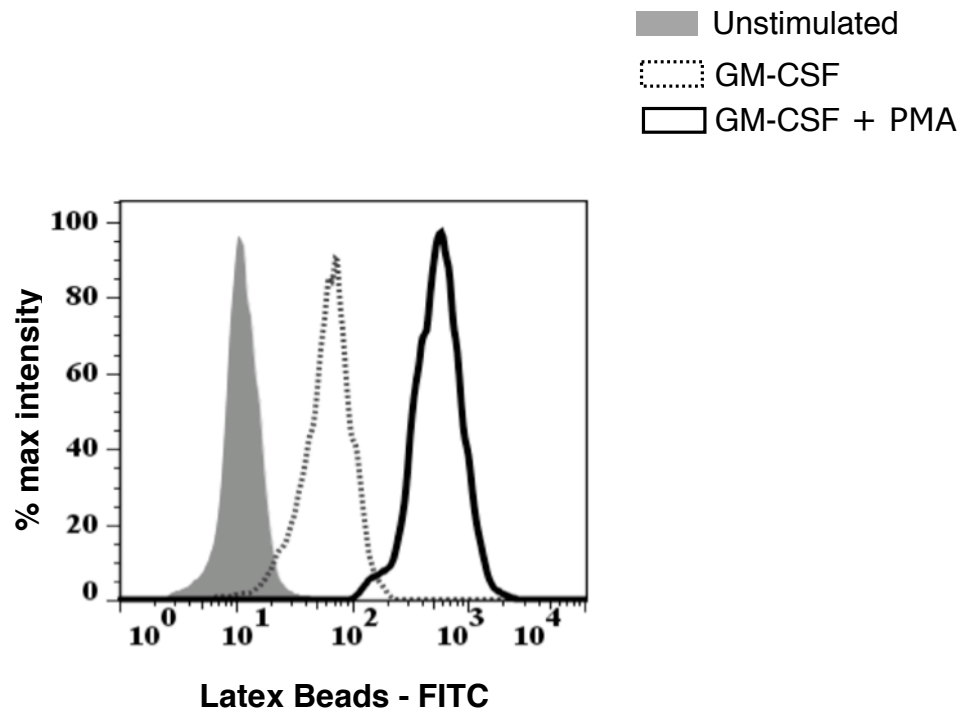


Fig 3.5: Cells differentiated with GM-CSF and PMA have increased phagocytic capacity.

U937 cells were differentiated with 50ng/ml GM-CSF and 50ng/ml GM-CSF with 5ng/ml PMA for 48h. Cells that were differentiated with GM-CSF and PMA had their phagocytic ability increase dramatically and were able to take up more fluorescent latex beads per unit time. A minimum of 10,000 cells was counted for each condition. Shaded peak: untreated U937. Dotted peak: U937 cells treated with 50ng/ml GM-CSF. Open peak: U937 cells treated with 50ng/ml GM-CSF and 5ng/ml PMA.

3.3 Use of latex beads for an *in vitro* phagosome model

Multiple receptors may be engaged simultaneously producing a complex and synergistic response during phagocytosis. The use of model systems will allow for the study of Fc γ receptors in isolation in which the engagement of other receptors is avoided or minimized.

Latex beads have been used extensively as a surrogate phagocytic target to study phagocytosis. These latex beads can be targeted for phagocytosis by a process called opsonization, which entails coating of its surface with proteins that are recognized by phagocytic receptors [16]. This provides one with the option of coating beads with protein molecules or with specific ligands that bind selectively to the receptors. Typically, latex beads that are opsonized with IgG molecules are used as a model for studying Fc γ receptor mediated phagocytosis [134, 135].

The process of phagocytosis is restricted to relatively large particles with a minimum size of 0.5 μ m [14]. To this end, we ensured that we specifically engage Fc γ receptors by conjugating 1 μ m carboxyl modified latex beads to BSA and subsequently incubating them with anti-BSA antibodies to form an IgG immune complex that will trigger an Fc γ signaling cascade.

Rabbit anti-BSA and mouse anti-BSA were used respectively to determine their association with human Fc receptors and to investigate for the most efficient Fc γ receptor phagocytosis of these latex beads. Our data demonstrates that while both rabbit and mouse IgG exhibited binding to human Fc γ receptors, the rabbit

IgG coated latex beads were recognized and internalized more rapidly via Fc receptors after 45 min of exposure at 37°C (**Fig 3.6**).

Confocal microscopy was used to visualize the interaction of IgG labeled latex beads with the Fc γ receptors present on the surface of U937 macrophages. Our results showed co-localization of the latex beads with the Fc γ receptors indicating that the latex beads interact with Fc γ receptors. Latex beads were then allowed to be internalized at 37°C for 5 min and 45 min respectively. The cells containing the latex bead phagosomes were stained for Rab 5, Rab 7 and LAMP-1 endocytic markers to evaluate the trafficking of latex beads into the cell interior after receptor engagement by checking for co-localization of these latex beads with stage specific endosomal markers (**Fig 3.7**). At 5 min post-internalization, phagosomes displayed co-localization with Rab 5, characterizing for early phagosomes and by 45 min, the phagosome has acquired Rab 7 indicating a late phagosome phenotype. Hence, phagocytosed latex beads were observed to undergo phagosome maturation through the gradual acquisition of these endosomal markers.

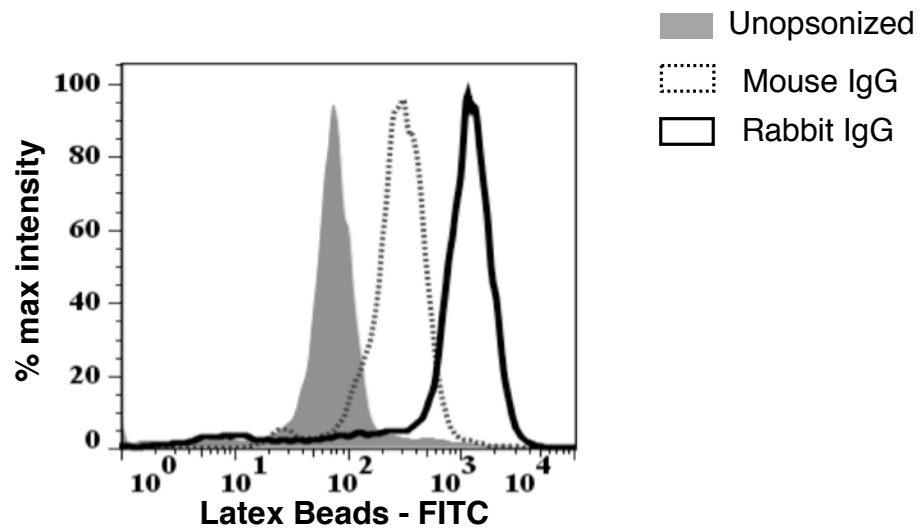


Fig 3.6: Rabbit IgG coated latex beads are most efficiently taken up via Fc receptors.

U937 macrophages were exposed to mouse or rabbit IgG opsonized latex beads allowing binding and internalization via Fc receptors. The uptake of rabbit IgG opsonized beads were more efficient in comparison to mouse IgG opsonized beads. Shaded peak: Unopsonized latex beads. Dotted peak: Mouse IgG latex beads. Open peak: Rabbit IgG latex beads.

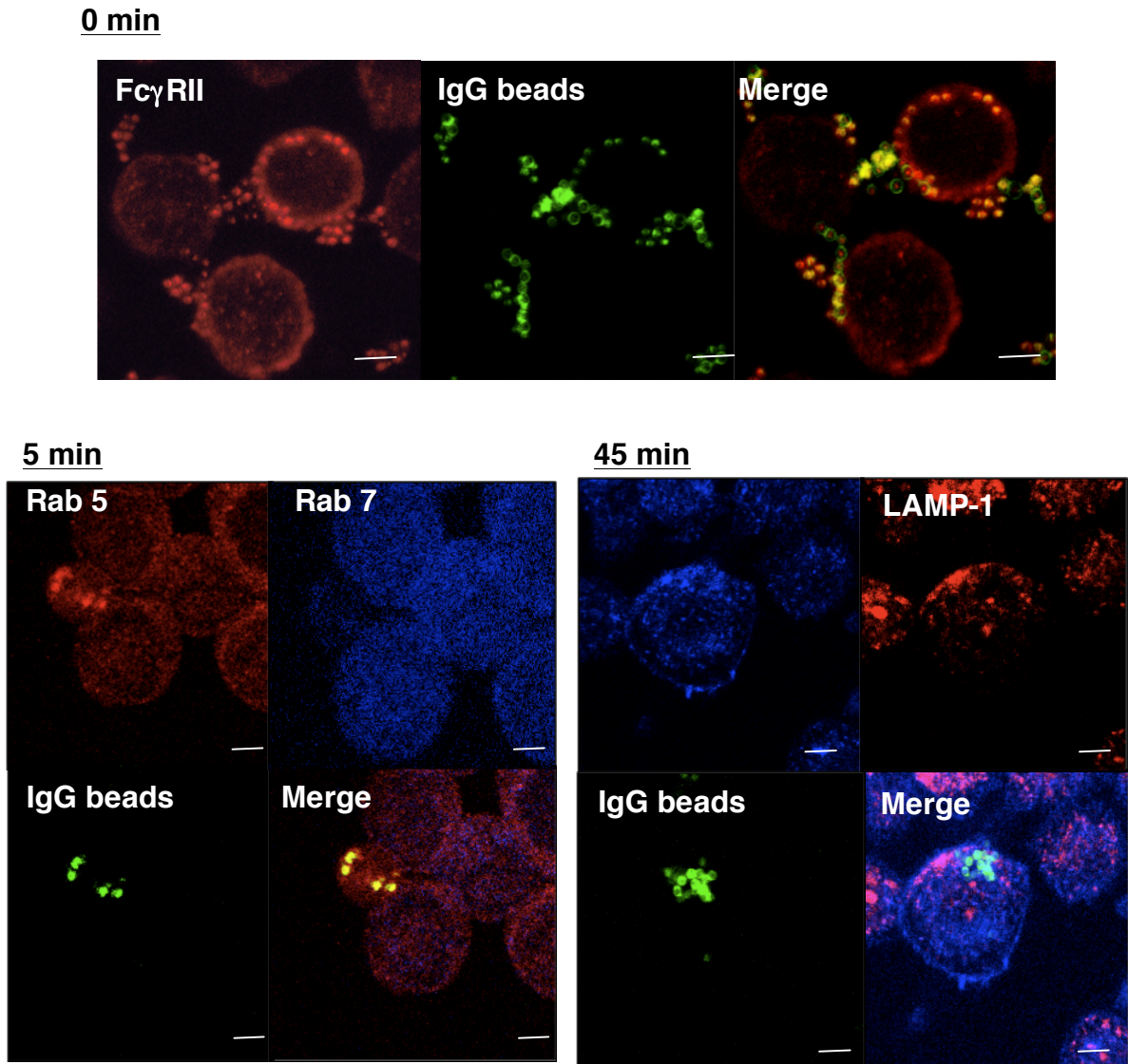


Fig 3.7: IgG particles interact with Fc γ receptors and is internalized into the phagolysosomal pathway.

U937 cells were fed with IgG coated latex beads. The co-localization of latex beads with Fc receptors observed indicated that the immune complexes were interacting with the Fc receptors. Incubation of the latex beads with the cells at 37°C allowed for the ingestion of the particles into the cells. The cells were stained with antibody specific for endocytic compartments such as Rab5, Rab7 or LAMP-1 and viewed using a confocal microscope. The cells containing phagosomes at 5 min post internalization exhibited co-localization with Rab5, an early endosome marker while the cells containing 45 min phagosomes co-localized well with Rab 7, a late endosomal marker. This therefore indicates that latex beads were delivered via Fc receptors and the phagosome gradually matures through the endocytic pathway. (Scale bar represents 5 μ m)

3.4 Isolation of maturing phagosomes with step sucrose gradients

Phagocytosis typically leads to the destruction of the internalized pathogen through a process termed “phagosome maturation”. In this maturation process the phagosome interacts sequentially with compartments of the endocytic pathway as it progresses and matures into a terminal phagolysosome whereby the target particle is digested [10, 136].

Phagosomes can be purified from other host cell organelles using a well-established protocol from Desjardins *et al*, 1994a. This is one of the “cleanest” methods to isolate phagosomes as it takes advantage of the possibility of inducing the formation of this compartment by feeding cells with latex beads. The low buoyant density of latex beads allow for the phagosomes to be isolated by flotation on step sucrose gradients, generating pure phagosome fractions (**Fig 3.7**).

The kinetics of maturation differs greatly depending on particles and cells employed. Therefore to begin our investigation into phagosome maturation, we first had to determine the time points in which we had phagosomes from representative stages of the entire process of phagosome maturation. The time points were determined by varying the time that macrophages were exposed to the latex beads at 37°C. As beads were pre-adsorbed onto cells at 4°C before internalization at 37°C, we were able to obtain a synchronized wave of phagosomes which proceed in a temporal order of maturation.

By performing western blot against molecules associated with distinct stages of the endocytic pathway, the time points chosen were 5 min, 45 min and 105 min as they correspond to different stages of phagocytosis. The 5 min phagosome expressed Rab 5, a protein on early endosomes thus representing early phagosomes; the 45 min phagosome expressed Rab 7, a late endosomal marker acquiring characteristics of late phagosomes and by 105 min, the phagosome expressed LAMP-1 which is predominantly present on lysosomes, the end compartment of the endocytic pathway and loses markers of early endocytic organelles such as Rab 5. Such phagosomes are referred to as phagolysosomes (**Fig 3.8**) [10].

The purity of the phagosome fractions was assessed by western blot analysis. Proteins derived from total cell extract and from purified phagosomes were resolved on SDS-PAGE gels. As compared to crude total extracts, purified phagosomes demonstrated the absence of contamination with Golgi membranes characterized by Golgi membrane marker 58k Golgi, but contained low levels of Calnexin, an endoplasmic reticulum (ER) marker. This indicates that some contamination with ER might be present. However, recent studies by Gagnon *et al*, 2002 have suggested that ER membranes could be recruited to phagosomes in order that the cell does not consume itself as it internalizes particles as large as the cell itself, allowing the maintenance of a relatively stable cell size without impaired function and viability (**Fig 3.9**).

The numbers of phagosomes loaded onto these gels for western blotting were normalized by measure of absorbance at 600 nm. A standard calibration curve may be obtained by measuring serial dilutions of these latex beads phagosomes, generating a linear correlation between absorbance and phagosome concentration. This straightforward measurement of phagosome concentration allows for the normalization of phagosomes from different time points (**Fig 3.10**).

This is further demonstrated by resolving equal amounts proteins as determined by the above method on SDS-PAGE gel after normalization and confirming equivalent protein levels by silver staining (**Fig 3.11**).

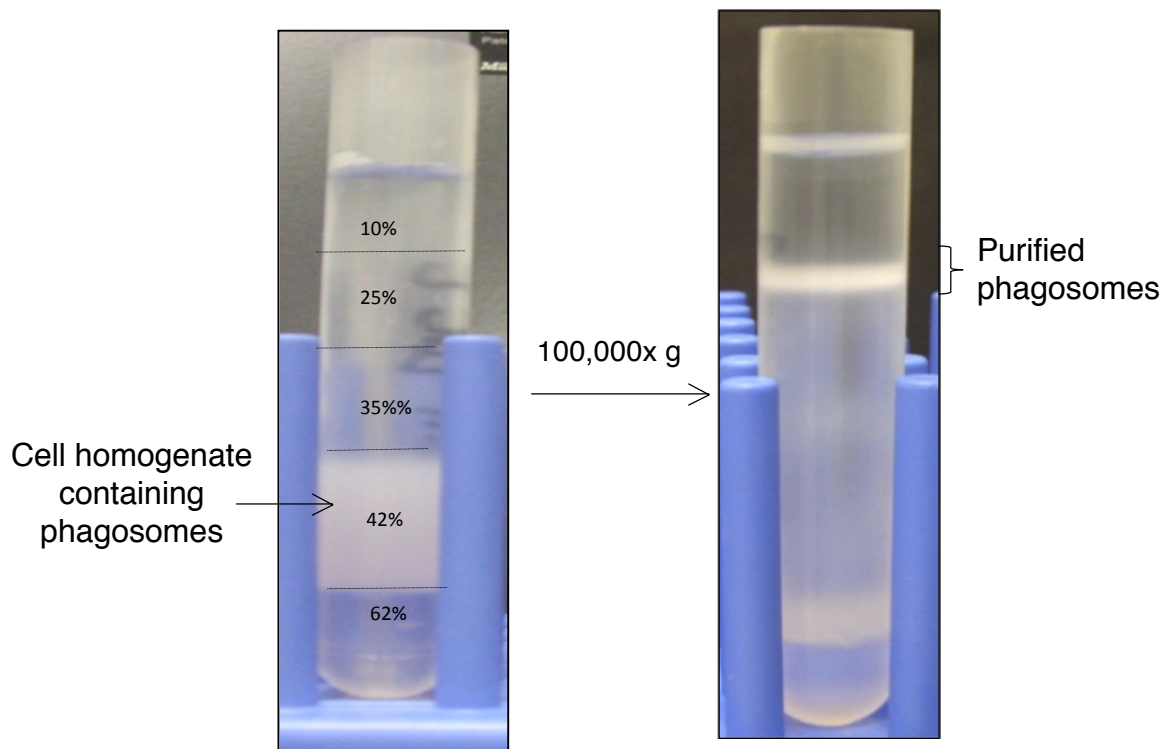


Figure 3.7: Latex bead phagosomes were isolated by flotation on step sucrose gradients.

Phagosomes were loaded near the bottom of the tube. By centrifugation at a speed of 100,000 x g, the low buoyancy of the latex beads allow for these beads to rise through the sucrose gradients while the rest of the cellular material are pelleted. Phagosomes were collected from the 10-25% sucrose interface.

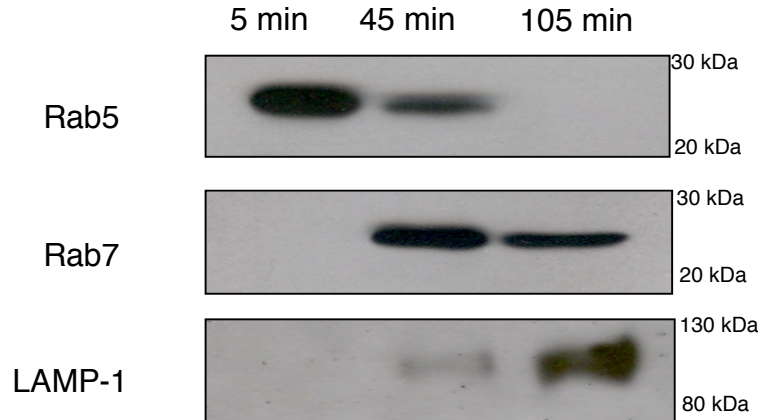


Fig 3.8: Latex bead phagosomes were isolated at different stages of maturation.

The maturation process can be monitored through the acquisition and loss of well-known markers from the endocytic pathway. This is often used to identify the stage of progression of phagosome maturation. Time points refer to the time elapsed after incubating the latex beads with cells at 37°C. As phagosomes age, they acquire Rab 5, an early endosome marker 5 min after formation; Rab 7, a late endosome marker 45 min after formation; and are enriched in LAMP-1, a lysosome marker 105 min after formation.

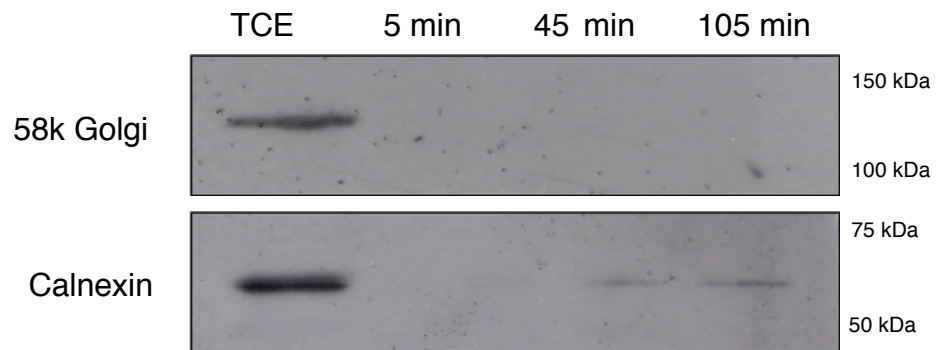


Fig 3.9: Phagosome isolates were devoid of major contamination from other intracellular organelles.

The contamination levels of phagosome extracts from different time points were assessed using diagnostic markers for ER (calnexin) and Golgi (58k Golgi) by western blotting. Total cell extracts (TCE) were loaded beside the phagosome fractions as a positive control.

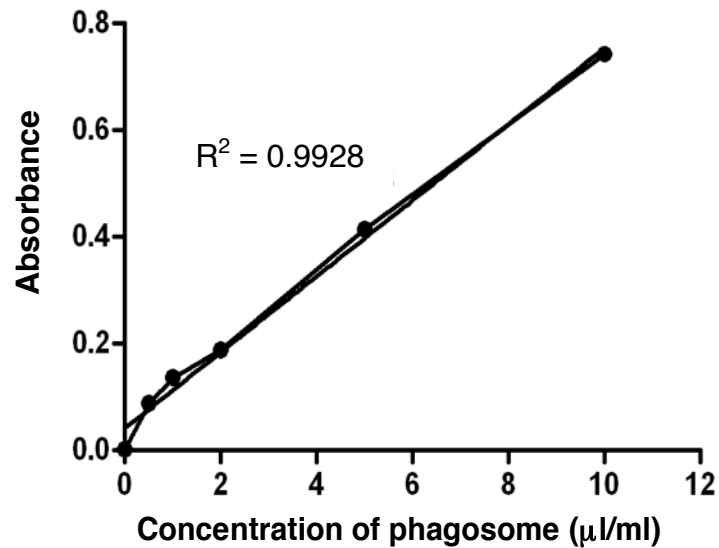


Fig 3.10: Phagosome concentration is normalized according to absorbance at 600nm.

The numbers of purified phagosomes between different samples were normalized precisely by measuring light scattering at OD_{600nm} . A standard curve can be generated by serial dilutions. This provides for straightforward quantification of phagosome numbers in a sample.

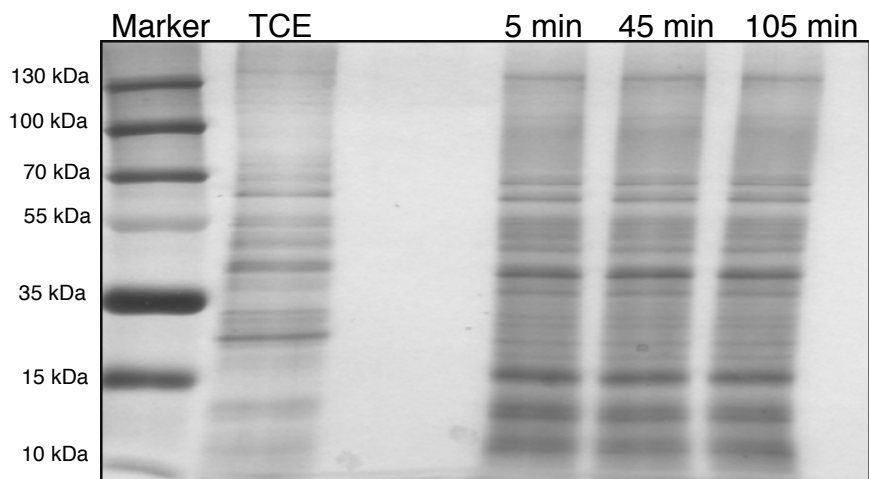


Fig 3.11: Equal loading of phagosomes was verified by silver stain.

Lanes were loaded with the same number of phagosomes, normalized by light scattering at 600nm. Total cell extract (TCE) were loaded next to the phagosome fractions. The comparison of the total cell extract lysate showed the unique band pattern of the phagosome fractions.

3.5 Extraction of plasma membrane

It is generally accepted that the composition of newly formed phagosomes resemble that of the plasma membrane as phagosomes appeared to be derived from its extension or inward displacement and are then extensively modified with time to allow the killing and degradation of their content [137].

Plasma membrane was isolated from cells using cationic colloidal silica on the basis of a method established by Chaney LK and Jacobson BS, 1983. The procedure consists of coating intact cells with cationic silica beads and polyacrylic acid at 4°C. Since the cells remain intact, the external face of the plasma membrane is selectively coated. The silica beads being positively charged, binds to the negatively charged plasma membrane. Polyacrylic acid is added to shield the exposed positive charges on the surface of the bound silica beads so that interactions with cellular debris are minimized. The addition of silica and polyacrylic acid greatly enhances the density of the plasma membrane and upon cell homogenization, large sheets of plasma membrane can be rapidly isolated by centrifugation on a Nycodenz gradient. Other intracellular membranes that are not silica coated will float and thus be removed from the pellet. [138].

Western blotting was used to determine the level of enrichment of plasma membrane and to evaluate the contamination by intracellular components. To monitor the efficacy of the silica beads in enriching for plasma membrane we included a total cell extract control and followed for the enrichment of a plasma

membrane marker (Na⁺K⁺ATPase)[139]. The purity of the plasma membrane fractions were judged by markers for Actin and Calnexin. These served as indicators for cytoplasmic proteins and ER respectively. Silica beads used to prepare for these fractions can perturb plasma membrane components generating artifacts, which will change the properties of the plasma membrane [140]. Hence, the concentration of silica beads to be used was optimized by titrating different concentrations of silica beads against a lipid raft marker, Flotillin [141]. High concentrations of silica beads were observed to artificially induce lipid raft formation. In all, the western blots revealed that the plasma membrane isolation technique employed provided us with highly purified silica-coated plasma membranes that were enriched in plasma membrane proteins but largely free of other contaminating cellular components (**Fig 3.12**).

The concentration of plasma membrane proteins was determined by Bradford assay and visualized for equivalent loading by silver stain (**Fig 3.13**)

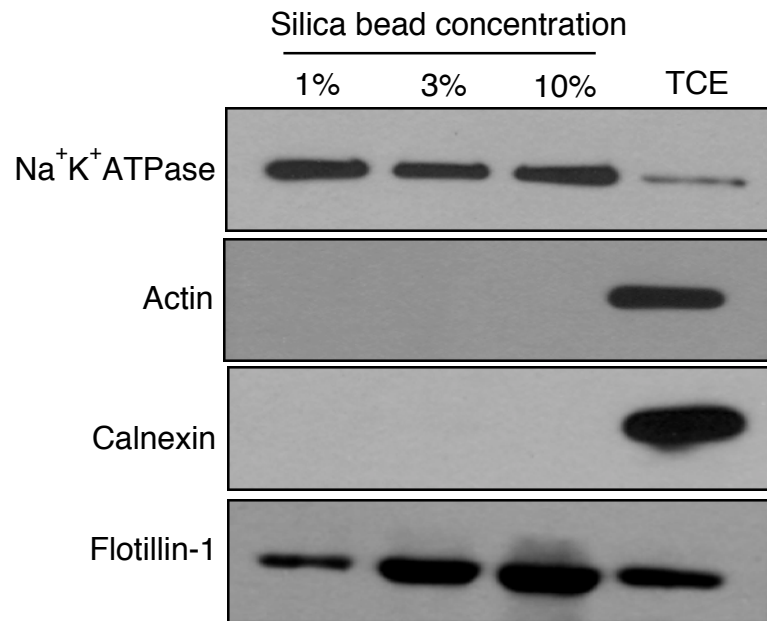


Fig 3.12: Coating of cells with cationic silica beads enables isolation of the plasma membrane from internal membranes.

The cationic silica beads adhere electrostatically to the negatively charged plasma membrane, ripping off large sheets of plasma membrane upon cell lysis. Western blot analysis of enriched plasma membrane fractions (Na⁺K⁺ATPase) were probed for contaminants such as cytoplasmic protein (actin) and ER (calnexin). The use of different concentration of silica beads was probed against a lipid raft marker (flotillin-1) to assess for the quality of plasma membrane. This revealed that at a low bead concentration of 1%, the silica beads did not induce any lipid raft artifact but at high bead concentrations lipid raft formation was observed.

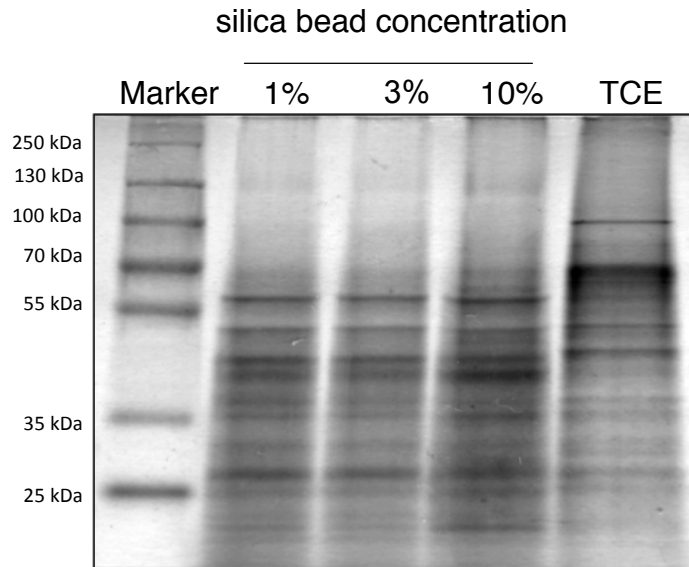


Fig 3.13: Silver staining of proteins in plasma membrane extracts.

Equal loading of protein in each sample onto each lane of SDS-PAGE gel was determined by Bradford assay and verified by silver stain.

3.6 Discussion

Phagocytosis, an active process for the uptake and subsequent clearance of internalized particles is an important immune response. Among the best-characterized phagocytic receptors are the Fc γ receptors that mediate the recognition of IgG immune complexes. Research has shown that mutations in Fc γ receptors or dysregulation in their signaling may lead to autoimmunity. A single amino acid polymorphism Ile232Thr in Fc γ RIIb has been identified in autoimmune systemic lupus erythmatosus (SLE).

To examine the effects of the wild type Fc γ RIIb (Fc γ RIIb^{232I}) and the polymorphic Fc γ RIIb (Fc γ RIIb^{232T}), we used a well-characterized human monocytic cell line U937 which provided useful as *in-vitro* human macrophages. We first sought to establish the panel of Fc γ receptors expressed by U937 cells. We showed that U937 constitutively expresses the activatory Fc γ RI and Fc γ RIIa but does not express the inhibitory Fc γ RIIb. The key difference between primary monocytes that are present in our body and U937 cells is that the primary monocytes express Fc γ RIIb, whereas U937 cells do not. However, the absence of Fc γ RIIb makes U937 an attractive cell line for studying the role of this inhibitory receptor as it allows for the generation of stable transfectants expressing either Fc γ RIIb^{232I} or Fc γ RIIb^{232T}. Plasmids encoding for the Fc γ RIIb^{232I} or Fc γ RIIb^{232T} were introduced into U937 cells by lentiviral transduction. We showed that these knock-in cell lines have equivalent expression of either the wild-type Fc γ RIIb^{232I} or

the polymorphic Fc γ RIIb^{232T} on the cell surface.

We showed that the differentiation of the promonocytic U937 cells to a macrophage-like phenotype with GM-CSF and PMA for 48 h increased its phagocytic capacity, and promoted the rapid uptake of latex beads. Therefore, in all our subsequent studies involving U937 cells, we pretreated the cells with GM-CSF and PMA for 48 h before the start of any experiment.

Phagocytosis is a receptor-mediated event and particles are most efficiently phagocytosed when they are opsonized with immunoglobulins. To initiate Fc receptor cross-linking and subsequent Fc-mediated internalization into the cell, we conjugated latex beads to IgG that can recognize human Fc γ receptors. We showed that latex beads coated with rabbit IgG were better recognized and taken up by Fc receptors as rabbit IgG binds more strongly to human Fc receptors than mouse IgG[142]. In addition, we verified that the uptake of IgG latex beads were via Fc receptors and examined the internalization and maturation processes using confocal microscopy.

Our western blots also showed that probing for markers along the endocytic pathway confirmed that the phagosomes harvested at the following timepoints: 5 min, 45 min and 105 min were sufficient to follow the transition from early phagosomes to phagolysosomes, giving a good overview of the entire process of phagosome maturation. Our 5 min phagosome contains Rab 5 and Rab 7

proteins resembling the composition of early phagosomes. In contrast, the presence of LAMP-1 in the 105 min phagosome represented the phagolysosome.

The use of latex beads as phagocytic targets allowed us to take advantage of its low buoyant density for the purification of these latex bead phagosomes on step sucrose gradients. We showed that we were able to efficiently isolate pure phagosome isolates at every stage of their complex maturation that were relatively free of contamination from other host organelles such as the ER and Golgi. The isolation of pure phagosomes will allow for comprehensive analysis of the composition and function governing phagosome maturation of wild-type Fc γ RIIb^{232I} and the polymorphic Fc γ RIIb^{232T}.

By measuring light scattering at 600nm, we were able to quantify the number of purified phagosomes. This provided us with a very straightforward way of normalizing the concentration of phagosomes that was yielded after sucrose gradient purification from different phagosome preparations.

In addition, we attempted to isolate intact plasma membrane sheets as phagosomes originate from the plasma membrane. We did this by the use of cationic silica beads and demonstrated that we were able to enrich for plasma membrane from cells with very high purity.

In summary, we have established a detailed experimental model system to investigate the implication of the Fc γ RIIb polymorphism in the context of Fc γ R mediated phagocytosis. These approaches will provide insights relevant for the

understanding of the intricate Fc γ receptor pathways that coordinate successful phagocytosis and to understand the mechanisms on how the Fc γ RIIb polymorphic variant, Fc γ RIIb^{232T} govern phagosome maturation and function that will ultimately lead to disease.

The next step is to utilize these systems to determine how these two receptors behave during IgG latex bead phagocytosis. This would include the study of U937 macrophages on IgG opsonized pathogen uptake and the consequences of these events in the activation of intracellular innate host defences during phagosome maturation. These studies are likely to contribute to our understanding of the way by which Fc γ RIIb and the mutant variant coordinate phagocytosis and phagosome maturation.

CHAPTER 4

RESULTS II: ANALYSING THE EFFECTS OF Fc γ RIIB^{232I} AND Fc γ RIIB^{232T} ON LATEX BEAD PHAGOCYTOSIS

4.1 Introduction

Activation of phagocytic receptors which recognizes and targets pathogens and foreign particles for degradation by phagocytosis is important for distinguishing invading foreign pathogens [15]. The target particles are enveloped by the plasma membrane and undergo an elaborate maturation process that parallels endosome maturation. During this process, the phagosome acquires degradative and microbicidal capabilities to promote the killing and destruction of the internalized particle [3].

As phagocytosis is a multi-step process initiated by particle recognition by activatory Fc γ receptors that detect and mediate internalization, and is regulated by Fc γ RIIb which is known to inhibit many features of this phagocytic response, the possibility these phagocytic receptors could have a crucial role in determining how a given target is processed is enticing. Considering also that pathogens are not killed by internalization per se but rather by the extremely hostile milieu of the phagolysosome, phagosome maturation is crucial for successful elimination of particle and in resolving infections. Therefore using inert targets such as IgG opsonized latex beads, we attempted to define how Fc γ RIIb^{232I} and Fc γ RIIb^{232T} regulate phagosome function and maturation.

4.2 Evaluation of phagocytic indexes of Fc γ RIIb^{232I} and Fc γ RIIb^{232T} macrophages

Macrophages are crucial players in the immune response to protect the host against the invasion of bacteria or viruses by phagocytosis. The phagocytic index demonstrates the performance of the macrophages in capturing foreign particles. With the notion that altered Fc γ RIIb activity in Fc γ RIIb^{232T} results in failure to negatively regulate the phagocytosis response, macrophages from these cell types are expected to exhibit a hyperactive phenotype. Moreover, observations made by Clatworthy et al., 2007 have demonstrated that humans homozygous for Fc γ RIIb^{232T} show increased phagocytosis of *Streptococcus pneumoniae in vitro*. Given that Fc γ RIIb inhibits Fc γ receptor mediated phagocytosis and that the polymorphic Fc γ RIIb^{232T} disrupts the negative inhibitory signaling, we sought to evaluate the phagocytic capabilities of Fc γ RIIb^{232I} and Fc γ RIIb^{232T} macrophages using FITC labeled IgG opsonized latex beads. Cells stably expressing equal quantities of either Fc γ RIIb^{232I} or the SLE-associated Fc γ RIIb^{232T} were allowed to ingest the fluorescent latex beads for 5 min, 45 min and 105 min. The number of fluorescent particles ingested by the cells were quantified using flow cytometry. The amount of fluorescence is directly proportional to the number of ingested particles allowing for the assessment of phagocytic index of these cells. Our result showed that Fc γ RIIb^{232I} macrophages ingested latex beads less avidly and macrophages expressing Fc γ RIIb^{232T} are more aggressive in ingesting opsonized latex beads per unit time at all time points measured (**Fig 4.1**).

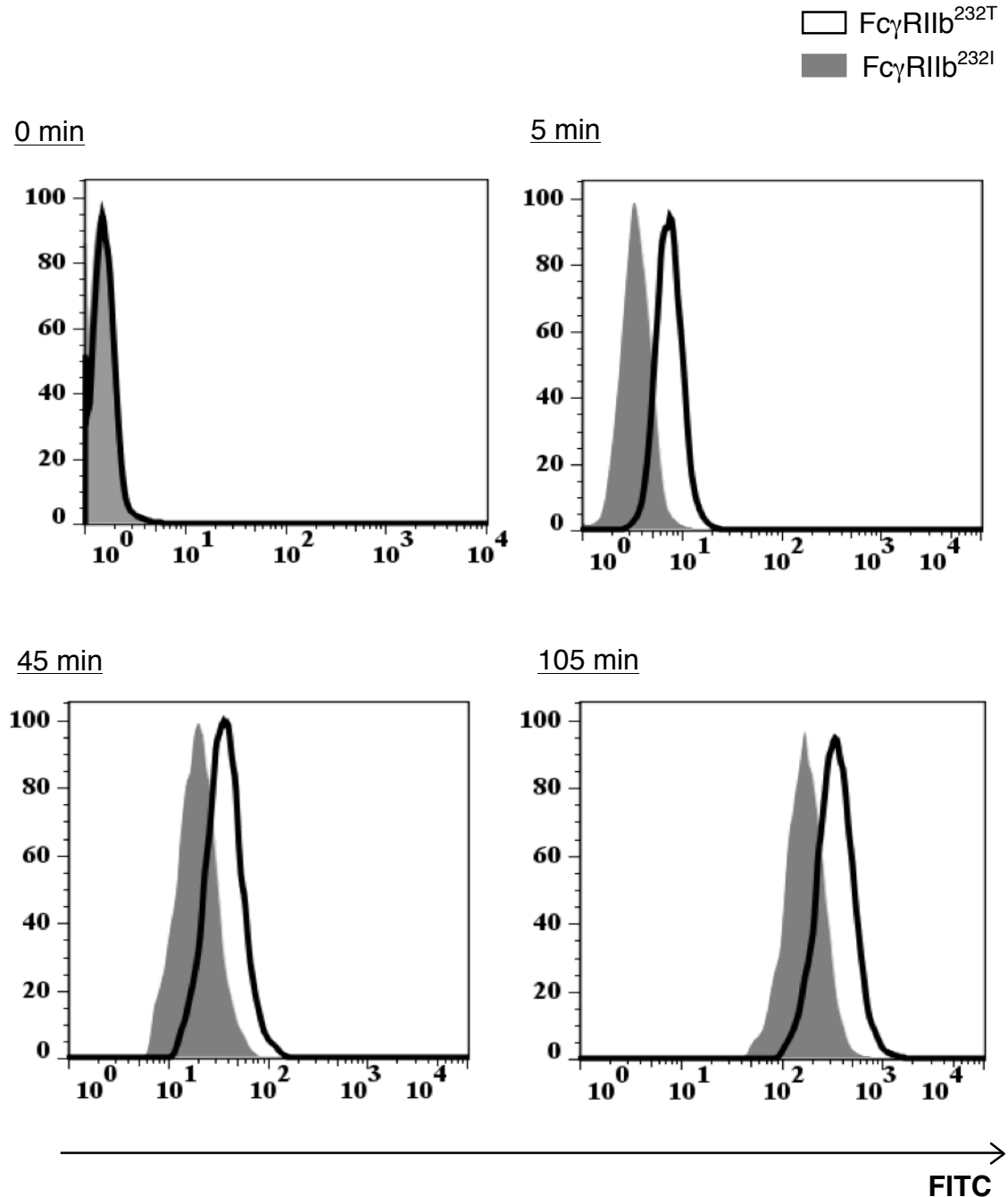


Fig 4.1: Fc γ RIIb^{232T} macrophages exhibit enhanced phagocytosis.

The phagocytic ability of macrophages were tested by exposing them to FITC labeled IgG opsonized latex beads. Macrophages expressing Fc γ RIIb^{232T} increased phagocytosis by ingesting more latex beads per macrophage. Phagocytosis of FITC-labeled latex beads was determined by fluorescein-activated cell sorter (FACS) analysis.

4.3 Assessment of phagosomal maturation

Internalization of pathogens per se is insufficient to mediate the destruction of pathogens. A phagosome undergoes a remodeling process termed phagosome maturation that converts a nascent phagosome into a potent microbicidal organelle through an ordered series of strictly choreographed membrane fusion and fission events that radically alter the composition of the phagosome [3, 12].

To reveal the relationship between phagocytic uptake and the ability of these macrophages to clear bacteria and foreign particles, we monitored for the maturation of these phagosomes isolated at 5 min, 45 min and 105 min time points by western blot analysis of protein markers for endosomal and lysosomal compartments that are known to interact with maturing phagosomes. These included Rab 5 which is detected in early phagosomes, Rab 7 found in the more mature late phagosome and LAMP-1 which is predominantly expressed on lysosomes to complete phagosome maturation [143].

The western blot data for Rab 5 and Rab 7 seems to imply that Fc γ RIIb^{232I} phagosomes containing the IgG latex beads are maturing at a faster kinetic than the Fc γ RIIb^{232T} variant (**Fig 4.2**). In Fc γ RIIb^{232T} phagosomes, Rab 5, which associates with early phagosomes, can still be detected after 45 min post internalization of IgG latex beads and after 105 min Rab 7 can still be detected on these phagosomes. Conversely, in Fc γ RIIb^{232I} phagosomes, Rab 5 was not detected at 45 min and Rab 7, which is present at later stages of maturation, was

recruited within 5 min. However, upon inspection of the expression of LAMP-1 protein which is characteristic of phagosome-lysosome fusion and signals the terminal stage of phagocytosis, we observed LAMP-1 on both Fc γ RIIb^{232I} and Fc γ RIIb^{232T} phagosomes by 45 min, which was more abundant at 105 min on phagosomes expressing Fc γ RIIb^{232T}. This suggests that although the interactions of Fc γ RIIb^{232T} phagosomes with the early and late endosomes are slightly delayed compared to Fc γ RIIb^{232I}, Fc γ RIIb^{232T} macrophages completes phagosome maturation more efficiently than Fc γ RIIb^{232I} macrophages as they culminate in the formation of phagolysosomes that are deemed critical for degradation of the internalized particle.

During phagosome maturation, as the internalized particle undergoes fusion interactions with increasingly acidified endosomes and lysosomes the phagosomal lumen will gradually be rendered acidic. Hence, to further evaluate phagosome maturation, we proceeded to measure the acidification of phagosomes following internalization.

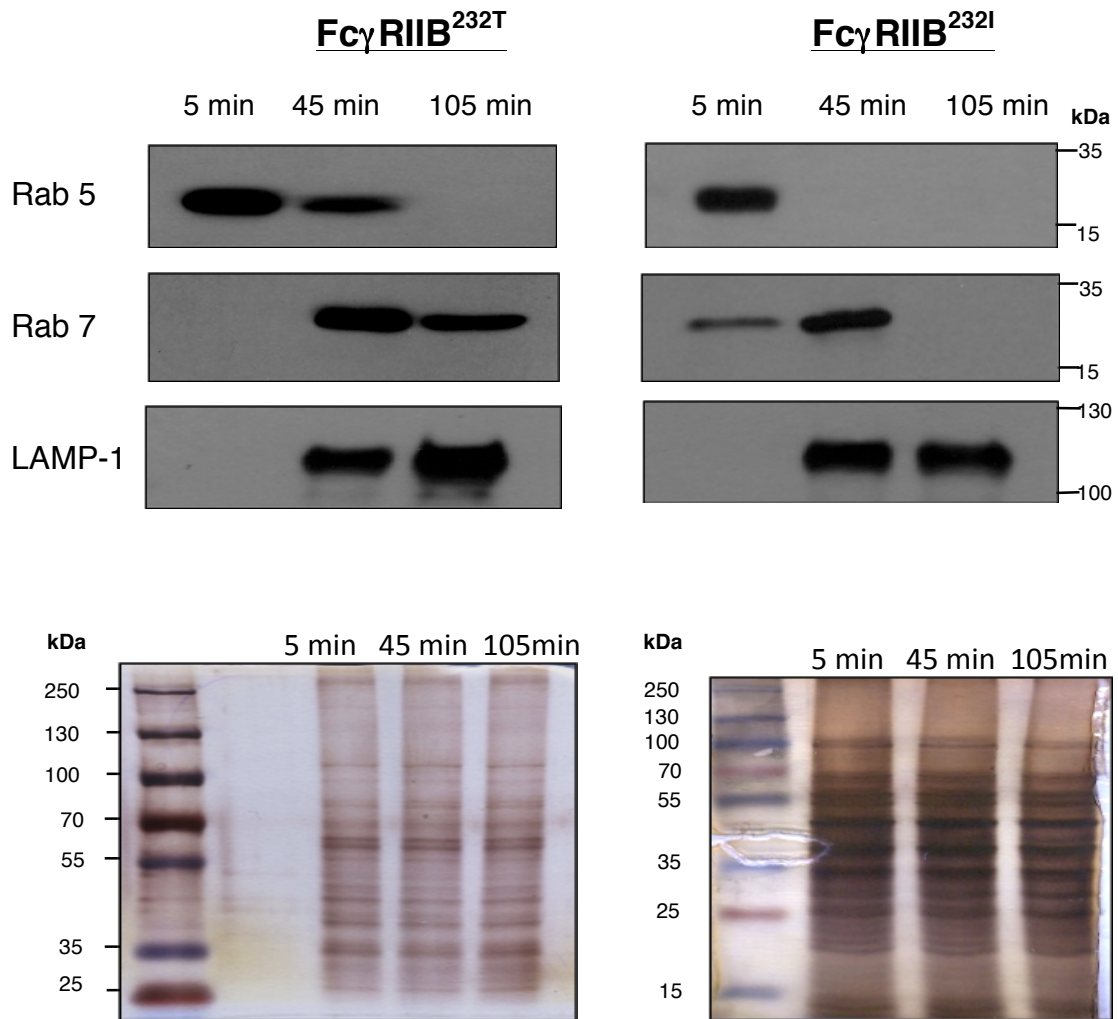


Fig 4.2: Fc γ RIIb^{232T} polymorphism on the cell surface is sufficient to enhance the rate of maturation of IgG opsonized beads.

Accordingly with the progression of the endocytic pathway, phagosomes mature with the acquisition or loss of characteristic endocytic vesicle markers and finally merge with lysosomes. Over a maturation time of 105 min, the enrichment of LAMP-1 on Fc γ RIIb^{232T} phagosomes indicates increased fusion events with lysosomes, which is the terminal compartment of the phagolysosome biogenesis pathway.

4.3 Assessment of phagosome acidification

A critical element of the maturation process is the gradual acidification of the phagosomal lumen; from a near neutral pH to a pH of less than 5. Fusion with early endosomes are marked by a mildly acidic pH of ~ 6 and after fusion with late endosomes, luminal pH is lowered to a moderate acidic pH ~ 5.5 . As maturation progresses and fuses with lysosomes, the phagosome lumen becomes extremely acidic and finally reaches a pH of 4.5 [10]. Thus, in addition to examining acquisition of endosomal and lysosomal protein markers, the acidification of the phagosomal lumen can also be used as an index of maturation.

This acidification is generated by proton-pumping vacuolar ATPase (V-ATPase). Acidification is essential during phagosome maturation. This is because it is only when the phagosome hits a sufficiently low pH can the phagocytosed particle be degraded as a result of the activity of many hydrolytic enzymes requiring acidic conditions. The acidic conditions also restrict microbial growth. Phagosome acidification is therefore of great importance for efficient and successful destruction of invading pathogens as the low pH creates a hostile environment for pathogens [3, 143].

The rate of phagosome acidification was assessed by following the internalization of IgG latex beads labeled with pHrodo™, a pH sensitive dye that is non-fluorescent at neutral pH but fluoresces red under acidic conditions for 5 min, 45

min and 105 min as the phagosomes matures to form a phagolysosome. By utilizing pHrodo™, pH within the phagosome can be quantified as its fluorescence increases with decreasing pH. Fluorescence was observed to be increasing as the phagosomes age in both cell lines but at all three time points that were monitored, Fc γ RIIb^{232T} macrophages displayed increased fluorescence suggesting that rate of acidification is rapid in comparison to the Fc γ RIIb^{232I} macrophages which exhibited weaker fluorescence indicating that phagosome acidification is occurring on a slower time scale. This supports our observation that phagosome maturation of Fc γ RIIb^{232T} is indeed more rapid (**Fig 4.3**).

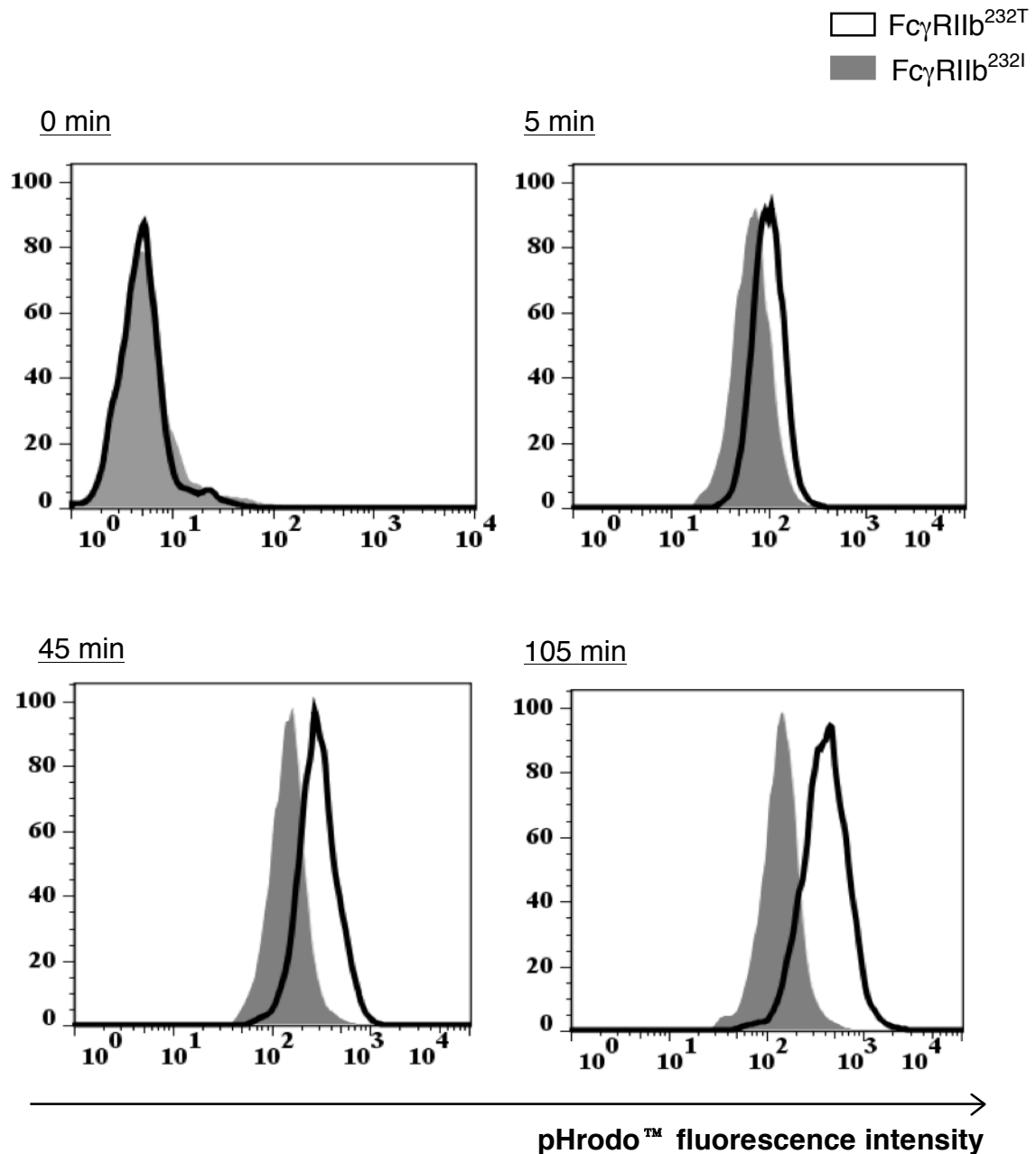


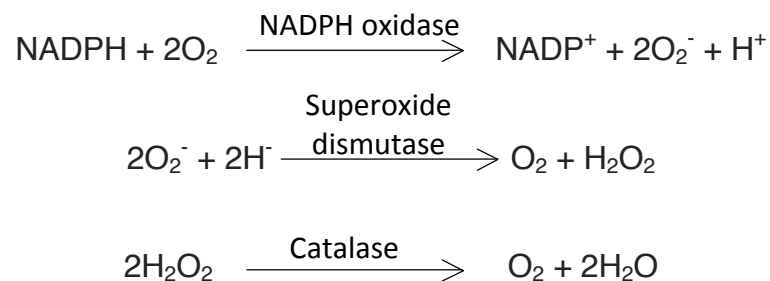
Fig 4.3: Phagosomes expressing Fc γ RIIb^{232T} displayed a more rapid acidification kinetic compared to Fc γ RIIb^{232I} phagosomes.

As phagosomes age, they interact with a series of increasingly acidified compartments of the endocytic pathway that lead to particle degradation. Fc γ RIIb^{232T} and Fc γ RIIb^{232I} macrophages were fed pHrodo™ labeled latex beads and incubated for 5 min, 45 min and 105 min. The Fc γ RIIb^{232T} variant exhibited increased fluorescence at all three time points indicating a faster acidification process.

4.4 Quantification of ROS produced in maturing phagosomes

During phagosome maturation, highly dynamic interactions of phagosomes with endomembranes of the phagocyte that rapidly acidify the phagosomal lumen is not an isolated event but coincides with the generation of toxic mediators such as reactive oxygen and nitrogen species thereby promoting killing of the internalized pathogen [3].

Reactive oxygen species (ROS) produced during particle ingestion is mediated through the involvement of nicotinamide adenine dinucleotide phosphate (NADPH) oxidase complex which exists in a disassembled state in quiescent cells but is rapidly assembled following phagocyte activation [3]. Upon activation, NADPH oxidase is formed by the Phox protein family which is composed of gp91^{phox}, p22^{phox}, p40^{phox}, p67^{phox}, p47^{phox} and Ras related C3 botulinum toxin substrate 2 (Rac2) [144]. This multi-protein NADPH oxidase shuttles electrons across the limiting membrane of the phagosome to yield the superoxide radical (O₂⁻), which is rapidly reduced by superoxide dismutase to form hydrogen peroxide (H₂O₂). Hydrogen peroxide is reduced by catalase to oxygen (O₂) and water (H₂O) [145].



The production of the phagocyte's oxidative arsenal confers bactericidal killing within the phagocyte. Patients with chronic granulomatous disease (CGD), a human genetic disorder, have a defect in phagocyte function where the lack of NADPH oxidase results in lack of ROS production and poor clearance of many bacterial and fungal pathogens [146, 147].

The ROS produced is confined within the phagosome vacuole and reacts directly with the phagosomal contents to contribute to pathogen eradication. For ROS production to be quantified, we incubated dihydrorhodamine123, a ROS sensitive dye which readily enters the phagosome and upon oxidation by reactive oxygen intermediates exhibits a fluorescence. The phagocyte's various oxidative species were measured by monitoring the fluorescence with flow cytometry as a readout. This allows for quantitative measurements of phagosomal ROS.

The accumulation of ROS was observed in the wild type Fc γ RIIb^{232I} was slight and gradual whereas the polymorphic Fc γ RIIb^{232T} displayed substantial amounts of ROS produced during phagocytosis especially after 45 min post internalization of latex beads. A sharp 2-fold increase in ROS production was observed during phagocytosis from 5 min to 45 min (**Fig 4.4**).

Stronger fluorescence values were detected at the 5 min, 45 min and 105 min time intervals in the polymorphic Fc γ RIIb^{232T} expressing phagocytes when compared to the wild-type Fc γ RIIb^{232I}. This fluorescence readout also indicated that larger amounts of oxidative products were formed upon phagocytosis in

these cells and supports the observation that Fc γ RIIb^{232T} phagocytes ingest a higher number of latex beads.

In addition, the observed rise in fluorescence at 45 min could be due to oxidative burst followed by a decline in fluorescence at 105 min. There are several possible reasons that could account for this decline in fluorescence: (1) reactive oxygen species are highly reactive short lived species that do not accumulate to very high levels; (2) diminishing fluorescence reflected termination of the respiratory burst; (3) substantial acidification during maturation may quench the fluorescence; or (4) the high concentration of proteases acquired during the maturation process could also influence the fluorescence of the dye.

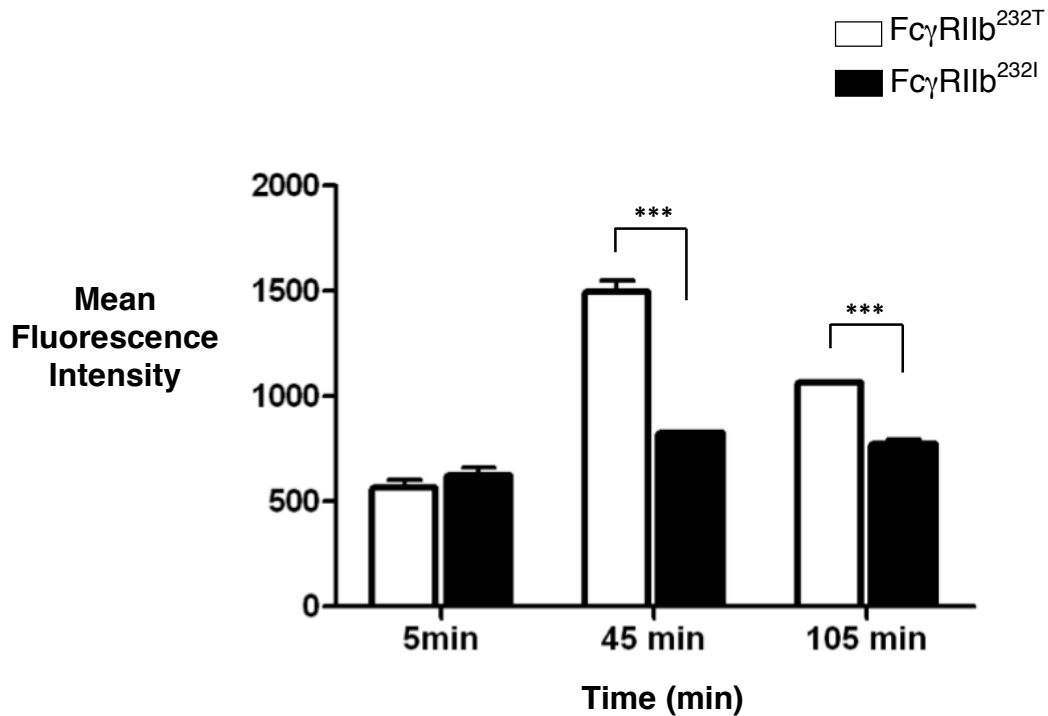


Fig 4.4: Fc γ RIIb^{232T} phagosomes produced more ROS over time compared to wild type Fc γ RIIb^{232I} phagosomes.

Reactive oxygen metabolite generation was examined by monitoring the fluorescence of oxidized dye formed via the reaction with oxygen species produced during phagocytosis by flow cytometry. The mean fluorescence of these cells reflects the rate of phagosomal ROS produced.

4.5 Impact of Fc γ R1Ib on calcium responses during phagocytosis

Calcium is a key signaling molecule that participates in a wide range of cellular activities including Fc γ receptor mediated phagocytosis in macrophages. Resting cells have an intracellular calcium [Ca²⁺] concentration of about 100 nM which is acutely elevated upon engagement of phagocytic receptors [148, 149]. The increase in [Ca²⁺] however is independent of particle internalization [150]. Although [Ca²⁺] is not required for phagocytic ingestion, studies have revealed that phagosome maturation is regulated more stringently by elevations of [Ca²⁺]. Malik and colleagues demonstrated that by preventing changes in intracellular calcium levels, phagosome-lysosome fusion was impaired [151].

More interesting are the observations of the dependence of the [Ca²⁺] response on Fc γ receptors expressed on the cell surface. For example, macrophages from Fc γ R1Ib knockout mice display a more robust calcium response than the wild type mice [152]. In addition, work by Myers and Swanson, 2002 indicate that the degree of calcium elevation correlates with the degree of activation of macrophages after Fc γ R ligation [149]. These studies reflect the possibility that phagocytic calcium responses are determined by the relative ratios of the different receptors on the cell surface and that the increased calcium responsiveness of the activated macrophages may be a result of reduced expression of Fc γ R1Ib.

Since cells stably expressing Fc γ RIIb^{232T} have shown to mediate a more aggressive phagocytosis as compared to Fc γ RIIb^{232I}, we explored the relative influence of Fc γ RIIb on calcium signaling during phagocytosis. To monitor [Ca²⁺] flux during phagocytosis, cells were pre-labeled with indo-1, a calcium indicator that fluoresces when [Ca²⁺] is bound. IgG latex beads were added to the labeled cells and [Ca²⁺] levels were recorded for 180 s during the course of receptor engagement leading to particle internalization. Ionomycin, a [Ca²⁺] ionophore which induces the release of calcium from intracellular stores such as the ER was used as a positive control [153]. This ensures that cells were properly loaded with indo-1 and to establish the maximum [Ca²⁺] flux response.

[Ca²⁺] levels were observed to increase upon addition of IgG latex beads. However, the amplitude of the calcium response of Indo-1 labelled U937 cells expressing the mutant Fc γ RIIb, Fc γ RIIb^{232T}, was higher than that generated by the wild type Fc γ RIIb^{232I}. The cells expressing Fc γ RIIb^{232I} appeared to generate a more subdued calcium flux response upon initiation of phagocytosis (**Fig 4.5**). The marked rise in [Ca²⁺] accompanying Fc γ RIIb^{232T} phagocytosis may suggest that the isoleucine to threonine mutation at position 232 in U937 transfectants enhances downstream phagocytic signaling leading to increased anti-microbial activities in the macrophages.

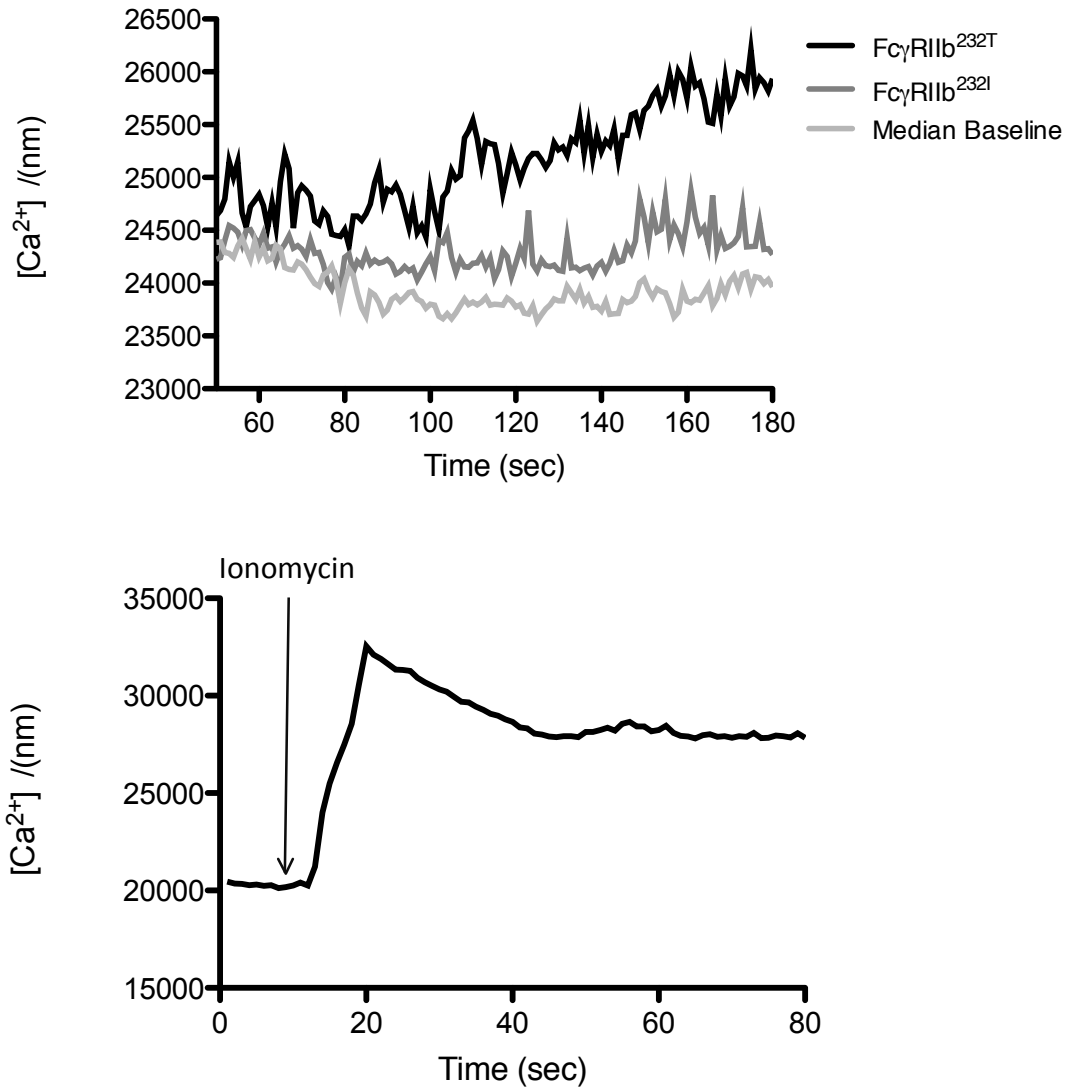


Fig 4.5: A more notable calcium response was observed during phagocytosis by $Fc\gamma RIIb^{232T}$ macrophages.

IgG latex beads were added to the cells expressing $Fc\gamma RIIb^{232I}$ and $Fc\gamma RIIb^{232T}$. $[Ca^{2+}]_i$ levels were monitored for 180s. Ionomycin (1mM final conc.) was used as a positive control for Indo-1 loading and maximum $[Ca^{2+}]_i$ flux.

4.6 Discussion

As a first line of defence against invading pathogens as well as for the clearance of apoptotic cells, the major function of phagocytosis is to mediate the internalization and elimination of these targets. During the course of phagosome maturation, an extraordinary array of microbicidal products are acquired that are essential for the efficient removal of internalized pathogens.

Phagocytosis is modulated by Fc receptors that are expressed on the cell surface. To study the relationship between the impact of the inhibitory Fc receptor on pathogen clearance, cells expressing the polymorphic Fc γ RIIb^{232T} and the wild type Fc γ RIIb^{232I} were allowed to internalize IgG coated latex beads for up to 105 min. Our results indicated that Fc γ RIIb^{232I} macrophages ingested latex beads less avidly than Fc γ RIIb^{232T} macrophages demonstrating enhanced phagocytosis of latex beads in Fc γ RIIb^{232T} macrophages.

As the role of the phagosome is to deliver the internalized material into a hydrolytic environment that will lead to its degradation, we next examined the influence of the amino acid 232 isoleucine to threonine mutation on the kinetics of phagosome maturation following particle internalization. This was accomplished by studying the recruitment of proteins associated with markers of phagolysosome maturation. We found that both the wild type Fc γ RIIb^{232I} and mutant Fc γ RIIb^{232T} acquired these markers of phagosome maturation but with differing kinetics of maturation. Fc γ RIIb^{232T} showed earlier acquisition of LAMP-1,

a phagolysosome marker implying that the mutation hastens the maturation process.

As phagosome maturation empowers the vacuole with a host of degradative properties central to the destruction of the invading pathogen, we proceeded to investigate the relationship between phagocytic activity and pathogen clearance in these cells. Detailed assays for phagosome maturation that are linked to the biological function of the phagosome as a degradative compartment were performed.

Firstly, we measured for the phagosome luminal pH during the maturation process, which is one of the key features of maturing phagosomes. Thus, the increasing acidity of the maturing phagosomal is a functional indicator of the phagosome maturation process. Phagosome acidification is an important maturation event that allows for the activation of digestive enzymes such as proteases and other lysosomal hydrolases that are involved in pathogen killing. Fc γ RIIb^{232T} macrophages exhibited a relatively rapid acidification of the phagosome in comparison to Fc γ RIIb^{232I} macrophages which displayed a slower acidification profile. This data supports the observation that macrophages expressing Fc γ RIIb^{232T} actually do mature more efficiently.

Phagosomal acidification is not the only microbicidal feature that is acquired during the maturation process. Macrophages also produce ROS which contribute to pathogen elimination. Therefore, we next sought to detect ROS produced in

Fc γ RIIb^{232I} and Fc γ RIIb^{232T} expressing cells. We observed that during phagocytosis, Fc γ RIIb^{232I} induced a gentler oxidative response in contrast to Fc γ RIIb^{232T} expressing cells which generated a higher production of ROS thus suggesting that it may participate more effectively in phagolysosome formation.

In addition to measurements of phagosome acidification and ROS production, we examined for intracellular calcium [Ca²⁺] elevations, which have been implicated in the regulation of early events in the phagocytic process. When phagocytosis was stimulated by the addition of IgG latex beads, an immediate increase in calcium signaling was observed. The [Ca²⁺] measurements also revealed that macrophages expressing the mutant Fc γ RIIb^{232T} exhibited a more robust [Ca²⁺] signaling than its wildtype Fc γ RIIb^{232I} counterpart. This is consistent with previous observations in which macrophages from Fc γ RIIb^{232T} mice exhibited heightened response in intracellular calcium flux [154].

Taken together, all our observations suggest that the Fc γ RIIb^{232T} macrophage is highly activated and aggressive in phagosome maturation – higher particle internalization was observed and this is coupled with an increased microbicidal activity. However, to prevent catastrophic autoimmune reactions, phagocytosis must be tightly regulated to limit damage to the host while allowing for optimal clearance and destruction of opsonized pathogens. This hyper-responsive state in Fc γ RIIb^{232T} macrophage may result from the failed negative regulation of phagocytosis.

The generation and release of microbicidal products such as hydrolytic enzymes and reactive oxygen species that are essential for normal host defense can result in significant tissue injury leading to autoimmunity and excessive inflammation if phagocytosis is not regulated [122]. Hence the inhibitory Fc γ RIIb plays a very important role in maintaining a delicate balance between adequate elimination of the pathogen to benefit the host and its failure which may result in a systemic inflammatory response.

While using targets such as latex beads provided for an excellent tool in dissecting the contributions of Fc γ RIIb^{232I} and Fc γ RIIb^{232T} in the mechanisms of phagocytosis, latex beads are inert and cannot be digested by cells. It would be interesting to investigate the interactions of these receptors on a pathogen to evaluate for the efficiency of phagocytosis. Therefore, we decided to extend our observations on a bacterial pathogen model to determine if the expression of Fc γ RIIb^{232I} and Fc γ RIIb^{232T} will contribute to functional differences in the phagocytic microbicidal machinery.

CHAPTER 5

RESULTS III: INVESTIGATING THE PHAGOCYtic BACTERICIDAL ACTION OF Fc γ RIIB^{232I} AND Fc γ RIIB^{232T} ON A PATHOGEN MODEL

5.1 Introduction

The immune response to phagocytosis must be controlled to ensure it is optimal for pathogen destruction while avoiding the consequences of excessive inflammation. Fc γ receptors are required for optimum immune activation. The balance of the activatory and inhibitory signals of these Fc receptors determines the threshold of phagocytosis and ensures for homeostatic clearance of invading pathogens. In this aspect, the inhibitory receptor Fc γ RIIb plays a pivotal role in providing an activation threshold, thereby regulating or terminating immune cell activation and hence contributes to immune homeostasis, which is crucial in inhibiting excessive inflammation [155].

We have shown that macrophages expressing Fc γ RIIb^{232T} displayed a more robust and efficient phagocytic response by engulfing latex beads at a higher rate, a faster kinetic in phagosome maturation and generated enhanced inflammatory responses characterized by higher levels of ROS and lower phagosomal pH compared to macrophages expressing Fc γ RIIb^{232I}.

In view of this, we sought to extend our observations of the phagocytic response of these macrophages on a physiological target such as the intracellular pathogen, *Mycobacterium bovis* (bacillus Calmette-Guérin) BCG, which typically resides within phagosomes [156].

5.2 Ensuring Fc receptor mediated phagocytic uptake

Bacterial pathogens display numerous ligands on their surface that allow for the recognition and engagement of multiple receptors which subsequently initiate internalization into the host cell [157].

Phagocytosis of mycobacteria such as *Mycobacterium bovis* BCG can be mediated by receptors such as complement receptors [158-160], mannose receptors [161], scavenger receptors [162-164], toll-like receptors [165] as well as Fc γ receptors [166].

To ensure the triggering of Fc receptor mediated phagocytosis of the mycobacteria, BCG was opsonized with an antibody targeting lipoarabinomannan (LAM), a major mycobacterial cell wall component (2F12) (a gift from Brandon Hanson, DSO Laboratories). As the terminal mannosyl units of LAM are ligands for the mannose receptor, the extent of BCG opsonization was examined by pretreatment of U937 cells with 2.5 mg/ml of mannan which inhibits uptake through mannose receptors [167] or pretreatment with a commercial Fc receptor blocking reagent which selectively blocks uptake via Fc receptors prior to infection. Treated cells were then allowed to phagocytose the 2F12 opsonized GFP labeled BCG (MOI 10) for up to 105 min and the fluorescence was monitored using flow cytometry.

While mannan pretreatment did not impact upon 2F12-BCG GFP internalization, blocking of Fc receptors abrogated the uptake of the opsonized BCG, strongly

indicating that entry is Fc receptor rather than mannose receptor mediated (**Fig 5.1**). Thus, we have established a model for Fc receptor mediated phagocytosis of mycobacteria.

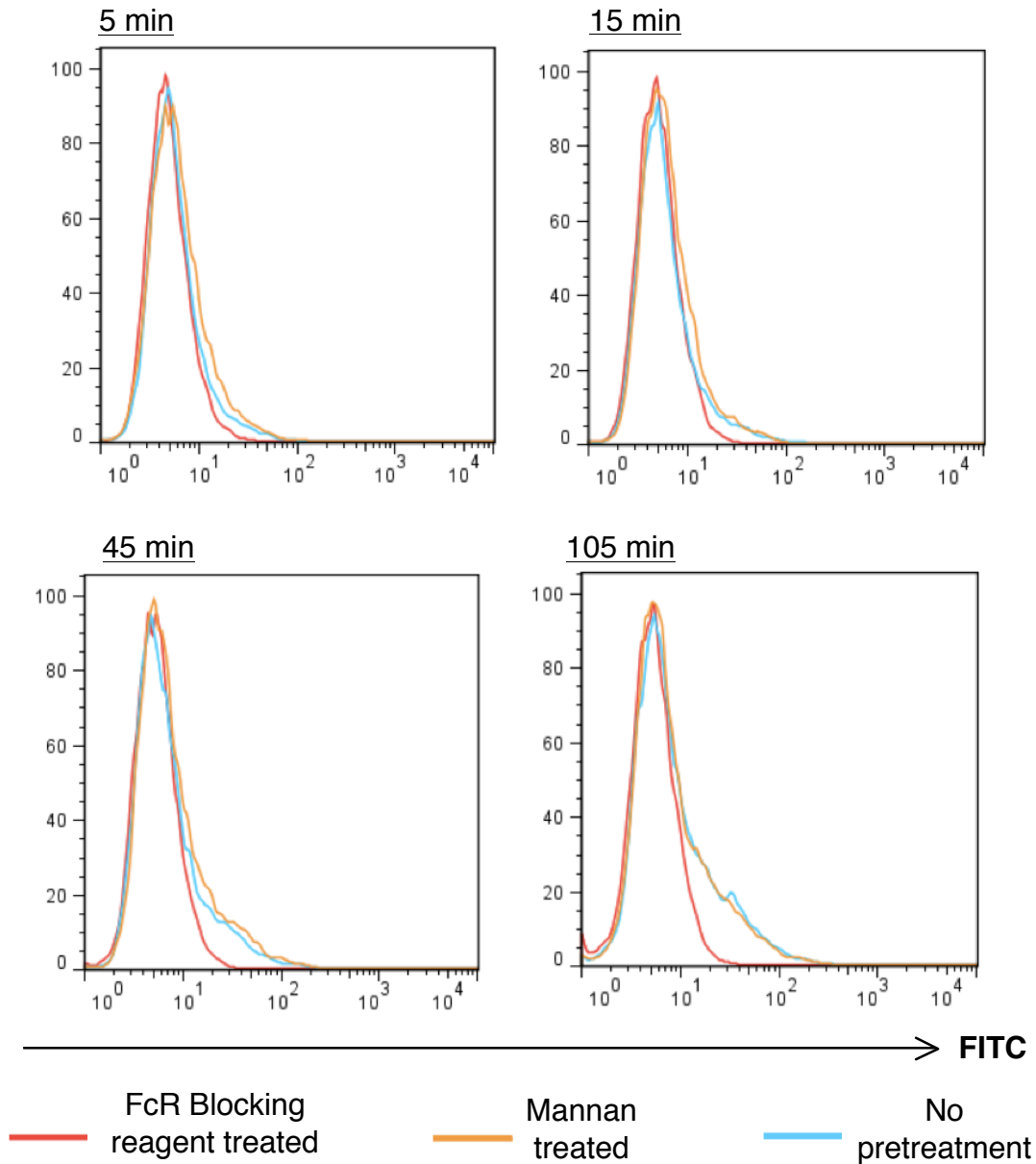


Fig 5.1: Anti-2F12 opsonized BCG activates Fc γ receptor mediated phagocytosis.

U937 cells were pre-incubated with either mannan or Fc receptor blocking reagent or left untreated as a control. IgG opsonized GFP labeled BCG were added to the cells. Binding of opsonized BCG to mannose receptors appeared to be inhibited with the addition of mannan as the uptake profile was similar to untreated cells suggesting that antibody opsonized GFP BCG engages Fc γ receptors for entry into the cell. Treatment of cells with Fc blocking reagent displayed reduced ability to phagocytose IgG-coated BCG, confirming that entry is indeed Fc receptor mediated.

5.3 Measurement of bacterial ingestion and killing

Inhibitory Fc receptors are well-established negative regulators of phagocytosis [38]. We have shown that the expression of Fc γ RIIb^{232T} results in hyperactive phagocytosis of latex bead particles however latex beads are inert particles and resistant to degradation by microbicidal products generated during phagocytosis. To pursue the understanding of the functional implications of this mutation in the context of phagocytosis, we studied for the ability of the wild type Fc γ RIIb^{232I} and the mutant Fc γ RIIb^{232T} inhibitory receptors on pathogen elimination, which is the key function of phagocytosis.

The efficiency of pathogen elimination was evaluated by measuring the ability of the macrophages to kill the bacteria they have internalized. Bacterial colonies were enumerated before and at the end of the infection period. A reduction in the numbers of colony-forming units (CFU) indicates that bacteria were killed by the macrophage while an increase in bacterial colonies indicates that bacteria were able to survive and replicate within the macrophages.

This was performed by infecting macrophages expressing Fc γ RIIb^{232I} and Fc γ RIIb^{232T} with BCG at an MOI of 2 for 1h. Extracellular bacteria were removed by washing and the amount of internalized bacteria was enumerated by plating the infected cell lysates onto 7H11 agar. The number of bacterial colonies represent bacterial uptake.

Macrophages expressing the mutant Fc γ RIIb^{232T} had more internalized BCG in contrast to its wild type Fc γ RIIb^{232I} counterpart (**Fig 5.2**). This mirrors the observation on the uptake of latex beads assayed previously and consistently illustrates that the phagocytic response to the uptake of foreign particles by macrophages is dramatically altered as a consequence of the mutation in Fc γ RIIb^{232T}.

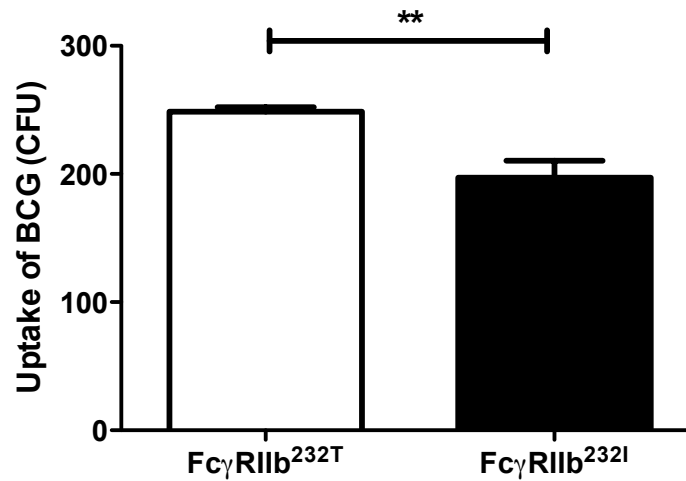


Fig 5.2: FcγRIIb^{232T} expressing macrophages internalize more mycobacteria.

Macrophages were infected with BCG for 1h after which the infected cells were lysed and internalized BCG were quantified. Compared with FcγRIIb^{232I}, macrophages expressing FcγRIIb^{232T} were significantly more efficient in the uptake of BCG into the cell. Data is representative of four independent experiment performed in quadruplicates **p < 0.01.

We next determined the killing kinetics of the internalized BCG by further incubating the infected macrophages over a period of seven days (**Fig 5.3**). The subsequent decrease in CFU of these bacteria following uptake of BCG on day one is indicative of initial killing. However, the exponential increase in CFU over time reflected the expansion of viable mycobacteria as the infected macrophages were unable to completely destroy the internalized BCG and which were able to grow and multiply within the cell.

The macrophages expressing Fc γ RIIb^{232T} showed a significantly lower increase in the percentage of viable CFU over the seven days compared to macrophages expressing Fc γ RIIb^{232I}. This signifies that the mutation in Fc γ RIIb^{232T} renders the macrophage with a greater capacity to limit or reduce the growth of bacteria, complementing data from phagocytosis of latex beads.

To evaluate the influence of the inhibitory Fc γ RIIb receptor and bacterial load on phagocytosis, macrophages were infected at an increased MOI of 1:10 (**Fig 5.4**). Macrophages both expressing the wild type Fc γ RIIb^{232I} and mutant Fc γ RIIb^{232T} showed increased phagocytosis when exposed to the five-fold increment in the number of BCG but the ability of the mutant Fc γ RIIb^{232T} to kill the phagocytosed BCG was still observed to be significantly more efficient. This confirms that the mutant receptor Fc γ RIIb^{232T} expressing macrophages have enhanced phagocytic activity as compared to the wild type Fc γ RIIb^{232I} expressing counterparts.

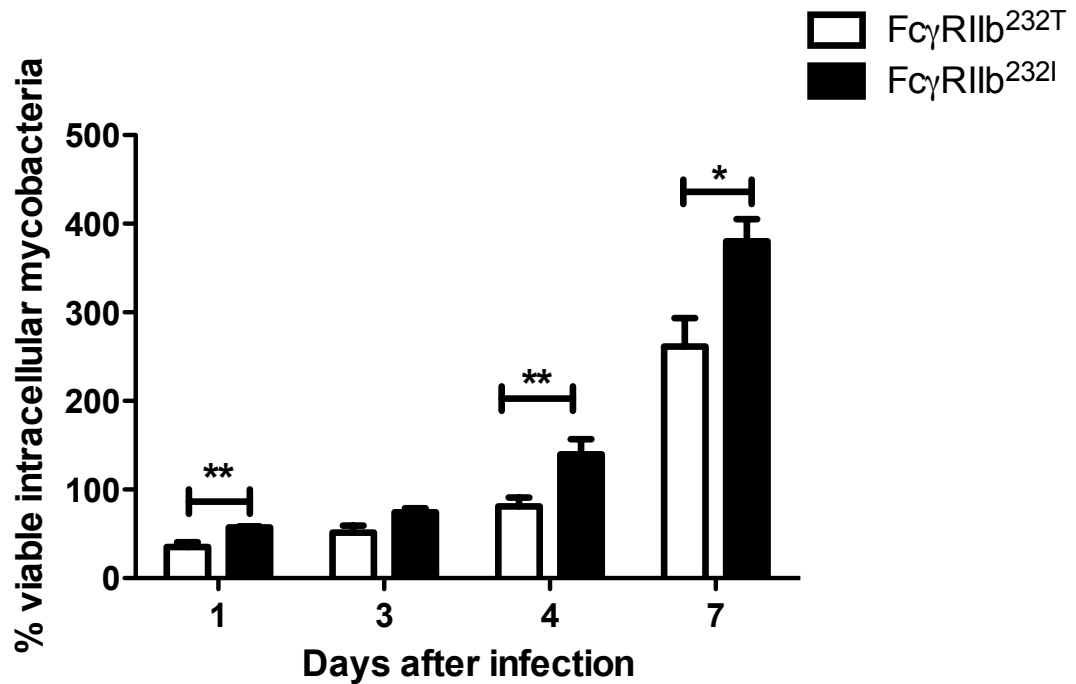


Fig 5.3: Macrophages expressing Fc γ R11b^{232T} have a much higher capacity to kill ingested bacteria as compared to Fc γ R11b^{232I} expressing macrophages.

The ability of the macrophages to kill the internalized bacteria was assessed by the number of CFU derived from macrophages that were lysed at several time points after post infection at a MOI of 2.

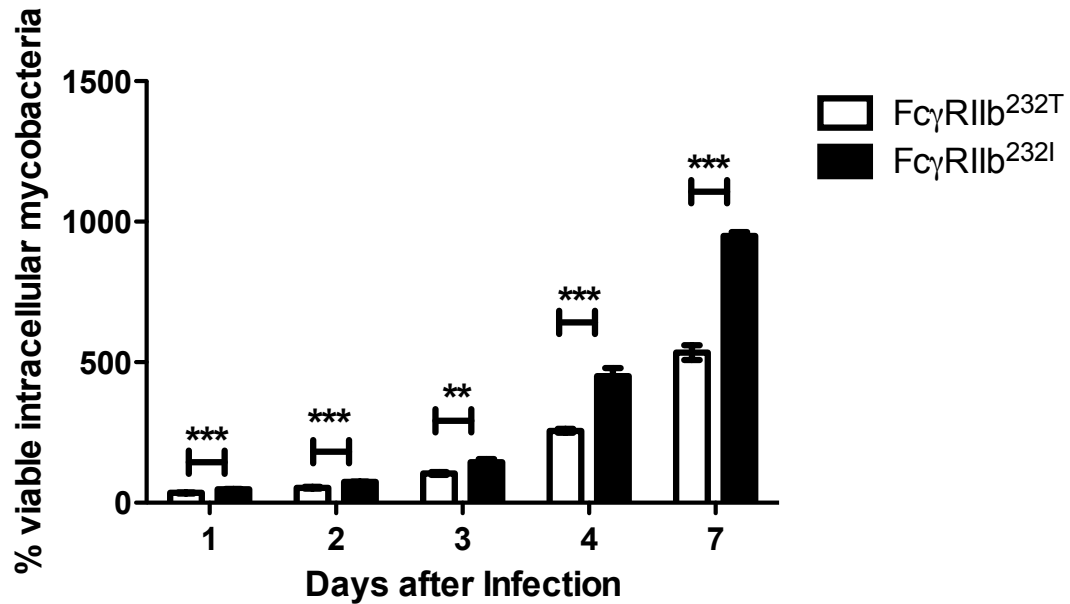


Fig 5.4: Killing capacities of macrophages were not affected by the increased bacterial burden.

Survival counts evaluating killing of BCG after infection of macrophages at a MOI of 10. Macrophages expressing Fc γ RIIb^{232T} were more efficient in bacterial killing as seen by the significantly slower increase in BCG CFU over time in comparison to macrophages expressing Fc γ RIIb^{232I}.

5.4 Assessment of inflammatory cytokines following phagocytosis

Inherent to their killing capacity, pathogen internalization by macrophages stimulates a robust inflammatory response, which is accompanied by the production of pro-inflammatory cytokines [157].

Cytokines are small protein molecules (8-26 kD), which are synthesized by cells of the immune system. Cytokines are important mediators of intracellular communication. Circulating concentrations of pro-inflammatory cytokines are low and undetectable in healthy individuals. However, their production is stimulated during host invasion resulting in the generation of an effective primary immune response for clearing an infection as they transiently upregulate macrophage functions such as phagocytosis and the release of inflammatory mediators [155, 168]. Cytokines can also increase the microbicidal potential of phagocytes. For example, IL-8 and TNF- α , are produced by monocytes, macrophages and other cell types at sites of infection for the recruitment other immune cells to the site of infection and thus are often found upregulated in infection [169]. The production of INF- γ has been documented to enhance the oxidative burst contributing to intracellular killing of pathogens. In addition, cytokines such as G-CSF participates in the phagocytic process by enhancing the levels of ROS produced by the cell [170]. However, studies have shown that an overwhelming production of these mediators can lead to multiple organ failure and ultimately shock and death [171].

Since Fc γ receptors are known to trigger inflammatory reactions in response to IgG opsonized pathogens, we sought out to assess the amplitude of the inflammatory responses of macrophages expressing Fc γ RIIb^{232I} or Fc γ RIIb^{232T} in response to pathogen internalization by measuring the secretion of cytokines after infection with opsonized BCG at MOI of 10. Cytokine production in response to phagocytosis of BCG was normalized by the deduction in basal levels of cytokine produced in uninfected controls. The culture supernatant was harvested after 24h and 48h post-infection and the cytokines secreted by the cells were assayed in duplicates using a 10-plex cytokine array. The panel of cytokines included: IL-1 β , IL-2, IL-6, IL-8, IL-10, G-CSF, MIP-1 α , MIP-1 β , INF- γ and TNF- α .

We found that after 24h post-infection, the levels of IL-1 β and TNF- α were similar in both cell types but were observed to be elevated after 48h post-infection in the macrophages expressing Fc γ RIIb^{232T} (**Fig 5.5**). Increased levels of IL-6, IL-8, G-CSF, INF- γ , MIP-1 α and MIP-1 β were detected in Fc γ RIIb^{232T} macrophages as compared to Fc γ RIIb^{232I} macrophages in response to BCG infection at both 24h (**Fig 5.6**) and 48h (**Fig 5.7**). However, low levels of IL-10, a potent deactivator of monocytes believed to limit the intensity of immune and inflammatory reactions were detected [172] (data not shown).

The heightened levels of cytokines are consistent with observations of overproduction of inflammatory cytokines found in SLE patients. For example, elevated levels of INF- γ [173, 174] and increased levels of IL-6 [175, 176] have

been found in the serum of SLE patients. High levels of TNF- α have also been reported in patients with SLE [176-178]. TNF- α has also been found to be a key player in the inflammatory diseases such as rheumatoid arthritis [179]. TNF- α also stimulates the production of IL-1 and IL-6 [180]. Elevated IL-6 has been closely correlated with disease activity in SLE [181]. More interestingly, overproduction of TNF- α and IL-6 have been shown to be associated with Fc γ RIIb deficient mice that demonstrated increased phagocytosis in response to *Streptococcus pneumoniae* [155].

These observations indicate that phagocytosis of BCG by macrophages expressing Fc γ RIIb^{232T} released higher levels of inflammatory cytokines reflecting a more pro-inflammatory response as compared to phagocytosis by Fc γ RIIb^{232I} macrophages. This also implies that the secretion of inflammatory cytokines appears to be very highly influenced by the expression of Fc γ RIIb on the cell surface. An overwhelming production of these inflammatory mediators may contribute to the amplification of tissue inflammation and organ damaged observed in patients with SLE [182-184].

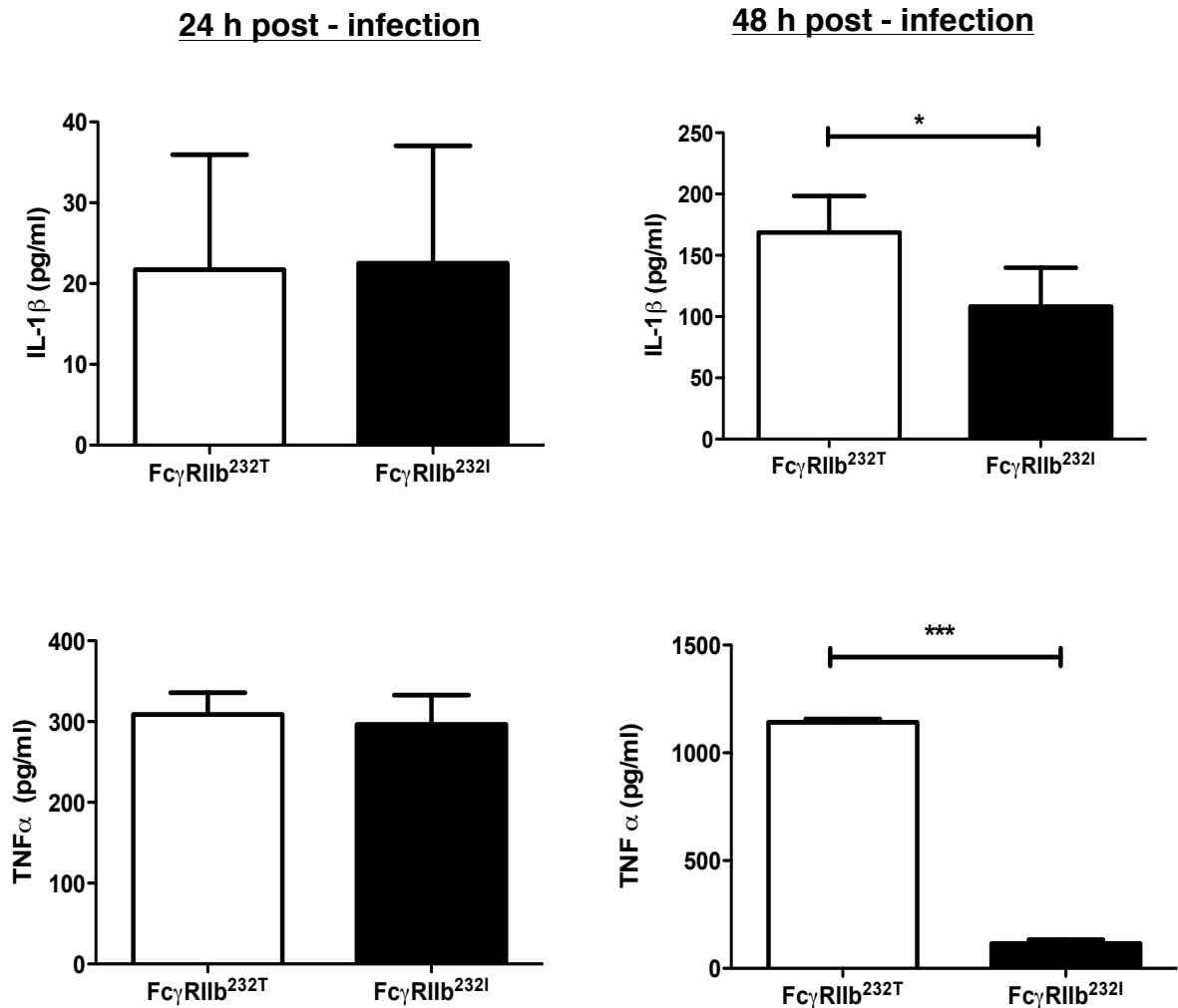


Fig 5.5: Macrophages expressing $Fc\gamma RIib^{232T}$ secrete higher levels of IL-1 β and TNF- α 48h following BCG infection.

Inflammatory response was assessed after incubation with opsonized BCG for 24h and 48h. IL-1 β and TNF- α levels were higher in $Fc\gamma RIib^{232T}$ only after 48h post-infection with IgG opsonized BCG.

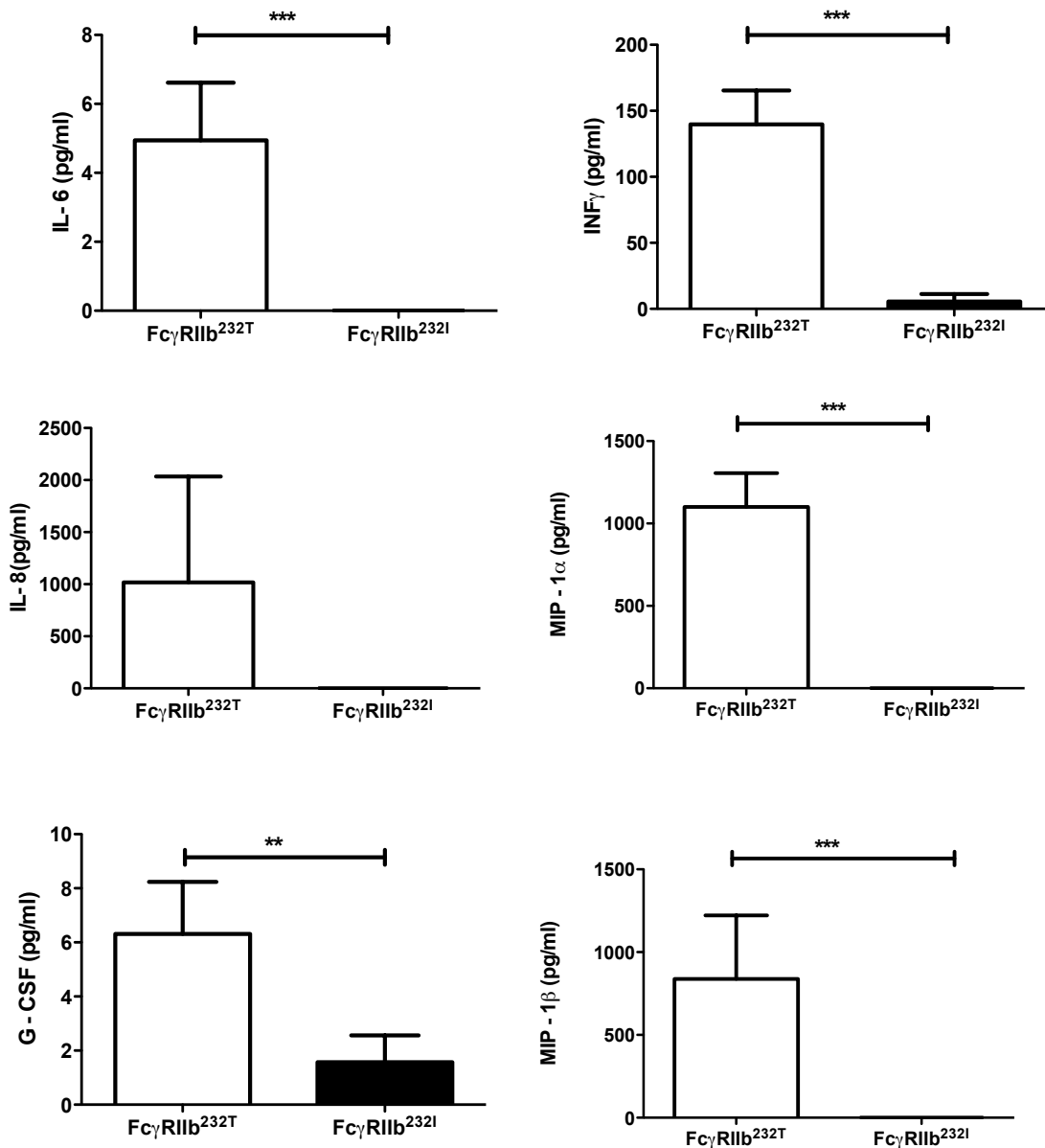
24 h post - infection

Fig 5.6: Pro-inflammatory cytokine secretion was enhanced by macrophages expressing Fc γ RIIb^{232T} following 24 h incubation with BCG.

Results were normalized against basal levels present in uninfected cells. We observed trends of significantly higher production of inflammatory cytokines 24 h after phagocytosis of IgG opsonized BCG in macrophages expressing Fc γ RIIb^{232T} compared to Fc γ RIIb^{232I}.

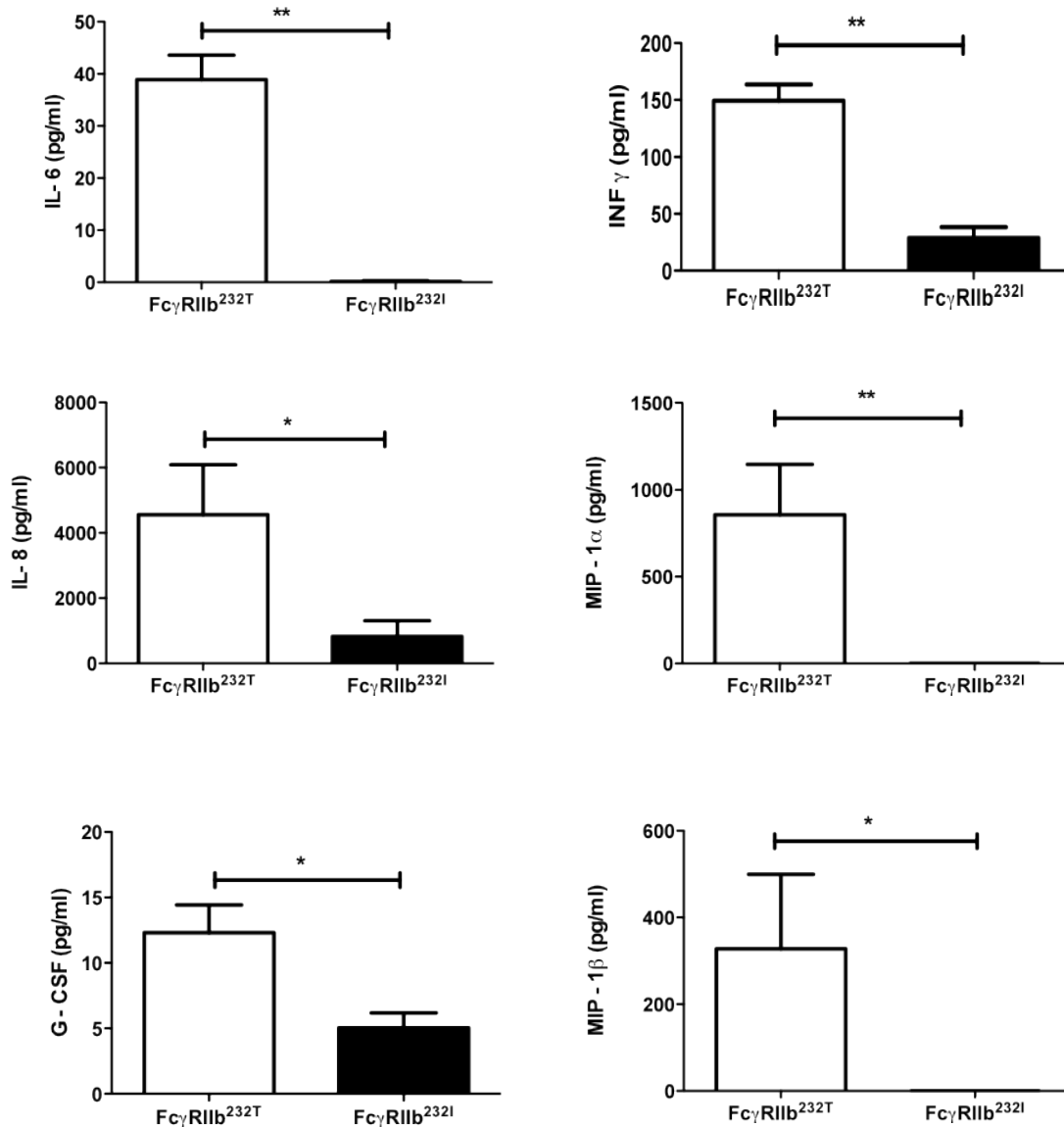
48 h post – infection

Fig 5.7: Increased production of pro-inflammatory cytokines 48 h after Fc γ receptor phagocytosis of BCG by Fc γ RIIb^{232T} macrophages.

Culture supernatant obtained from 48 h incubation with IgG opsonized BCG was examined for the secretion of cytokines. Production of inflammatory cytokines in response to phagocytosis of BCG was exaggerated in macrophages expressing Fc γ RIIb^{232T} compared to Fc γ RIIb^{232I}.

5.5 Discussion

Fc receptors bind to IgG opsonized pathogens to mediate phagocytosis, yet the macrophage may bind and internalize a pathogen but yet not be able to kill it. Since pathogen elimination is the key function of phagocytosis, we examined the killing capacity of macrophages expressing Fc γ RIIb^{232I} and Fc γ RIIb^{232T} against bacterial pathogens such as *Mycobacterium bovis* BCG and measured a panel of pro-inflammatory cytokines secreted during this process.

Effective opsonization of *Mycobacterium bovis* BCG by anti-2F12 ensures binding and internalization of the bacteria via Fc γ receptors for killing by macrophages expressing either the wild type or the mutant inhibitory Fc γ receptor, Fc γ RIIb^{232I} and Fc γ RIIb^{232T} respectively.

Similar to observations obtained with latex beads, experiments performed with BCG displayed increased bacterial uptake in macrophages expressing the mutant Fc γ RIIb^{232T} receptor in comparison to the wild type Fc γ RIIb^{232I} verifying that the targeted mutation in the inhibitory receptor is sufficient for macrophages to exhibit a hyper-aggressive phenotype in which these macrophages ingest increased amounts of foreign particles or pathogens.

The ability of the macrophage to kill the internalized bacteria was measured by a straightforward assay in which bacterial colonies are enumerated before and after a killing period. Intracellular bacterial killing was expressed as a percentage relative to the number of bacteria ingested. Accordingly, the kinetic studies

revealed that of Fc γ RIIb^{232T} had an enhanced ability in controlling intracellular BCG relative to wild type Fc γ RIIb^{232I} during the 7-day assay period. In addition, we also found that the function of this killing ability was not affected by bacterial load.

It would appear that a lower internalization rate of BCG by Fc γ RIIb^{232I} leads to a decreased intracellular killing capacity while in Fc γ RIIb^{232T}, the increased number of ingested bacteria leads to an enhancement of killing capacity. This suggests the demand in the number of internalized bacteria might influence the activation of killing mechanisms in the cell.

During phagocytosis of pathogens, infected macrophages trigger classical pro-inflammatory cytokine cascades as a powerful bactericidal mechanism in addition to a wide variety of mediators to kill and neutralize pathogens. The secretion of inflammatory cytokines is important in generating an effective primary immune response and in clearing an infection. Thus, we sought to analyze the secretion of a panel of these inflammatory cytokines in response to pathogen killing when macrophages expressing the wild type Fc γ RIIb^{232I} and the mutant Fc γ RIIb^{232T} were differentially activated in response phagocytosis.

Cytokine production was induced following interaction with IgG opsonized BCG. Macrophages expressing Fc γ RIIb^{232T} were observed to result in a more pro-inflammatory profile with increased levels of IL-6, IL-8, G-CSF, INF- γ , MIP-1 α and

MIP-1 β 24 h and 48 h after phagocytosis of BCG, while levels of IL-1 β and TNF- α were significantly enhanced 48 h post-phagocytosis.

These results suggest the contribution of the inhibitory receptor and its targeted disruption of function in the tight regulation of inflammatory mediators produced during an immune response, thereby limiting the cytokine-driven inflammation caused by the excessive release, which may otherwise lead to autoimmunity [185].

In summary, the data demonstrates that the expression of the mutant Fc γ RIIb^{232T} results in heightened phagocytic responses and superior bactericidal activity and is associated with the enhanced production of pro-inflammatory cytokines induced by Fc receptor-mediated phagocytosis. This highlights the importance of Fc γ RIIb in preventing excessive or inappropriate cell activation, which is associated with autoimmunity.

CHAPTER 6

RESULTS IV: Lipidomic Fingerprinting and Analysis

6.1 Introduction

Although numerous studies have demonstrated that the lipid environment at the phagocytic cup and the phagosome plays a critical role in orchestrating signaling events leading to successful phagocytosis [57, 84], a comprehensive and quantitative analysis of the lipid composition during phagocytosis has yet to be conducted.

To better understand the molecular mechanisms involved in phagocytosis, we sought to comprehensively characterize the lipid composition of latex bead phagosomes via an LC-MS/MS platform. This will allow us to determine which lipids are present and the concentration of each lipid at each specific phagocytosis stage. Additionally, the effect of the presence/absence of Fc γ RIIb^{232T} on the lipid composition was assessed to provide insights into the understanding of the effect of the polymorphic Fc γ RIIb^{232T}.

6.2 Lipid composition of plasma membrane

As phagosome membranes are believed to derive from the plasma membrane, individual lipid classes from the plasma membrane were measured. Lipids were extracted using Bligh and Dyer extraction method and subjected to mass spectrometry (for details, please refer to Chapter 2, Materials and Methods). The composition of the plasma membrane may provide important information regarding lipids present or involved during initial stage of phagocytosis such as the interaction of the target particle with the cell.

Analyses of the total lipid fraction of the individual lipid classes of the plasma membrane were shown in **Fig 6.1**. Plasma membranes are enriched in sphingolipids and sterols. Correspondingly, lipids extracted from plasma membranes of U937 $\text{Fc}\gamma\text{RIIb}^{232\text{I}}$ and $\text{Fc}\gamma\text{RIIb}^{232\text{T}}$ macrophages were most abundant in PC and cholesterol. PC comprised of ~ 30 to 50 % of total lipid while cholesterol made up ~ 20 to 40 % of the total lipid. The levels of PC, PG, Cer and Cho species were significantly different between $\text{Fc}\gamma\text{RIIb}^{232\text{I}}$ and $\text{Fc}\gamma\text{RIIb}^{232\text{T}}$. The concentration of other lipid species such as PE, PS, PI and SM were similar in both cell types, however, detailed analyses reveal many significant differences in the distribution of individual lipid species between the plasma membrane of cells from $\text{Fc}\gamma\text{RIIb}^{232\text{I}}$ and $\text{Fc}\gamma\text{RIIb}^{232\text{T}}$ (**Fig 6.2**).

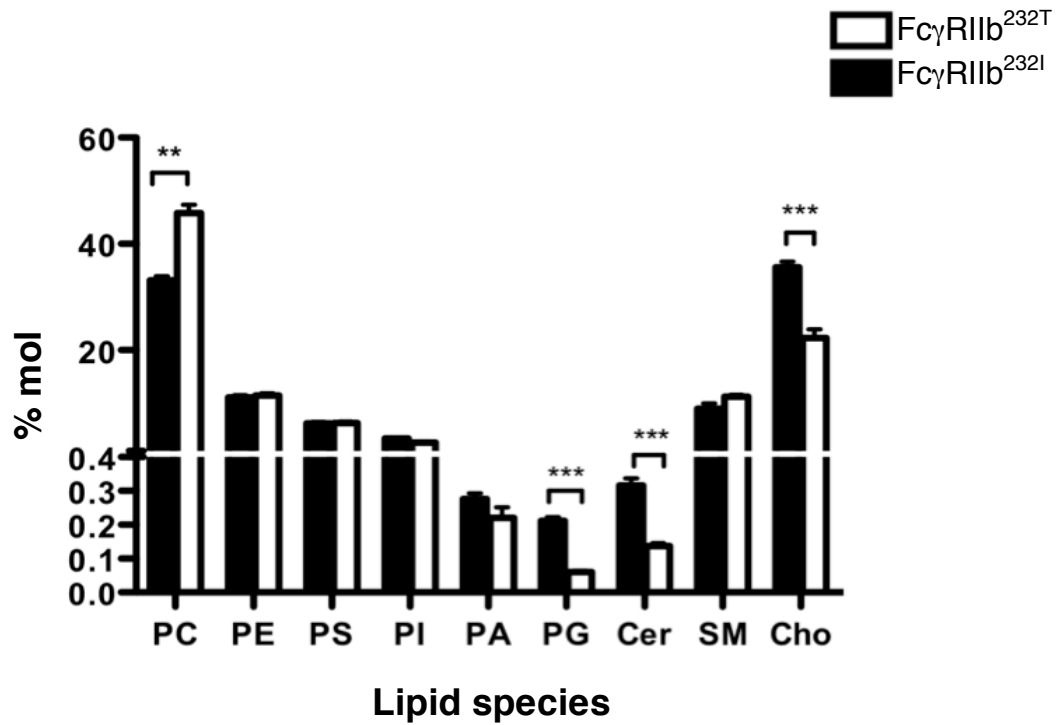


Fig 6.1: Major lipid species in the plasma membrane.
Comparison of total molar fraction of phospholipid and sphingolipid species in plasma membrane.

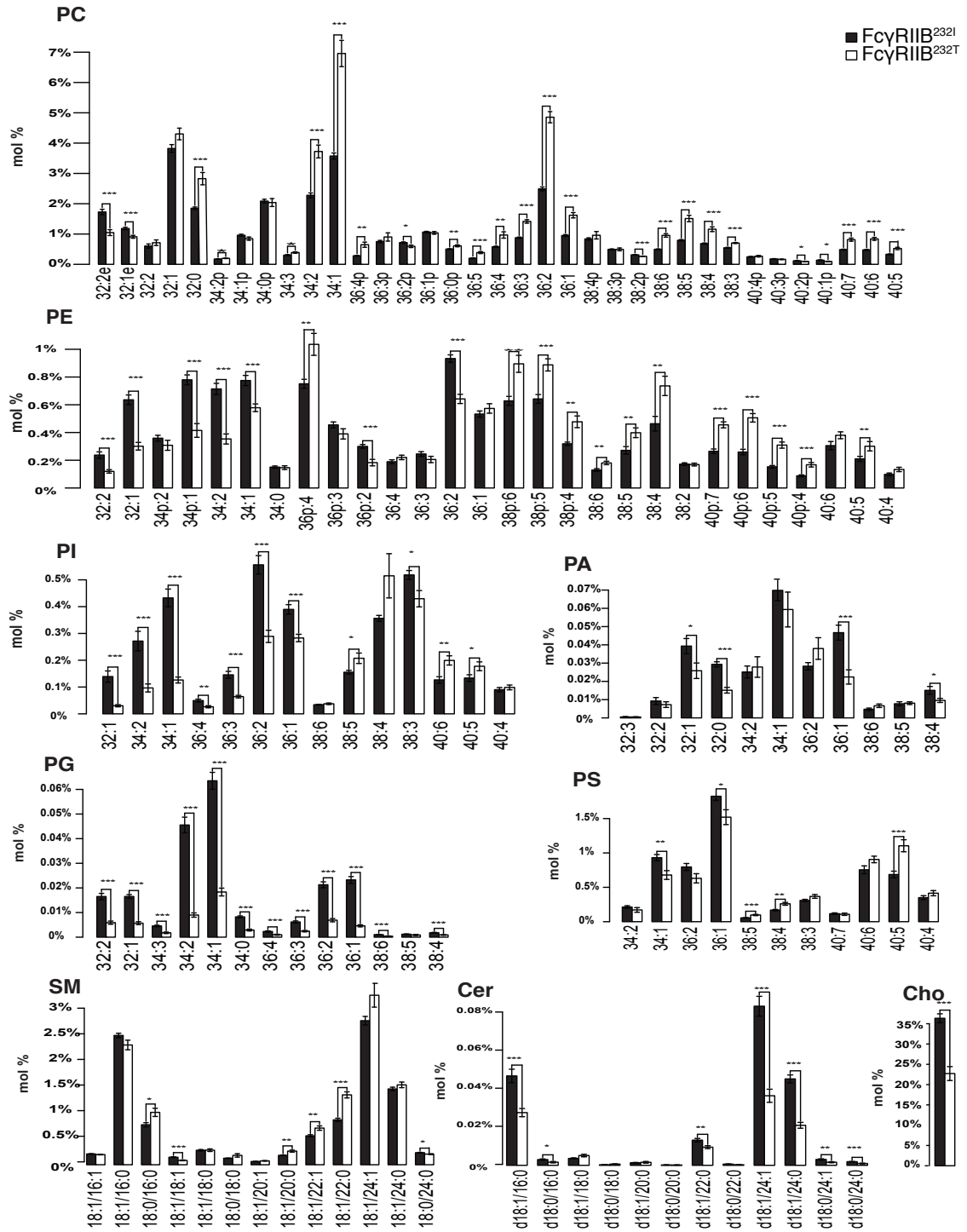


Fig 6.2: Individual lipid species in the plasma membrane revealed significant differences between FcγRIIb^{232I} and FcγRIIb^{232T} macrophages.

In addition, plasma membrane expressing the wild type Fc γ RIIb^{232I} also expresses significantly higher levels of Cer and Cho. The increased levels of Cer and Cho hint that the substitution of the wild type Fc γ RIIb^{232I} for the polymorphic Fc γ RIIb^{232T} on the plasma membrane can affect the properties of plasma membrane. To investigate if the length of the acyl chains of the phospholipids were affected, we quantified the acyl chains accordingly: Short (up to 32 C atoms), medium (up to 36 C atoms) and long chain species (\geq 38 C in acyl chains). The differences are illustrated in **Fig 6.3**. Fc γ RIIb^{232I} was detected to have trends showing higher levels of short and medium acyl chains and lower levels of long acyl chains with the exception of PC in which Fc γ RIIb^{232T} had higher levels of medium acyl chains (\sim 28 mol % vs \sim 18 mol %). The reverse trends were observed for plasma membrane expressing Fc γ RIIb^{232T}. For example, compared to PE acyl chains of Fc γ RIIb^{232T}, plasma membranes expressing Fc γ RIIb^{232I} contained more PE species with 32 carbon chains (\sim 1 mol % vs \sim 0.5 mol %) and 36 carbons (\sim 6 mol % vs \sim 5 mol %) but fewer PE species with more than 38 carbons (\sim 4 mol % vs \sim 6 mol %).



 FcγRIIb^{232T}

 FcγRIIb^{232I}

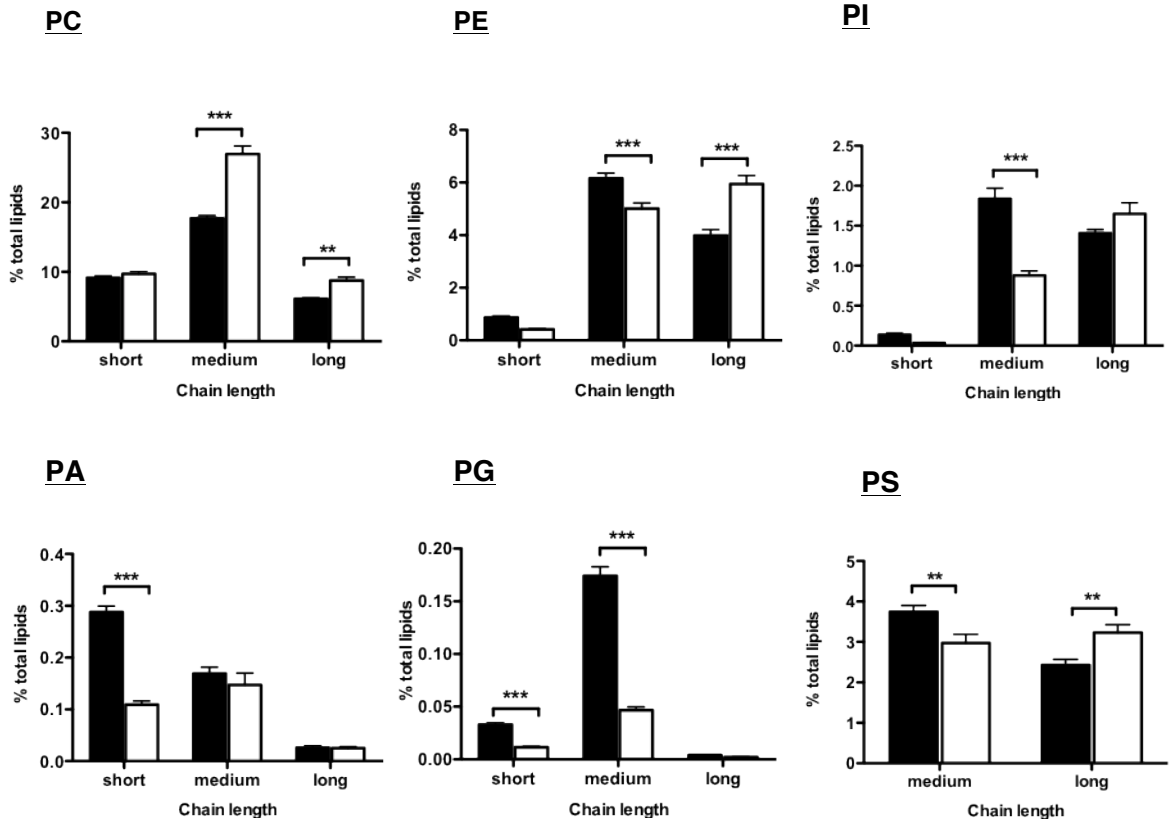


Fig 6.3: FcγRIIb^{232T} resulted in increased levels of phospholipid species with long acyl chains.

Lipid profiles demonstrate that FcγRIIb^{232I} contains higher levels of short chain phospholipid species while FcγRIIb^{232T} consisted of higher phospholipids with long acyl chains.

We quantified the degree of saturation to further investigate the impact on Fc γ RIIb^{232I} and/or Fc γ RIIb^{232T} on the plasma membrane (**Fig 6.4**).

PC and PE, both major structural phospholipids of the plasma membrane display a trend of polyunsaturated species with ≥ 3 double bonds in Fc γ RIIb^{232T} containing membranes. An increase in the number of double bonds increases membrane fluidity. In contrast, plasma membrane expressing Fc γ RIIb^{232I} was observed to have a trend of more saturated, monounsaturated and disaturated lipids and a reduction in polyunsaturated lipids. For instance, the concentration of polyunsaturated PC and polyunsaturated PE species detected were ~ 15 mol % vs ~ 23 mol % and ~ 6 mol % vs 8 mol % respectively.

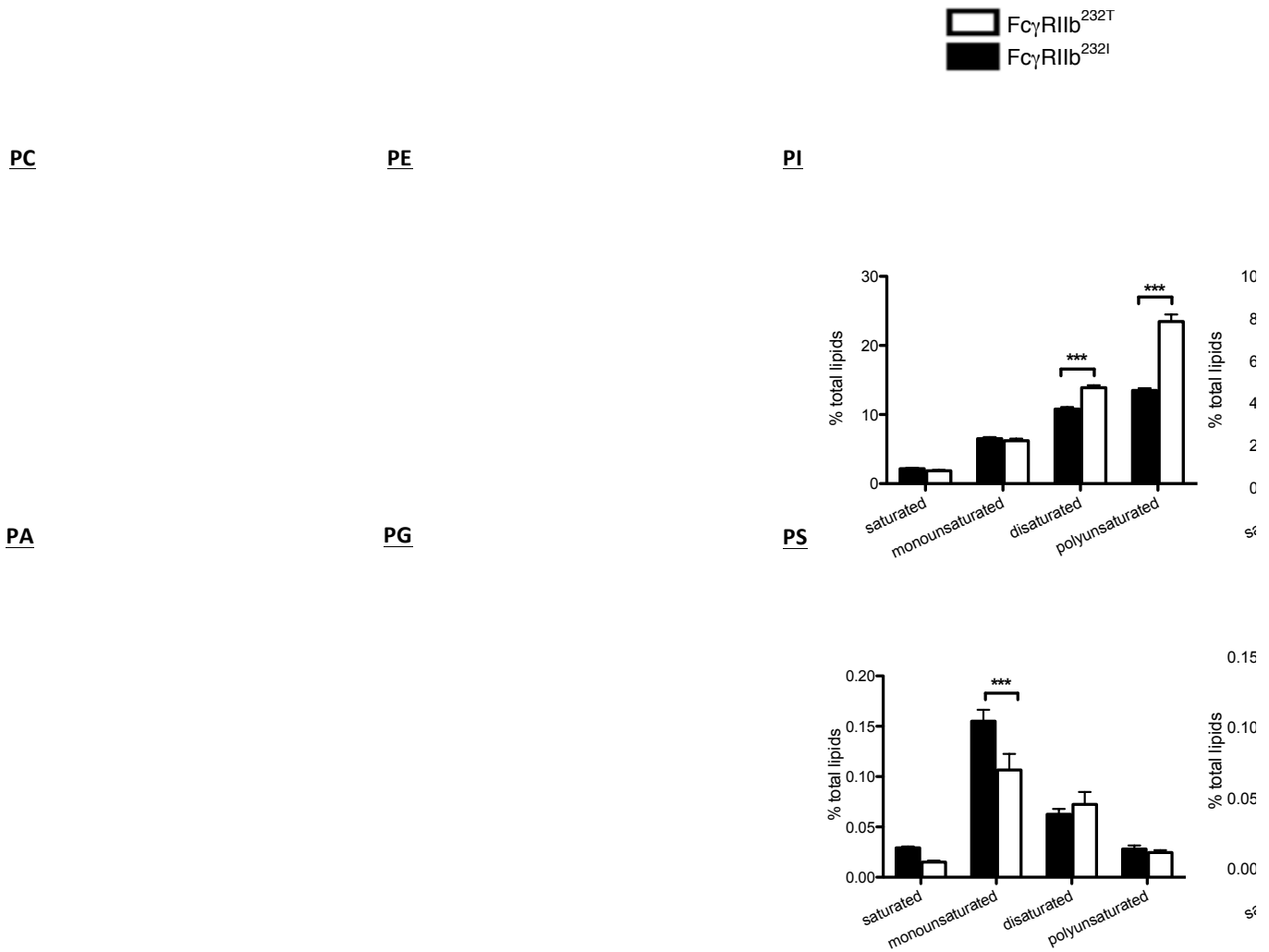


Fig 6.4: Impact of Fc γ RIIb^{232I} or Fc γ RIIb^{232T} on saturation of plasma membrane phospholipids.

More saturated, monounsaturated and disaturated phospholipids were detected in plasma membrane expressing Fc γ RIIb^{232I} compared to its polymorphic Fc γ RIIb^{232T} variant, which displayed increase in the levels of polyunsaturated phospholipids.

6.3 Lipid composition in maturing phagosomes

After determining the lipid composition of the plasma membrane, the next step was to examine and monitor the lipid composition changes as phagosomes age. Highly purified phagosomes were isolated at 5 min (early phagosome), 45 min (late phagosome) and 105 min (phagolysosome) to study the potential significance of the lipid composition during phagosome maturation. Additionally, we aimed to analyze if there were differences in lipid composition of phagosomes derived from plasma membrane expressing the wild type inhibitory receptor FcγRIIb^{232I} from the polymorphic inhibitory receptor FcγRIIb^{232T}. These differences are summarized in **Fig 6.5**. Our lipidomic analysis revealed comparable concentration of the classes of lipids in both cell types. The most abundant lipids detected in phagosome membranes were PC and Cho. Interestingly, differences in lipid trends from major lipid classes were observed. For example, in FcγRIIb^{232I} phagosomes; PC, PE, and SM levels increase as phagosomes mature while Cho decrease. The progressive decline in Cho levels could be attributed to the fission and fusion process as the phagosome progresses along the endocytic pathway. Maturing phagosomes also exhibited an increase in LBPA. LBPA is enriched in late endosomes and lysosomes.

In contrast, FcγRIIb^{232T} phagosomes displayed the reverse trend with PC, PE, and SM levels decreasing and Cho levels increasing as phagosomes mature. These differences in major lipid classes revealed that the phagosomal membrane

between the Fc γ RIIb^{232I} and Fc γ RIIb^{232T} are distinct and could contribute to differences in phagosome function and/or maturation.

While there are no significant changes for the levels of most lipid classes, we compared the individual lipid species during phagosome maturation to examine the consequences of Fc γ RIIb^{232T} mutation in greater detail. The resulting comparison of phagosome lipids from Fc γ RIIb^{232I} and Fc γ RIIb^{232T} illustrates striking differences in individual levels of many lipid species (**Fig 6.6, refer to Appendix 2**).

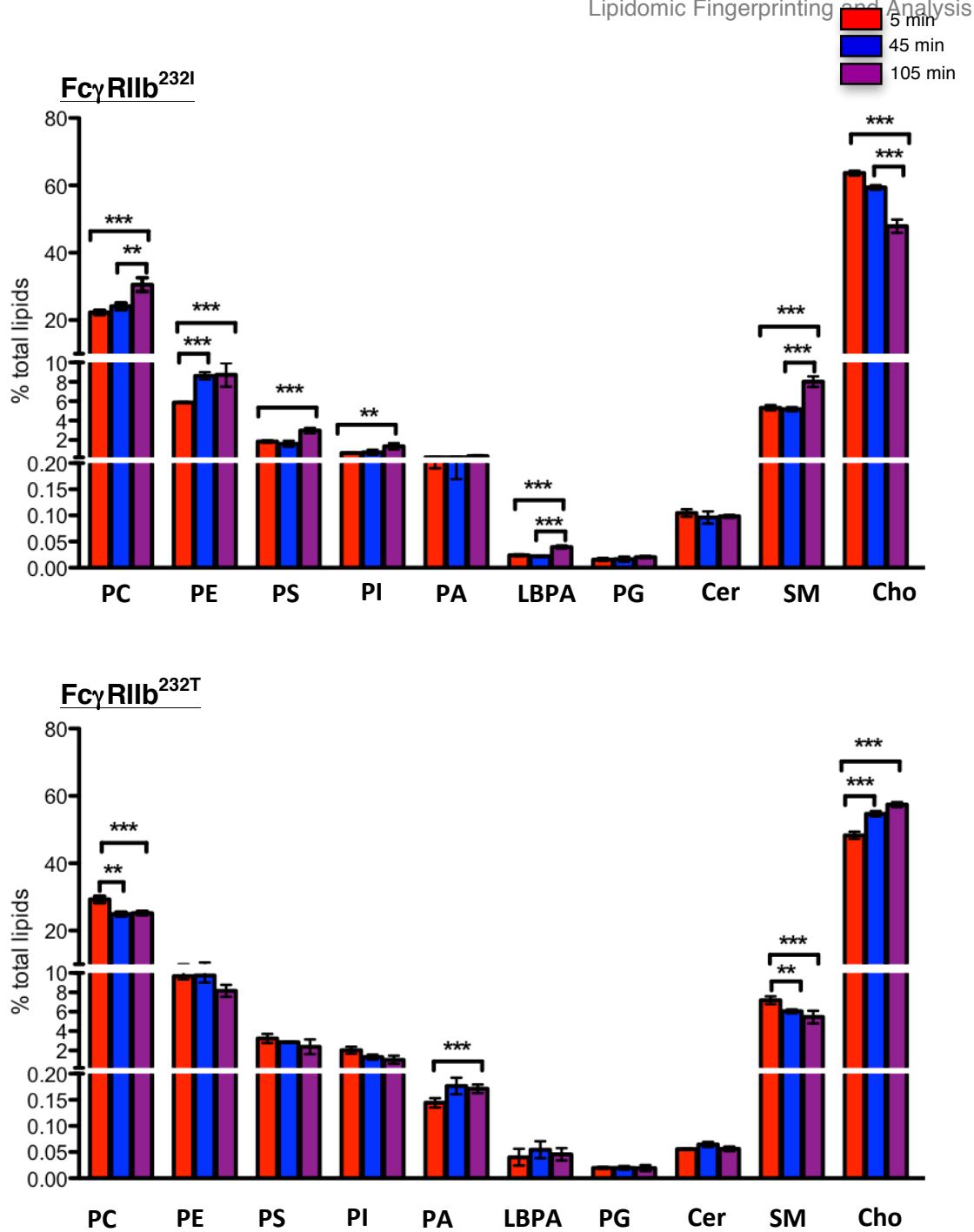


Fig 6.5: Comparison of phagosomal lipids from Fc γ RIIb^{232I} and Fc γ RIIb^{232T} macrophages.

Lipid composition of phagosomal membranes isolated after 5 min (red bars), 45 min (blue bars) and 105 min (purple bars). The data are a representative set of three independent experiments containing 24 samples per time point (n = 3).

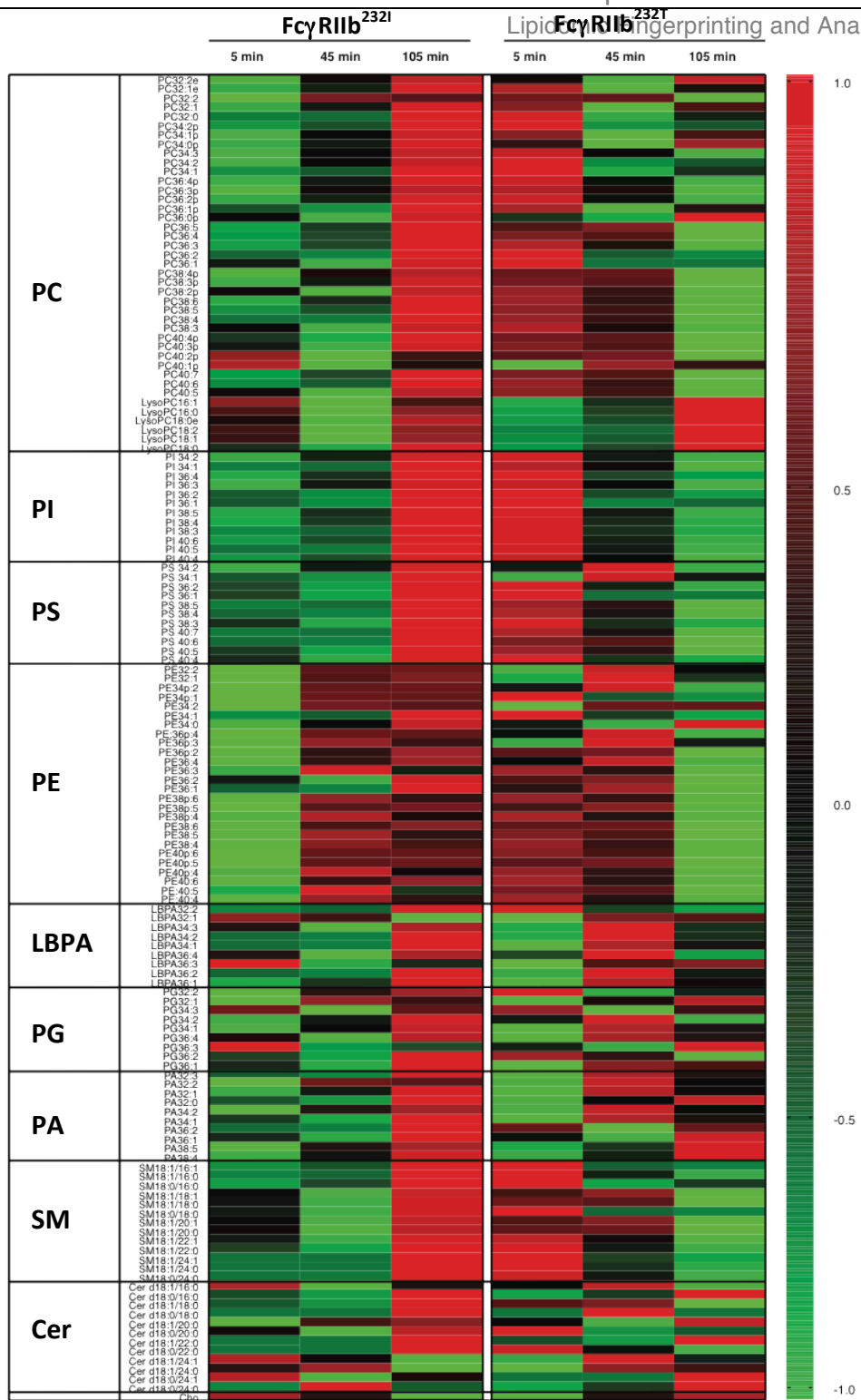


Fig 6.6: Heatmap representation of changes in individual lipid species of phagosome lipids.

Mole percent (Mol %) of individual lipid species was averaged across time to obtain the z – value. The data are a representative set containing three samples.

6.4 Comparison of lipid profiles between plasma membrane and phagosomes

Our quantitative analysis allows us to monitor lipid changes as the phagosome is formed at the plasma membrane and its progress through maturation. This will allow us to monitor the lipid changes that occur during this process and will enable us to compare between the functional Fc γ RIIb^{232I} and its polymorphic variant Fc γ RIIb^{232T}. A summary of the lipid species analyzed in the plasma membrane and phagosomes is presented in **Fig 6.7**. Intriguingly, the most abundant lipid species detected in phagosomal membrane was Cho (~ 40 mol % to ~ 60 mol %) compared to (~ 20 mol to ~ 35 mol %) in plasma membrane. Phagosomes have significantly lower levels of PS, PE and PI compared to plasma membrane. SM concentrations in maturing phagosomes, on the other hand, are similar to the levels found in plasma membrane. This reveals that the lipid composition of the plasma membrane is distinctly different from that of phagosome membranes.

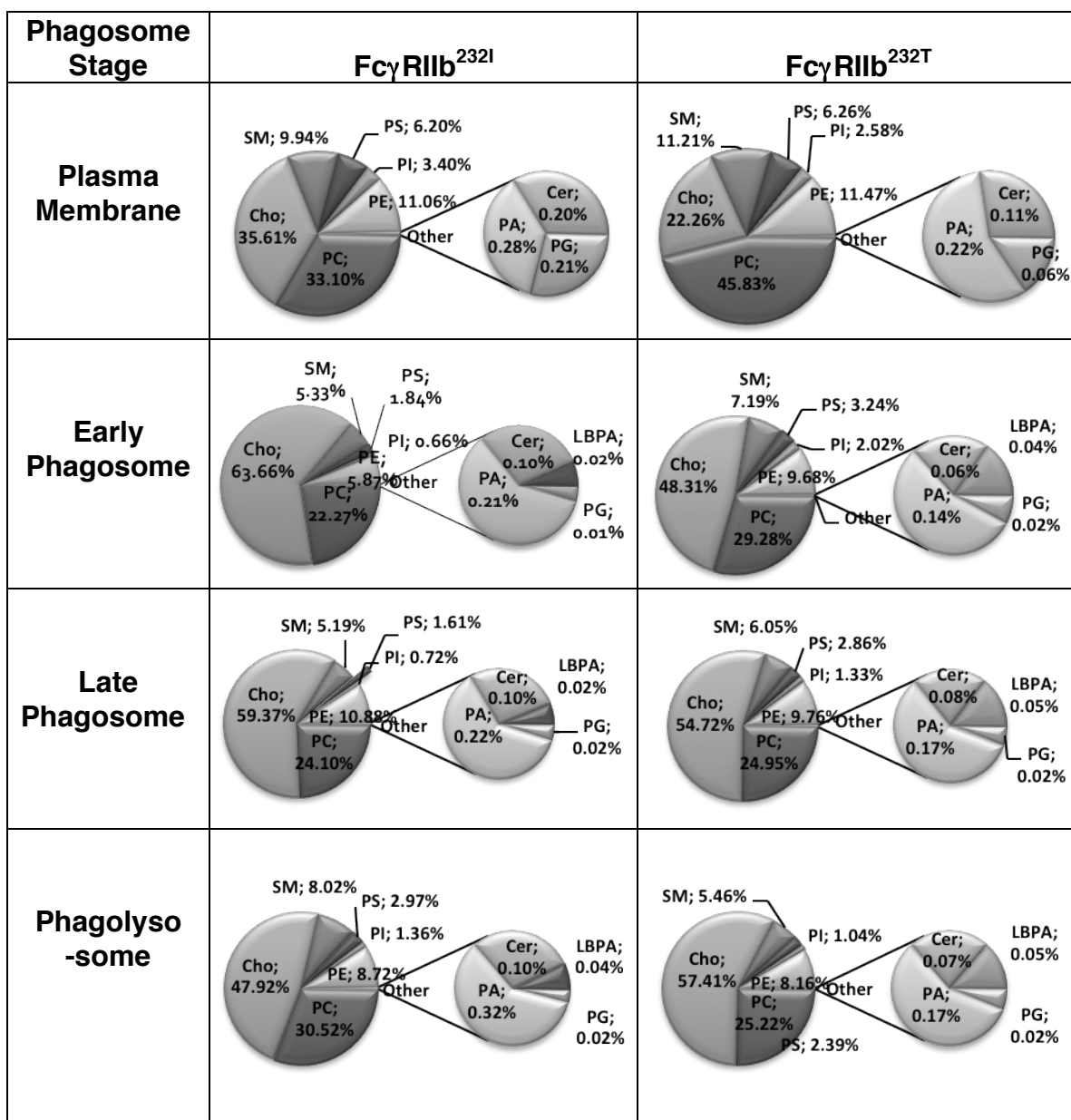


Fig 6.7: The lipid composition of the plasma membrane differed significantly from that of phagosome membranes.
The results shown in this figure are representative of several independent experiments.

Interestingly phagosome fractions showed an overall similarity for the distribution of the different lipid species during its maturation process. Substantial differences were also observed between Fc γ RIIb^{232I} and Fc γ RIIb^{232T}. This implies that a single mutation in the transmembrane domain of Fc γ RIIb has the capacity to modify their lipid composition. The most interesting finding was the level of ceramide present in these membrane fractions. Ceramide was observed to be elevated in plasma membrane and phagosomes expressing Fc γ RIIb^{232I} in contrast to the very low levels of ceramide observed in Fc γ RIIb^{232T}. The polymorphic variant Fc γ RIIb^{232T} has been linked to its exclusion from lipid rafts. Ceramide is a strong promoter of lipid raft formation. A study by Abdel Shakor et al., 2004 contributed further evidence for the importance of ceramide in phagocytosis and raft formation. Their data indicated that ceramide is produced at the onset of Fc γ RII activation and controls receptor clustering and association with lipid rafts. To reveal the potential enrichment or exclusion of Fc γ RIIb with lipid rafts, we scrutinized and compared individual ceramide species. **Fig 6.8** illustrates the heterogeneity in ceramide lipid species that is not apparent in absolute levels of entire class. The ceramide profile demonstrated that Fc γ RIIb^{232I} contained higher levels of Cer d18:1/16:0, d18:1/22:0, d18:1/24:1, d18:1/24:0.

Reports have shown that sphingomyelinase is activated upon Fc γ receptor crosslinking, which leads to the generation of ceramide, and that ceramide can induce the formation of ordered domains. More recently, Magnenau et al., 2011 showed that phagocytosis induces and requires a high membrane order. Highly

ordered membranes are a hallmark of lipid rafts. To investigate if there are differences in membrane order in potentially recruiting Fc γ RIIb or in phagosome function as postulated by others, we measured for the contribution of lipid rafts during phagocytosis **Fig 6.9**. In Fc γ RIIb^{232I} cells, the concentration of raft-forming lipids remained high whereas in Fc γ RIIb^{232T}, the concentration was significantly lower suggesting that “lipid rafts” could be sufficient in regulating the recruitment and subsequent phagosome formation and maturation.

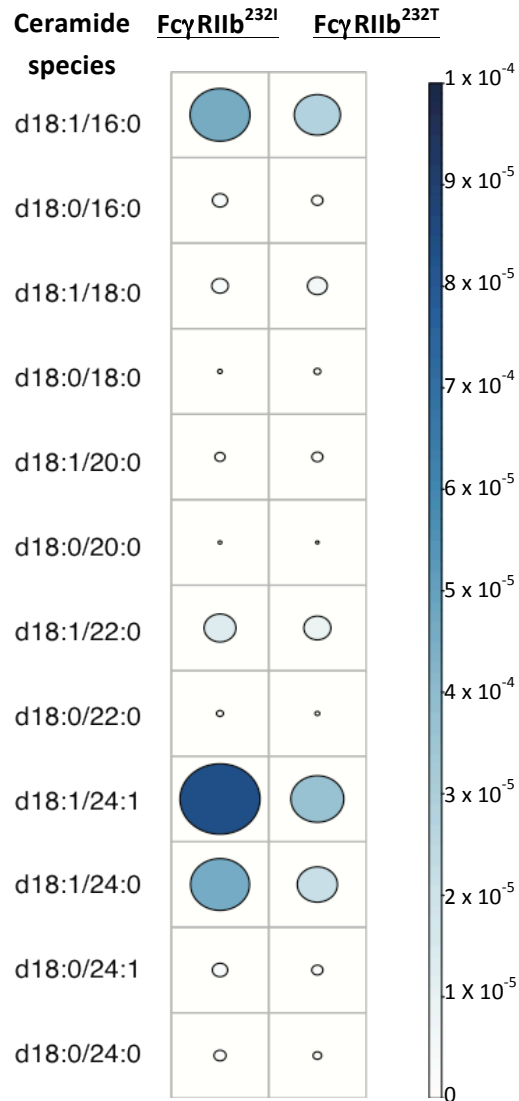


Fig 6.8: Comparison of ceramide species in both the FcγRIIb^{232I} and FcγRIIb^{232T} phagosomes.

Many of the ceramide species in FcγRIIb^{232I} is more abundant than in FcγRIIb^{232T} as illustrated by the larger and/or darker circle.

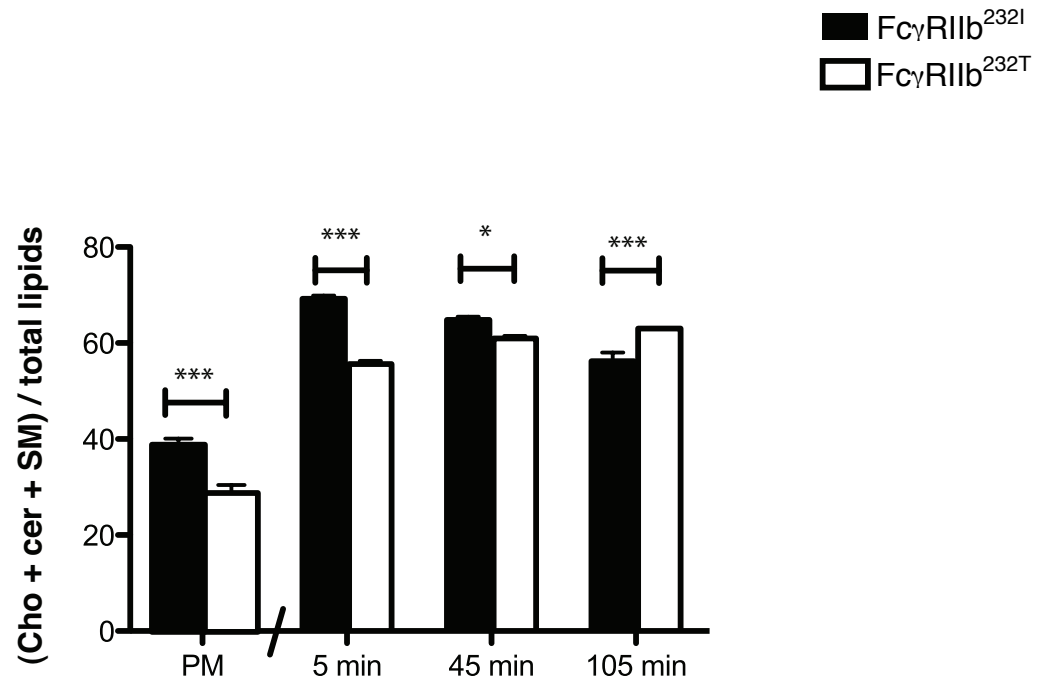


Fig 6.9: Raft lipids were enriched in cells expressing Fc γ RIIb^{232I}.

The concentration of lipid rafts is significantly lower in cells that express the mutant Fc γ RIIb^{232T} suggesting that the mutation in Fc γ RIIb^{232T} has an effect on lipid rafts.

6.4 Discussion

The lipidome of maturing phagosomes was determined by liquid chromatography-mass spectrometry. The use of mass spectrometry would allow for precise identification and quantification of changes in the phagosome lipidome during the phagocytosis. Lipid compositions of phagosome from the different time points were compared to that of the host plasma membrane from which they were derived. It is generally assumed that lipid composition in nascent and early phagosomes resemble the composition of the plasma membrane. Quantification of lipid species has shown that the lipid composition of these maturing phagosomes are distinctly different from the plasma membrane suggesting that Fc γ R cross-linking drives a distinct membrane remodeling process.

It has to be taken into account that the phagosome isolates exhibit a different degree of purity than that of plasma membrane fractions. The use of plasma membrane for comparative lipid analysis depends critically on the purity of plasma membrane preparations. The isolates are also representatives of maturation. One has to exercise care in the interpretation of results.

In addition to studying the lipidome of maturing phagosomes, the effect of Fc γ R1Ib receptor on phagocytosis was investigated. Since, Fc γ R1Ib lipid raft association is required for the initiation of signal transduction events upon receptor crosslinking we decided to look closely at membrane raft lipids. The results of this comprehensive study revealed the potential of ceramide in

phagosome function and maturation. Reduced levels of ceramide were detected in plasma membrane and phagosomal membranes bearing Fc γ RIIb^{232T} in contrast to Fc γ RIIb^{232I}.

The striking differences in ceramide levels suggests that changes in ceramide level can lead to significant functional consequences. These alterations in ceramide might be reflected in the increased phagocytic activity of the phagosomes resulting in the autoimmune disease SLE due to its failure to associate with lipid rafts. Considering that ceramide has been shown to self-associate and induce membrane order, we postulate that ceramide rafts cluster around cross-linked Fc γ Rs resulting in signaling platforms which could protect the activated receptors. Therefore, we decided to study in more detail the effect of ceramide on Fc γ RIIb receptor to determine if there is a functional link between the ceramide and Fc γ RIIb.

CHAPTER 7

RESULTS V: INVESTIVGATING THE ROLE OF CERAMIDE IN PHAGOCYTOSIS

7.1 Introduction

The plasma membrane constitutes the initial barrier against infection by intracellular pathogens [116]. Recent studies indicate that specialized domains of the plasma membrane, termed rafts, are central for the organization of receptors and signaling molecules [100, 186].

Sphingomyelin (SM) is the main sphingolipid component of plasma membrane rafts and is predominantly found in the outer leaflet of the plasma membrane. Upon activation by transmembrane receptor crosslinking, acid sphingomyelinase (ASMase) translocates to the outer leaflet of the plasma membrane where it hydrolyzes SM resulting in the generation of ceramide [115]. Ceramide promotes raft formation into large platforms and reorganizes the membrane that may result in the trapping of receptors in ceramide-enriched membrane domains [187, 188]. For instance, ceramide production have been shown to be involved in the clustering of CD40 and CD95 receptors in the lipid raft domains [189].

Cell surface ceramide generation has also been shown to control Fc γ RII clustering and phosphorylation in lipid rafts, which are important for inducing the phagocytosis of opsonized pathogens. When U937 cells were treated with bacterial sphingomyelinase before cross-linking of Fc γ RII, a synergistic increase in ceramide generation was observed [99, 115]. Although there is evidence that Fc γ RII receptors are influenced by ceramide, we do not know whether ceramide can also regulate the expression and recruitment of Fc γ RII receptors. In addition,

Floto et al., 2005 have reported that a mutation in the key residues within the transmembrane region of Fc γ RIIb Ile232Thr reduces its association with lipid rafts.

Studies by Hinkovska-Galcheva et al., 2003 have demonstrated that the inhibition of ceramide generation enhances phagocytosis and high levels of ceramide disrupt phagocytosis. This suggests ceramide as an important molecule in the regulation of phagocytosis. Similarly, ceramide levels have also been reported to increase after triggering phagocytosis and continues to accumulate until its termination [190].

Consistent with the potential role of ceramide in phagocytosis, we have previously demonstrated that cells expressing the impaired function of the inhibitory receptor Fc γ RIIb^{232T} have significantly less ceramide than its wildtype Fc γ RIIb^{232I} counterpart.

Hence, given the ability of ceramide to promote receptor co-segregation into (or exclusion from) raft microdomains, ceramide may be of importance for the efficiency of pathogen uptake into the cell and also for modulating phagocytic responses. Therefore to examine the role of ceramide in the phagocytosis of IgG opsonized BCG, we manipulated the level of ceramide expressed on U937 cells.

7.2 Generation and characterization of cell lines

The manipulation of the levels of ceramide at the plasma membrane was achieved by the over-expression or silencing of the enzyme ASMase which is involved in its synthesis. ASMase is encoded by a single gene, sphingomyelin phosphodiesterase 1(SMPD1)[191].

Accordingly, in U937 cells stably expressing FcγRIIb^{232T}, we overexpressed SMPD1 by lentiviral transduction. Since the transduced cells expressed GFP, its fluorescence was used to determine the transduction efficiency using flow cytometry. Flow cytometry sorted GFP positive cells were cultured for further experiments. To compare the impact of ceramide on phagosome function, shRNA targeting SMPD1 was performed on U937 cells expressing FcγRIIb^{232I} to induce gene silencing. These newly generated cell lines will allow the examination of both loss-of-function and gain-of-function of ceramide in U937 cells.

The expression levels of SMPD1 were measured by RT-PCR. Increased mRNA levels of SMPD1 were observed in cells that were overexpressed for SMPD1 relative to FcγRIIb^{232T} cells. The SMPD1 knockdown also demonstrated a decreased expression of SMPD1 relative to the FcγRIIb^{232I} cells. Actin was used as an internal control for gene expression (**Fig 7.1**). At the protein level, expression of SMPD1 also reflected reduced SMPD1 levels in shSMPD1 FcγRIIb^{232I} cells and an increase SMPD1 levels in SMPD1FcγRIIb^{232T} cells (**Fig**

7.2). The level of ceramide on the plasma membrane of these cells was determined by flow cytometry based on the specific binding of an anti-ceramide antibody to the intact cells. A decrease in plasma membrane was observed after SMPD1 gene silencing. Ceramide levels also rose in parallel with increased SMPD1 gene expression (**Fig 7.3**).

We proceeded to examine the lipid composition of the plasma membrane by mass spectrometry. Lipid profiles for both SMPD1Fc γ RIIb^{232T} and shSMPD1Fc γ RIIb^{232I} cells confirmed the enhancement and suppression of SMPD1 respectively. Ceramide levels in the plasma membrane of SMPD1Fc γ RIIb^{232T} were amplified in comparison to Fc γ RIIb^{232T}, whereas in the plasma membrane of shSMPD1Fc γ RIIb^{232I}, ceramide levels were lowered when compared to Fc γ RIIb^{232I} macrophages. The level of ceramide induced in SMPD1Fc γ RIIb^{232T} was also comparable to Fc γ RIIb^{232I}. This was also the case for shSMPD1Fc γ RIIb^{232I} and Fc γ RIIb^{232T} (**Fig 7.4**).

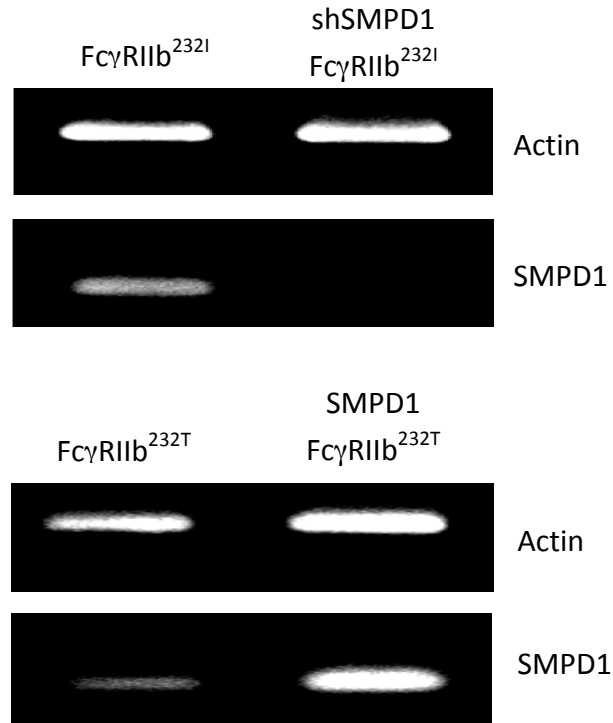


Figure 7.1: Establishing the expression of SMPD1 gene in transduced U937 cell lines.

Specific overexpression of SMPD1 was achieved with pLenti6/viralV5 lentiviral expression vector encoding for SMPD1. Silencing for SMPD1 gene was achieved by shRNAs in pLKO.1 lentiviral vector. mRNA levels were assessed by RT-PCR. Primers that were specific for actin was also included in the reaction mix to confirm equivalent amounts of RNA was used in each reaction.

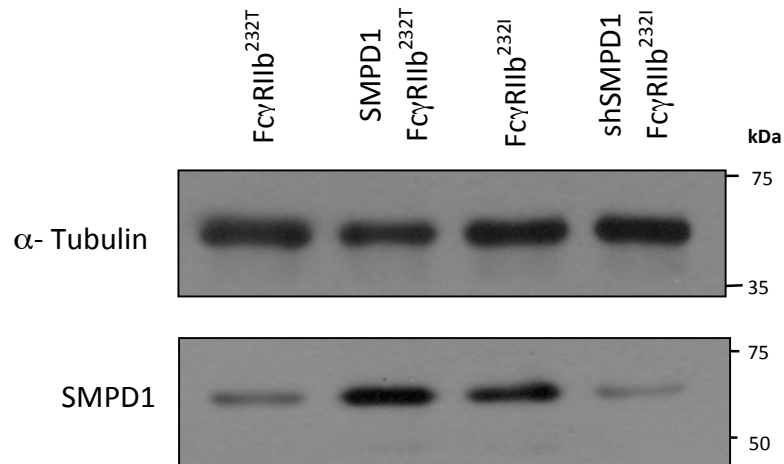


Figure 7.2: SMPD1 expression levels were confirmed by western blotting. Western blot analysis of the U937 transduced variants confirmed that SMPD1 is upregulated in SMPD1 Fc γ RIIb^{232T} cells but is downregulated in shSMPD1 Fc γ RIIb^{232I}. α -Tubulin was used as a loading control.

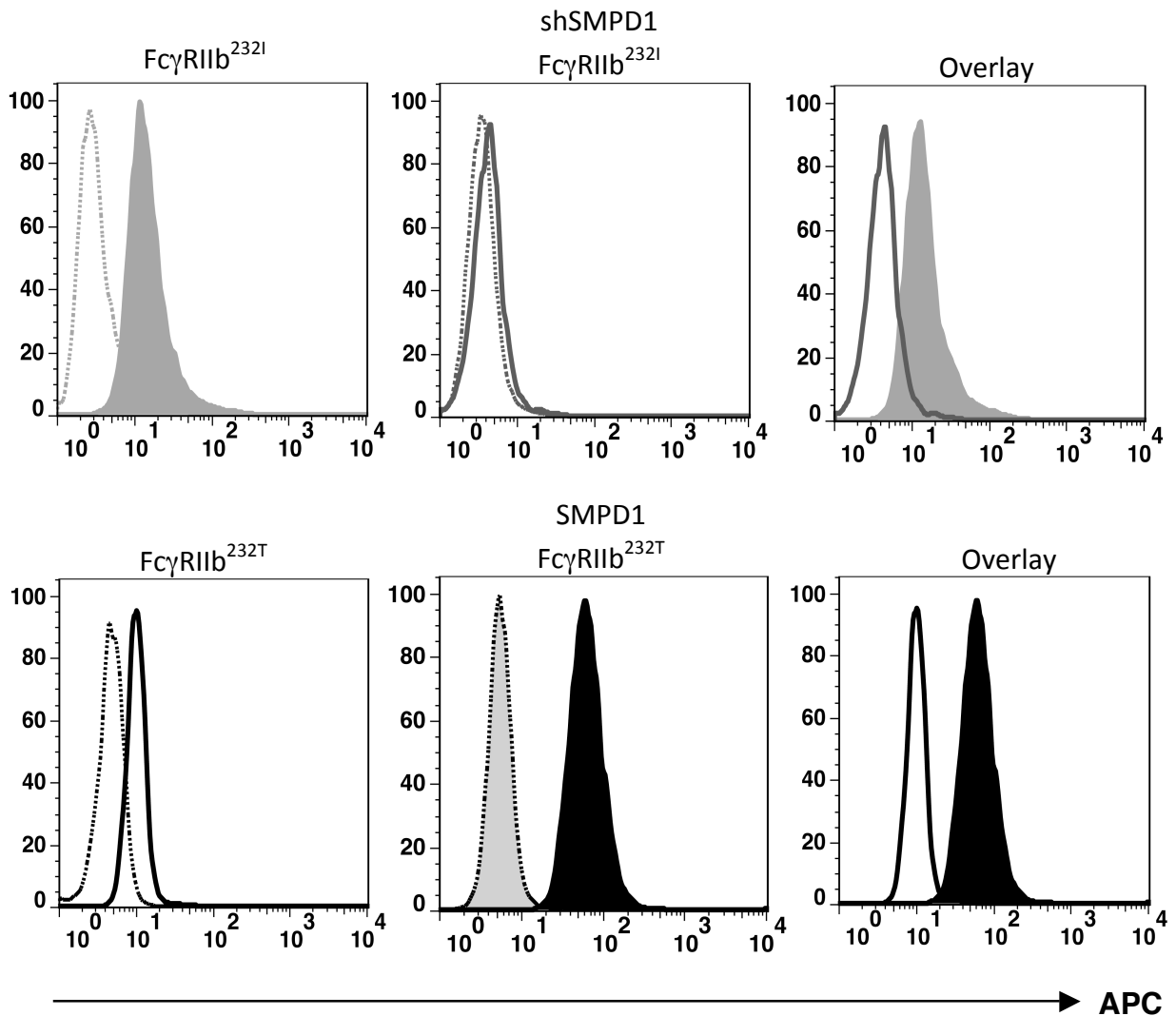


Figure 7.3: Surface expression of ceramide was altered after over-expression or silencing of SMPD1 gene.

Ceramide was detected on the surface of intact U937 cells using anti-ceramide IgM binding and evaluated by flow cytometry. The dotted peaks show the relevant isotype control. Solid peaks reflect ceramide staining.

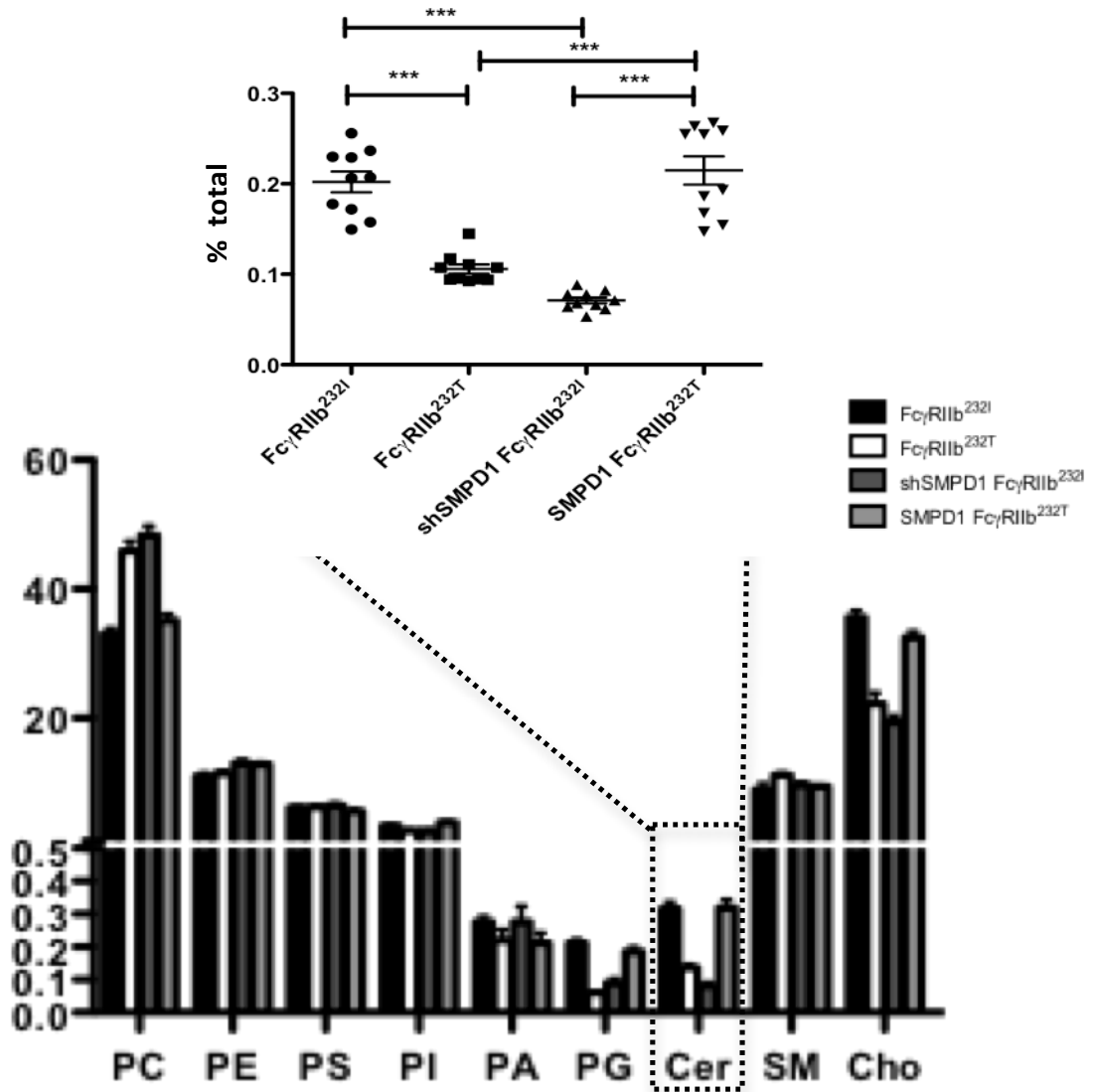


Figure 7.4: SMPD1 can modify the levels of ceramide on the plasma membrane.

Lipid composition of total lipids plasma membrane of $Fc\gamma RIIB^{232I}$, $Fc\gamma RIIB^{232T}$, $shSMPD1 Fc\gamma RIIB^{232I}$ and $SMPD1 Fc\gamma RIIB^{232T}$ cells was measured by LC-ESI-MS. Data is representative of 10 independent experiments.

7.3 Effect of ceramide on BCG killing and cytokine secretion

Ceramide has been shown to be essential for pathogen infection and survival. For example, cells deficient in ASM prevented the internalization of *Pseudomonas* by lung epithelial cells resulting in a blockage in apoptosis and enhanced inflammatory response [192]. Gublins and colleagues, 2006 have also demonstrated that infection of cells with *Neisseria gonorrhoeae* required ceramide. Cells treated with imipramine, an ASM inhibitor could not efficiently internalize *N. gonorrhoeae* until ceramide levels were restored [193]. Interestingly, when murine ASM knock-out macrophages were challenged with *Listeria Monocytogenes*, the cells were able to uptake the pathogen efficiently but were not able to restrict the growth of this pathogen as the maturation of these phagosomes into phagolysosomes is impaired leading to an enhanced cytokine release [103]. More recently, mice that are genetically deficient in ASM have been reported to exhibit an increased bacterial burden, increased phagocytic activity and a more pronounced cytokine storm [194]. These investigations indicate that the ceramide composition of the cell membrane has a very important role in bacterial infection and its subsequent fate within the cell.

Here, we determine if altering the ceramide level plays a role the infection and phagocytosis of U937 macrophages by the intracellular bacterial pathogen BCG. BCG was used as a model organism to analyse the antimicrobial defense mechanism in these cells. Macrophages were infected with BCG at an MOI of 2.

Infected cells were cultured over seven days, and cells were periodically lysed for the enumeration of CFU as described in Chapter 2: Materials and Methods.

In BCG infected cells, ceramide induced SMPD1 $Fc\gamma RIIb^{232T}$ cells showed a significant reduction in the bacterial uptake into the cell as compared to $Fc\gamma RIIb^{232T}$. In contrast, shSMPD1 $Fc\gamma RIIb^{232I}$ cells were able to rapidly engulf these phagocytic targets demonstrating that cells exhibiting less ceramide have a dramatically increased phagocytic ability. This also indicates that the expression level of ceramide on the cell surface can influence the interaction of a cell with the target and eventually internalization into the cell (**Fig 7.5**).

An initial killing of internalized mycobacteria was observed for both SMPD1 $Fc\gamma RIIb^{232T}$ and shSMPD1 $Fc\gamma RIIb^{232I}$ at day one post-infection. The infected macrophages were both not able to completely destroy the internalized bacteria allowing for any viable bacteria to replicate within the cell as reflected by the exponential increase in CFU over time.

The SMPD1 $Fc\gamma RIIb^{232T}$ macrophages showed a significant increase in CFU over time as compared to macrophages expressing the $Fc\gamma RIIb^{232T}$ thus reflecting a less aggressive phagocytic machinery. Conversely, ceramide deficient shSMPD1 $Fc\gamma RIIb^{232I}$ resulted in more significant bacterial killing as compared to $Fc\gamma RIIb^{232I}$ reflecting more aggressive phagocytosis and possibly a defective $Fc\gamma RIIb$ mediated phagocytic function. It is also worthy to note that there was no significant variability in the number of macrophages of both cell types at each of

the seven day period, signifying that the differences in number of mycobacteria were not due to differences in macrophage cell numbers but due to differences in the intrinsic ability of the macrophage to control the intracellular mycobacteria replication (**Fig 7.6**).

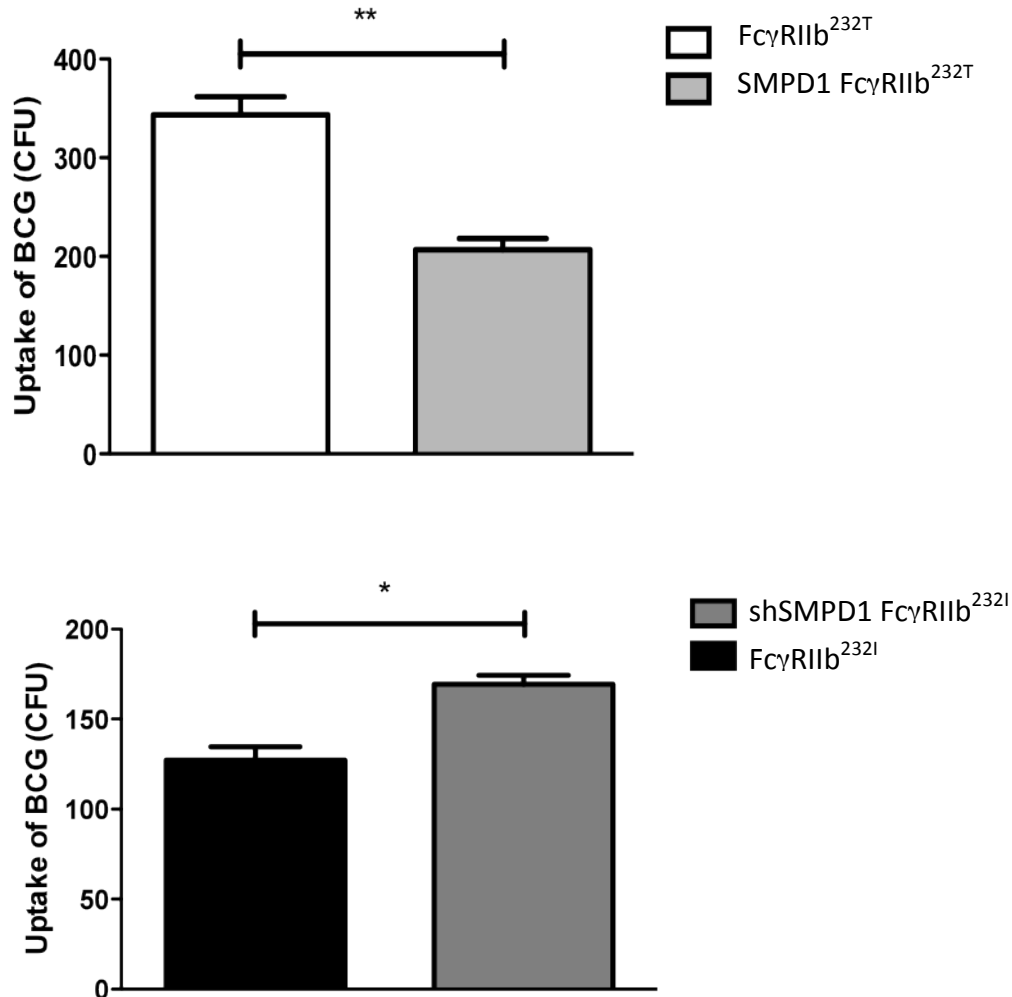


Fig 7.5: High level of ceramide retards the uptake of BCG into macrophages.

A reduction in internalization was observed in cells with higher ceramide composition. In contrast, internalization was increased in cells deficient in ceramide. Macrophages were infected with BCG for 1 h, after which the internalized mycobacteria were lysed and viable BCG were quantified. Macrophages which displayed higher levels of ceramide on the cell surface were observed to have restricted the phagocytic ability while a lower level of ceramide was found to promote the ingestion of IgG opsonized BCG. (* $p < 0.05$; ** $p < 0.01$)

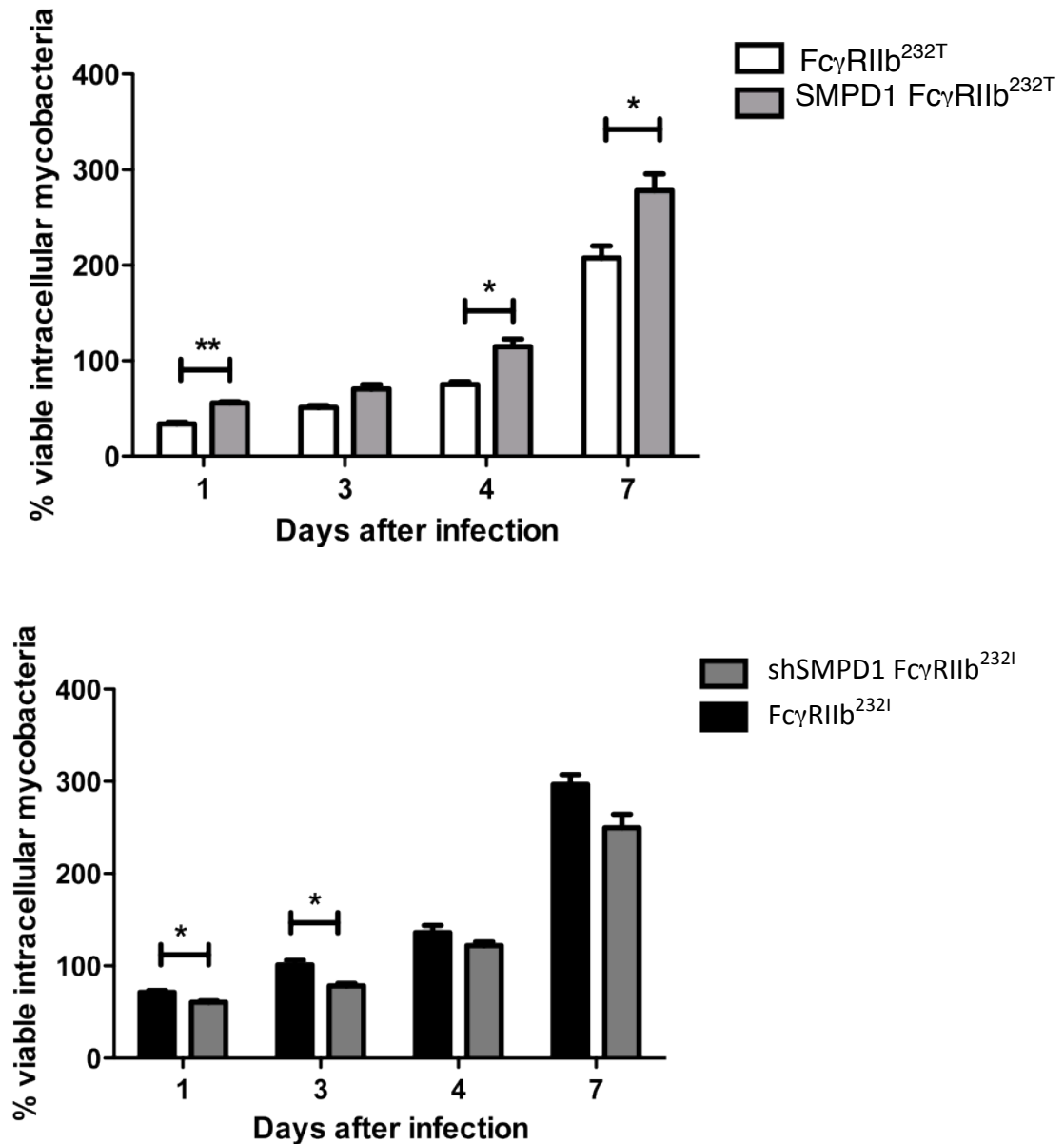


Fig 7.6: Ceramide mediated raft modification is critical for pathogen survival.

An increase in ceramide level in SMPD1 Fc γ RIIb^{232T} U937 macrophages enhances mycobacteria growth within the cell whereas ASM induced reduction of ceramide causes a marked reduction in mycobacteria growth. The ability of the infected macrophages with less ceramide leads to enhanced bactericidal activity and efficiency in controlling in mycobacteria numbers. (*p < 0.05; **p < 0.01)

These findings link ceramide as an important mediator in phagocytosis and show that ceramide is sufficient to determine the phagocytic ability of the cell.

To further explore the involvement of ceramide in Fc γ receptor mediated phagocytosis, we assayed for the differences, if any, in cytokine production by the BCG infected macrophages expressing different levels of ceramide. Pro-inflammatory cytokines upregulate phagocytosis and their production is tightly regulated to limit the negative effects due to a prolonged cytokine-driven inflammation. The amplitude of the inflammatory responses is believed to depend on the ratio of the activating and the inhibitory Fc γ receptors [195].

A 17-plex cytokine array was performed and cytokines studied included IL-1 β , IL-2, IL-4, IL-5, IL-6, IL-7, IL-8, IL-10, IL-12, IL-13, IL-17, G-CSF, GM-CSF, INF- γ , MCP-1, MIP-1 β , TNF- α . Macrophages were infected with BCG at an MOI of 10. Supernatant was collected at 24h and 48h post-infection for cytokine array analysis. Cytokine production in response to BCG infection was normalized by the deduction of basal levels of cytokine production in uninfected controls.

The pattern of cytokine secretion was strikingly different when macrophages from cells expressing less ceramide were exposed to IgG opsonized BCG compared to SMPD1 Fc γ RIIb^{232T} and Fc γ RIIb^{232I} macrophages which have more ceramide. We observed trends of higher production of the pro-inflammatory cytokines IL-6, IL-8, IL-12, G-CSF, INF- γ and TNF- α at both 24h (**Fig 7.7**) and 48h (**Fig 7.8**)

post-infection in cells with less ceramide. Recently, IL-12 has been implicated in enhancing phagocytosis and intracellular killing of *Mycobacterium tuberculosis* [196]. We also observed higher production of the anti-inflammatory IL-10 from macrophages expressing more ceramide as compared to macrophages with less ceramide (**Fig 7.10**). A study conducted by Xu *et al.*, 2006 demonstrated that high IL-10 production by macrophages in the absence of pro-inflammatory cytokines allows the phagocyte to efficiently clear early apoptotic cells in a silent and non-inflammatory fashion [197]. The remaining cytokines included in the 17-plex were either undetected, or could not be accurately measured as a result of experimental conditions (data not shown).

Our results strongly indicate that the level of ceramide present on the cell can affect the amplitude of cytokine secretion in response to phagocytosis. Lower levels of ceramide will lead to the excessive secretion of pro-inflammatory cytokines in response to IgG mediated phagocytosis. Conversely, increasing ceramide levels can limit the production of these inflammatory cytokines.

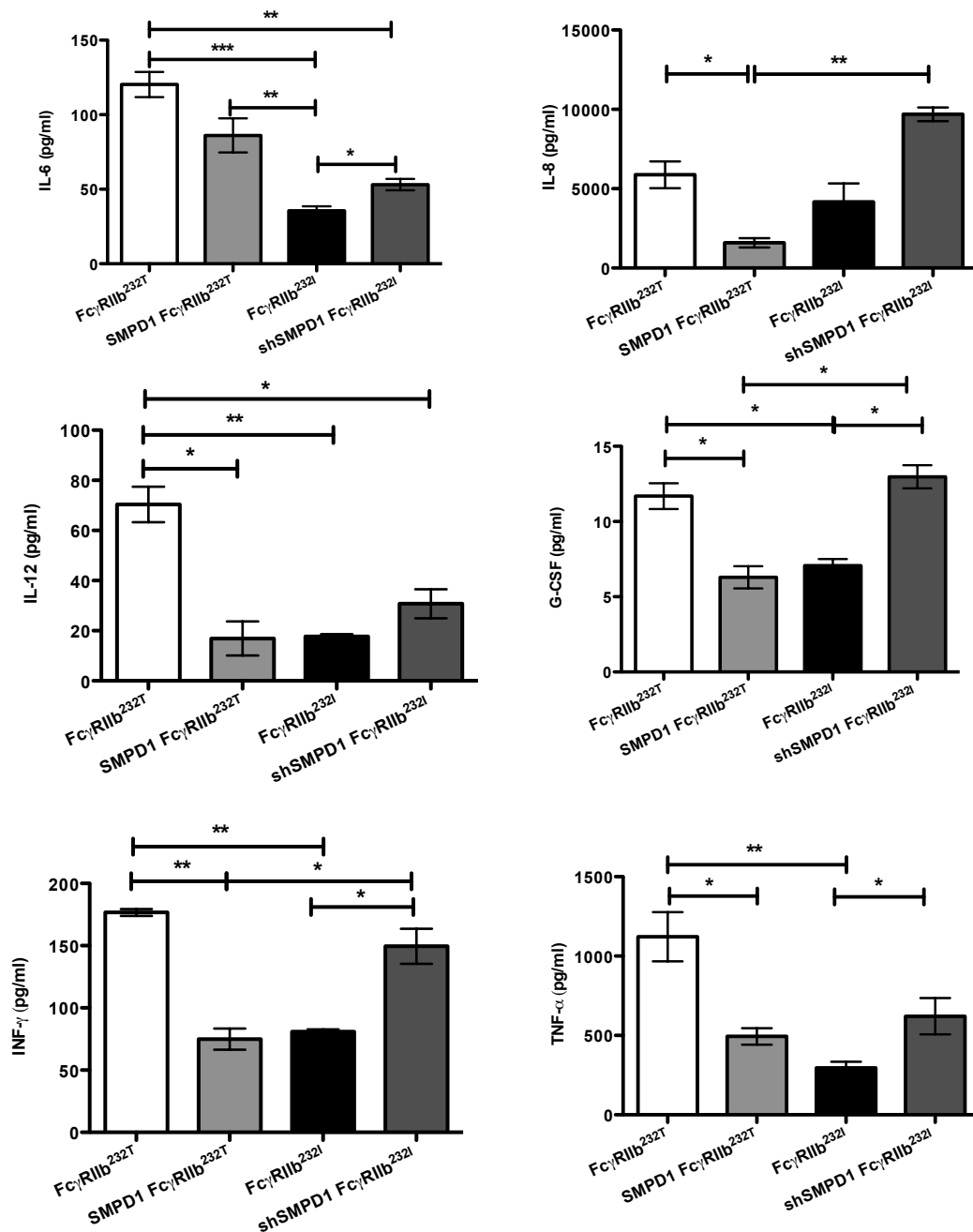


Fig 7.7: Ceramide influences the secretion of pro-inflammatory cytokines. Cytokine production (24h post phagocytosis) was determined after BCG infection of U937 cells with excess or reduced levels of ceramide. The overproduction of pro-inflammatory cytokines by Fc γ RIIb^{232T} macrophages was significantly reduced with increased ceramide in SMPD1 Fc γ RIIb^{232T} macrophages. Conversely, ceramide deficient shSMPD1 Fc γ RIIb^{232I} treated macrophages were observed to increase their production of pro-inflammatory cytokines as compared to cytokine secretion by Fc γ RIIb^{232I} cells.

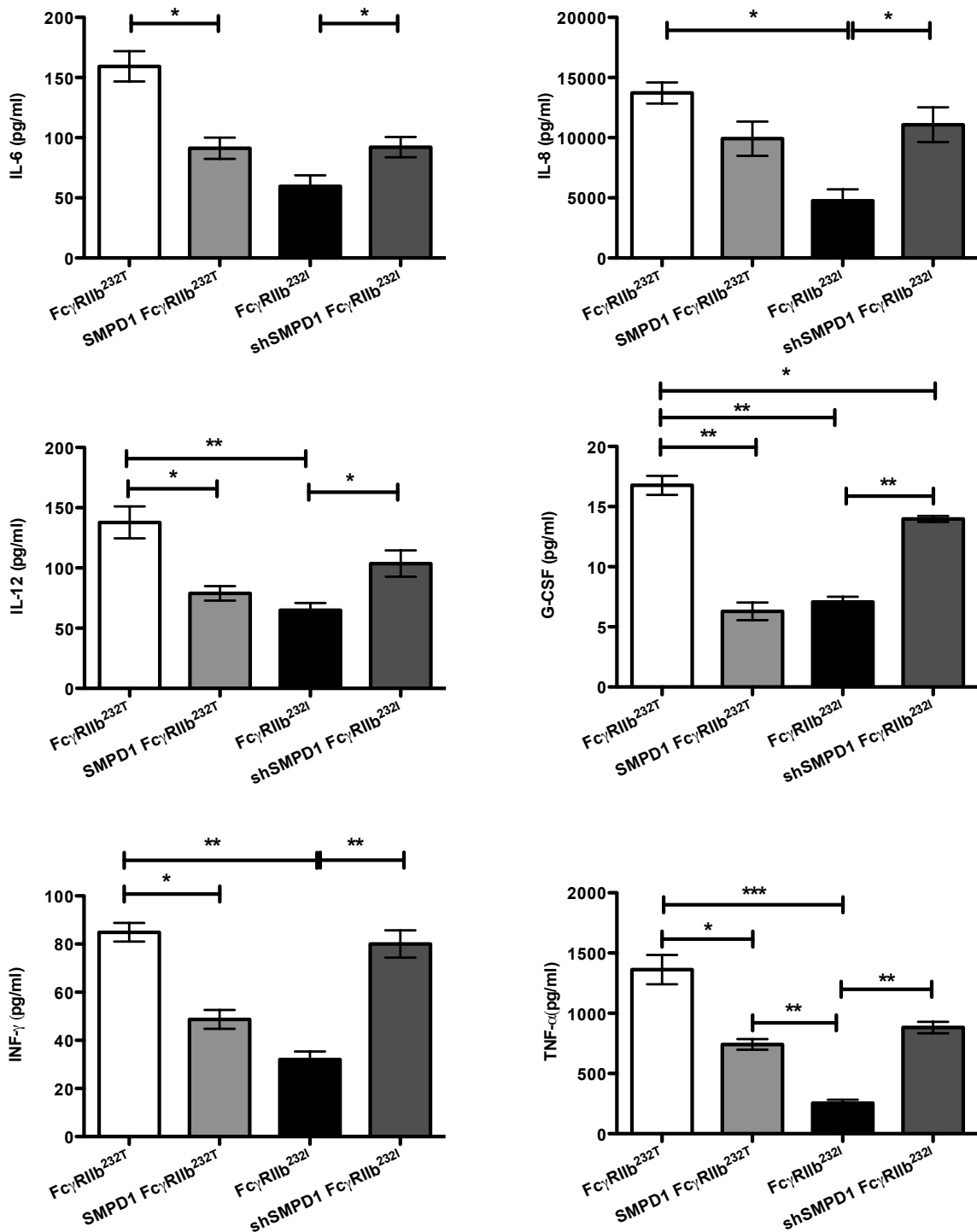


Fig 7.8: A low level of ceramide enhances excessive cytokine production after 48h Fc γ R phagocytosis.

Similar to observations after 24h post-infection, SMPD1 Fc γ RIIb^{232I} blocks excessive cytokine secretion while shSMPD1 Fc γ RIIb^{232T} promotes cytokine production.

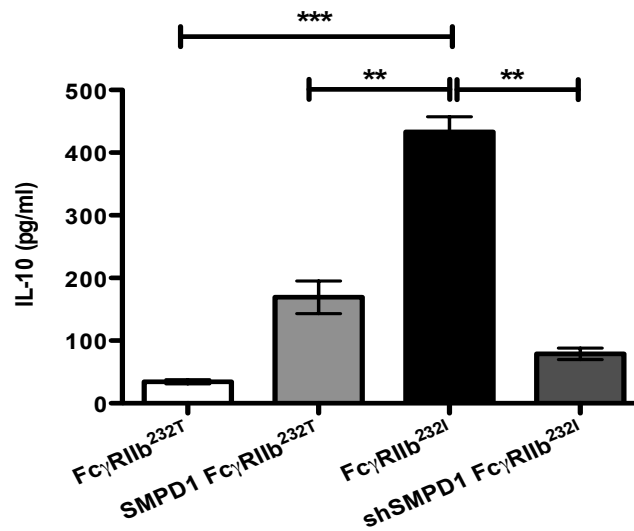
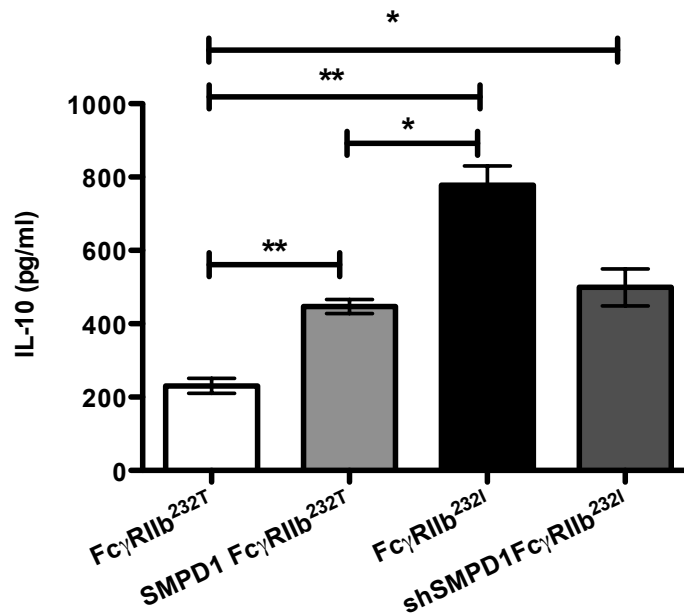
24h post-infection48h post-infection

Fig 7.9: Production of IL-10 in culture supernatant after Fc γ R phagocytosis. Inhibition of ceramide generation in shSMPD1 Fc γ RIIb^{232I} macrophages decreases IL-10 production. High levels of IL-10 were observed in macrophages with higher levels of ceramide that is, SMPD1 Fc γ RIIb^{232T} and Fc γ RIIb^{232T}.

7.4 Discussion

Studies have shown that mutation in the 232-position of Fc γ RIIb results in a loss of association with lipid rafts. Consistent with this notion, our lipid analysis on Fc γ RIIb^{232T} and Fc γ RIIb^{232I} U937 cell lines indicated the involvement of ceramide lipid rafts in regulating these inhibitory receptors as was discussed in the previous chapter.

To assess if ceramide membrane changes affect Fc γ RIIb function, we generated transgenic cell lines that selectively over-express SMPD1, the ASM encoding gene, on Fc γ RIIb^{232T} U937 knock-in cells. In addition, the SMPD1 gene was silenced in Fc γ RIIb^{232I} U937 knock-in cell lines. This resulted in stable cell lines that over-expressed or were deficient in ceramide to allow normalization in the inhibitory signaling in the SMPD1 Fc γ RIIb^{232T} cell and an aberrant level of inhibitory signaling in the shSMPD1 Fc γ RIIb^{232I} cell.

When IgG-opsonized BCG was exposed to Fc γ RIIb^{232T}, there was an increased uptake of these pathogens into the cell. However, when a higher level of ceramide was present on the SMPD1 Fc γ RIIb^{232T} cell, the rate of internalization was significantly reduced. Similarly, when less ceramide was present in shSMPD1 Fc γ RIIb^{232I}, phagocytic internalization was enhanced. Our results indicate that ceramide rafts are a central component of the phagocytic interaction between the phagocytic target and the cell.

We also monitored the rate of bacterial killing within the cell over seven days.

SMPD1 Fc γ RIIb^{232T} showed a decrease in killing capacity in comparison to Fc γ RIIb^{232T} macrophages. In addition, enhanced pathogen killing was observed in shSMPD1 Fc γ RIIb^{232I} when compared to Fc γ RIIb^{232I}. This demonstrates that decreasing ceramide will induce an aberrant activation of phagocytosis that contributes to overactive macrophages. Our finding suggests a novel function of ceramide in the regulation of Fc γ receptor mediated phagocytosis and its effect on phagosome function and maturation.

To determine if the level of ceramide can lead to a differential production of cytokines in response to phagocytosis, we studied a large panel of 17 cytokines. We found that ceramide-deficient cells exhibited elevated pro - inflammatory cytokine accumulation in response to IgG mediated. A trend of higher IL-6, IL-8, IL-12, G-CSF, INF- γ and TNF- α production but lower levels of anti-inflammatory IL-10 production in Fc γ RIIb^{232T} and shSMPD1 Fc γ RIIb^{232I} were observed. Similarly, SMPD1 Fc γ RIIb^{232T} secreted lower levels of pro-inflammatory cytokines as compared to Fc γ RIIb^{232T} upon IgG mediated phagocytosis. This showed that the alteration of expression levels of ceramide can affect the secretion of cytokines and that increasing ceramide may downregulate the excess pro-inflammatory cytokines produced.

In summary, in the comparison of the SMPD1 Fc γ RIIb^{232T} versus shSMPD1 Fc γ RIIb^{232I} expressing macrophages, our data shows that the shSMPD1 Fc γ RIIb^{232I} variant is associated with a more aggressive phagocytic response as

characterized by the enhanced bacterial killing and the upregulation of pro-inflammatory cytokines. These results demonstrate the involvement of ceramide in differentially regulating phagocytosis internalization and its subsequent maturation. This led us to conclude that a sufficiently high level of ceramide is crucial in recruiting the inhibitory receptor for unwanted cellular activation and autoimmunity. These observations also put forward the hypothesis that the generation of ceramide rich microdomains by ASM is required to generate a signaling platform for functional Fc γ RIIb signaling.

CHAPTER 8

DISCUSSION

Discussion

Phagocytosis is a critical component of our innate immune defense. The best-characterized cellular receptors that mediate this process are the receptors for IgG. These receptors are termed Fc γ receptors. During the early stages of phagocytosis, Fc γ receptors are activated by the IgG-opsonized target particle. Extensive membrane remodeling occurs driving the pseudopods of the plasma membrane to encircle the target particle. This results in its uptake into the cell in a membrane bound organelle known as a phagosome [3, 15].

Fc γ receptors can be broadly separated into activatory and inhibitory receptors based on the presence of an Immuno-Tyrosine Activatory Motif (ITAM) or Immuno-Tyrosine Inhibitory Motif (ITIM) in their cytoplasmic domains. The inhibitory receptor is proposed to regulate and dampen the activation response mediated by the activatory receptor. As such, the magnitude of the phagocytic response is regulated by the activity between the activatory Fc γ receptors and the inhibitory Fc γ R11b receptor [38]. This has important implications in autoimmunity as impaired negative regulation results in overwhelming inflammation leading to the development of autoimmune diseases [22].

A transmembrane mutation in the Fc γ R11b receptor coding for the substitution of isoleucine to threonine at position 232 has been identified to be associated with the pathogenesis of systemic lupus erythematosus (SLE) by abolishing its inhibitory function [42, 55]. In a study published in *Science*, McGaha and

colleagues show that the restoration of Fc γ RIIb expression on B cells using a lentiviral construct could prevent autoimmune disease in Fc γ RIIb-deficient mice [44]. Although numerous studies have demonstrated this association of the polymorphism with susceptibility to SLE, it has also been shown to confer protection against malaria in Asian population where malaria is endemic [40, 49, 53].

A number of studies have shown increased phagocytosis in cells with dysfunctional Fc γ RIIb^{232T} [54, 155] but how this receptor is involved in the process of particle internalization and pathogen destruction is poorly characterized.

The governing aim for this project was to investigate the effect of the Fc γ RIIb receptor and/or its mutant variant on phagosome function and maturation. To this end, we employed a human myelomonocytic cell line, U937. U937 expresses Fc γ RI and Fc γ RIIa but does not express Fc γ RIIb, making it an ideal cell line for studying the role of this receptor in phagocytosis. We generated U937 cell lines stably transfected with either the wild type inhibitory receptor (Fc γ RIIb^{232I}) or the mutated inhibitory (Fc γ RIIb^{232T}) receptor. The expression levels of the native Fc γ receptors were unaffected in transfected cells and similar levels of Fc γ RIIb were expressed. This allowed us to examine the differences between the wild-type Fc γ RIIb^{232I} inhibitory receptor and the polymorphic Fc γ RIIb^{232T} receptor.

In Chapter 3, we utilized IgG-opsonized latex beads as a surrogate for immune complexes as well as IgG-opsonized microbes to engage Fc γ receptors and showed that cells exposed to these latex beads were taken up via Fc receptors and delivered into the cells. Phagosomes were generated and isolated using a well-established protocol by Desjardins et al., 1994. The low buoyant density of latex beads allows phagosomes to be isolated by flotation on step sucrose gradients in a region where other organelles are not detected. Latex bead phagosomes were isolated at different time points: 5 min, 45 min and 105 min to study all the stages of phagocytosis.

Earlier in Chapter 4, we found that macrophages expressing Fc γ RIIb^{232T} were able to elicit a more aggressive phagocytic response as they showed an increased rate of internalization into the cell for destruction. However, a delayed phagosome maturation kinetic was observed. Fc γ RIIb^{232T} phagosomes initially fuse slowly with endosomes but subsequently fuse efficiently with the lysosomal compartment. We speculated that this was due to accelerated internalization of high concentrations of beads into cells which delays fusion with the endosomal compartment. We also noted that there was an increase in the production of reactive oxygen species, phagosome acidification and a more robust elevation in intracellular calcium; processes that accompany phagocytosis.

In Chapter 5, we measured for the ability of these macrophages in ingesting and destroying a bacterial pathogen. Although latex beads are a good model system for studying phagocytosis, unlike bacteria, they cannot be digested and

eliminated by the macrophages. The bactericidal activity of a macrophage is a culmination of its ability to bind, ingest and kill bacteria as the macrophage may bind, or bind and internalize a bacterium, yet not be able to kill it. We used *Mycobacterium bovis* BCG as our pathogen as we had access to an anti-human antibody targeting lipoarabinomannan (LAM), a major mycobacterial cell wall component. This ensures that the pathogen is IgG-opsonized and thus resulting in a Fc γ receptor-mediated uptake. Our results revealed that macrophages expressing the mutant Fc γ RIIb^{232T} had increased phagocytic activity as they were able to ingest more IgG opsonized BCG per unit time and were able to clear more of the ingested BCG. In addition, a more pronounced inflammatory environment was also observed in contrast to macrophage phagosomes expressing Fc γ RIIb^{232I}.

As part of this study, we also wanted to determine the lipid composition of maturing phagosomes as the role of lipids involved in phagocytosis is poorly characterized. More specifically, we aimed to focus on the lipid biology in Fc γ receptor signaling as studies by Floto et al., 2005 show that Fc γ RIIb^{232T} mediates its effect through an exclusion from lipid rafts, and is therefore unable to interact with activatory Fc γ Rs and exert their inhibitory effect.

In Chapter 6, the lipidome of plasma membrane and phagosomes were determined by mass spectrometry. Phagosomes have been proposed to originate from invagination and scission of the plasma membrane. Therefore, we purified plasma membrane via the use of cationic silica beads that adhere

electrostatically to the plasma membrane to examine marked changes in the lipid composition as phagosomes mature. It is generally assumed that the lipid composition in early phagosomes will resemble the lipid composition of the plasma membrane. However, quantification of the lipid species present in the plasma membrane and the phagosomes revealed distinctly different lipid composition suggesting that Fc γ R crosslinking drives a distinct membrane remodeling process.

It has to be taken into account that the phagosome isolates exhibit a different degree of purity than that of the plasma membrane fractions. The use of plasma membrane for comparative lipid analysis depends critically on the purity of the plasma membrane preparations. The isolates are also representatives of maturation. Care has to be exercised in the interpretation of results.

Additionally, we assessed the effect of Fc γ RIIb receptor on the lipid composition of plasma membrane. Most striking was the level of ceramide observed between the plasma membrane of Fc γ RIIb^{232I} and Fc γ RIIb^{232T}. Fc γ RIIb^{232I} plasma membrane had almost twice the concentration of ceramide detected in Fc γ RIIb^{232T}. This was interesting because the loss of function of Fc γ RIIb^{232T} has been linked to its exclusion from lipid rafts.

In the past years, numerous research groups have suggested a novel mechanism on the ability of ceramide lipid rafts in mediating the aggregation/clustering of receptor molecules. The generation of ceramide at the

plasma membrane transforms small “resting” rafts into “active” platforms. This fusion of small rafts into large platforms causes the reorganization of intracellular signaling molecules. The clustering and trapping of receptors ultimately provides a high concentration of signaling molecules which amplifies signaling into the cell. In addition, the generation of ceramide within rafts also permits very tight packing of lipids and strongly stabilizes the lipid rafts [186, 187].

This ceramide-triggered microdomain fusion which generate larger, stable platforms, have also been documented to be involved in many aspects of infection such as the internalization of pathogens, intracellular maturation of phagosomes, induction of apoptosis upon infection and regulation of cytokine release [104, 186]. Although ceramide has been recognized as a key signalling molecule in phagocytosis, the exact mechanism(s) by which ceramide performs its function are not completely understood.

An increasing body of work on ceramide signaling has provided clues to show that most receptors trigger a stimulus that activates acid sphingomyelinase (ASMase), which hydrolyzes sphingomyelin predominantly found on the outer leaflet of the plasma membrane to generate ceramide [100, 186]. ASMase has also been detected at the phagosomal cup [99]. Although studies have also demonstrated enhanced phagocytosis through the inhibition of ceramide synthesis and ceramide has been described to be a negative regulator of phagocytosis as its accumulation correlates with the termination of the phagocytic response [112, 190], the precise relationship between phagocytosis,

ASMase, the conversion of sphingomyelin to ceramide, ceramide and Fc γ R11b receptor remains unsolved.

Abdel Shakor et al., 2004 contributed further evidence for the importance of ceramide in phagocytosis and raft formation. Their data indicated that ceramide is produced at the onset of Fc γ R11 activation and controls receptor clustering and its association with lipid rafts. This led us to realize that the coalescence of receptors could result in a modification of the lipid environment surrounding them.

The purpose of Chapter 7 was to study the implications of ceramide in phagocytosis with respect to Fc γ R11b in greater detail. We generated two more cell lines; one that over-expresses ceramide and another that is deficient in ceramide. The objective was to investigate if ceramide causes differences in the phagosome function and maturation in these cells.

It was observed that cells which over-expressed ceramide resulted in a dramatic shift from hyperaggressive macrophages to macrophages with a lower degree of phagocytic activity possibly restoring the balance between the activatory Fc γ receptor and the inhibitory Fc γ R11b receptor. However, we cannot also rule out the possibility that the presence of more ceramide on the cell membrane leads to enhanced trapping the Fc γ R11b receptor molecules which are outside of the lipid rafts upon activation which may account for controlling over-activation of phagocytosis. Ceramide rich cells internalized less BCG and also exhibited a more subdued killing profile. In contrast, cells deficient in ceramide led to an

upregulation of their phagocytic ability by internalizing and destroying a higher number of mycobacteria as well as releasing an increased level of inflammatory cytokines.

Our results indicate that ceramide rich rafts are a central component of the initial interactions between the target IgG particle and the host cell. The results also suggest that increasing ceramide on cells re-establishes the function of Fc γ RIIb receptor.

While the importance of receptor clustering for signal initiation during phagocytosis has been long known, little is still known on the mechanism for such clustering. Here, we propose that ceramide-rich membrane rafts provide residency for Fc γ RIIb receptors on U937 cells, and by doing so they provide a platform for which Fc γ RIIb can initiate or carry out its function.

In conclusion, our study provides evidence for the importance of ceramide in establishing microdomains that could recruit Fc γ RIIb and that the magnitude of phagocytosis could be modulated by ceramide.

Finally, a major challenge for the future is to gain a full understanding of the specific ceramide species present within the outer and inner leaflets of the membrane, and, more importantly, if the production of distinct ceramide species within specific leaflets has distinct metabolic and physiological consequences for the cell. The level of how much ceramide needed for this process could also be a major contributing factor. In addition, as the modulation of plasma membrane

lipids is an early event in the response to various stimuli, a greater understanding of the lipids at the plasma membrane is needed to fully appreciate the intricacies of the phagocytic signal transduction.

APPENDICES

Appendices

Appendix 1: Optimized MRM parameters for lipid species detected by

LC-MS/MS

ESI-	Q1	Q3	Dwell Time (ms)	Declustering Potential (V)	Collision Energy (V)	Cell Exit Potential (V)
PG32:2	717.6	153	12	-80	-50	-5
PG32:1	719.6	153	12	-80	-50	-5
PG34:3	743.7	153	12	-80	-53	-5
PG34:2	745.7	153	12	-80	-53	-5
PG34:1	747.7	153	12	-80	-55	-5
PG34:0	749.7	153	12	-90	-55	-5
PG36:4	769.7	153	12	-90	-55	-5
PG36:3	771.7	153	12	-90	-55	-5
PG36:2	773.7	153	12	-90	-55	-5
PG36:1	775.7	153	12	-90	-55	-5
PG38:6	793.7	153	12	-90	-55	-5
PG38:5	795.7	153	12	-90	-55	-5
PG38:4	797.7	153	12	-90	-55	-5
PE32:2	686.6	196.1	12	-90	-55	-3
PE32:1	688.6	196.1	12	-90	-55	-3
PE34p:2	698.6	196.1	12	-90	-55	-3
PE34p:1	700.6	196.1	12	-100	-55	-3
PE34:2	714.6	196.1	12	-100	-55	-3
PE34:1	716.6	196.1	12	-100	-55	-3
PE34:0	718.6	196.1	12	-100	-55	-3

Appendices

PE:36p:4	722.6	196.1	12	-100	-55	-3
PE36p:3	724.6	196.1	12	-100	-55	-3
PE36p:2	726.6	196.1	12	-100	-55	-3
PE36:4	738.65	196.1	12	-100	-55	-3
PE36:3	740.65	196.1	12	-100	-55	-3
PE36:2	742.65	196.1	12	-100	-55	-3
PE36:1	744.7	196.1	12	-100	-55	-3
PE38p:6	746.7	196.1	12	-100	-55	-3
PE38p:5	748.7	196.1	12	-100	-55	-3
PE38p:4	750.7	196.1	12	-100	-55	-3
PE38:6	762.7	196.1	12	-100	-55	-3
PE38:5	764.7	196.1	12	-100	-55	-3
PE38:4	766.7	196.1	12	-100	-55	-3
PE38:2	770.7	196.1	12	-100	-55	-3
PE40p:7	772.7	196.1	12	-100	-55	-3
PE40p:6	774.7	196.1	12	-100	-55	-3
PE40p:5	776.7	196.1	12	-100	-55	-3
PE40p:4	778.7	196.1	12	-100	-55	-3
PE40:6	790.7	196.1	12	-100	-55	-3
PE:40:5	792.7	196.1	12	-100	-55	-3
PE:40:4	794.7	196.1	12	-100	-55	-3
PI 32:1	807.7	241	12	-100	-55	-5
PI 34:2	833.7	241	12	-100	-60	-5
PI 34:1	835.7	241	12	-100	-60	-5
PI 36:4	857.7	241	12	-100	-60	-5
PI 36:3	859.7	241	12	-100	-60	-5

Appendices

PI 36:2	861.7	241	12	-100	-60	-5
PI 36:1	863.7	241	12	-100	-60	-5
PI 38:6	881.7	241	12	-100	-60	-5
PI 38:5	883.7	241	12	-100	-60	-5
PI 38:4	885.7	241	12	-100	-65	-5
PI 38:3	887.7	241	12	-100	-65	-5
PI 40:6	909.8	241	12	-100	-65	-5
PI 40:5	911.8	241	12	-100	-65	-5
PI 40:4	913.8	241	12	-100	-65	-5
PS34:2	758.7	671.6	12	-90	-25	-5
PS 34:1	760.7	673.6	12	-90	-25	-5
PS 36:2	786.7	699.6	12	-90	-25	-5
PS 36:1	788.7	701.6	12	-90	-25	-5
PS 38:5	808.7	721.7	12	-90	-26	-5
PS 38:4	810.7	723.7	12	-90	-26	-5
PS 38:3	812.7	725.7	12	-90	-26	-5
PS 40:7	832.7	745.7	12	-90	-26	-5
PS 40:6	834.7	747.7	12	-90	-26	-5
PS 40:5	836.7	749.7	12	-90	-26	-5
PS 40:4	838.7	751.7	12	-90	-26	-5
PA32:3	641.6	153	12	-90	-55	-3
PA32:2	643.6	153	12	-90	-55	-3
PA32:1	645.6	153	12	-90	-55	-3
PA32:0	647.6	153	12	-90	-55	-3
PA34:2	671.6	153	12	-90	-55	-3
PA34:1	673.6	153	12	-90	-55	-3

Appendices

PA36:2	699.6	153	12	-90	-55	-3
PA36:1	701.6	153	12	-90	-55	-3
PA38:6	719.6	153	12	-90	-55	-3
PA38:5	721.6	153	12	-90	-55	-3
PA38:4	723.6	153	12	-90	-55	-3

ESI-	Q1	Q3	Dwell Time (ms)	Declustering Potential (V)	Collision Energy (V)	Cell Exit Potential (V)
PC32:2e	718.7	184.1	15	90	60	3
PC32:1e	720.7	184.1	15	90	60	3
PC32:2	730.7	184.1	15	90	60	3
PC32:1	732.7	184.1	15	90	60	3
PC32:0	734.7	184.1	15	90	60	3
PC34:2p	742.7	184.1	15	90	60	3
PC34:1p	744.7	184.1	15	90	60	3
PC34:0p	746.7	184.1	15	90	60	3
PC34:3	756.7	184.1	15	90	60	3
PC34:2	758.7	184.1	15	90	60	3
PC34:1	760.7	184.1	15	90	60	3
PC36:4p	766.7	184.1	15	90	60	3
PC36:3p	768.7	184.1	15	90	60	3
PC36:2p	770.7	184.1	15	90	60	3
PC36:1p	772.7	184.1	15	90	60	3
PC36:0p	774.7	184.1	15	90	60	3
PC36:5	780.8	184.1	15	90	60	3
PC36:4	782.8	184.1	15	90	60	3

Appendices

PC36:3	784.8	184.1	15	90	60	3
PC36:2	786.8	184.1	15	90	60	3
PC36:1	788.8	184.1	15	90	60	3
PC38:4p	794.8	184.1	15	90	60	3
PC38:3p	796.8	184.1	15	90	60	3
PC38:2p	798.8	184.1	15	90	60	3
PC38:6	806.8	184.1	15	90	60	3
PC38:5	808.8	184.1	15	90	60	3
PC38:4	810.8	184.1	15	90	60	3
PC38:3	812.8	184.1	15	90	60	3
PC40:4p	822.8	184.1	15	90	60	3
PC40:3p	824.8	184.1	15	90	60	3
PC40:2p	826.8	184.1	15	90	60	3
PC40:1p	828.8	184.1	15	90	60	3
PC40:7	832.8	184.1	15	90	60	3
PC40:6	834.8	184.1	15	90	60	3
PC40:5	836.8	184.1	15	90	60	3
SM18:1/16:0	703.7	184.1	15	90	60	3
SM18:0/16:0	705.7	184.1	15	90	60	3
SM18:1/18:1	729.8	184.1	15	90	60	3
SM18:1/18:0	731.8	184.1	15	90	60	3
SM18:0/18:0	733.8	184.1	15	90	60	3
SM18:1/20:1	757.7	184.1	15	90	60	3
SM18:1/20:0	759.7	184.1	15	90	60	3
SM18:1/22:1	785.8	184.1	15	90	60	3
SM18:1/22:0	787.8	184.1	15	90	60	3

Appendices

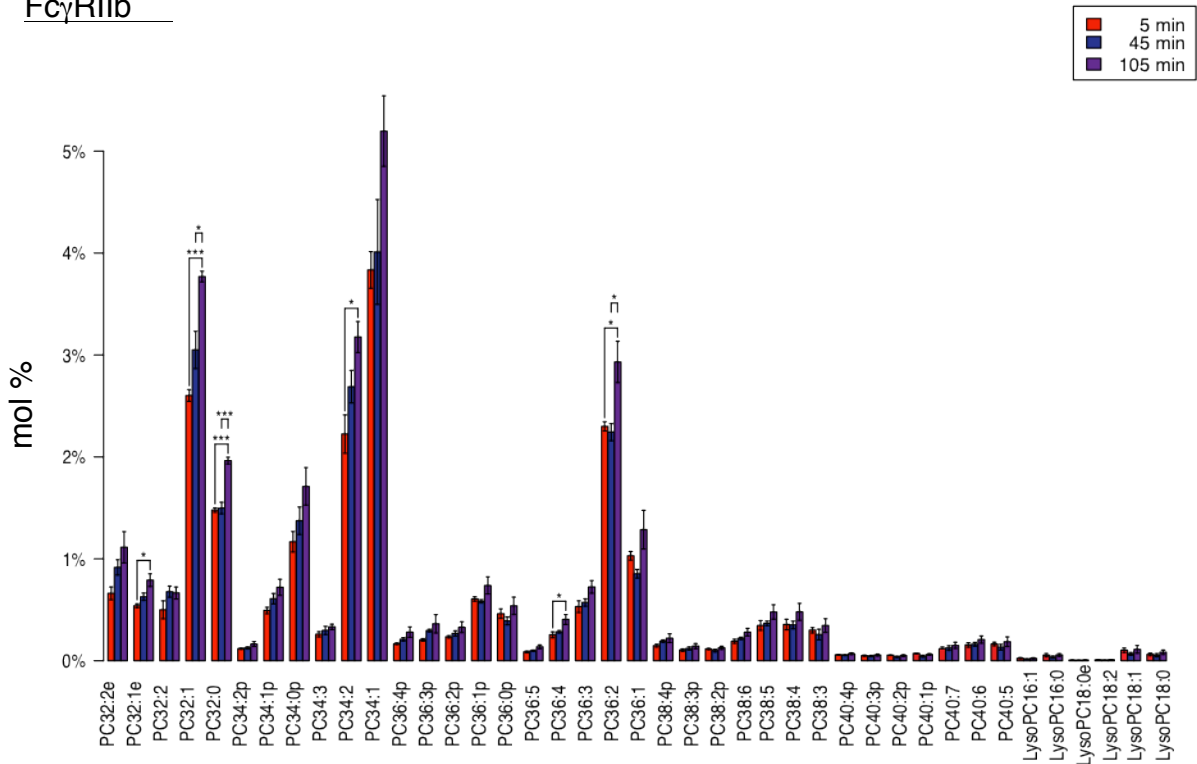
SM18:1/24:1	813.9	184.1	15	90	60	3
SM18:1/24:0	815.9	184.1	15	90	60	3
SM18:0/24:0	817.9	184.1	15	90	60	3
Cer d18:1/16:0	538.7	264.4	15	50	50	3
Cer d18:0/16:0	540.7	266.4	15	50	50	3
Cer d18:1/18:0	566.7	264.4	15	50	50	3
Cer d18:0/18:0	568.7	266.4	15	50	50	3
Cer d18:1/20:0	594.7	264.4	15	50	50	3
Cer d18:0/20:0	596.7	266.4	15	50	50	3
Cer d18:1/22:0	622.7	264.4	15	50	50	3
Cer d18:0/22:0	624.7	266.4	15	50	50	3
Cer d18:1/24:1	648.7	264.4	15	50	50	3
Cer d18:1/24:0	650.7	264.4	15	50	50	3
Cer d18:0/24:1	650.7	266.4	15	50	50	3
Cer d18:0/24:0	652.7	266.4	15	50	50	3

APCI	Q1	Q3	Dwell Time (ms)	Declustering Potential (V)	Collision Energy (V)	Cell Exit Potential (V)
Cholesterol	369.3	161	50	30	40	15

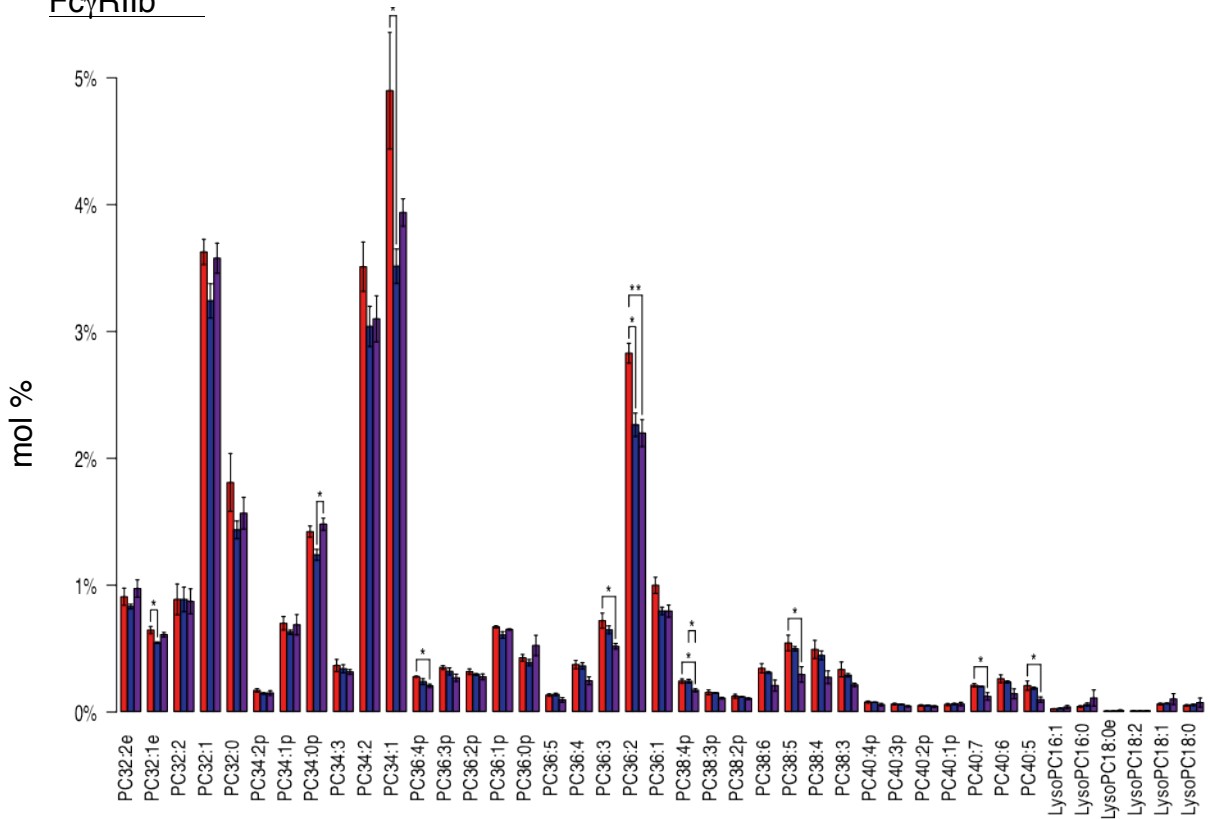
Appendix 2: Trends of individual lipid species in maturing phagosomes

Phosphatidylcholine (PC)

FcγRIIb^{232I}

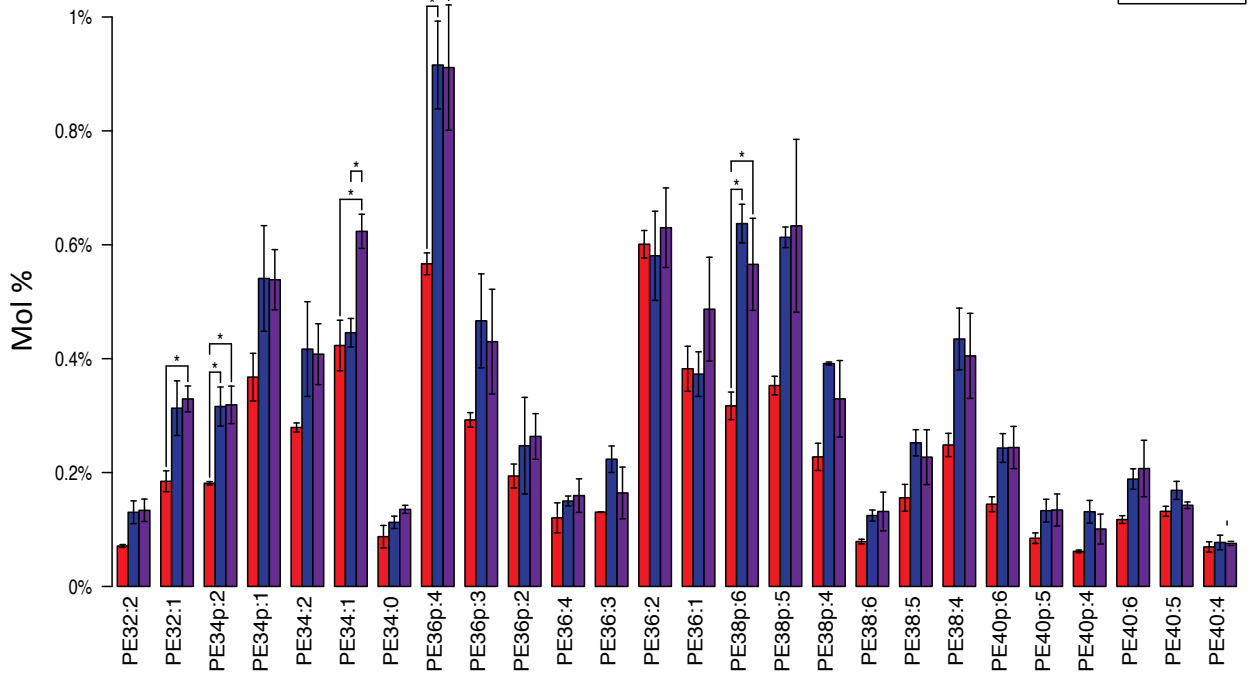


FcγRIIb^{232T}

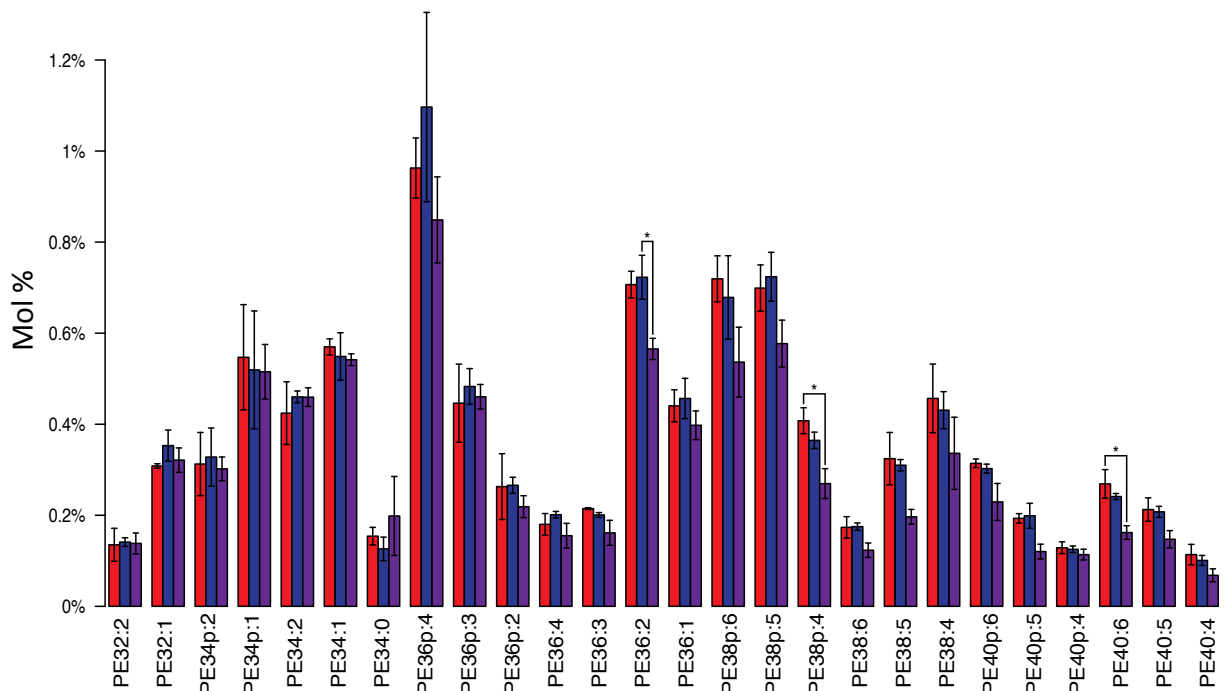


Phosphatidylethanolamine (PE)

^{232I}
FcγRIIb

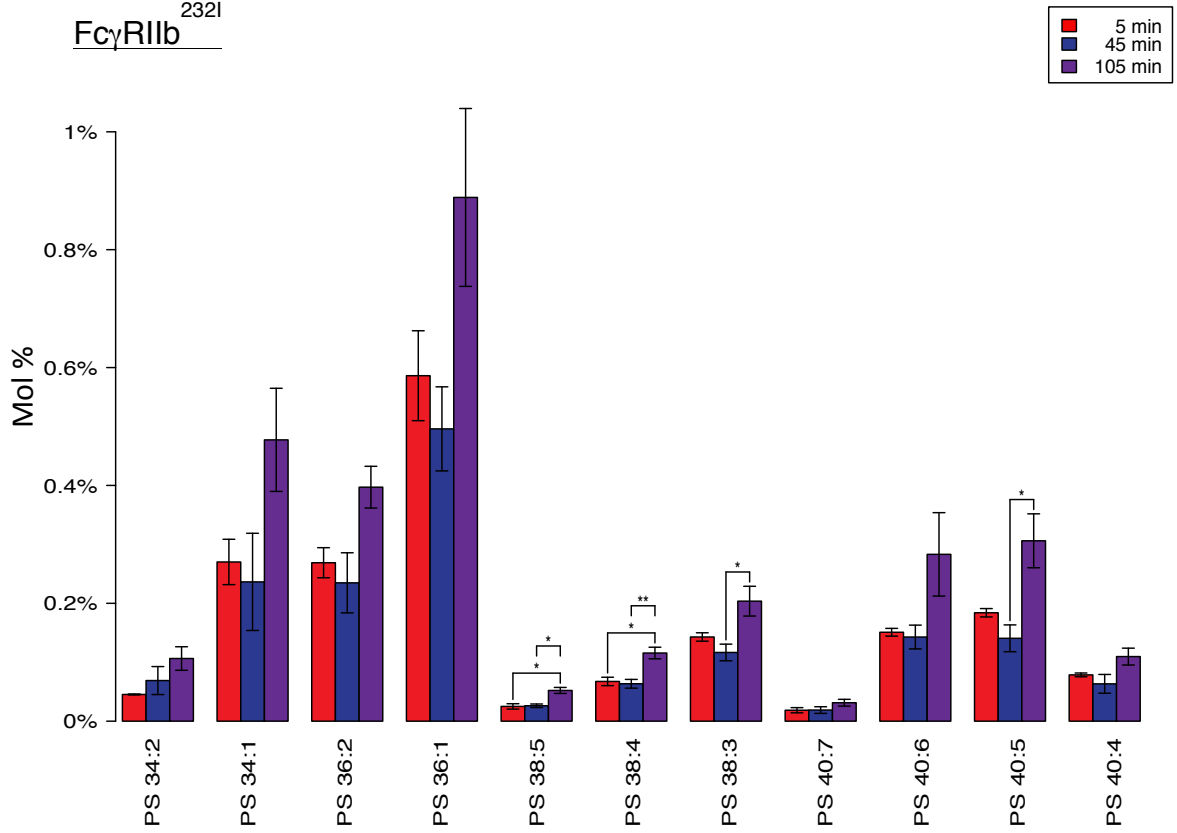


^{232T}
FcγRIIb

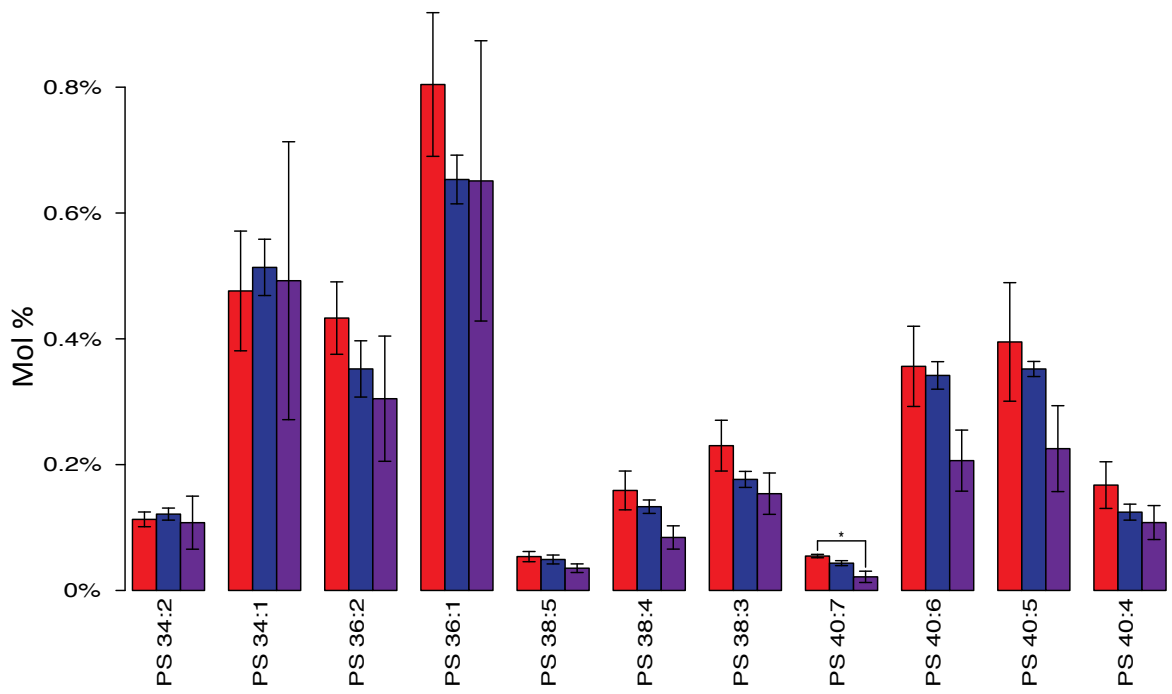


Phosphatidylserine (PS)

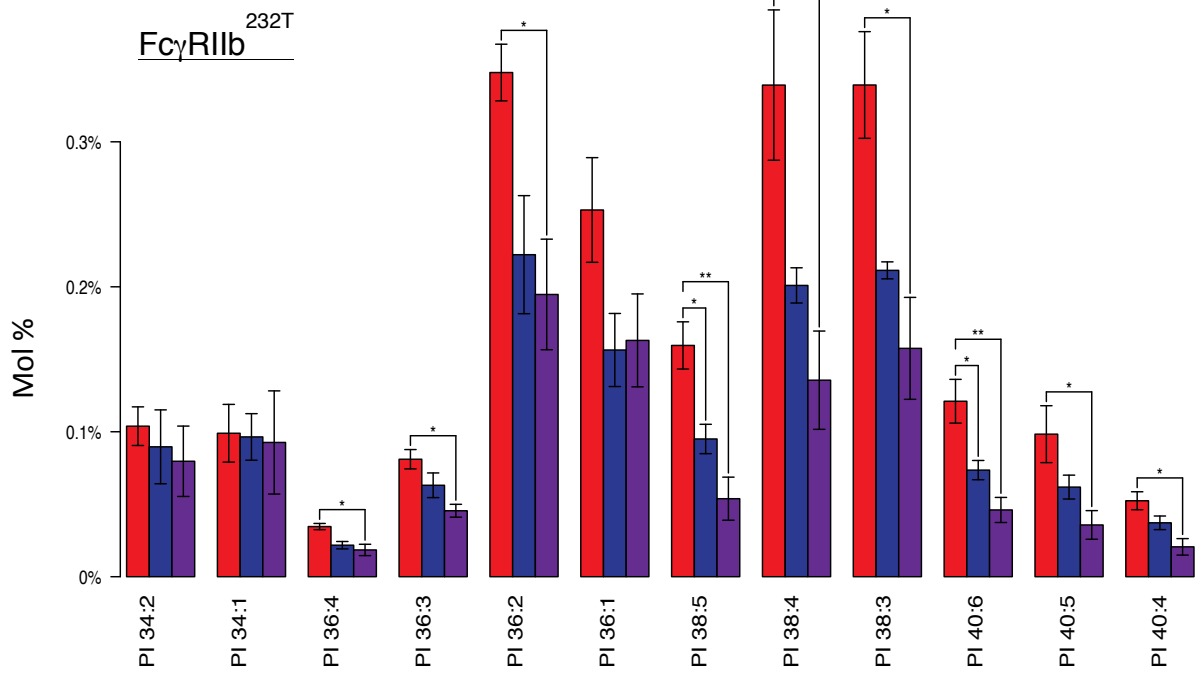
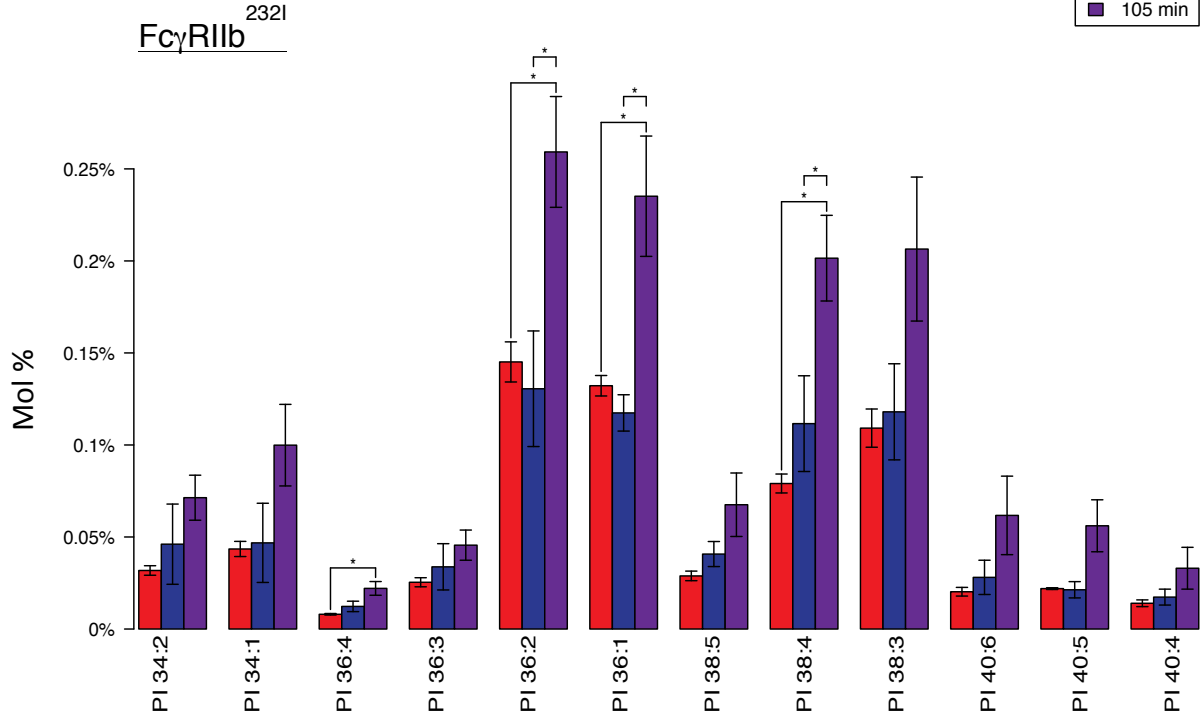
FcγRIIb^{232I}

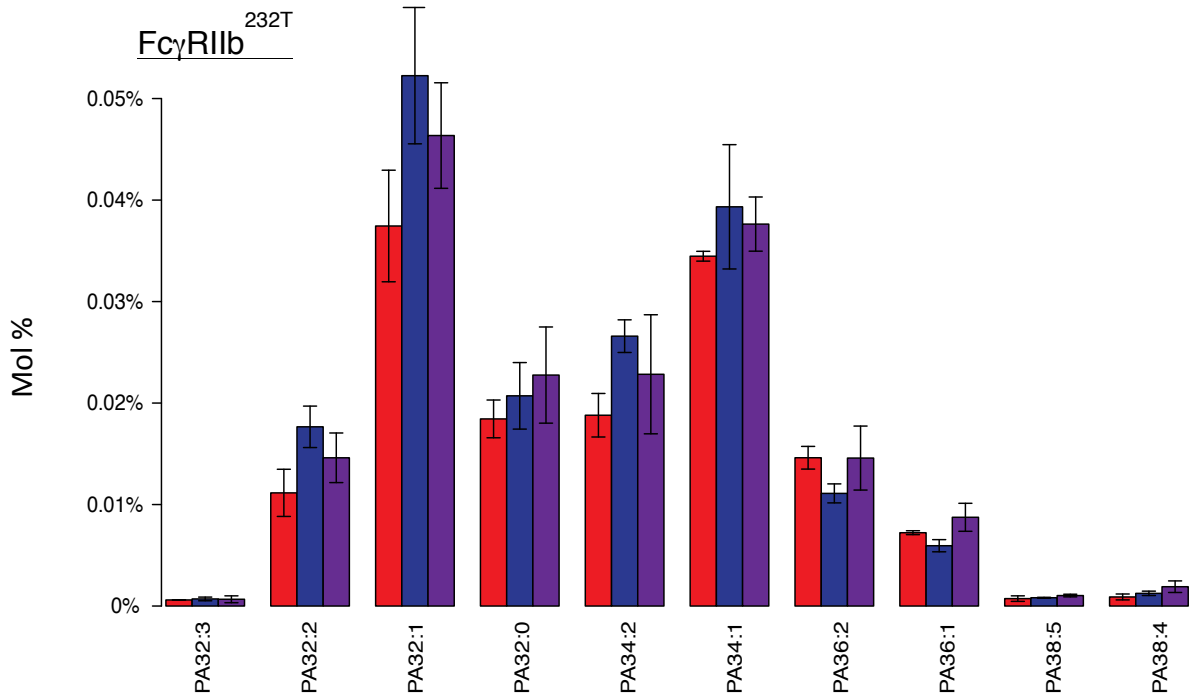
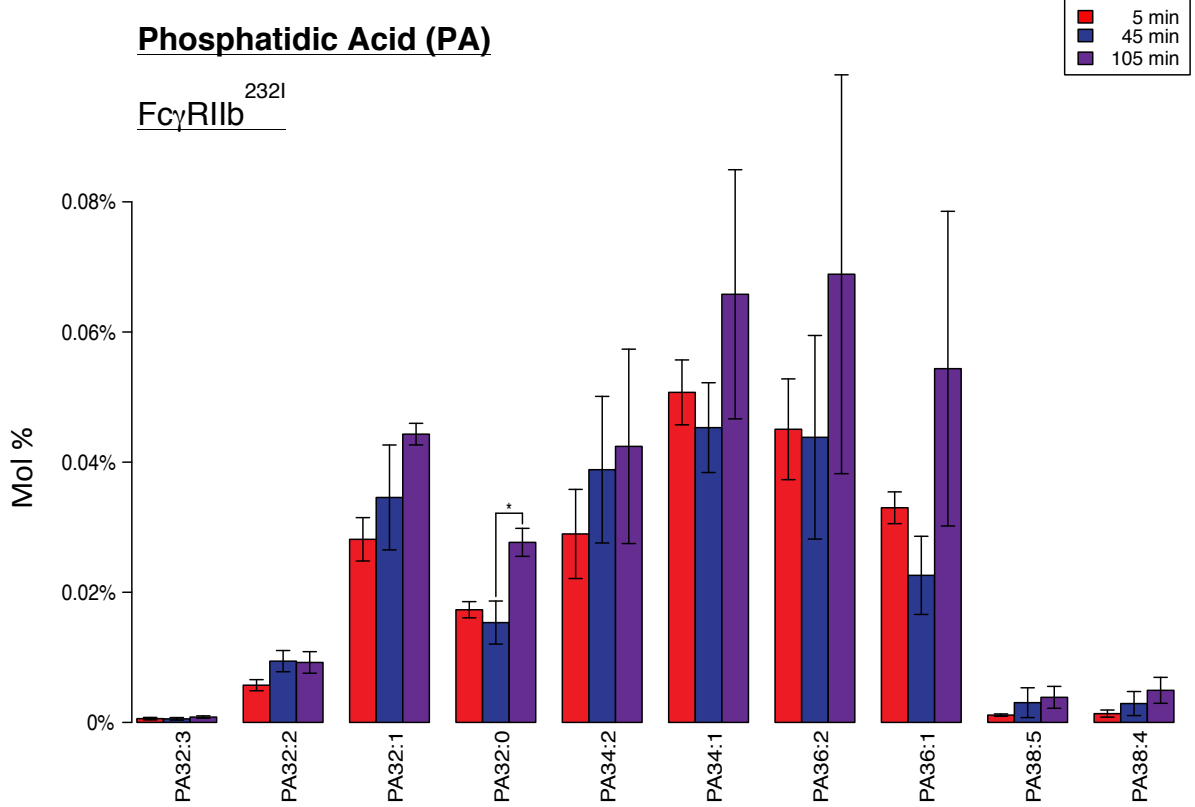


FcγRIIb^{232T}



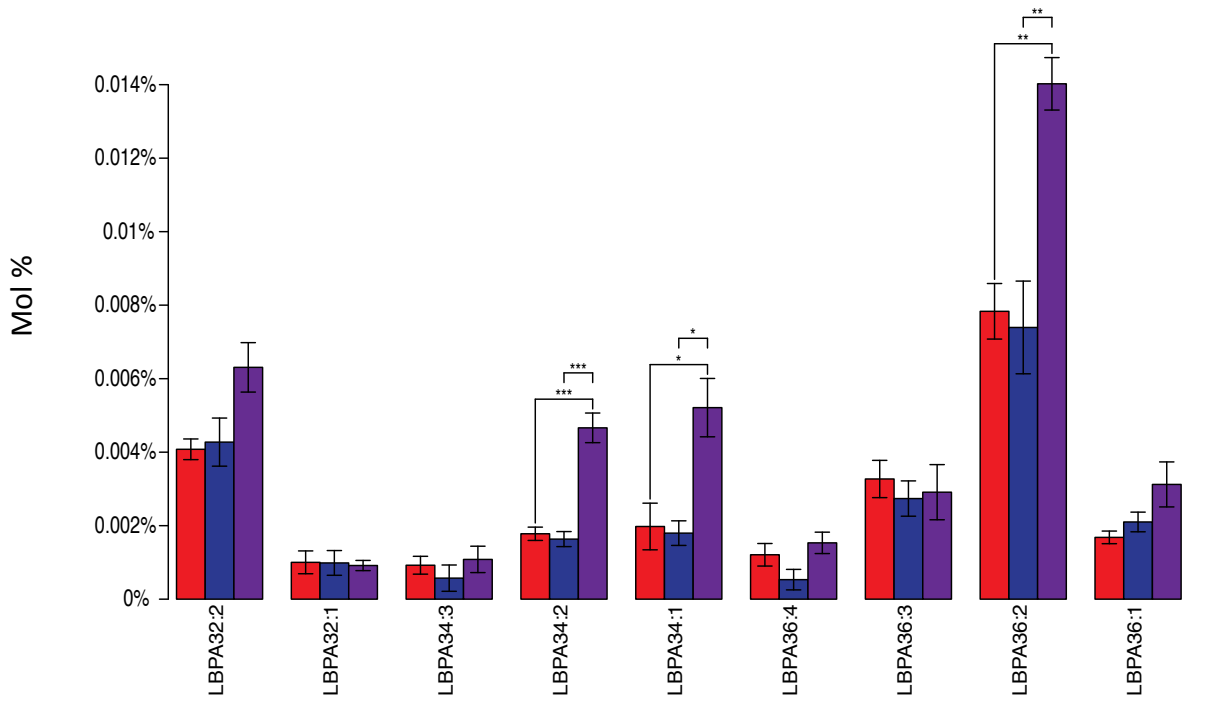
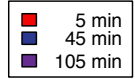
Phosphatidylinositol (PI)



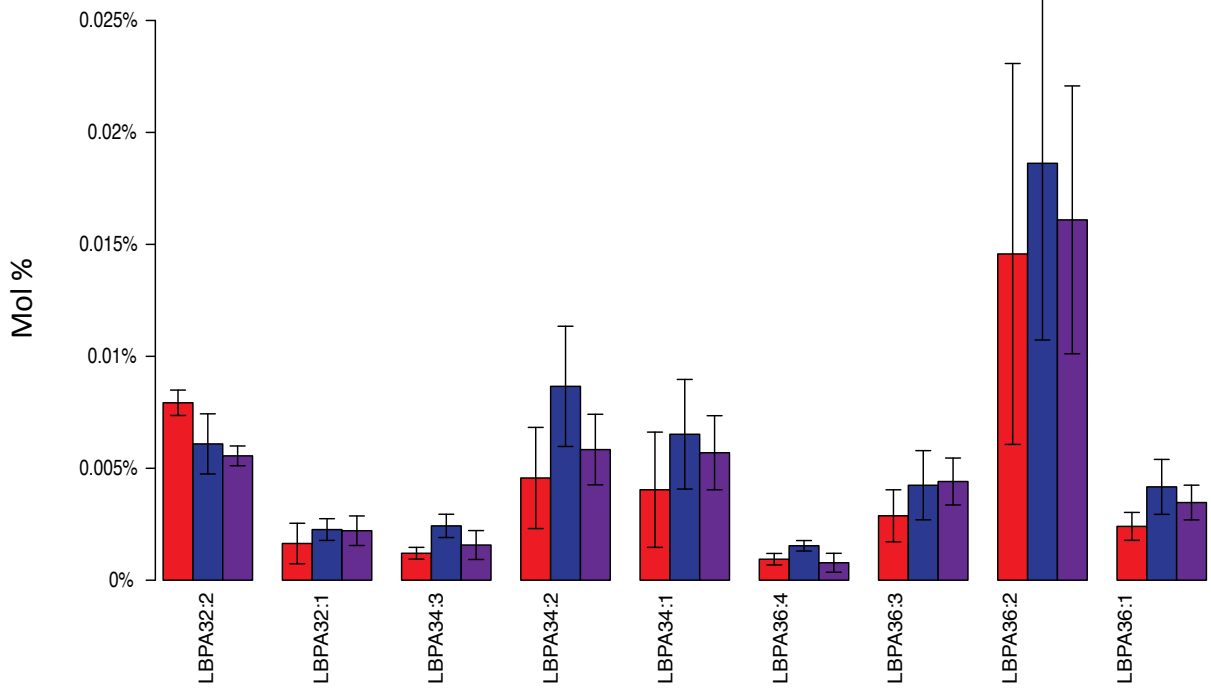


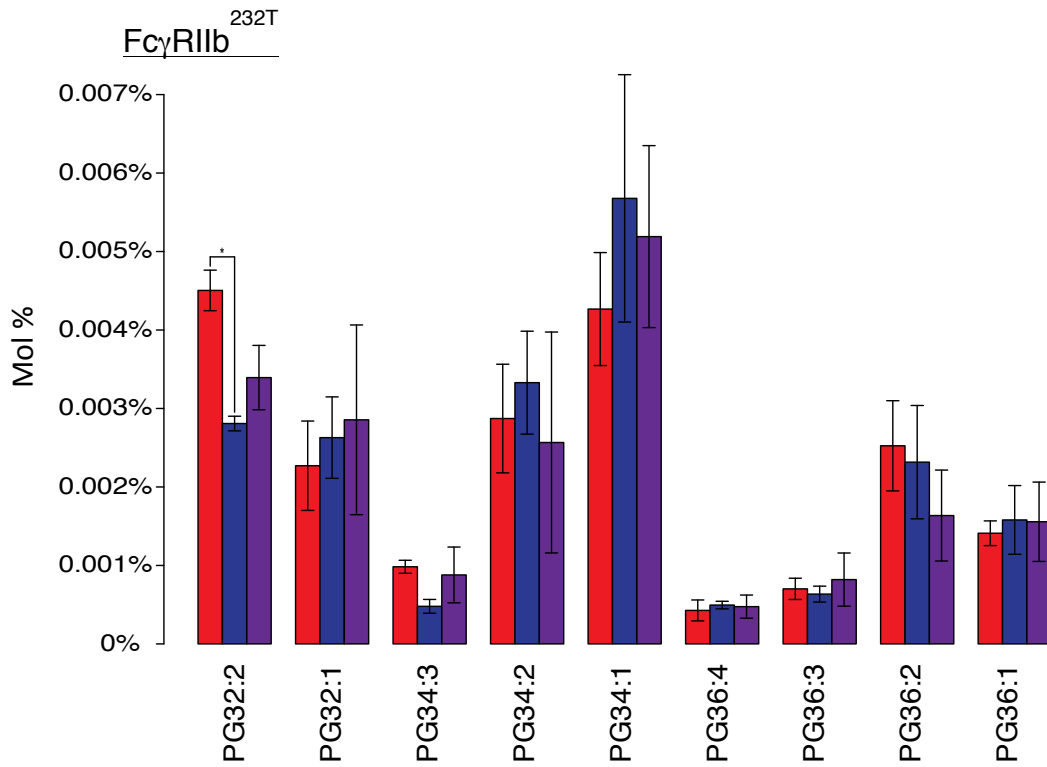
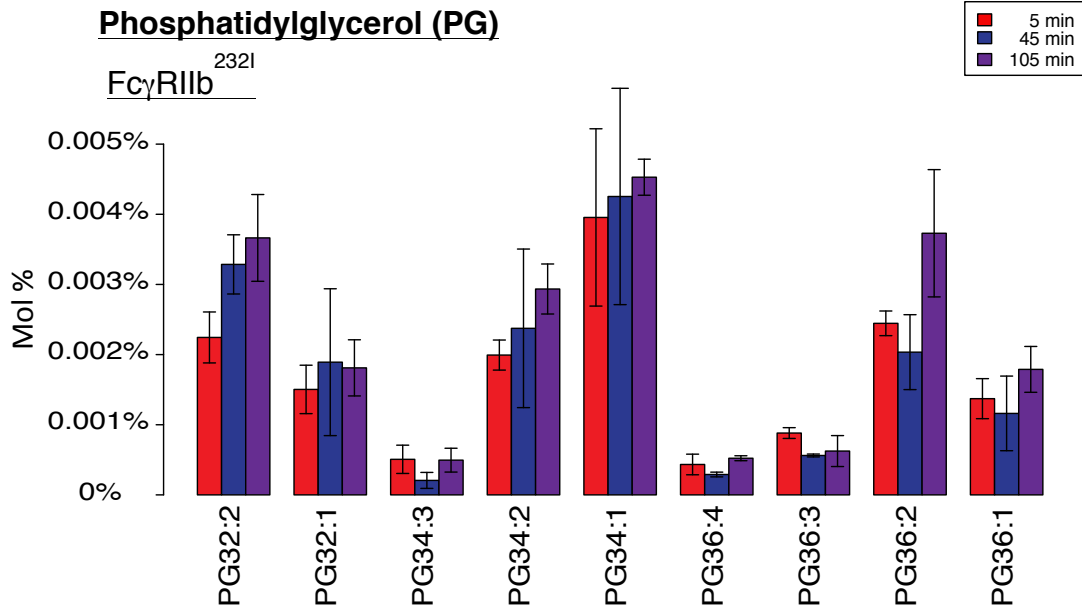
Lysobisphosphatidic Acid (LBPA)

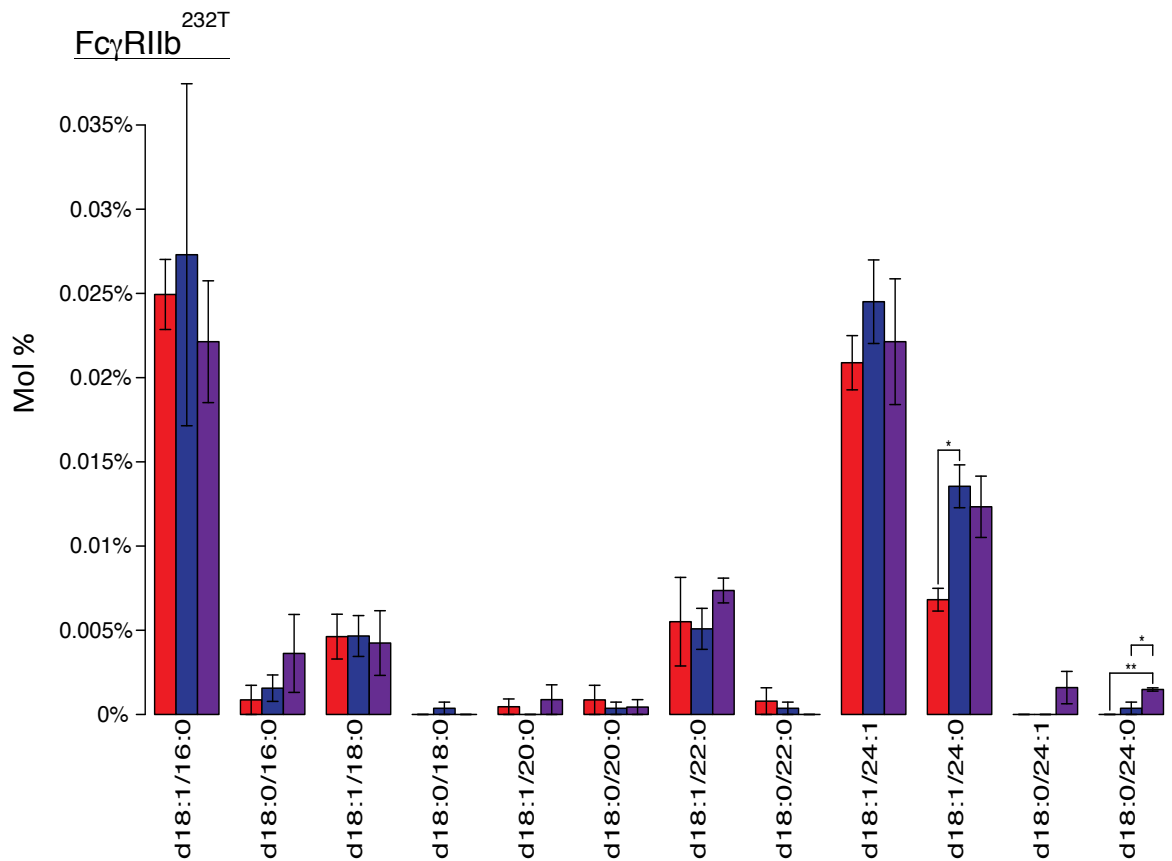
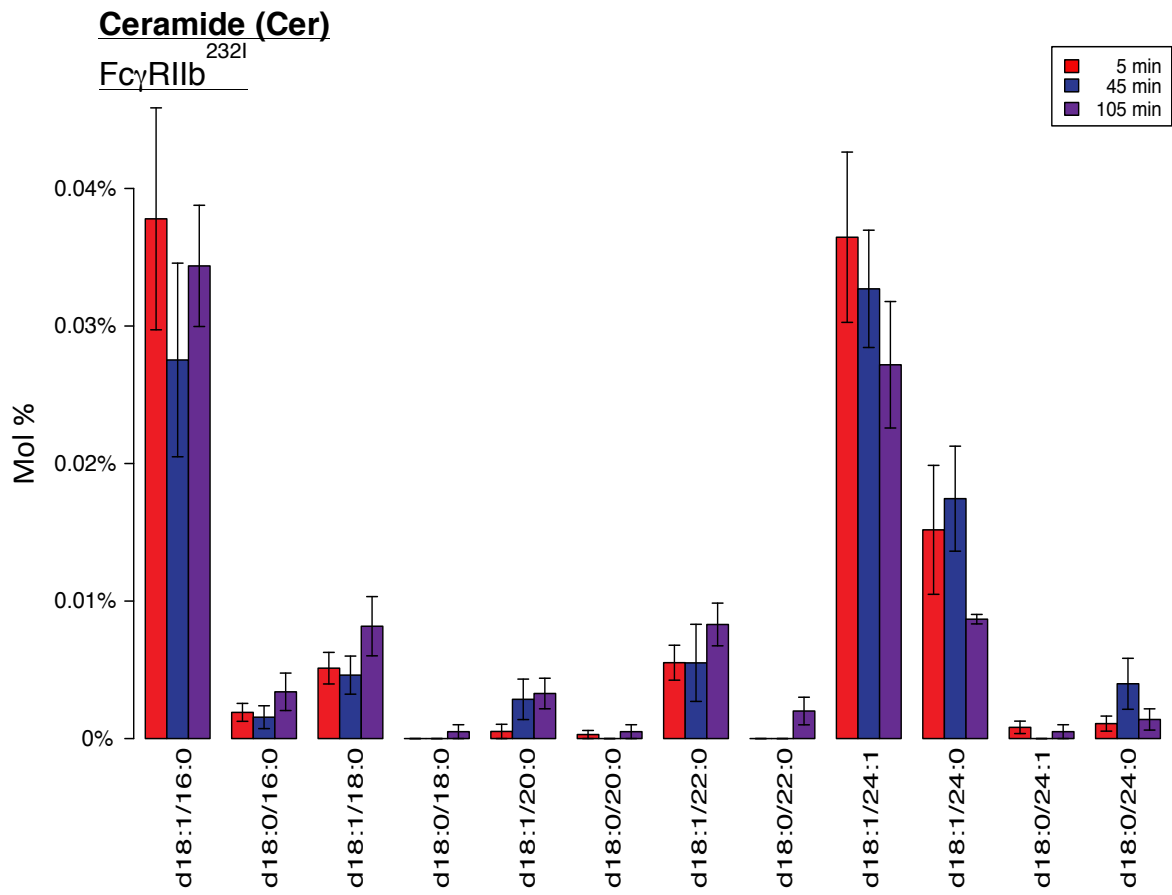
FcγRIIb^{232I}

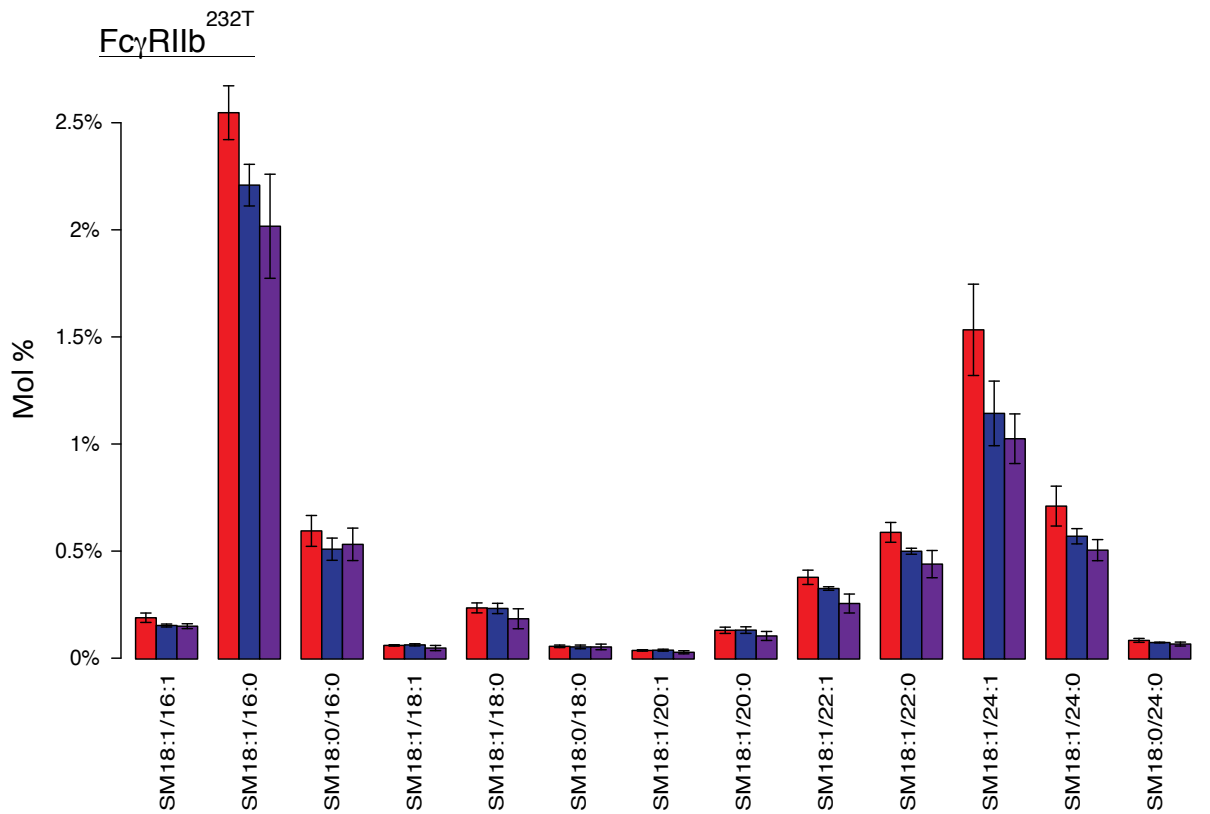
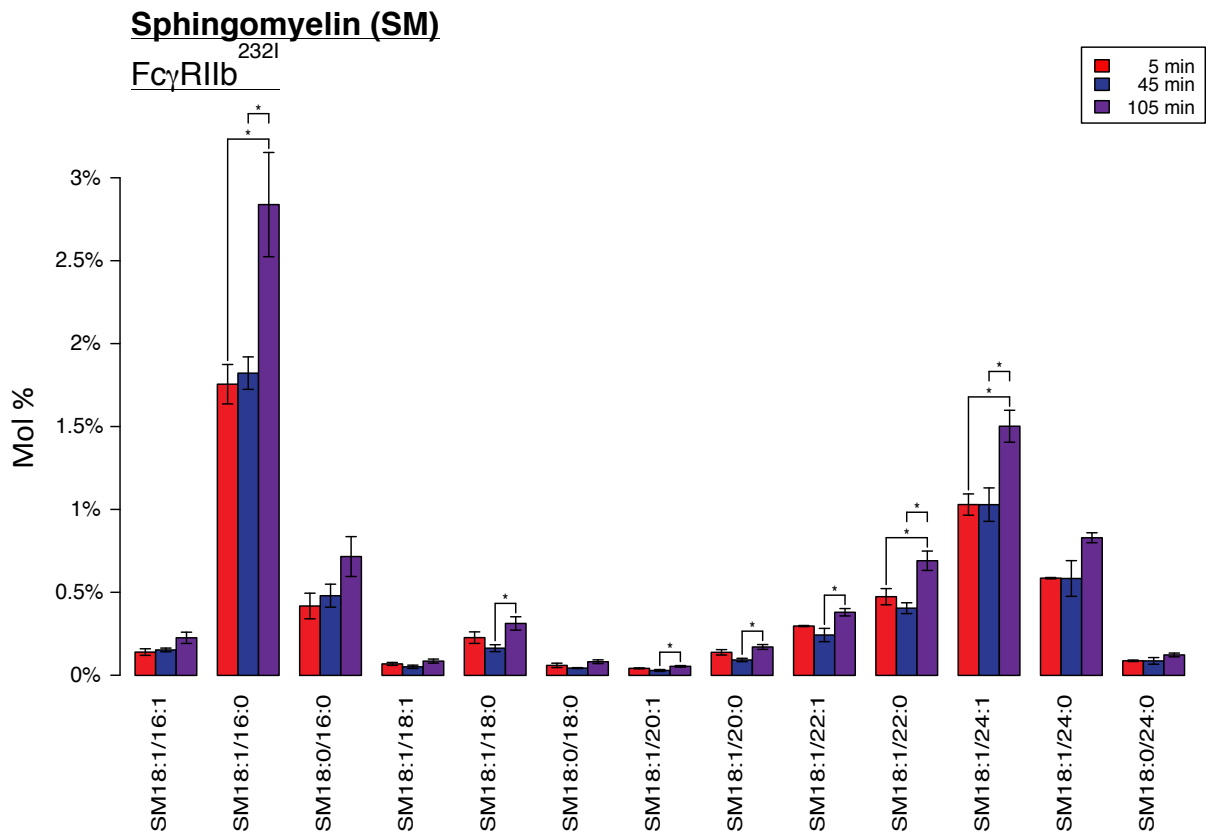


FcγRIIb^{232T}



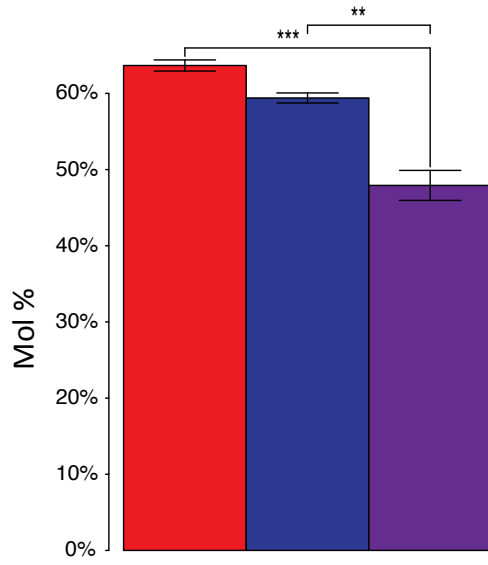




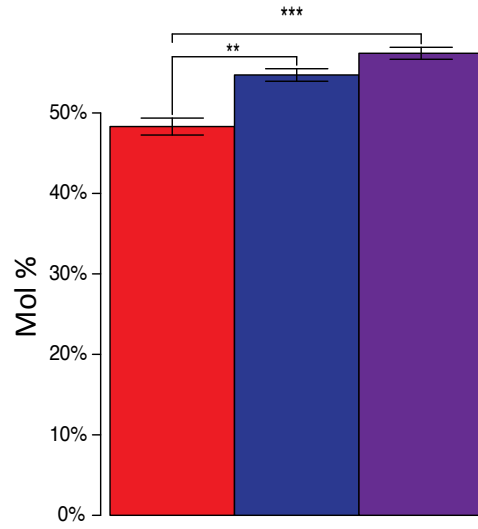
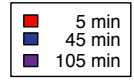


Cholesterol (Cho)

FcγRIIb^{232I}



FcγRIIb^{232T}



REFERENCE

References

1. Aderem, A., *How to eat something bigger than your head*. Cell, 2002. **110**(1): p. 5-8.
2. Rogers, L.D. and L.J. Foster, *Contributions of proteomics to understanding phagosome maturation*. Cell Microbiol, 2008. **10**(7): p. 1405-12.
3. Flannagan, R.S., V. Jaumouille, and S. Grinstein, *The Cell Biology of Phagocytosis*. Annual review of pathology, 2011.
4. Tan, S.Y. and M.K. Dee, *Elie Metchnikoff (1845-1916): discoverer of phagocytosis*. Singapore medical journal, 2009. **50**(5): p. 456-7.
5. Russell, D.G., et al., *The macrophage marches on its phagosome: dynamic assays of phagosome function*. Nature reviews. Immunology, 2009. **9**(8): p. 594-600.
6. Stuart, L.M. and R.A. Ezekowitz, *Phagocytosis and comparative innate immunity: learning on the fly*. Nat Rev Immunol, 2008. **8**(2): p. 131-41.
7. Niedergang, F. and P. Chavrier, *Signaling and membrane dynamics during phagocytosis: many roads lead to the phagos(R)ome*. Curr Opin Cell Biol, 2004. **16**(4): p. 422-8.
8. Brown, E.J., *Phagocytosis*. Bioessays, 1995. **17**(2): p. 109-117.
9. Rabinovitch, M., *Professional and non-professional phagocytes: an introduction*. Trends in cell biology, 1995. **5**(3): p. 85-7.
10. Vieira, O.V., R.J. Botelho, and S. Grinstein, *Phagosome maturation: aging gracefully*. Biochem J, 2002. **366**(Pt 3): p. 689-704.
11. Scott, C.C., R.J. Botelho, and S. Grinstein, *Phagosome maturation: a few bugs in the system*. J Membr Biol, 2003. **193**(3): p. 137-52.
12. Flannagan, R.S., G. Cosio, and S. Grinstein, *Antimicrobial mechanisms of phagocytes and bacterial evasion strategies*. Nat Rev Microbiol, 2009. **7**(5): p. 355-66.

13. Tjelle, T.E., T. Lovdal, and T. Berg, *Phagosome dynamics and function*. Bioessays, 2000. **22**(3): p. 255-63.
14. Botelho, R.J. and S. Grinstein, *Phagocytosis*. Current biology : CB, 2011. **21**(14): p. R533-8.
15. Aderem, A. and D.M. Underhill, *Mechanisms of phagocytosis in macrophages*. Annu Rev Immunol, 1999. **17**: p. 593-623.
16. Stuart, L.M. and R.A. Ezekowitz, *Phagocytosis: elegant complexity*. Immunity, 2005. **22**(5): p. 539-50.
17. Swanson, J.A. and A.D. Hoppe, *The coordination of signaling during Fc receptor-mediated phagocytosis*. J Leukoc Biol, 2004. **76**(6): p. 1093-103.
18. Allen, L.A. and A. Aderem, *Mechanisms of phagocytosis*. Current opinion in immunology, 1996. **8**(1): p. 36-40.
19. Yeung, T. and S. Grinstein, *Lipid signaling and the modulation of surface charge during phagocytosis*. Immunol Rev, 2007. **219**: p. 17-36.
20. Fairn, G.D. and S. Grinstein, *How nascent phagosomes mature to become phagolysosomes*. Trends Immunol, 2012. **33**(8): p. 397-405.
21. Takai, T., *Roles of Fc receptors in autoimmunity*. Nature reviews. Immunology, 2002. **2**(8): p. 580-92.
22. Takai, T., *Fc receptors and their role in immune regulation and autoimmunity*. J Clin Immunol, 2005. **25**(1): p. 1-18.
23. Sanchez-Mejorada, G. and C. Rosales, *Signal transduction by immunoglobulin Fc receptors*. Journal of leukocyte biology, 1998. **63**(5): p. 521-33.
24. Ravetch, J.V., *Fc receptors*. Current opinion in immunology, 1997. **9**(1): p. 121-5.
25. Steinberg, B.E., C.C. Scott, and S. Grinstein, *High-throughput assays of phagocytosis, phagosome maturation, and bacterial invasion*. American journal of physiology. Cell physiology, 2007. **292**(2): p. C945-52.

26. van Sorge, N.M., W.L. van der Pol, and J.G. van de Winkel, *Fcγ₁R polymorphisms: Implications for function, disease susceptibility and immunotherapy*. *Tissue Antigens*, 2003. **61**(3): p. 189-202.
27. Niederer, H.A., et al., *Fcγ₂R1B, Fcγ₂R2B, and systemic lupus erythematosus*. *Ann N Y Acad Sci*, 2010. **1183**: p. 69-88.
28. Woof, J.M. and D.R. Burton, *Human antibody-Fc receptor interactions illuminated by crystal structures*. *Nat Rev Immunol*, 2004. **4**(2): p. 89-99.
29. Nimmerjahn, F. and J.V. Ravetch, *Fcγ receptors: old friends and new family members*. *Immunity*, 2006. **24**(1): p. 19-28.
30. Jovanovic, V., et al., *Fc γ₁ receptor biology and systemic lupus erythematosus*. *International journal of rheumatic diseases*, 2009. **12**(4): p. 293-8.
31. Tarasenko, T., J.A. Dean, and S. Bolland, *Fcγ₂R1B as a modulator of autoimmune disease susceptibility*. *Autoimmunity*, 2007. **40**(6): p. 409-17.
32. Fossati, G., R.C. Bucknall, and S.W. Edwards, *Fcγ receptors in autoimmune diseases*. *European journal of clinical investigation*, 2001. **31**(9): p. 821-31.
33. Ravetch, J.V. and S. Bolland, *IgG Fc receptors*. *Annu Rev Immunol*, 2001. **19**: p. 275-90.
34. Reefman, E., et al., *Fcγ receptors in the initiation and progression of systemic lupus erythematosus*. *Immunology and cell biology*, 2003. **81**(5): p. 382-9.
35. Willcocks, L.C., K.G. Smith, and M.R. Clatworthy, *Low-affinity Fcγ receptors, autoimmunity and infection*. *Expert reviews in molecular medicine*, 2009. **11**: p. e24.
36. Joshi, T., J.P. Butchar, and S. Tridandapani, *Fcγ receptor signaling in phagocytes*. *Int J Hematol*, 2006. **84**(3): p. 210-6.
37. Smith, K.G. and M.R. Clatworthy, *Fcγ₂R1B in autoimmunity and infection: evolutionary and therapeutic implications*. *Nature reviews. Immunology*, 2010. **10**(5): p. 328-43.

38. Nimmerjahn, F. and J.V. Ravetch, *Fcγ receptors as regulators of immune responses*. Nat Rev Immunol, 2008. **8**(1): p. 34-47.
39. May, R.C. and L.M. Machesky, *Phagocytosis and the actin cytoskeleton*. Journal of cell science, 2001. **114**(Pt 6): p. 1061-77.
40. Li, X., et al., *A novel polymorphism in the Fcγ receptor IIB (CD32B) transmembrane region alters receptor signaling*. Arthritis Rheum, 2003. **48**(11): p. 3242-52.
41. Blank, M.C., et al., *Decreased transcription of the human FCGR2B gene mediated by the -343 G/C promoter polymorphism and association with systemic lupus erythematosus*. Hum Genet, 2005. **117**(2-3): p. 220-7.
42. Kono, H., et al., *FcγRIIB Ile232Thr transmembrane polymorphism associated with human systemic lupus erythematosus decreases affinity to lipid rafts and attenuates inhibitory effects on B cell receptor signaling*. Hum Mol Genet, 2005. **14**(19): p. 2881-92.
43. Blank, M.C., et al., *Decreased transcription of the human FCGR2B gene mediated by the -343 G/C promoter polymorphism and association with systemic lupus erythematosus*. Human genetics, 2005. **117**(2-3): p. 220-7.
44. McGaha, T.L., B. Sorrentino, and J.V. Ravetch, *Restoration of tolerance in lupus by targeted inhibitory receptor expression*. Science, 2005. **307**(5709): p. 590-3.
45. Bolland, S., et al., *Genetic modifiers of systemic lupus erythematosus in FcγRIIB(-/-) mice*. The Journal of experimental medicine, 2002. **195**(9): p. 1167-74.
46. Tsokos, G.C., *Systemic lupus erythematosus*. The New England journal of medicine, 2011. **365**(22): p. 2110-21.
47. Mok, C.C. and C.S. Lau, *Pathogenesis of systemic lupus erythematosus*. Journal of clinical pathology, 2003. **56**(7): p. 481-90.
48. Boross, P., et al., *The inhibiting Fc receptor for IgG, FcγRIIB, is a modifier of autoimmune susceptibility*. J Immunol, 2011. **187**(3): p. 1304-13.

49. Kyogoku, C., et al., *Fcgamma receptor gene polymorphisms in Japanese patients with systemic lupus erythematosus: contribution of FCGR2B to genetic susceptibility*. *Arthritis Rheum*, 2002. **46**(5): p. 1242-54.
50. Chu, Z.T., et al., *Association of Fcgamma receptor IIb polymorphism with susceptibility to systemic lupus erythematosus in Chinese: a common susceptibility gene in the Asian populations*. *Tissue Antigens*, 2004. **63**(1): p. 21-7.
51. Siriboonrit, U., et al., *Association of Fcgamma receptor IIb and IIIb polymorphisms with susceptibility to systemic lupus erythematosus in Thais*. *Tissue Antigens*, 2003. **61**(5): p. 374-83.
52. Pradhan, V., et al., *Fc gamma R IIB gene polymorphisms in Indian systemic lupus erythematosus (SLE) patients*. *The Indian journal of medical research*, 2011. **134**(2): p. 181-5.
53. Willcocks, L.C., et al., *A defunctioning polymorphism in FCGR2B is associated with protection against malaria but susceptibility to systemic lupus erythematosus*. *Proceedings of the National Academy of Sciences of the United States of America*, 2010. **107**(17): p. 7881-5.
54. Clatworthy, M.R., et al., *Systemic lupus erythematosus-associated defects in the inhibitory receptor FcgammaRIIb reduce susceptibility to malaria*. *Proceedings of the National Academy of Sciences of the United States of America*, 2007. **104**(17): p. 7169-74.
55. Floto, R.A., et al., *Loss of function of a lupus-associated FcgammaRIIb polymorphism through exclusion from lipid rafts*. *Nat Med*, 2005. **11**(10): p. 1056-8.
56. van der Meer-Janssen, Y.P., et al., *Lipids in host-pathogen interactions: pathogens exploit the complexity of the host cell lipidome*. *Prog Lipid Res*, 2010. **49**(1): p. 1-26.
57. Bohdanowicz, M. and S. Grinstein, *Role of phospholipids in endocytosis, phagocytosis, and macropinocytosis*. *Physiol Rev*, 2013. **93**(1): p. 69-106.
58. Eyster, K.M., *The membrane and lipids as integral participants in signal transduction: lipid signal transduction for the non-lipid biochemist*. *Adv Physiol Educ*, 2007. **31**(1): p. 5-16.

59. Engelman, D.M., *Membranes are more mosaic than fluid*. Nature, 2005. **438**(7068): p. 578-80.
60. van Meer, G., D.R. Voelker, and G.W. Feigenson, *Membrane lipids: where they are and how they behave*. Nat Rev Mol Cell Biol, 2008. **9**(2): p. 112-24.
61. Leventis, P.A. and S. Grinstein, *The distribution and function of phosphatidylserine in cellular membranes*. Annu Rev Biophys, 2010. **39**: p. 407-27.
62. Wymann, M.P. and R. Schneider, *Lipid signalling in disease*. Nature reviews. Molecular cell biology, 2008. **9**(2): p. 162-76.
63. van Meer, G., D.R. Voelker, and G.W. Feigenson, *Membrane lipids: where they are and how they behave*. Nature reviews. Molecular cell biology, 2008. **9**(2): p. 112-24.
64. Steinberg, B.E. and S. Grinstein, *Pathogen destruction versus intracellular survival: the role of lipids as phagosomal fate determinants*. J Clin Invest, 2008. **118**(6): p. 2002-11.
65. Simons, K. and J.L. Sampaio, *Membrane organization and lipid rafts*. Cold Spring Harb Perspect Biol, 2011. **3**(10): p. a004697.
66. Hermansson, M., K. Hokynar, and P. Somerharju, *Mechanisms of glycerophospholipid homeostasis in mammalian cells*. Progress in lipid research, 2011. **50**(3): p. 240-57.
67. Han, X. and R.W. Gross, *Shotgun lipidomics: electrospray ionization mass spectrometric analysis and quantitation of cellular lipidomes directly from crude extracts of biological samples*. Mass Spectrom Rev, 2005. **24**(3): p. 367-412.
68. Alfred H. Merrill, J., *Biochemistry of Lipids, Lipoproteins and Membranes*. 5 ed, ed. D.E.V.a.J.E. Vance 2008: Elsevier.
69. McMahon, H.T. and J.L. Gallop, *Membrane curvature and mechanisms of dynamic cell membrane remodelling*. Nature, 2005. **438**(7068): p. 590-6.
70. van Meer, G. and H. Sprong, *Membrane lipids and vesicular traffic*. Curr Opin Cell Biol, 2004. **16**(4): p. 373-8.

71. Piomelli, D., G. Astarita, and R. Rapaka, *A neuroscientist's guide to lipidomics*. Nat Rev Neurosci, 2007. **8**(10): p. 743-54.
72. Pike, L.J., *Lipid rafts: heterogeneity on the high seas*. Biochem J, 2004. **378**(Pt 2): p. 281-92.
73. Yeung, T., et al., *Contribution of phosphatidylserine to membrane surface charge and protein targeting during phagosome maturation*. J Cell Biol, 2009. **185**(5): p. 917-28.
74. Wenk, M.R., *The emerging field of lipidomics*. Nat Rev Drug Discov, 2005. **4**(7): p. 594-610.
75. Verkleij, A.J. and J.A. Post, *Membrane phospholipid asymmetry and signal transduction*. J Membr Biol, 2000. **178**(1): p. 1-10.
76. Bou Khalil, M., et al., *Lipidomics era: accomplishments and challenges*. Mass Spectrom Rev, 2010. **29**(6): p. 877-929.
77. Shevchenko, A. and K. Simons, *Lipidomics: coming to grips with lipid diversity*. Nat Rev Mol Cell Biol, 2010. **11**(8): p. 593-8.
78. Yeung, T., et al., *Membrane phosphatidylserine regulates surface charge and protein localization*. Science, 2008. **319**(5860): p. 210-3.
79. Vance, J.E. and R. Steenbergen, *Metabolism and functions of phosphatidylserine*. Prog Lipid Res, 2005. **44**(4): p. 207-34.
80. Holthuis, J.C. and T.P. Levine, *Lipid traffic: floppy drives and a superhighway*. Nat Rev Mol Cell Biol, 2005. **6**(3): p. 209-20.
81. Iyer, S.S., et al., *Phospholipases D1 and D2 coordinately regulate macrophage phagocytosis*. J Immunol, 2004. **173**(4): p. 2615-23.
82. Corrotte, M., et al., *Dynamics and function of phospholipase D and phosphatidic acid during phagocytosis*. Traffic, 2006. **7**(3): p. 365-77.
83. van Meer, G. and A.I. de Kroon, *Lipid map of the mammalian cell*. J Cell Sci, 2011. **124**(Pt 1): p. 5-8.

84. Yeung, T., et al., *Lipid metabolism and dynamics during phagocytosis*. *Curr Opin Cell Biol*, 2006. **18**(4): p. 429-37.
85. Cosio, G. and S. Grinstein, *Analysis of phosphoinositide dynamics during phagocytosis using genetically encoded fluorescent biosensors*. *Methods Mol Biol*, 2008. **445**: p. 287-300.
86. Lee, W.L., et al., *Quantitative analysis of membrane remodeling at the phagocytic cup*. *Mol Biol Cell*, 2007. **18**(8): p. 2883-92.
87. Coppolino, M.G., et al., *Inhibition of phosphatidylinositol-4-phosphate 5-kinase I α impairs localized actin remodeling and suppresses phagocytosis*. *J Biol Chem*, 2002. **277**(46): p. 43849-57.
88. Scott, C.C., et al., *Phosphatidylinositol-4,5-bisphosphate hydrolysis directs actin remodeling during phagocytosis*. *J Cell Biol*, 2005. **169**(1): p. 139-49.
89. Botelho, R.J., et al., *Localized biphasic changes in phosphatidylinositol-4,5-bisphosphate at sites of phagocytosis*. *J Cell Biol*, 2000. **151**(7): p. 1353-68.
90. Cox, D., et al., *A requirement for phosphatidylinositol 3-kinase in pseudopod extension*. *J Biol Chem*, 1999. **274**(3): p. 1240-7.
91. Chevallier, J., et al., *Lysobisphosphatidic acid controls endosomal cholesterol levels*. *J Biol Chem*, 2008. **283**(41): p. 27871-80.
92. Matsuo, H., et al., *Role of LBPA and Alix in multivesicular liposome formation and endosome organization*. *Science*, 2004. **303**(5657): p. 531-4.
93. Ikonen, E., *Cellular cholesterol trafficking and compartmentalization*. *Nat Rev Mol Cell Biol*, 2008. **9**(2): p. 125-38.
94. Maxfield, F.R. and I. Tabas, *Role of cholesterol and lipid organization in disease*. *Nature*, 2005. **438**(7068): p. 612-21.
95. Kwiatkowska, K. and A. Sobota, *The clustered Fc γ receptor II is recruited to Lyn-containing membrane domains and undergoes phosphorylation in a cholesterol-dependent manner*. *Eur J Immunol*, 2001. **31**(4): p. 989-98.

96. Loike, J.D., et al., *Statin inhibition of Fc receptor-mediated phagocytosis by macrophages is modulated by cell activation and cholesterol*. *Arterioscler Thromb Vasc Biol*, 2004. **24**(11): p. 2051-6.
97. Corbett-Nelson, E.F., et al., *Signaling-dependent immobilization of acylated proteins in the inner monolayer of the plasma membrane*. *J Cell Biol*, 2006. **174**(2): p. 255-65.
98. Huynh, K.K., E. Gershenson, and S. Grinstein, *Cholesterol accumulation by macrophages impairs phagosome maturation*. *J Biol Chem*, 2008. **283**(51): p. 35745-55.
99. Korzeniowski, M., et al., *Fc gamma RII activation induces cell surface ceramide production which participates in the assembly of the receptor signaling complex*. *Cell Physiol Biochem*, 2007. **20**(5): p. 347-56.
100. Gulbins, E. and P.L. Li, *Physiological and pathophysiological aspects of ceramide*. *Am J Physiol Regul Integr Comp Physiol*, 2006. **290**(1): p. R11-26.
101. Liu, P. and R.G. Anderson, *Compartmentalized production of ceramide at the cell surface*. *J Biol Chem*, 1995. **270**(45): p. 27179-85.
102. Utermohlen, O., et al., *Fusogenicity of membranes: the impact of acid sphingomyelinase on innate immune responses*. *Immunobiology*, 2008. **213**(3-4): p. 307-14.
103. Schramm, M., et al., *Acid sphingomyelinase is required for efficient phagolysosomal fusion*. *Cell Microbiol*, 2008. **10**(9): p. 1839-53.
104. Riethmuller, J., et al., *Membrane rafts in host-pathogen interactions*. *Biochim Biophys Acta*, 2006. **1758**(12): p. 2139-47.
105. Anes, E., et al., *Selected lipids activate phagosome actin assembly and maturation resulting in killing of pathogenic mycobacteria*. *Nat Cell Biol*, 2003. **5**(9): p. 793-802.
106. Simons, K. and D. Toomre, *Lipid rafts and signal transduction*. *Nat Rev Mol Cell Biol*, 2000. **1**(1): p. 31-9.
107. Pike, L.J., *Lipid rafts: bringing order to chaos*. *J Lipid Res*, 2003. **44**(4): p. 655-67.

108. Vieira, F.S., et al., *Host-cell lipid rafts: a safe door for micro-organisms?* Biol Cell, 2010. **102**(7): p. 391-407.
109. Zajchowski, L.D. and S.M. Robbins, *Lipid rafts and little caves. Compartmentalized signalling in membrane microdomains.* Eur J Biochem, 2002. **269**(3): p. 737-52.
110. Munro, S., *Lipid rafts: elusive or illusive?* Cell, 2003. **115**(4): p. 377-88.
111. Kono, H., et al., *Spatial raft coalescence represents an initial step in Fc gamma R signaling.* J Immunol, 2002. **169**(1): p. 193-203.
112. Hinkovska-Galcheva, V., et al., *Enhanced phagocytosis through inhibition of de novo ceramide synthesis.* J Biol Chem, 2003. **278**(2): p. 974-82.
113. Megha and E. London, *Ceramide selectively displaces cholesterol from ordered lipid domains (rafts): implications for lipid raft structure and function.* J Biol Chem, 2004. **279**(11): p. 9997-10004.
114. Grassme, H., J. Riethmuller, and E. Gulbins, *Biological aspects of ceramide-enriched membrane domains.* Prog Lipid Res, 2007. **46**(3-4): p. 161-70.
115. Abdel Shakor, A.B., K. Kwiatkowska, and A. Sobota, *Cell surface ceramide generation precedes and controls Fc gamma RII clustering and phosphorylation in rafts.* J Biol Chem, 2004. **279**(35): p. 36778-87.
116. Manes, S., G. del Real, and A.C. Martinez, *Pathogens: raft hijackers.* Nat Rev Immunol, 2003. **3**(7): p. 557-68.
117. Harkewicz, R. and E.A. Dennis, *Applications of mass spectrometry to lipids and membranes.* Annu Rev Biochem, 2011. **80**: p. 301-25.
118. Wenk, M.R., *Lipidomics: new tools and applications.* Cell, 2010. **143**(6): p. 888-95.
119. Pulfer, M. and R.C. Murphy, *Electrospray mass spectrometry of phospholipids.* Mass Spectrom Rev, 2003. **22**(5): p. 332-64.
120. Navas-Iglesias, N., A. Carrasco-Pancorbo, and L. Cuadros-Rodriguez, *From lipids analysis towards lipidomics, a new challenge for the analytical*

- chemistry of the 21st century. Part II: Analytical lipidomics. Trac-Trends in Analytical Chemistry*, 2009. **28**(4): p. 393-403.
121. Hu, C., et al., *Analytical strategies in lipidomics and applications in disease biomarker discovery*. *J Chromatogr B Analyt Technol Biomed Life Sci*, 2009. **877**(26): p. 2836-46.
 122. Gresham, H.D., et al., *Negative regulation of phagocytosis in murine macrophages by the Src kinase family member, Fgr*. *The Journal of experimental medicine*, 2000. **191**(3): p. 515-28.
 123. Dai, X., et al., *Differential signal transduction, membrane trafficking, and immune effector functions mediated by FcγRI versus FcγRIIa*. *Blood*, 2009. **114**(2): p. 318-27.
 124. Griffiths, G. and L. Mayorga, *Phagosome proteomes open the way to a better understanding of phagosome function*. *Genome biology*, 2007. **8**(3): p. 207.
 125. Li, Q., et al., *Analysis of phagosomal proteomes: from latex-bead to bacterial phagosomes*. *Proteomics*, 2010. **10**(22): p. 4098-116.
 126. Desjardins, M. and G. Griffiths, *Phagocytosis: latex leads the way*. *Current opinion in cell biology*, 2003. **15**(4): p. 498-503.
 127. Sundstrom, C. and K. Nilsson, *Establishment and characterization of a human histiocytic lymphoma cell line (U-937)*. *International journal of cancer. Journal international du cancer*, 1976. **17**(5): p. 565-77.
 128. Geissler, K., et al., *Effects of recombinant human colony stimulating factors (CSF) (granulocyte-macrophage CSF, granulocyte CSF, and CSF-1) on human monocyte/macrophage differentiation*. *Journal of immunology*, 1989. **143**(1): p. 140-6.
 129. Harris, P. and P. Ralph, *Human leukemic models of myelomonocytic development: a review of the HL-60 and U937 cell lines*. *Journal of leukocyte biology*, 1985. **37**(4): p. 407-22.
 130. Hass, R., et al., *TPA-induced differentiation and adhesion of U937 cells: changes in ultrastructure, cytoskeletal organization and expression of cell surface antigens*. *European journal of cell biology*, 1989. **48**(2): p. 282-93.

131. Liesveld, J.L., et al., *Expression of IgG Fc receptors in myeloid leukemic cell lines. Effect of colony-stimulating factors and cytokines.* Journal of immunology, 1988. **140**(5): p. 1527-33.
132. Niedel, J.E., L.J. Kuhn, and G.R. Vandenbark, *Phorbol diester receptor copurifies with protein kinase C.* Proceedings of the National Academy of Sciences of the United States of America, 1983. **80**(1): p. 36-40.
133. Liu, W.S. and C.A. Heckman, *The sevenfold way of PKC regulation.* Cellular signalling, 1998. **10**(8): p. 529-42.
134. Mellman, I.S., et al., *Internalization and degradation of macrophage Fc receptors during receptor-mediated phagocytosis.* The Journal of cell biology, 1983. **96**(3): p. 887-95.
135. Kusner, D.J., C.F. Hall, and S. Jackson, *Fc gamma receptor-mediated activation of phospholipase D regulates macrophage phagocytosis of IgG-opsinized particles.* Journal of immunology, 1999. **162**(4): p. 2266-74.
136. Desjardins, M., et al., *Molecular characterization of phagosomes.* J Biol Chem, 1994. **269**(51): p. 32194-200.
137. Haas, A., *The phagosome: compartment with a license to kill.* Traffic, 2007. **8**(4): p. 311-30.
138. Chaney, L.K. and B.S. Jacobson, *Coating cells with colloidal silica for high yield isolation of plasma membrane sheets and identification of transmembrane proteins.* The Journal of biological chemistry, 1983. **258**(16): p. 10062-72.
139. Morth, J.P., et al., *A structural overview of the plasma membrane Na⁺,K⁺-ATPase and H⁺-ATPase ion pumps.* Nature reviews. Molecular cell biology, 2011. **12**(1): p. 60-70.
140. Chan, R., et al., *Retroviruses human immunodeficiency virus and murine leukemia virus are enriched in phosphoinositides.* Journal of virology, 2008. **82**(22): p. 11228-38.
141. Dermine, J.F., et al., *Flotillin-1-enriched lipid raft domains accumulate on maturing phagosomes.* The Journal of biological chemistry, 2001. **276**(21): p. 18507-12.

142. Antonsson, A. and P.J. Johansson, *Binding of human and animal immunoglobulins to the IgG Fc receptor induced by human cytomegalovirus*. J Gen Virol, 2001. **82**(Pt 5): p. 1137-45.
143. Kinchen, J.M. and K.S. Ravichandran, *Phagosome maturation: going through the acid test*. Nature reviews. Molecular cell biology, 2008. **9**(10): p. 781-95.
144. Kohchi, C., et al., *ROS and innate immunity*. Anticancer research, 2009. **29**(3): p. 817-21.
145. Forman, H.J. and M. Torres, *Reactive oxygen species and cell signaling: respiratory burst in macrophage signaling*. American journal of respiratory and critical care medicine, 2002. **166**(12 Pt 2): p. S4-8.
146. Beaman, L. and B.L. Beaman, *The role of oxygen and its derivatives in microbial pathogenesis and host defense*. Annual review of microbiology, 1984. **38**: p. 27-48.
147. Heyworth, P.G., A.R. Cross, and J.T. Curnutte, *Chronic granulomatous disease*. Current opinion in immunology, 2003. **15**(5): p. 578-84.
148. Berridge, M.J., P. Lipp, and M.D. Bootman, *The versatility and universality of calcium signalling*. Nature reviews. Molecular cell biology, 2000. **1**(1): p. 11-21.
149. Myers, J.T. and J.A. Swanson, *Calcium spikes in activated macrophages during Fcγ receptor-mediated phagocytosis*. Journal of leukocyte biology, 2002. **72**(4): p. 677-84.
150. Nunes, P. and N. Demaurex, *The role of calcium signaling in phagocytosis*. Journal of leukocyte biology, 2010. **88**(1): p. 57-68.
151. Malik, Z.A., G.M. Denning, and D.J. Kusner, *Inhibition of Ca²⁺ signaling by Mycobacterium tuberculosis is associated with reduced phagosome-lysosome fusion and increased survival within human macrophages*. The Journal of experimental medicine, 2000. **191**(2): p. 287-302.
152. Clynes, R., et al., *Modulation of immune complex-induced inflammation in vivo by the coordinate expression of activation and inhibitory Fc receptors*. The Journal of experimental medicine, 1999. **189**(1): p. 179-85.

153. Yoshida, S. and S. Plant, *Mechanism of release of Ca²⁺ from intracellular stores in response to ionomycin in oocytes of the frog Xenopus laevis*. J Physiol, 1992. **458**: p. 307-18.
154. Pritchard, N.R., et al., *Autoimmune-prone mice share a promoter haplotype associated with reduced expression and function of the Fc receptor FcγRII*. Current biology : CB, 2000. **10**(4): p. 227-30.
155. Clatworthy, M.R. and K.G. Smith, *FcγRIIb balances efficient pathogen clearance and the cytokine-mediated consequences of sepsis*. J Exp Med, 2004. **199**(5): p. 717-23.
156. Deretic, V. and R.A. Fratti, *Mycobacterium tuberculosis phagosome*. Mol Microbiol, 1999. **31**(6): p. 1603-9.
157. Underhill, D.M. and A. Ozinsky, *Phagocytosis of microbes: complexity in action*. Annual review of immunology, 2002. **20**: p. 825-52.
158. Cywes, C., et al., *Nonopsonic binding of Mycobacterium tuberculosis to complement receptor type 3 is mediated by capsular polysaccharides and is strain dependent*. Infection and immunity, 1997. **65**(10): p. 4258-66.
159. Cywes, C., et al., *Nonopsonic binding of Mycobacterium tuberculosis to human complement receptor type 3 expressed in Chinese hamster ovary cells*. Infection and immunity, 1996. **64**(12): p. 5373-83.
160. Schorey, J.S., M.C. Carroll, and E.J. Brown, *A macrophage invasion mechanism of pathogenic mycobacteria*. Science, 1997. **277**(5329): p. 1091-3.
161. Schlesinger, L.S., S.R. Hull, and T.M. Kaufman, *Binding of the terminal mannosyl units of lipoarabinomannan from a virulent strain of Mycobacterium tuberculosis to human macrophages*. Journal of immunology, 1994. **152**(8): p. 4070-9.
162. Tailleux, L., B. Gicquel, and O. Neyrolles, *[DC-SIGN, a key receptor of Mycobacterium tuberculosis?]*. Medecine sciences : M/S, 2003. **19**(6-7): p. 658-60.
163. Schafer, G., et al., *The role of scavenger receptor B1 in infection with Mycobacterium tuberculosis in a murine model*. PloS one, 2009. **4**(12): p. e8448.

164. Zimmerli, S., S. Edwards, and J.D. Ernst, *Selective receptor blockade during phagocytosis does not alter the survival and growth of Mycobacterium tuberculosis in human macrophages*. American journal of respiratory cell and molecular biology, 1996. **15**(6): p. 760-70.
165. Means, T.K., et al., *Human toll-like receptors mediate cellular activation by Mycobacterium tuberculosis*. Journal of immunology, 1999. **163**(7): p. 3920-7.
166. Armstrong, J.A. and P.D. Hart, *Phagosome-lysosome interactions in cultured macrophages infected with virulent tubercle bacilli. Reversal of the usual nonfusion pattern and observations on bacterial survival*. The Journal of experimental medicine, 1975. **142**(1): p. 1-16.
167. Diaz-Silvestre, H., et al., *The 19-kDa antigen of Mycobacterium tuberculosis is a major adhesin that binds the mannose receptor of THP-1 monocytic cells and promotes phagocytosis of mycobacteria*. Microbial pathogenesis, 2005. **39**(3): p. 97-107.
168. Netea, M.G., et al., *Proinflammatory cytokines and sepsis syndrome: not enough, or too much of a good thing?* Trends in immunology, 2003. **24**(5): p. 254-8.
169. Baggiolini, M., B. Dewald, and B. Moser, *Human chemokines: an update*. Annu Rev Immunol, 1997. **15**: p. 675-705.
170. Ouadrhiri, Y. and Y. Sibille, *Phagocytosis and killing of intracellular pathogens: interaction between cytokines and antibiotics*. Curr Opin Infect Dis, 2000. **13**(3): p. 233-240.
171. Netea, M.G., et al., *Proinflammatory cytokines and sepsis syndrome: not enough, or too much of a good thing?* Trends Immunol, 2003. **24**(5): p. 254-8.
172. de Waal Malefyt, R., et al., *Interleukin 10(IL-10) inhibits cytokine synthesis by human monocytes: an autoregulatory role of IL-10 produced by monocytes*. The Journal of experimental medicine, 1991. **174**(5): p. 1209-20.
173. al-Janadi, M., et al., *Cytokine profile in systemic lupus erythematosus, rheumatoid arthritis, and other rheumatic diseases*. Journal of clinical immunology, 1993. **13**(1): p. 58-67.

174. Bauer, J.W., et al., *Elevated serum levels of interferon-regulated chemokines are biomarkers for active human systemic lupus erythematosus*. PLoS medicine, 2006. **3**(12): p. e491.
175. Grondal, G., et al., *Cytokine production, serum levels and disease activity in systemic lupus erythematosus*. Clinical and experimental rheumatology, 2000. **18**(5): p. 565-70.
176. Sabry, A., et al., *Proinflammatory cytokines (TNF-alpha and IL-6) in Egyptian patients with SLE: its correlation with disease activity*. Cytokine, 2006. **35**(3-4): p. 148-53.
177. Studnicka-Benke, A., et al., *Tumour necrosis factor alpha and its soluble receptors parallel clinical disease and autoimmune activity in systemic lupus erythematosus*. British journal of rheumatology, 1996. **35**(11): p. 1067-74.
178. Gabay, C., et al., *Circulating levels of tumor necrosis factor soluble receptors in systemic lupus erythematosus are significantly higher than in other rheumatic diseases and correlate with disease activity*. The Journal of rheumatology, 1997. **24**(2): p. 303-8.
179. Shankar, S. and R. Handa, *Biological agents in rheumatoid arthritis*. J Postgrad Med, 2004. **50**(4): p. 293-9.
180. Davis, L.S., J. Hutcheson, and C. Mohan, *The role of cytokines in the pathogenesis and treatment of systemic lupus erythematosus*. J Interferon Cytokine Res, 2011. **31**(10): p. 781-9.
181. Linker-Israeli, M., et al., *Elevated levels of endogenous IL-6 in systemic lupus erythematosus. A putative role in pathogenesis*. J Immunol, 1991. **147**(1): p. 117-23.
182. Munoz, L.E., et al., *Autoimmunity and chronic inflammation - two clearance-related steps in the etiopathogenesis of SLE*. Autoimmunity reviews, 2010. **10**(1): p. 38-42.
183. Singh, R.R., *SLE: translating lessons from model systems to human disease*. Trends in immunology, 2005. **26**(11): p. 572-9.

184. Dijstelbloem, H.M., J.G. van de Winkel, and C.G. Kallenberg, *Inflammation in autoimmunity: receptors for IgG revisited*. Trends in immunology, 2001. **22**(9): p. 510-6.
185. Tincani, A., et al., *Inflammatory molecules: a target for treatment of systemic autoimmune diseases*. Autoimmunity reviews, 2007. **7**(1): p. 1-7.
186. Bollinger, C.R., V. Teichgraber, and E. Gulbins, *Ceramide-enriched membrane domains*. Biochim Biophys Acta, 2005. **1746**(3): p. 284-94.
187. Stancevic, B. and R. Kolesnick, *Ceramide-rich platforms in transmembrane signaling*. FEBS Lett, 2010. **584**(9): p. 1728-40.
188. Truman, J.P., et al., *Acid sphingomyelinase in macrophage biology*. Cell Mol Life Sci, 2011. **68**(20): p. 3293-305.
189. Grassme, H., et al., *Ceramide-rich membrane rafts mediate CD40 clustering*. J Immunol, 2002. **168**(1): p. 298-307.
190. Suchard, S.J., et al., *Ceramide inhibits IgG-dependent phagocytosis in human polymorphonuclear leukocytes*. Blood, 1997. **89**(6): p. 2139-47.
191. Schuchman, E.H., et al., *Structural organization and complete nucleotide sequence of the gene encoding human acid sphingomyelinase (SMPD1)*. Genomics, 1992. **12**(2): p. 197-205.
192. Grassme, H., et al., *Host defense against Pseudomonas aeruginosa requires ceramide-rich membrane rafts*. Nat Med, 2003. **9**(3): p. 322-30.
193. Hauck, C.R., et al., *Acid sphingomyelinase is involved in CEACAM receptor-mediated phagocytosis of Neisseria gonorrhoeae*. FEBS Lett, 2000. **478**(3): p. 260-6.
194. Jbeily, N., et al., *Hyperresponsiveness of mice deficient in plasma-secreted sphingomyelinase reveals its pivotal role in early phase of host response*. J Lipid Res, 2012. **54**(2): p. 410-24.
195. Clynes, R., et al., *Modulation of immune complex-induced inflammation in vivo by the coordinate expression of activation and inhibitory Fc receptors*. J Exp Med, 1999. **189**(1): p. 179-85.

196. Jiang, L.N., et al., [*The Enhanceing effect of IL-12 on phagocytosis and killing of Mycobacterium tuberculosis by neutrophils in tuberculosis patients*]. *Xi Bao Yu Fen Zi Mian Yi Xue Za Zhi*, 2011. **27**(11): p. 1191-4.
197. Xu, W., et al., *IL-10-producing macrophages preferentially clear early apoptotic cells*. *Blood*, 2006. **107**(12): p. 4930-7.